ISBN 978-82-326-3936-6 (printed version)
ISBN 978-82-326-3937-3 (electronic version)
ISSN 1503-8181

Gunvor Bjerkelund Røkke

Doctoral Thesis

Doctoral theses at NTNU, 2019:169

Gunvor Bjerkelund Røkke

Regulation of photosynthesis in heterokont algae

NTNU
Norwegian University of
Science and Technology
Faculty of Natural Sciences
Department of Biotechnology and Food Science

NTNU
Norwegian University of
Science and Technology

Doctoral theses at NTNU, 2019:169

NTNU

NTNU
Norwegian University of
Science and Technology

Gunvor Bjerkelund Røkke

Regulation of photosynthesis in heterokont algae

Thesis for the degree of Philosophiae Doctor

Trondheim, 05 2019

Norwegian University of Science and Technology
Faculty of Natural Sciences
Department of Biotechnology and Food Science

NTNU
Norwegian University of
Science and Technology

NTNU
Norwegian University of Science and Technology

Thesis for the degree of Philosophiae Doctor

Faculty of Natural Sciences
Department of Biotechnology and Food Science

ISBN 978-82-326-3936-6 (printed version)
ISBN 978-82-326-3937-3 (electronic version)
ISSN 1503-8181

Doctoral theses at NTNU, 2019:169

Printed by Skipnes Kommunikasjon as

Acknowledgements

Even though the thesis you are now holding in your hands has my name on its front page, it would never have been written, and my defence day would never have come, if it were not for all of the wonderful people who have helped me throughout these past years. Therefore, I have a debt of gratitude to my amazing colleges, who have helped me carry out experiments I could never have done on my own (unless I had cloned myself, but that was obviously not within the scope of my PhD), been there to answer all my questions, and made these years leading up to my defence interesting and memorable.

First and foremost, I wish to thank my main supervisor, associate professor Martin Hohmann-Marriott. Thank you for always being available, even when you were in New Zealand with a 12-hour time difference between us. Thank you for always being patient, and never seeming to get even a little bit annoyed when you had to explain a concept to me that you had already explained three times before. You have been the best supervisor I could possibly ask for.

I also want to thank my co-supervisors, professor Olav Vadstein and professor Atle M. Bones. Thank you for giving me the opportunity to pursue a PhD, and for letting me use your labs.

One person to whom I really owe an infinite amount of thanks is Thor Bernt Melø, who spent so much time helping me out in the lab, especially when I was new to spectroscopy. He was the one I could always go and talk to when Martin was in New Zealand and I needed an answer right away. I realize that you were never officially one of my supervisors, and not obligated to help me or spend any time on me, which makes me all the more grateful that you did. I have enjoyed both working and having coffee breaks with you more than words can possibly say.

I also wish to thank professor Eivind Almaas. Thank you for working with me on building the chloroplast model, and for igniting my interest in metabolic modelling by making it fun and interesting back when I was a master student, and I took your systems biology course without knowing much about programming. Thank you also for giving me the opportunity to be a part of the NTNU iGEM team in 2011, to be a team leader in 2012, and to be an advisor for

the team in 2013. I am pretty sure I would not have been here, writing this thesis, if it were not these experiences.
A big thank you to my lab family - adjunct associate professor Rahmi Lale; postdoctor Swapnil Vilas Bhujbal; my fellow PhD students Anne Vogel, Maxime Fages-Lartaud, Erland Årstøl, Lisa Tietze and Alex Wong; PhD graduates Jake Lamb and Alice Mühlroth; and Kerstin Engelhardt and Ingerid Onsager - for being such amazing colleagues. I enjoyed the interesting discussions, the Monday morning coffee breaks, and being part of a great group.
Thank you also to Per Winge, Torfinn Sparstad and Marianne Nymark at the Department of Biology.
Two people without whom this thank-you list would not be complete are the two master students I was lucky enough to mentor, and with whom I also became very good friends: Ksenia Gulyaeva and Nhung Pham. I am so grateful because it was the two of you I had the opportunity to mentor, and nobody else. You are both fantastic people, and I am so happy to know you!
If you have read this far, you have probably gotten the idea by now – my PhD has been quite enjoyable thanks to all the fantastic people I have been able to work with. But research in itself can be a challenge, and on those days when nothing worked in the lab, and I really started wondering why on earth I put myself through this, I have been even more grateful for my friends (you know who you are). Thank you for being there for me, and for giving life more dimensions than only research.
Last but not least, I want to thank my parents, who have always let me follow my dreams, who have always been there to support me, and who catch me when I fall.

And finally; a big thank you to my algae for cooperating with me, and giving me some interesting results to write about!

Summary

Several heterokont algae have emerged as model organisms, due to their ability to produce and store large amounts of lipids, which are of interest as a resource for fuel and food production. The photosynthetic machineries of heterokont algae are, however, not as well understood as the ones of their plant and green algal counterparts.

One part of this thesis reviews lipid metabolism in heterokont algae and develops a computational model to explore and compare chloroplast lipid metabolism in the heterokont algae *Nannochloropsis* and *Phaeodactylum,* and in the green alga *Chlamydomonas*. This chloroplast model also includes a detailed representation of the photosynthetic electron transport chain and carbon fixation.

The main focus of the thesis is the exploration of the photosynthetic machinery of the heterokont algae *Nannochloropsis* and *Phaeodactylum* using chlorophyll fluorescence techniques.

The results indicate that the photosynthetic machinery of the investigated heterokont algae is tuned fundamentally differently than in green algae and plants. In heterokont algae, pulses of light that exceed the light intensity of maximum sunlight do not provoke a complete reduction of the photosynthetic electron transport chain. The reduction state of the photosynthetic electron transport chain modulates the distribution of excitation energy between the two photosystems in plants and green algae. However, this tuning response termed a state transition, has not been identified in heterokont algae. Having revealed that the photosynthetic machinery of heterokont algae is not completely reduced by bright light, I manipulated the photosynthetic machinery of *Nannochloropsis oceanica* and *Phaeodactylum tricornutum* by oxygen depletion and the application of inhibitors to achieve a completely reduced photosynthetic electron transport chain. These studies demonstrate a redistribution of excitation energy that appears to be redox-mediated. To demonstrate the dynamic distribution of excitation energy in heterokont algae, chlorophyll fluorescence emission at 77 K was used, a technique that also I specifically reviewed for heterokont algae.

The work presented in this thesis contributes significantly to the understanding of the photosynthetic machineries of heterokont algae. In particular, the work performed in this thesis demonstrates for the first time the redox-dependent distribution of excitation energy between the two photosystems of heterokont algae. The results have an impact on understanding the evolution and eco-physiological adaptations of heterokont algae, and also clarify the use of chlorophyll fluorescence techniques in heterokont algae.

List of publications

Paper I

Mühlroth, Alice; Li, Keshuai; Røkke, Gunvor; Winge, Per; Olsen, Yngvar; Hohmann-Marriott, Martin F.; Vadstein, Olav; Bones, Atle M. (2013) **Pathways of lipid metabolism in marine algae, co-expression network, bottlenecks and candidate genes for enhanced production of EPA and DHA in species of Chromista**. *Marine Drugs*, vol. 11, pp. 4662 – 4697, DOI: 10.3390/md11114662

Paper II

Røkke, Gunvor; Melø, Thor Bernt; Hohmann-Marriott, Martin Frank (2017) **The plastoquinone pool of *Nannochloropsis oceanica* is not completely reduced during bright light pulses**. *PLoS One*, vol. 12: e0175184, DOI: 10.1371/journal.pone.0175184

Paper III

Røkke, Gunvor Bjerkelund; Melø, Thor Bernt; Mühlroth, Alice; Vadstein, Olav; Bones, Atle M.; Hohmann-Marriott, Martin F. (2019) **Unique photosynthetic electron transport tuning and excitation distribution in heterokont algae**. *PLoS One*, vol. 14: e0209920, DOI: 10.1371/journal.pone.0209920

Paper IV

Lamb, Jacob Joseph; Røkke, Gunvor; Hohmann-Marriott, Martin Frank (2018) **Chlorophyll fluorescence emission spectroscopy of oxygenic organisms at 77 K**. *Photosynthetica*, vol. 56, pp. 105 – 124, DOI: 10.1007/s11099-018-0791-y

Paper V

Røkke, Gunvor Bjerkelund; Hohmann-Marriott, Martin Frank; Almaas, Eivind. **An adjustable algal chloroplast plug-and-play model for genome-scale metabolic models.**

Manuscript prepared for submission

Additional publications

Røkke, Gunvor; Korvald, Eirin; Pahr, Jarle; Øyås, Ove; Lale, Rahmi (2014) **BioBrick assembly standards and techniques and associated software tools**. In: Valla, Svein & Lale, Rahmi (Eds.), *DNA cloning and assembly methods* (pp. 1 – 24). New York, USA: Springer Science+Business Media

Posters

Poster at the 12th Nordic Photosynthesis Congress 2014
Title: *Comparing the light acclimation mechanisms in Nannochloropsis oceanica and Chlamydomonas reinhardtii*
Authors: Røkke, Gunvor; Hohmann-Marriott, Martin F.
Date: 14th – 17th of October 2014
Location: Uppsala University, Sweden

Electronic poster at the Photosynthesis Gordon Research Conference 2015
Title: *Investigating the photosynthetic apparatus of Nannochloropsis oceanica CCMP 1779*
Authors: Røkke, Gunvor; Hohmann-Marriott, Martin Frank
Date: 28th of June – 3rd of July 2015
Location: Bentley University, Massachusetts, USA

Electronic poster at the Norwegian Plant Biology Conference 2016
Title: *Investigating the protection mechanisms of the photosynthetic apparatus of Nannochloropsis oceanica*
Authors: Røkke, Gunvor; Melø, Thor Bernt; Hohmann-Marriott, Martin Frank
Date: 15th – 17th of June 2016
Location: NTNU, Trondheim

Popular science communications

Competition: PhD Grand Prix, 2015

Name of presentation: *Green revolution!*

Comment: 3rd place out of 7 contestants

Date: 5th of March 2015

Location: NTNU, Trondheim

Competition: Forsker Grand Prix, 2015

Name of presentation: *Fantastiske alger*

Comment: Joint 5th place of 10 contestants

Date: 24th of September 2015

Location: Byscenen, Trondheim

The presentation can be found at the NRK website:

https://tv.nrk.no/serie/kunnskapskanalen/2015/MDDP17004215 (at 10:44 min)

Invited talks

Invited talk at the Annual Meeting of NITO

Title: *Kræsjkursj i algeforskning*

Arranged by: NITO (Norges ingeniør- og teknologiorganisasjon)

Date: 17th of March 2016

Location: Britannia hotell, Trondheim

List of abbreviations

ACP	Acyl-carrier protein
ADP	Adenosine diphosphate
ATP	Adenosine triphosphate
CCCP	carbonylcyanide *m*-chlorophenylhydrazone
Chl	Chlorophyll
CLH	*Chromera velia*-like light-harvesting complex
CoA	Coenzyme A
DBMIB	2,5-dibromo-6-isopropyl-3-methyl-1,4-benzoquinone
DCMU	3-(3,4-dichlorophenyl)-1,1-dimethylurea
DGDG	Digalactosyl diacylglycerol
FCP	Fucoxanthin chlorophyll protein
FBA	Flux balance analysis
FNR	Ferredoxin-$NADP^+$ reductase
LC-PUFA	Long-chain poly-unsaturated fatty acid
LHC	Light-harvesting complex
LHCI	Light-harvesting complex associated with PSI
LHCII	Light-harvesting complex associated with PSII
MGDG	Monogalactosyl diacylglycerol
$NADP^+$	Nicotinamide adenine dinucleotide phosphate
NADPH	Reduced nicotinamide adenine dinucleotide phosphate
NDH	NADH oxidase-like complex
Ndh	NADPH dehydrogenase
NPQ	Non-photochemical quenching
PAM	Pulse amplitude modulated / Pulse amplitude modulation
PGR5	Proton gradient regulation 5
PGRL1	PGR5-like photosynthetic phenotype 1
PSI	Photosystem I
PSII	Photosystem II
PUFA	Poly-unsaturated fatty acid
redCAP	red lineage chlorophyll *a*/*b* binding-like proteins
RuBisCO	Ribulose-1,5-bisphosphate carboxylase / oxygenase

SQDG	Sulfoquinovosyl diacylglycerol
VCP	Violaxanthin / vaucheriaxanthin chlorophyll protein

Contents

1. Introduction

1.1. Microalgae

Microalgae are unicellular algae that can be found in almost any environment on earth (Borowitzka & Moheimani, 2013). They are an extremely diverse group of organisms, and may range in size from a few micrometres up to several hundred micrometres. Although nobody knows how many species of microalgae actually exist, it has been estimated that the number could be between 200,000 and 800,000 (Kim, 2015).

Microalgae can grow in oceans, rivers, ponds and lakes, and the different species thrive in a wide range of light intensities, temperatures, salinities and pH values. Microalgae are extremely important for primary production. About half of the total global primary production occurs in the oceans (Boyd, et al. 2014), and unicellular phytoplankton is responsible for almost the entire oceanic primary production (Falkowski et al. 2004). Diatoms alone are thought to have a primary production comparable to all the world's rainforests (Lucentini, 2005). Microalgae also form the basis of several food chains, making them the source of 70 % of the world's biomass (Kim, 2015).

In recent years, microalgae have moved into the spotlight and been the subject of an increasing number of studies due to their potential and versatility.

Many microalgae are able to produce and store very high amounts of fatty acids. Certain species of microalgae can store an amount of lipids equivalent to more than half their own weight. This makes them an interesting source of biodiesel, since these fatty acids could be used as substrate in the transesterification reaction that produces biodiesel (Lam & Lee, 2012). Microalgae are much better suited for biodiesel production than the crops that are currently being used, as microalgae have higher growth rates, higher rates of lipid production, and higher photosynthetic efficiency (Miao et al. 2004). In addition, they do not occupy arable land, which is already scarce and desperately needed for food production for an ever-increasing human population (Johnson & Wen, 2009). Microalgae also produce carbohydrates, which in most cases can be found in the outer layer of their cell walls (Chen et al. 2013). These carbohydrates could be

fermented in order to produce bioethanol, which is an alternative biofuel to fossil-resource derived gasoline (Naik et al. 2010).

The algal lipids that are relevant for biodiesel production are mostly unsaturated. But most microalgae also have an impressive production of poly-unsaturated fatty acids (PUFAs). This makes microalgae a potential ingredient both in human food and in fish feed (Patil et al. 2007; Vanthoor-Koopmans et al. 2013).

Microalgae also produce valuable chemicals, and several species of algae have been the subjects of studies aimed at screening for bioactive compounds, such as anti-cancer and antimicrobial agents (Borowitzka, 1995; Shanab et al. 2012). Due to their photosynthetic abilities, algae are also eager producers of pigments that could be utilized as antioxidants in food, pharmaceuticals and cosmetics (Lubián et al. 2000).

While the applications of microalgae for generating biomolecules are almost endless, one additional important field of usage worth mentioning here is their ability to capture nutrients from wastewater (Kim, 2015). Valuable nutrients escaping into the oceans is an increasing problem, especially if these nutrients are a limited resource, such as phosphorous. Algal biomass derived from nutrient trapping could subsequently be used as a fertilizer, thus allowing re-use of the nutrients (Aslan & Kapdan, 2006).

1.2. Evolution of microalgae

All microalgae are thought to have developed as a result of one or several endosymbiotic events (McFadden, 2001), and until very recently, it has been assumed that all organisms with a chloroplast are descendants of one particular cyanobacterium (Keeling, 2004; McFadden, 2001).

Fossil records indicate that cyanobacteria have existed for between 2.72 and 3.5 billion years (Hohmann-Marriott & Blankenship, 2011), while the history of microalgae started around 1.6 billion years ago, when a non-photosynthetic eukaryote engulfed a cyanobacterium and kept it as an organelle (Yoon et al. 2004). This initial photosynthetic eukaryote gave rise to green algae, red algae, and glaucophytes (Keeling, 2004). A secondary endosymbiotic event involving red algae gave rise to the chromalveolates, including the heterokont algae. This is assumed to have occurred approximately 1.3 billion years ago (Yoon et al. 2004). Green algae, on the other hand, later gave rise to land plants about 5 million years ago (Morris et al. 2018).

The cyanobacterium that was engulfed in a eukaryotic cell has over time lost or transferred most of its original genes to its eukaryotic host. Current chloroplasts depend on several proteins that are now encoded in the nuclear genome. These are synthesized in the cytoplasm, tagged with a transit peptide, and targeted to the chloroplast (Keeling, 2004). The chloroplast, however, still encodes most of the gene products that are needed for building the protein complexes involved in the photosynthetic electron transport chain (Pfannschmidt et al. 1999).

1.3. Photosynthesis

Photosynthesis is the most important biological process on Earth, as it is the foundation of all ecosystems on the Earth's surface. If it were not for the first photosynthetic microorganisms (Hohmann-Marriott & Blankenship, 2011), there would be no oxygen in the atmosphere, and since the majority of the organisms inhabiting this planet depend on oxygen as their primary electron acceptor, an atmosphere without oxygen would have prevented the evolution of most complex organisms.

Photosynthesis has traditionally been seen as two distinct, yet connected set of reactions; the light reactions and the carbon reactions. The light reactions are those carried out by the protein complexes of the photosynthetic electron transport chain taking place in the thylakoids, while the reactions of carbon fixation involved in the Calvin-Benson cycle, are referred to as the carbon reactions.

The ultimate goal of the light-dependent reactions is to create adenosine triphosphate (ATP) and reduced nicotinamide adenine dinucleotide phosphate (NADPH), which is subsequently being used in the Calvin-Benson cycle to fix CO_2. The Calvin-Benson cycle is a cyclic pathway consisting of 13 reactions. A critical step in this cycle is the reaction which is responsible for binding CO_2, which is catalysed by the enzyme Ribulose-1,5-bisphosphate carboxylase/oxygenase (RuBisCO) (Gong et al. 2018).

The product of the Calvin-Benson cycle is the three-carbon molecule glyceraldehyde-3-phosphate (alternatively dihydroxyacetonephosphate), which is the basic building block for all organic components in autotrophic algae.

1.3.1. The photosynthetic electron transport chain

Before an alga can use the chemical and redox energy contained in ATP and NADPH for carbon fixation and glyceraldehyde-3-phosphate production, these molecules must first be produced, or more precisely re-generated from adenosine diphosphate (ADP) and nicotinamide adenine dinucleotide phosphate ($NADP^+$), respectively. Algae and plants do this by utilizing the energy contained in sunlight.

The photosynthetic electron transport chain uses the energy in sunlight to split water into molecular oxygen and protons, while sending the electrons derived from water-splitting on a journey through three membrane-bound electron-transporting protein complexes: photosystem II (PSII), the cytochrome b_6f complex, and photosystem I (PSI). In the photosynthetic electron transport chain, electrons are passed from a donor molecule with higher energy to an acceptor molecule with lower energy until it reaches PSI, where the energy from sunlight is used to move the electrons to high-energy iron-sulphur clusters within PSI.

In summary, the photosynthetic electron transport chain increases the redox energy of the electrons passing through it from $\sim$0.8 eV (when bound to water) to $\sim$ – 0.3 eV (when bound to NADPH) (Govindjee et al. 2017).

1.3.1.1. Light-harvesting antennae

Light-harvesting complexes come in so many different shapes and sizes that it is likely that they have evolved several times during the course of evolution (Hohmann-Marriott & Blankenship, 2011). Their function, however, is conserved, as they are all united in one task – to collect sunlight and funnel the captured light-energy to the photosystem they are connected to.

In eukaryotes, the main classes of light-harvesting complexes (LHCs) consist of transmembrane proteins with three hydrophobic transmembrane alpha-helix domains that bind chlorophylls and carotenoids. The light-harvesting complexes coupled to PSII (LHCII) in green algae and plants usually have a size of ~ 25 kDa, and each bind 12 – 16 pigment molecules (Croce & Van Amerongen, 2014). The light-harvesting complexes of green algae contain chlorophyll *a* and *b,* while heterokont algae usually contain chlorophyll *a* and *c*. As an example; in *Phaeodactylum*, a light-harvesting complex typically contains 6 chl *a*, 4 chl *c* and 5 – 6 carotenoids, which in diatoms could be fucoxanthin, lutein, diadinoxanthin or diatoxanthin (Gundermann & Büchel, 2014).

LHCII complexes are coupled to PSII through the proteins CP43 (PsbC) and CP47 (PsbB), which funnel the excitation energy to the reaction center core of PSII (Drop et al. 2014).

Several classes of light-harvesting complexes exist, and the naming, function and pigment composition of these varies from organism to organism (further described in sections 1.5.1, 1.5.2 and 1.5.3).

Studies of energy transfer within light-harvesting complexes have shown that the excitation energy within them can be transferred from xanthophylls to chlorophyll *b* to chlorophyll *a* via Förster energy transfer (Van Amerongen & Van Grondelle, 2001).

In green algae and land plants, LHCIIs usually exists as trimeric complexes (Drop et al. 2014, Nagao et al. 2013), and on average, four trimers are present per reaction center of PSII (Van Amerongen & Van Grondelle, 2001). Light-harvesting complexes contain ~ 70 % of the pigments involved in photosynthesis (Croce et al. 1999), and even though PSII also contains

chlorophylls, and would continue working even in the absence of its light-harvesting complexes, its light-harvesting efficiency would be strongly reduced.

1.3.1.2. Photosystem II

PSII in most organisms consists of approximately 20 protein subunits (Gimpel et al. 2015). The overall function of PSII is to generate electrons from water splitting. Electrons are subsequently passed on to electron carriers embedded in the protein complex, linking the PSII reaction center with the plastoquinone pool (Lubitz et al., 2008).

The water splitting activity of PSII is catalysed within the oxygen-evolving complex, which is situated at the lumenal side of the thylakoid membrane. It contains a manganese cluster, which is the catalytic site where water splitting occurs. In order to split water, the manganese cluster cycles through a continuous loop of five steps, called the S-cycle. In each S-cycle step, four electrons are generated from two molecules of water, while four protons are released into the thylakoid lumen and one molecule of oxygen is generated (Cox et al. 2014).

Each electron released as a result of S-cycle activity is passed on to a tyrosine residue, termed Y_Z, which is situated between the oxygen-evolving complex and the reaction center of PSII (Shinopoulos & Brudvig, 2012).

The PSII reaction center core houses a pair of chlorophyll molecules, commonly termed P_{680}, which are situated at the interface between the proteins D1 (PsbA) and D2 (PsbD). Peripheral light-harvesting complexes channel the excitation energy to P680 via the core antennae proteins CP47 (PsbB) and CP43 (PsbC), which combined contain around 35 molecules of chlorophyll *a* (Umena et al. 2011). When P_{680} is excited, one electron escapes the reaction center chlorophyll pair, and is donated to a series of downstream electron carriers. The empty electron 'hole' in P_{680} is filled with an electron from Yz. When leaving P_{680}, the electron first reaches pheophytin, which is a chlorophyll molecule where the central magnesium atom is replaced by two protons. From pheophytin, the electron travels further to the PSII-bound Q_A, and subsequently to Q_B. The two

latter electron acceptors are both quinones. Q_A is permanently bound to PSII, while Q_B is mobile, and leaves PSII when it is fully loaded with two electrons and two protons, and becomes part of the plastoquinone pool (Pospíšil, 2009).
Even though P_{680}^+ is usually reduced by Y_Z, which facilitates electron transfer from the oxygen-evolving complex to the oxidized reaction center, P_{680}^+ could also be reduced by a plastoquinol molecule from the plastoquinone pool (Pospíšil, 2009). This alternative electron pathway in PSII occurs via the PSII donor side cytochrome b_{559} and a carotenoid molecule (the two alternative electron pathways of PSII are shown in Figure 1). It is assumed that this alternative electron transport pathway in PSII serves as a safety valve that could be used to prevent the accumulation of P_{680}^+, which is extremely oxidizing, and could lead to the formation of reactive oxygen species, which in turn could damage the photosynthetic machinery (Pospíšil, 2009).
In conditions where the plastoquinone pool is highly reduced and Q_A is unable to pass on its electron, electrons could also move backwards from the reaction center, via Y_Z, and eventually end up back where they came from, in the manganese cluster of the oxygen evolving complex (Lomoth et al. 2006). This process is called charge recombination (Rappaport et al. 2002).
Charge recombination, occurring on a time scale of milliseconds, is a much slower process than the electron transfer occurring from the reaction center to Q_A. Charge recombination is therefore more likely to occur if the electron is blocked from moving to Q_B. The manganese cluster is more prone to accept an electron from Y_Z when it is in its S_2 state, moving it back to S_1 (Rappaport et al. 2002).
Molecules resembling plastoquinones can also be bound to the Q_B binding pocket of PSII. The molecule 3-(3,4-dichlorophenyl)-1,1-dimethylurea (DCMU) has a structure similar to a plastoquinone molecule, and binds strongly to the Q_B binding pocket. However, DCMU will not be reduced by Q_A. DCMU will therefore remain in the binding pocket, and block the electron flow between Q_A and Q_B.

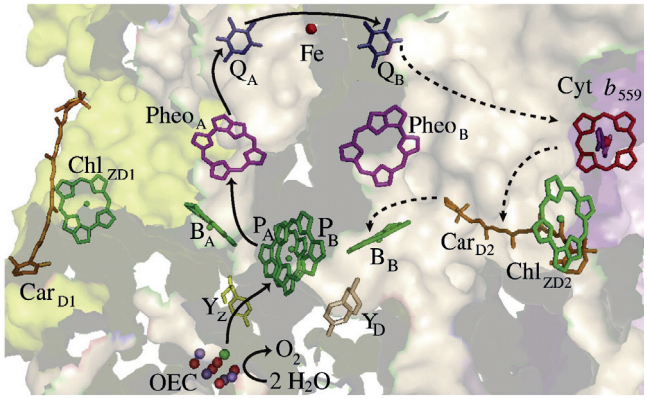

Figure 1: The two alternative electron transport pathways of PSII (figure taken from Shinopoulos & Brudvig, 2012)

1.3.1.3. The plastoquinone pool

Plastoquinone is the first mobile electron carrier of the photosynthetic electron transport chain, being responsible for transporting electrons between PSII and the next photosynthetic protein complex, the cytochrome b_6f complex. Plastoquinones are quite abundant in the thylakoid membrane, with about 10 plastoquinone molecules per PSII (Tikhonov, 2014).

An oxidized plastoquinone molecule can bind to the Q_B binding pocket of PSII, which is situated towards the stromal side of the thylakoid membrane (Rochaix, 2011). There, it undergoes two rounds of reductions by receiving electrons from Q_A. After receiving electrons, two protons from the stromal side of the membrane are bound to keep the electron carrier charge-neutral.

The reduced plastoquinone molecule (plastoquinol) has a lower affinity for the Q_B binding site than an oxidized plastoquinone molecule (Müh et al. 2012). The plastoquinol therefore leaves PSII and travels through the thylakoid membrane to the cytochrome b_6f complex, where it binds to the Q_o site situated on the lumenal side of the complex (Tikhonov, 2014).

One function of the plastoquinone pool is of course to transport electrons between two of the photosynthetic protein complexes, but it also has another

important function – it translocates protons from the stromal side of the thylakoid membrane to the lumenal side. When the two protons were bound during the reduction of plastoquinone, these protons were taken from the stromal side of the membrane. When the protons are released again upon binding of plastoquinol to the cytochrome b_6f complex, the same protons are released on the lumenal side of the membrane.
This imbalance in proton concentration between the two sides of the thylakoid membrane serves two important purposes. Firstly, it is used for generating ATP from ADP (see section 1.3.1.7 about ATP synthase). Secondly, the magnitude of the proton concentration on the lumenal side of the thylakoid membrane plays an important role in the onset of mechanisms involved in photoprotection (see section 1.3.2).

1.3.1.4. The cytochrome b_6f complex

The cytochrome b_6f complex is the second electron transferring protein complex in the photosynthetic electron transport chain, but unlike PSII and PSI, it is not driven by light. The cytochrome b_6f complex is a homodimer, with each monomer consisting of eight protein units. The four major subunits of each monomer are the Rieske iron-sulphur protein, cytochrome *f*, cytochrome b_6 and subunit IV (Kurisu et al. 2003).
The electron transfer pathway through the b_6f complex is commonly referred to as the Q-cycle, and was discovered by Peter Mitchell in 1976 (Mitchell, 1976). There are two possible pathways an electron can follow through the b_6f complex, and during the Q-cycle, both electron routes are used.
When a fully reduced plastoquinol molecule docks to the Q_o binding site of the cytochrome b_6f complex, the two electrons carried by the plastoquinol follow different paths. The first electron transferred from plastoquinol to the b_6f complex reduces the iron-sulphur cluster of the Rieske protein. From the reduced iron-sulphur cluster of the Rieske protein, the electron is passed on to cytochrome *f*, which again passes it on to one of the mobile electron carrier

plastocyanin (in some algae cytochrome c_6) (Tikhonov, 2014, Nelson & Yocum, 2006).

The second electron on the semiquinone that is still docked to the Q_o site of the cytochrome b_6f complex is transferred to heme b_l, which passes on its electrons to a pair of hemes, heme b_h and heme c_i. This heme pair is able to accept two electrons and subsequently use these to reduce an oxidized plastoquinone molecule at the Q_i site of the cytochrome b_6f complex, which is located towards the stromal side of the thylakoid membrane. During a full Q-cycle, the b_6f complex therefore uses two plastoquinol molecules, which are oxidized at the Q_o site, in order to generate one additional plastoquinol molecule at the Q_i site. The protons used to keep the plastoquinol molecule generated at the Q_i site charge-neutral are taken from the stromal side of the thylakoid membrane. The plastoquinol molecule is released back into the plastoquinone pool, and when it is oxidized again at the Q_o site, the protons are released into the thylakoid lumen. The activity of the Q-cycle therefore increases the proton gradient build-up over the thylakoid membrane (Joliot & Joliot 1994; Kurisu et al. 2003). The detailed mechanism of the Q-cycle is shown in Figure 2.

During normal cytochrome b_6f complex function, the Rieske iron-sulphur protein oscillates between two positions within the cytochrome b_6f complex (Brugna et al. 2000; Darrouzet et al. 2000). These oscillations bring different prosthetic groups into proximity with each other, and allow for different possible electron transfers. Since the Q-cycle depends on two different electron transport routes through the cytochrome b_6f complex, this continuous movement of the Rieske protein is essential for normal Q-cycle function.

Most inhibitors of the cytochrome b_6f complex have molecular shapes resembling plastoquinol, and target the Q_o site of the complex. One inhibitor frequently used to stop electron transport at the Q_o site is 2,5-dibromo-6-isopropyl-3-methyl-1,4-benzoquinone (DBMIB).

In conditions that generally lead to a reduced plastoquinone pool, such as anaerobic conditions (Diner & Mauzerall 1973), the plastoquinone reduction process occurring at the Q_i site will be impaired, due to the lack of available plastoquinones. In these conditions, it has been shown that both the cytochrome bc_1 complex of mitochondria (Wikström & Krab 1986) and the cytochrome b_6f

complex of chloroplasts (Joliot & Joliot, 1994) can use a semiquinone molecule from the Q_o site in order to keep generating plastoquinol at the Q_i site. This process is called the semiquinone cycle, and although the semiquinone cycle will yield a smaller proton gradient than the Q-cycle, it will keep the electron transport through the complex functional.

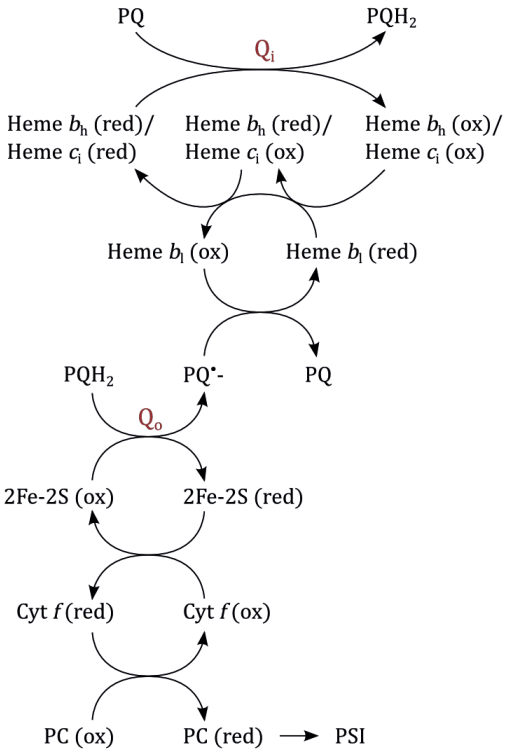

Figure 2: The mechanism of the Q-cycle, depending on two alternative electron transport pathways through the cytochrome b_6f complex. During the oxidation of one plastoquinol molecule at the Q_o site, one electron will be transferred to plastocyanin via cytochrome *f*, while the other will be transported to heme b_l and further to the heme pair consisting of heme b_h and heme c_i close to the Q_i site. At the Q_i site, the electron will be used to reduce a plastoquinone molecule in the first half-cycle of the Q-cycle, while the semiquinone created during the first half-cycle will be further reduced to a plastoquinol during the completion of the cycle.

1.3.1.5. Plastocyanin

From the cytochrome b_6f complex, electrons are loaded onto the mobile electron carrier plastocyanin, a copper-binding monomeric protein with the tertiary shape of a β-barrel (Moore et al. 1988), having a size of 10,5 kDa (Grossman et al. 1982). Plastocyanin receives electrons from the cytochrome *f* subunit of the cytochrome b_6f complex, and subsequently travels through the lumenal space to PSI, transporting one electron at a time.
Usually, plastocyanin transport between the cytochrome b_6f complex and PSI is not a rate limiting step in the photosynthetic electron transport chain, but it has been shown that certain external factors, for example osmotic stress, are able to reduce the space between the thylakoid membranes of a granum from about 50 Å to approximately 15 Å. Under these circumstances, plastocyanin, which has an approximate size of 40 x 32 x 28 Å, could become a major bottleneck for electron transport (Cruz et al. 2001).

1.3.1.6. Photosystem I

Photosystem I is the second light-driven protein complex in the photosynthetic electron transport chain. Its exact protein composition varies between different oxygenic organisms. In cyanobacteria, PSI usually contains 11 – 12 subunits, while in higher plants, the number of subunits is usually 14 – 15 (Nelson & Yocum, 2006; Karapetyan et al. 1999). The core complex also binds from ~ 90 to ~ 160 chlorophyll molecules (in higher plants, PSI contains 167 chlorophylls, and 192 light harvesting pigments altogether), 2 phylloquinones and 3 Fe_4S_4 clusters (Ben-Shem et al. 2003; Mazor et al. 2017).
The reaction center of PSI possesses a chlorophyll pair commonly referred to as P_{700}, which is located at the interface between the heterodimeric PsaA and PsaB. When P_{700} is excited, it donates an electron to the PSI primary electron acceptor A_0, which is a chlorophyll molecule. The electron hole in P_{700} is filled by a reduced plastocyanin. The reduced A_0 transfers its electron to the phylloquinone A_1, and A_1 transfers it further to the first of three Fe_4S_4 clusters of PSI, F_x

(Jagannathan & Golbeck, 2009; Nelson & Yocum, 2006). From the reaction center chlorophyll pair to F_x, there are two pseudo-symmetrical electron transport routes, one located within PsaA, and one located within PsaB. These two alternative routes both include the cofactors A_0 and A_1 (Nelson & Yocum, 2006). F_x is the first common electron acceptor, and the point where the two alternative electron paths meet. From F_x, the electron is transferred via the iron-sulphur clusters F_A and F_B, (Jagannathan & Golbeck, 2009; Nelson & Yocum, 2006) to a ferredoxin. The electron path through PSI is shown in Figure 3.

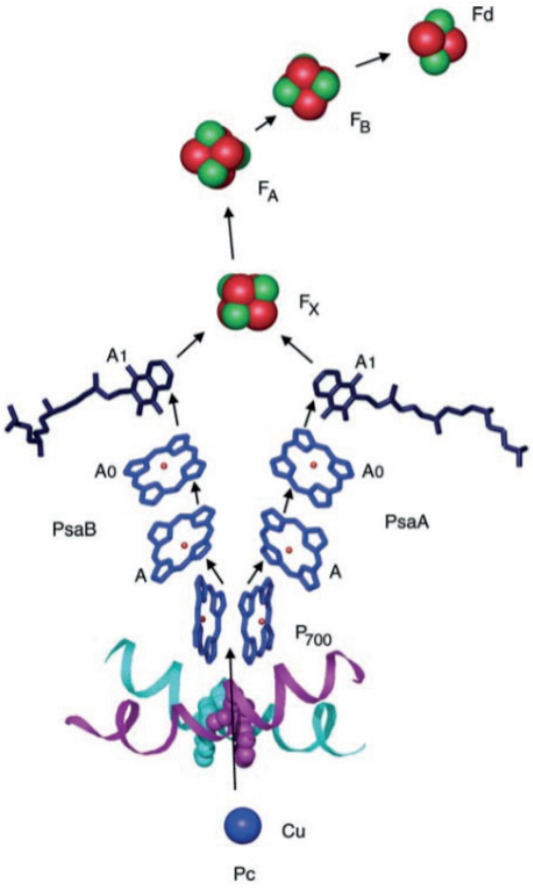

Figure 3: Electron transport path through PSI. When receiving excitation energy from the peripheral antennae, the reaction center P_{700} donates an electron to A_0, while P_{700}^+ is re-reduced by plastocyanin. From A_0, the electron is transported through the complex by A_1, F_x, F_A and F_B, before being used to reduced ferredoxin (figure taken from Nelson & Yocum, 2006)

F_A and F_B are located within the PsaC subunit on the stromal side of PSI. PsaC, along with the adjacent subunits PsaD and PsaE, form a docking site for the soluble electron acceptor ferredoxin (or in certain algae flavodoxin) (Sétif et al. 2002), which transfers electrons to the stromal enzyme Ferredoxin-$NADP^+$ reductase (FNR). FNR accepts two electrons from ferredoxins, and uses these to generate NADPH from $NADP^+$ (Kurisu et al. 2001).
In higher plants, PSI exist as monomeric complexes, while in cyanobacteria, PSI usually operate as trimers (Nelson & Yocum, 2006; Karapetyan et al. 1999). PSI also has external light-harvesting complexes (in higher plants, PSI has four associated light-harvesting complexes), which are closely energetically linked to the reaction center by approximately 20 strategically placed chlorophyll molecules (Ben-Shem et al. 2003; Qin et al. 2015). The PSI-associated light-harvesting complexes are distinctly different from those associated with PSII (for details on the light-harvesting complexes of *Nannochloropsis*, *Phaeodactylum* and *Chlamydomonas*, see sections 1.5.1 – 1.5.3). There is also evidence that in most photosynthetic organisms, the light-harvesting complexes associated with PSI are bound more strongly to the core complex than the light-harvesting complexes associated with PSII (Basso et al. 2014; Gardian et al. 2007; Caffarri et al. 2009).

1.3.1.7. ATP synthase

ATP, along with NADPH, is the product of the light reactions that fuel carbon fixation. What drives the regeneration of ATP from ADP is the difference in proton concentration between the thylakoid lumen and the stroma. This proton gradient is generated by the proton release from the PSII-mediated water oxidation, the transport of protons across the thylakoid membrane, with plastoquinone acting as a proton shuttle between PSII and the cytochrome b_6f complex, and from the activity of the Q-cycle.
ATP contains a large amount of chemical energy stored in the bonds linking its three phosphate groups together. The process of re-generating ATP from ADP is carried out by the protein complex ATP synthase in a three-step reaction.

Photosynthetic ATP synthases consist of two main protein domains, the catalytic F_1 domain, and the F_0 domain, which is responsible for powering the F_1 domain while it is performing the highly energy-demanding reaction of ATP generation. The catalytic F_1 domain consists of the 5 subunits α, β, γ, δ, and ε in a 3:3:1:1:1 ratio (Seelert et al. 2000). The α and β subunits form three catalytic seats where ADP can be bound, while the γ, δ and ε subunits form the basis for connection between the two domains of the enzyme complex.
The F_0 domain consists of a, b and c subunits in the ratio 1:2:10-14 (Arechaga et al. 2002), where the amount of c-subunits depends on the organism in question. Compared to the other, rather static protein complexes involved in photosynthesis, ATP synthase is different. It resembles a molecular machine, and contains a rotor and a stator (Seelert et al. 2000; Stock et al. 2000).
The rotor is made up by the ring-structured c-units of the F_0 domain and the γ and ε subunits of the F_1 domain (Nakamoto et al. 2008). The c-ring is coupled to an ion channel, and when protons escape back to the stroma through this ion channel, it gives the c-ring movement, which is transmitted to the ε and γ subunits. The γ subunit is partially incorporated in the catalytic domain made up by α and β units. When the γ subunit rotates with the c-ring, it introduces conformational changes in the catalytic subunits. These conformational changes drive the three-step ATP-generating reaction.

1.3.1.8. Cyclic electron transport around PSI

Cyclic electron transport is an alternative to the linear electron transport. The pathway for linear electron transport starts with water splitting at PSII, and ends with the reduction of $NADP^+$ downstream of PSI.
However, the ratio of ATP production to NADPH production during linear electron transport is fixed, and it therefore does not allow for dynamic ATP and NADPH requirements. In conditions where the cell might need a higher ATP:NADPH ratio than linear electron transport is able to produce, cyclic electron transport might occur. Cyclic electron transport 'recycles' electrons by sending them back to the plastoquinone pool instead of using them to reduce

$NADP^+$. This diminishes the NADPH production while increasing the proton gradient over the thylakoid membrane, which in turn increases ATP production. There is evidence of two distinct cyclic electron transport pathways in plants, the PGR5/PGRL1 pathway, and the NDH dependent pathway (Yamori & Shikanai, 2016).

The main pathway, the PGR5/PGRL1 pathway, features the proteins Proton Gradient Regulation 5 (PGR5) and PGR5-like Photosynthetic Phenotype 1 (PGRL1), and is proposed to be able to reduce the plastoquinone pool using NADPH as its electron donor (Johnson, 2011). In *Chlamydomonas*, a supercomplex consisting of the PSI supercomplex, light-harvesting complexes, the cytochrome b_6f complex, ferredoxin-NADP reductase and PGRL1, has been isolated, and this has been proposed to be responsible for cyclic electron transport via the PGR5/PGRL1 pathway (Iwai et al. 2010). This finding has, however, been disputed (Nawrocki et al. 2019). The same supercomplex has not been detected in higher plants. The exact mechanism of the PGR5/PGRL1 pathway is still being debated (Yamori & Shikanai, 2016).

The other pathway shown to be involved in cyclic electron transport in plants is the NDH pathway. This pathway is driven by the multisubunit complex NADH oxidase-like complex (NDH) (Johnson, 2011). This complex accepts electrons directly from ferredoxin, and subsequently reduces the plastoquinone pool.

In plants, drought, extreme temperatures and light of high intensity have been shown to trigger cyclic electron transport (Johnson, 2011). Conditions that trigger state transitions (see section 1.3.2.1), such as high-intensity light and anaerobic conditions, have also been shown to increase the ratio between cyclic and linear electron transport in several organisms (Finazzi et al. 1999; Johnson, 2011; Yamori & Shikanai, 2016).

1.3.1.9. Carbon fixation

The ultimate goal of the photosynthetic electron transport chain is to generate energy for the Calvin-Benson cycle, which is responsible for carbon fixation. Carbon fixation is costly for the cells, and the cycle is driven by ATP and NADPH created by the photosynthetic electron transport chain. The Calvin-Benson cycle was discovered around 1950 (Calvin & Benson, 1949; Benson et al. 1950), and is a branched cyclic pathway consisting of 13 reactions (Figure 4). The most important reaction within this cycle is the reaction responsible for capturing CO_2, which is catalysed by the enzyme Ribulose-1,5-bisphosphate carboxylase/oxygenase (RuBisCO) (Yeates & Wheatley, 2017).
As the name implies, this particular enzyme is able to bind not only CO_2, but also O_2. The reaction of binding O_2 instead of CO_2 to Ribulose-1,5-bisphosphate is the starting point of photorespiration, which competes with the Calvin-Benson cycle.

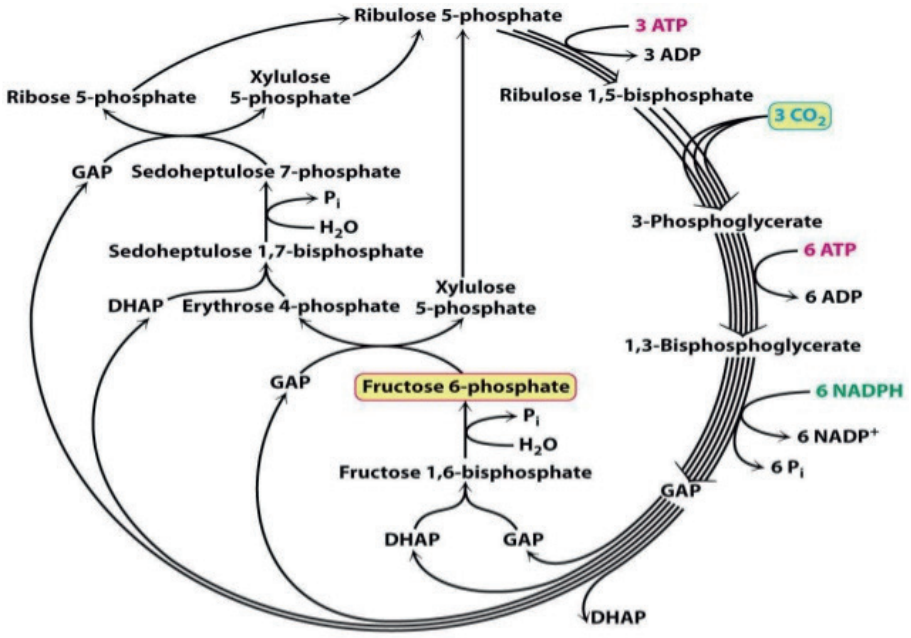

Figure 4: The reactions of the Calvin-Benson cycle (Figure taken from Tymoczko et al. 2011)

Since the Calvin-Benson cycle is essential for the growth of all oxygen-producing organisms, one would think that there would have been a strong evolutionary pressure to eliminate photorespiration. However, photorespiration is an important reaction pathway in its own right, being the main pathway for production of the amino acids glycine and serine in plants and algae (Betsche, 1983). Photorespiration may be a necessary compromise, since the atmosphere contains more oxygen than CO_2, making photorespiration hard to control, especially as O_2 and CO_2 are similar in size.
The most important feature of RuBisCO is undoubtedly its carboxylase activity, and its participation in the Calvin-Benson cycle. For every three CO_2 molecules fixed, the Calvin-Benson cycle produces one molecule of glyceraldehyde-3-phosphate / dihydroxyacetonephosphate, and uses 9 molecules of ATP and 6 of NADPH.
Glyceraldehyde-3-phosphate and dihydroxyacetonephosphate are three-carbon compounds that are the basis for all organic matter in plants and algae, including lipids (Guschina & Harwood, 2006).

1.3.1.10. Lipid biosynthesis in algae

Glyceraldehyde-3-phosphate and dihydroxyacetonephosphate are both intermediates of the glycolysis. They can thus be converted into pyruvate, which in turn can be converted into acetyl-coenzyme A (CoA). Acetyl-CoA can be converted into malonyl-CoA by the enzyme Acetyl-CoA carboxylase, and malonyl-CoA serves as the starting point for the *de novo* synthesis of fatty acids taking place in the chloroplasts of algae (Figure 5). In this process, the malonyl group is linked to an acyl-carrier protein (ACP), and malonyl-ACP is subsequently elongated by two carbon atoms (coming from acetyl-CoA) at a time, in a sequence of four reactions steps (Blatti et al. 2013). The original malonyl-ACP is elongated to C16:0, and subsequently transferred from the acyl-carrier protein and back to coenzyme A. Palmitoyl-CoA (C16:0) can be elongated further to stearoyl-CoA (C18:0), and the acyl-CoA molecules are then

transported to cytosol, and subsequently to the smooth endoplasmic reticulum. Here, both the enzymes involved in the synthesis of long-chain polyunsaturated fatty acids (LC-PUFAs) as well as the enzymes involved in the synthesis of triacylglycerols (TAGs) are located (Mühlroth et al. 2013). Elongated PUFAs can be transported back to the chloroplast, and used in the synthesis of the glycolipids monogalactosyldiacylglycerol (MGDG), digalactosyldiacylglycerol (DGDG) or the sulfolipid sulfoquinovosyldiacylglycerol (SQDG) (Guschina & Harwood, 2006).

In certain algae, such as *Nannochloropsis*, eicosapentaenoic acid (EPA, C20:5 $^{\Delta 5,8,11,14,17}$) is the endpoint of the LC-PUFA synthesis (Vieler et al. 2012), while others are able to produce docosahexaenoic acid (DHA, C22:6 $^{\Delta 4,7,10,13,16,19}$). An example of a group of microalgae that are able to produce relatively large amounts of DHA, are thraustochytrids (Chang et al. 2013).

Several factors are known to affect the lipid production of algae, and much research has also been carried out on this particular topic with regards to optimizing overall lipid yield, or the production of certain classes of lipids.

As lipids can serve as an energy reserve for an alga, several stress conditions, for example low availability of nutrients, are known to increase the production of storage triacylglycerols (Guihéneuf & Stengel, 2013). Osmotic stress, pH and temperature are also factors that are known to have an effect on the production and storage of triacylglycerols (Sharma et al. 2012). The production of LC-PUFAs, on the other hand, is known to increase in low temperatures (Schüller et al. 2017). LC-PUFAs have lower melting points than saturated fatty acids of the same lengths, and they are thus used by cells to increase the fluidity of membranes. When the temperature is decreased, algae therefore increase their LC-PUFA production, to retain their membrane fluidity.

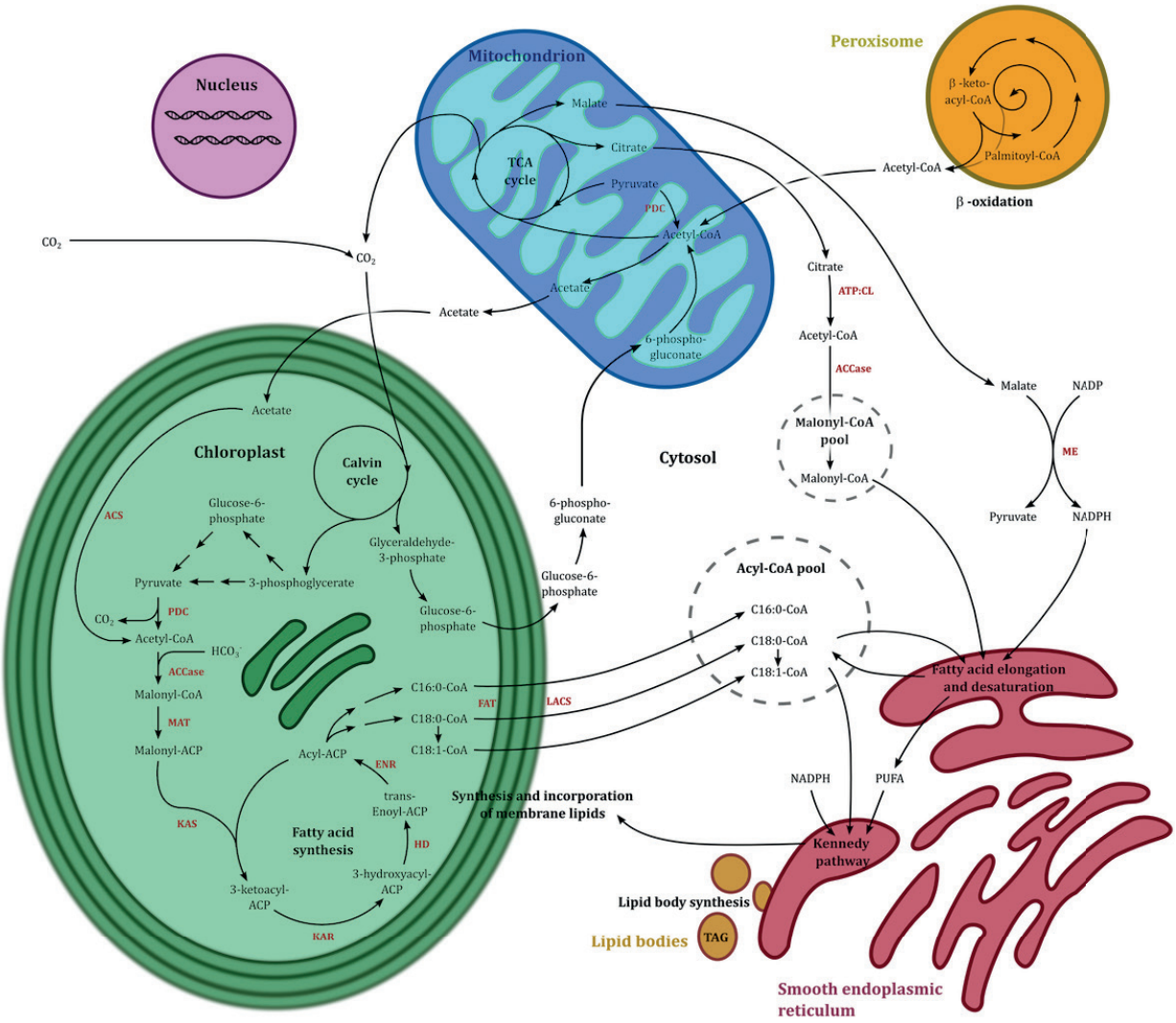

Figure 5: Organelle localization of different parts of lipid metabolism in algae (Figure taken from Mühlroth et al. 2013)

1.3.2. Photoprotection mechanisms

For marine microalgae, efficient photoprotection is essential.
In the ocean, microalgae are continuously subjected to rapidly changing light environments. Within minutes, an alga being transported by the current can travel from shadow to full sunlight (MacIntyre et al. 2000). Additionally, waves can act like lenses, and the light intensity an alga might experience can exceed even the full intensity of sunlight (Schubert et al. 2001). Because of these ever-changing light environments in the ocean, marine algae have developed mechanisms helping them stabilize the amount of photons that eventually reach the reaction centers of their photosystems.
Several modes of photoprotection are present in algae (Malnoë, 2018), with state transitions (Haldrup, 2001; Wollman, 2001), the xanthophyll cycle (Jahns & Holzwarth, 2012; Demming-Adams & Adams, 1996), xanthophyll-dependent photoprotection (Jahns & Holzwarth, 2012; Derks et al. 2015, Bína et al. 2017, 2), and the photoprotective effect of cyclic electron flow (Huang et al. 2015; Huang et al. 2016; Ananyev et al. 2017) being the most extensively explored (Figure 6).
PSII is more prone to light-induced damage than PSI. Both state transitions and the actions of the xanthophyll cycle and q_E are therefore initiated in conditions where PSII is susceptible to light-induced damage (Derks et al. 2015), while cyclic electron flow is able to protect both photosystems (Huang et al. 2016).
Which photoprotective mechanism is utilized during light stress varies between different algae. In *Chlamydomonas*, the main photoprotective mechanism is state transitions (Takahashi, 2006; Depège et al. 2003), while *Nannochloropsis* utilizes heat dissipation by xanthophyll cycle pigments (Lubián & Montero, 1998; Gentile & Blanch, 2001), and has so far been thought to not carry out state transitions. *Phaeodactylum*, on the other hand, carries out a parallel version of the xanthophyll cycle converting diadinoxanthin into diatoxanthin in conditions of increased light stress (Schumann, 2007). *Phaeodactylum*, as *Nannochloropsis*, has also been assumed not to carry out state transitions (Owens, 1986).

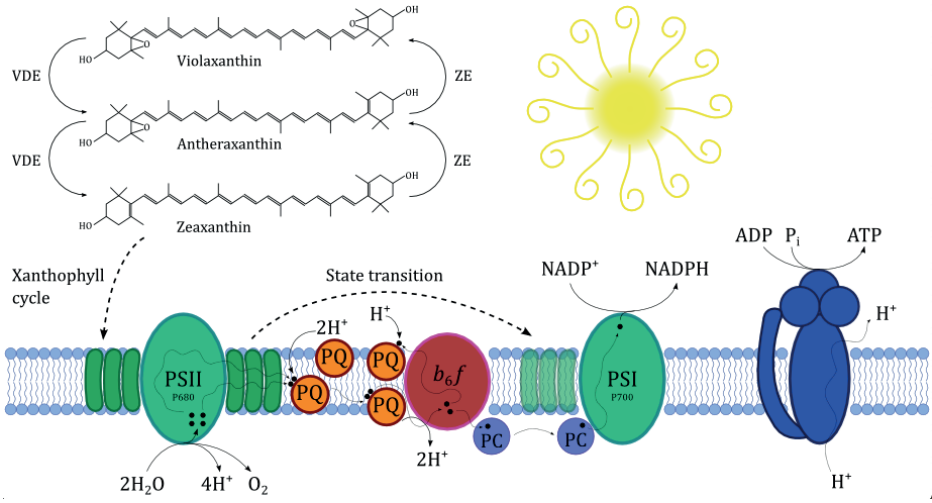

Figure 6: Regulation of electron transport by photoprotection mechanisms
In the photosynthetic electron transport chain, PSII is prone to damage by reactive oxygen species, which will occur if the complex receives more excitation energy than it needs for driving charge-separation. Therefore, most plants and algae have evolved mechanisms for regulating how much excitation energy is transferred to the PSII reaction center. One of these mechanisms is the xanthophyll cycle, where the light harvesting pigment violaxanthin is converted to the photoprotective pigment zeaxanthin. The other major photoprotective mechanism is state transitions, where light-harvesting complexes associated with PSII are disconnected from the complex, and in some cases instead coupled to PSI.

1.3.2.1. State transitions

State transitions have been extensively studied in plants and green algae (Takahashi et al. 2006; Shapiguzov et al. 2010; Ünlü et al. 2014; Nawrocki et al. 2016) and in cyanobacteria (Calzadilla et al. 2019).
While changes in phycobilisome association between PSI and PSII are the basis of state transition in cyanobacteria (Joshua & Mullineaux, 2004), in plants and green algae, state transitions involve a rearrangement of the light-harvesting

complexes associated with PSII and PSI. In what is traditionally viewed as state 1, the LHCII complexes are functionally linked to PSII. In conditions where electrons cannot be effectively disposed of by PSII due to a reduced plastoquinone pool, LHCIIs dissociate from PSII and are instead coupled to PSI (Haldrup et al. 2001; Snellenburg et al. 2017). This mechanisms gives the plants and algae using this mode of photoprotection an opportunity to fine-tune the excitation energy balance between their two photosystems (Nawrocki et al. 2016).

Recent studies indicate that during state 2, LHCII complexes could also form fluorescence quenching aggregates instead of being coupled to PSI (Miloslavina et al. 2009; Goss & Lepetit, 2015).

In *Chlamydomonas*, state transitions are one of the most important mechanisms the alga uses to protect itself against light stress (Kargul et al. 2005; Takahashi et al. 2006; Iwai et al. 2008; Ünlü et al. 2014).

In *Chlamydomonas reinhardtii*, the mechanism of state transitions has been the subject of many independent studies (Wollman, 2001; Snellenburg et al. 2017; Fujita et al. 2018). Studies focusing on the mechanism of initiation have shown that in *Chlamydomonas*, the structural dynamics of the cytochrome b_6f complex and the presence of reduced plastoquinone molecules are key participants.

The Rieske protein of the b_6f complex alternates between being proximal and distal to the thylakoid membrane, as described earlier (Brugna et al. 2000; Darrouzet et al. 2000). When the Rieske protein is in its proximal position, it is able to activate the kinase responsible for state transitions. When the Rieske protein oscillates back to its distal position, the kinase is released and can phosphorylate the LHCII complexes. The kinase phosphorylates LHCII at amino acid residues located towards the stromal side of the thylakoid membrane (Wollman, 2001).

The identity of the kinase responsible for initiating state transitions remained unknown until 2003, when it was identified as the Stt7 protein (Depège et al. 2003). In *Arabidopsis thaliana*, the STN7 kinase, which is a homologue to the Stt7 protein, has been identified (Shapiguzov et al. 2010), while the phosphatase reversing the process has been identified as the Tap38/Pph1 protein (Shapiguzov et al. 2010).

Once phosphorylated, LHCIIs dissociate from PSII, and thus make PSII less susceptible to light-induced damage. The physical movement of phosphorylated light-harvesting complexes is proposed to occur because of electrostatic repulsion that arises between the light-harvesting complexes, which are negatively charged because of the phosphorylation, and PSII, which is also negatively charged (Wollman, 2001). In *Chlamydomonas*, there is also a physical separation between the majority of PSII and PSI complexes. The grana stacks are enriched in PSII, while most PSI complexes reside in the stroma lamellae (Finazzi et al. 2002). Grana stacks are more negatively charged than the stroma lamellae, which might also be one of the reasons for the physical movement of the phosphorylated light-harvesting complexes away from the grana stacks.
In *Chlamydomonas*, the cytochrome b_6f complexes can be found both in the grana stacks and in the stroma lamellae. In state 1, most cytochrome b_6f complexes reside in the grana stacks, while in state 2, a fraction of the cytochrome b_6f complexes will also travel to the stroma lamellae (Wollman, 2001). In state 2, the stroma lamellae will thus contain the majority of LHCII, cytochrome b_6f complexes, and PSI. These are the main components of the complex proposed to be responsible for cyclic electron transport via the PGR5/PGRL1 pathway in *Chlamydomonas* (Iwai et al. 2010), and as a result, the rate of cyclic electron transport to linear electron transport increases during a state transition (Finazzi et al. 2002).
In *Nannochloropsis*, state transitions have so far not been reported, and in *Phaeodactylum*, state transitions have been declared to be absent (Owens, 1986). A state transition in a heterokont alga would moreover have a different underlying structural mechanism than the state transitions carried out by plants and green algae, as the architecture of their thylakoid membranes are quite distinct. The secondary plastids of heterokont algae have been shown to form lamellae consisting of three thylakoids (Bedoshvili et al. 2009), instead of the usual grana stacks and stroma lamellae observed in green algae and plants. In heterokont algae, PSII and PSI have also not been thought to occupy different areas of the thylakoid (Bína et al. 2017, 1), even though large membrane areas enriched in PSI have recently been demonstrated in red light-treated cells of *Phaeodactylum tricornutum* (Bína et al. 2016). A state transition in a heterokont

algae, would thus likely involve a re-coupling of light-harvesting complexes between the two photosystems, rather than a physical movement of light-harvesting complexes from one area of the thylakoid to another.

1.3.2.2. The xanthophyll cycle

The xanthophyll cycle is a photoprotective process occurring internally in the light harvesting antennae usually associated with PSII.
A single light-harvesting complex usually contains 3 – 4 carotenoids (Croce et al. 1999). In certain algae, such as *Nannochloropsis*, violaxanthin is one of the pigments frequently found in both the light-harvesting complexes as well as in the minor monomeric antenna proteins (Goss & Lepetit, 2015). Violaxanthin is a light-harvesting pigment, but it can be converted to the photoprotective pigment zeaxanthin via the intermediate antheraxanthin in a two-step de-epoxidation process termed the xanthophyll cycle.
The enzyme responsible for this two-step de-epoxidation is Violaxanthin de-epoxidase, which is located in the thylakoid lumen. Its pH optimum is around 5.2 in most algae performing the xanthophyll cycle, and it requires ascorbate as a cofactor (Goss & Jakob, 2010). In high-intensity light conditions, the rate of water splitting and plastoquinone transport will increase, resulting in a decreased pH in the thylakoid. When the lumenal pH drops below ~ 6.2 (Pfündel & Dilley, 1993; Hager & Holocher, 1994), Violaxanthin de-epoxidase will be activated and start converting violaxanthin into zeaxanthin. It has also been proposed that the PsbS protein, which is protonated at low pH values, and is known to act like a pH sensor (Jahns & Holzwarth, 2012), plays an important role in the onset of the xanthophyll cycle.
Current models suggest that excitation energy captured by chlorophylls can be transferred to zeaxanthin and subsequently dissipated as heat, via both excitation energy transfer and charge transfer (Park et al. 2019). The proposed mechanism of heat dissipation is described in Figure 7.

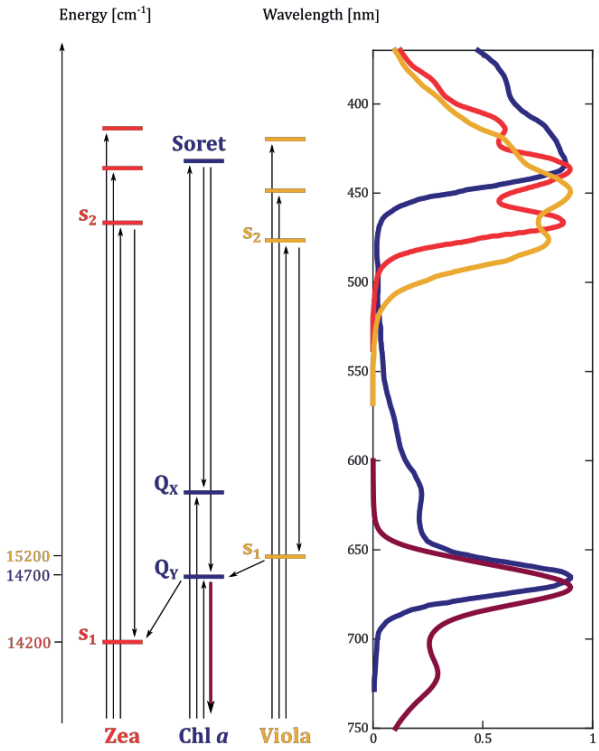

Figure 7: Energy level diagram and absorption spectrum for violaxanthin, chlorophyll *a* and zeaxanthin.

The s_1 band of violaxanthin is located above the Q_Y band for chlorophyll *a*, while the S_1 band for zeaxanthin lies below the Q_Y band of chlorophyll *a*. Violaxanthin can therefore transfer energy to chlorophyll *a*, and chlorophyll *a* can transfer excitation energy to zeaxanthin via excitation energy transfer. Energy can also be dissipated as heat via charge transfer between chlorophyll *a* and zeaxanthin (Park et al. 2019). The latter pathway for heat-dissipation is not shown in this figure.

Values of the S_1 energy levels for violaxanthin and zeaxanthin, and the value of the Q_Y level of chlorophyll *a* were extracted from Frank et al. 1994. The absorption data for violaxanthin was extracted from Takaichi & Shimada, 1992, absorption data for zeaxanthin was extracted from Kuwabara et al. 1999, absorption data for chlorophyll *a* was extracted from Chen & Blankenship, 2011, and the fluorescence data for chlorophyll a was taken from Prahl, 2017.

Violaxanthin de-epoxidase exists as a monomer located in the thylakoid lumen (Jahns et al. 2009), but once activated, the enzyme forms active dimers, and binds to the thylakoid membrane. In its dimeric, activated state, a catalytic site forms, which is able to bind one molecule of violaxanthin and two molecules of the cofactor ascorbate (Goss & Lepetit, 2015). The conversion of violaxanthin into zeaxanthin does not only depend on the presence of activated Violaxanthin de-epoxidase enzymes, but also on the presence of the galactolipid monogalactosyldiacylclycerol (MGDG), which solubilizes the violaxanthin molecules, and makes them available for the enzyme (Schaller et al. 2010).
The conversion of violaxanthin into the photoprotective pigment zeaxanthin occurs on a time scale of 10 – 30 minutes (Jahns et al. 2009), and when zeaxanthin has been formed, this is incorporated into the light harvesting antennae. Experiments performed on spinach have confirmed that especially the minor PSII antennae proteins CP29 and CP26 are enriched in xanthophyll cycle pigments (Goss et al. 1997).
When the cell is no longer in need of photoprotection, zeaxanthin will be converted back to light-harvesting violaxanthin by adding the same two epoxy-groups that Violaxanthin de-epoxidase removed in its step-wise conversion of violaxanthin into antheraxanthin, and from antheraxanthin into zeaxanthin. The reverse reactions, from zeaxanthin to antheraxanthin, and from antheraxanthin back to violaxanthin, are driven by the enzyme Zeaxanthin epoxidase, (Jahns et al. 2009). Zeaxanthin epoxidase is located at the stromal side of the thylakoid membrane, possibly weakly bound to the membrane (Goss & Lepetit, 2015). The enzyme has a broad pH optimum around pH 7.5 in most organisms carrying out the xanthophyll cycle (Jahns et al. 2009), and is strongly inhibited at pH values below 6 (Gilmore et al. 1994). The enzyme requires NADPH and molecular oxygen as cofactors, which means that the back-reaction from zeaxanthin to violaxanthin will be impaired in anaerobic conditions. Several studies have also shown that Zeaxanthin epoxidase in general is sensitive to stress. Both light stress and cold stress might severely limit the activity of the enzyme (Öquist & Huner, 2003; Reinhold et al. 2008). Generally, the conversion of zeaxanthin back to violaxanthin carried out by Zeaxanthin epoxidase takes 5 to 10 times longer

than the de-epoxidation reactions carried out by Violaxanthin de-epoxidase (Jahns et al. 2009), which means that the photoprotection provided by the presence of zeaxanthin can be relatively long-lasting.

The normal xanthophyll cycle and its driving enzymes, Violaxanthin de-epoxidase and Zeaxanthin epoxidase, can be found in higher plants, ferns, mosses and the species belonging to the Chlorophyta division (Jahns et al. 2009). Diatoms, belonging to the class of Bacillariophyceae, have a similar, yet distinct xanthophyll cycle. Diatoms contain the light harvesting pigment diadinoxanthin, which is converted directly to the photoprotective pigment diatoxanthin during light stress. This conversion is driven by the enzyme Diadinoxanthin de-epoxidase, which, as Violaxanthin de-epoxidase, is activated by acidification of the thylakoid lumen caused by extensive water splitting and electron transport. Diadinoxanthin de-epoxidase is, however, activated at a higher pH than Violaxanthin de-epoxidase. The enzyme has a pH optimum of 5.5 (in contrast to Violaxanthin de-epoxidase's optimum of 5.2), and it is activated when the pH drops below 6.5 (in constrast to Violaxanthin de-epoxidase, which is activated when the pH falls below 6.2). Some Diadinoxanthin de-epoxidase activity can be demonstrated even at neutral pH values of around 7 (Goss & Jakob, 2010). The de-epoxidation of diadinoxanthin also requires ascorbate as a cofactor, and depends on the presence of the galactolipid MGDG.

The conversion of diatoxanthin back to diadinoxanthin is driven by the enzyme Diatoxanthin epoxidase. This enzyme shares several similarities with Zeaxanthin epoxidase. It is a stromal enzyme, and it requires NADPH and oxygen as cofactors. However, one difference between the two epoxidation enzymes is that Diatoxanthin epoxidase is almost completely inhibited in high-intensity light, while Zeaxanthin epoxidase is not (Mewes & Richter, 2002). The rate of epoxidation is also faster for Diatoxanthin epoxidase than for Zeaxanthin epoxidase (Goss & Jakob, 2010).

1.3.2.3. PsbS- / Lhcx-dependent photoprotection

Zeaxanthin might be able to dissipate excitation energy as heat, but the exact mechanism of zeaxanthin-dependent photoprotection is complex, and involves several key players in addition to zeaxanthin.

Just as the conversion of violaxanthin to zeaxanthin by violaxanthin de-epoxidase, or the conversion of diadinoxanthin to diatoxanthin by diadinoxanthin de-epoxidase, the formation of the quenching sites proposed to be involved in zeaxanthin-dependent photoprotection also depends heavily of the build-up of a proton gradient (Goss & Lepetit, 2015).

Even though the exact mechanism of zeaxanthin-dependent photoprotection is yet unknown, the mechanism of initiation has been increasingly studied in the later years. It has been revealed that zeaxanthin-dependent photoprotection likely involve two distinct sites in the thylakoid membrane where excitation energy is dissipated as heat. The formation of these is proposed to be mediated by the PSII subunit PsbS, which is present in higher plants and green algae (Jahns & Holzwarth, 2012). The PsbS protein is proposed to be pigment free, and instead functions as a pH sensor (Dominici et al. 2002). In conditions when the lumenal pH decreases, PsbS is protonated at two glutamate residues situated towards the lumen (Li et al. 2004). This protonation triggers conformational changes of the thylakoid membrane (Kiss et al. 2008; Betterle et al. 2009), and also leads to the formation of two quenching sites, termed Q1 and Q2, which carries out separate modes of photoprotection occurring at different time scales (Jahns & Holzwarth, 2012; Derks et al. 2015). Q1 is proposed to consist of light-harvesting complexes having detached from PSII to form aggregates, while Q2 can be found in minor light-harvesting complexes being functionally linked to PSII. Both these quenching sites are proposed to depend completely or partially on the presence of zeaxanthin, and on the ability of this particular xanthophyll to dissipate excess excitation energy as heat (Jahns & Holzwarth, 2012).

The presence of the two distinct sites, Q1 and Q2, related to photoprotection in the PSII-associated light-harvesting complex have also been detected in diatoms (Miloslavina et al. 2009). As in the case of higher plants, Q1 is formed by

aggregates of light-harvesting complexes detaching from PSII during conditions increasing the pH gradient over the thylakoid membrane, while Q2 is formed in light-harvesting complexes still attached to PSII (Miloslavina et al. 2009).
A similar pH sensor protein as PsbS in plants has so far not been detected in diatoms, but photoprotection has been shown to depend heavily on the Lhcx protein, in addition to the heat-dissipative xanthophyll diatoxanthin (Goss & Lepetit, 2015).
In *Nannochloropsis*, the same photoprotective sites as in higher plants and diatoms have not been identified. Yet, two kinetically different modes of zeaxanthin-dependent photoprotection have been demonstrated. A fast mode of photoprotection seems to depend both on the concentration of zeaxanthin present, and on the pH gradient, while a slower mode of photoprotection seems to be directly dependent on the amount of zeaxanthin (Bína et al. 2017, 2).
Nannochloropsis, just like *Phaeodactylum*, contains light-harvesting complexes of the type Lhcx, and it is assumed that Lhcx proteins are important for the fast mode of heat-dissipative photoprotection in *Nannochloropsis* (Bína et al. 2017, 2).
Green algae do not have PsbS, but a related protein called LhcsR (Bonente et al. 2011). This protein is proposed to act like a pH sensor in a similar fashion as PsbS in higher plants, and to initiate a change in the light-harvesting complexes from a light-harvesting state to an energy-dissipating state during conditions triggering a low lumenal pH (Liguori et al. 2013).

1.3.2.4. The role of cyclic electron flow in photoprotection

In several plants and some algae, the shift from linear to cyclic electron flow has been shown to play a major role in photoprotection (Huang et al. 2015). The other major mechanisms involved in photoprotection; the xanthophyll cycle, q_E and state transitions, are all aimed at preferentially protecting PSII from light stress. Cyclic electron flow stands out by also playing a role in photoprotection of PSI.

Especially in conditions where photosynthetic carbon fixation is limited, such as drought stress in plants, PSI is prone to photodamage because the lack of $NADP^+$ in these conditions will lead to over-reduction of the iron-sulphur clusters downstream of P_{700} (Huang et al. 2012). The onset of cyclic electron transport will lead to a shift in the ratio of NADPH to $NADP^+$. More $NADP^+$ will be available because NADPH can now donate electrons to the plastoquinone pool, and this will in turn relieve the redox stress on the iron-sulphur clusters within PSI.

Cyclic electron flow does not only protect PSI, but also PSII. When cyclic electron transport is active, protons are being transported across the thylakoid membrane through the activity of the Q-cycle, and this increased proton gradient can activate the xanthophyll cycle and protonate PsbS, thus protecting PSII from photodamage.

It has also been shown that the stability of the oxygen-evolving complex of PSII depends on the presence of Ca^{2+}, and that the increased proton concentration in the thylakoid lumen due to the activity of cyclic electron flow increases the activity of H^+/Ca^{2+} antiporters pumping Ca^{2+} into the lumenal space (Huang et al. 2016).

It has recently been shown that desert microalgae, which are especially prone to draught stress, can maintain high growth rates in extreme light intensities with minimal effect of light-harvesting complex-based photoprotection, by employing cyclic electron transport (Ananyev et al. 2017).

1.3.3. Chlorophyll fluorescence

According to Govindjee (1995), "chlorophyll fluorescence is red and beautiful". According to others, it is merely a waste product of light harvesting. Still, what most researchers working with a photosynthetic organism could agree upon is that the assessment of chlorophyll fluorescence can be an extremely useful tool when trying to gain insight into the photosynthetic machinery of an organism. However, interpreting chlorophyll fluorescence data is a complex task, as chlorophyll fluorescence is modulated by many physiological processes and physical parameters (Govindjee, 1995).

When one of the light-harvesting complexes of a plant or an alga absorbs a photon, the energy of the photon is used to promote an electron into a higher excited state. When excited electrons return to their ground states, the energy can be emitted as fluorescence, or in other words, as a photon of a longer wavelength than the original photon exciting the electron. In a photosynthetic context, fluorescence is a waste of captured energy that could have been used to drive charge separation. In photosynthetic systems, with energetically coupled pigments, less than 1% of the captured energy is lost as fluorescence (Govindjee, 1995).

Excitation energy has four fates: 1) It can be used to drive photochemistry, 2) it can be disposed of as heat (see section 1.3.2.2 on the xanthophyll cycle), 3) it can contribute to the formation of a triplet-state chlorophyll, or 4) it can be sent off as light with a shifted wavelength – fluorescence.

1.3.3.1. The Kautsky curve

The chlorophyll fluorescence transient that can be observed when a leaf or a solution of algae is subjected to continuous light after having been acclimated to darkness was first observed by Hans Kautsky in 1931, and it has therefore since been called a Kautsky curve (Figure 8).

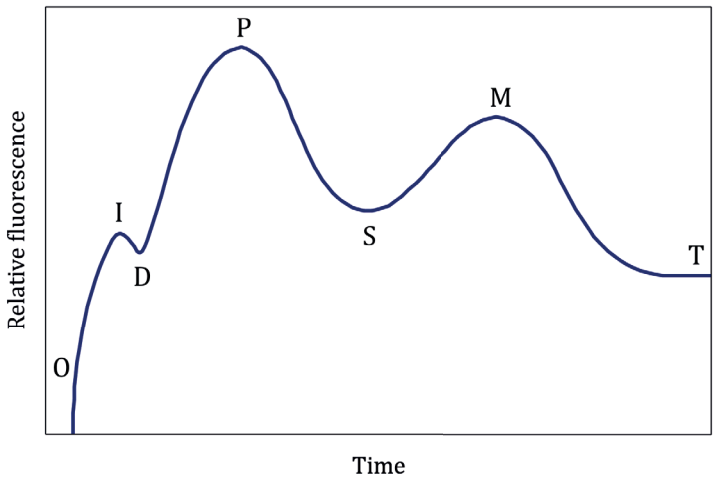

Figure 8: A standard Kautsky curve, digitized from Govindjee & Papageorgiou (1971)

In the Kautsky curve in Figure 8, different parts of the curve have been labelled, and these local maxima or minima can be related to events occurring in the photosynthetic electron transport chain after the onset of illumination. The time points of the local minima or maxima also give valuable insight into the kinetics of electron transfer through PSII, as approximately 90 % of the fluorescence yield at room temperature originates from PSII (Govindjee, 1995).
The inflection points of the Kautsky curve are thought to represent different phases of electron transport and fluorescence quenching.
The main chlorophyll fluorescence modulator of the photosynthetic electron transport chain is Q_A (Govindjee, 1995). When a PSII is exposed to light, a charge separation occurs, and an electron will be transferred from the reaction center chlorophyll pair to the primary electron acceptor Q_A within 250 – 300 ps

(Krause, 1991). When Q_A is reduced, the reaction center is said to be closed, as a new electron cannot be transferred to Q_A until the first electron is transported further in the electron transport chain. An electron is transferred to an oxidized quinone or a semiquinone bound to the Q_B site with a half time of approximately 300 μs, or 1.3 – 2 ms if a plastoquinone is not already present at the Q_B site (De Wijn & Van Gorkom, 2001). While the reaction center is closed, the energy trapped by the light-harvesting complexes cannot be used for charge separation. Therefore, energy captured by the pigments is instead disposed of as fluorescence. When a leaf or an alga is suddenly exposed to light, the reduction of Q_A is relatively synchronized across all PSIIs present in the sample. As the reaction centers are gradually closing, the fluorescence is gradually rising, until the point where all reaction centers are closed (inflection point I in the Kautsky curve shown in Figure 8). Eventually, the electrons sitting on Q_A will be transferred further to Q_B, and, and the fluorescence will briefly decrease (inflection point D in Figure 8). This brief decrease in fluorescence will be enhanced by the quenching effect of oxidized electron donors, in particular P_{680}^+, (Laisk & Oja, 2018). From the local minimum D to the overall fluorescence maximum P, two processes are prevailing. Firstly, a second (or third) round of electrons are transferred to Q_A, causing the fluorescence to rise, and secondly; the initial electrons will start to reach the plastoquinone pool. Even though Q_A is considered the main quencher of chlorophyll fluorescence, other components of the photosynthetic electron transport chain can also modulate fluorescence, and one important component known be directly responsible for the fluorescence yield is the redox state of the plastoquinone pool. It has been proposed that oxidized plastoquinones are able to quench fluorescence directly (Vernotte et al. 1979; Haldimann & Tsimilli-Michael, 2005). As more and more plastoquinone molecules are reduced, this quenching effect is lost, and the fluorescence will therefore gradually increase until the plastoquinone pool is completely reduced, at point P in the Kautsky curve. This will occur approximately 1 s after the onset of illumination (Maxwell & Johnson, 2000). Alternatively, it has been proposed that oxidized plastoquinones do not quench fluorescence themselves, but rather that the presence of a plastoquinone or semiquinone bound at the Q_B site is able to modulate fluorescence (Prášil et al. 2018).

The OIDP transient is also commonly called the fast transient, while the PSMT transient that follows, occurring on the time scale of minutes, is referred to as the slow transient (Govindjee, 1995).
The PSMT transient has proved more difficult to elucidate (Govindjee, 1995), but it is generally assumed that the reduction in fluorescence yield occurring between inflection point P and S on the Kautsky curve is due to the light-induced activation of enzymes involved in carbon fixation, and the onset of photoprotection mechanisms (Maxwell & Johnson, 2000), while the fluorescence increase between S and M (at least in *Chlamydomonas reinhardtii*) has been shown to be due to a reverse state transition (State 2 → State 1) (Kodru et al. 2015).

1.3.3.2. Mechanisms involved in photochemical and non-photochemical fluorescence quenching

The most important use of excitation energy is to drive charge separation. The amount of excitation energy that is not used for charge separation has been termed non-photochemical quenching (NPQ), and can be further divided into fluorescence quenching categories.
The most important fluorescence quenching mechanisms involved in non-photochemical quenching in photosynthetic organisms have traditionally been labelled as high-energy state quenching (q_E), state transitions (q_T) and photoinhibitory quenching (q_I) (Lavaud & Lepetit, 2013). These quenching components are active to different extents in different organisms.
The high energy state quenching, q_E, is a fast type of quenching, usually observed between several seconds and up to 5 minutes after the onset of illumination (Goss & Lepetit, 2015; Erickson et al. 2015). In plants, the relaxation of q_E occurs on the same time scale: several seconds to several minutes (Erickson et al. 2015). In diatoms, however, the relaxation has been shown to be much slower than in plants (Goss et al. 2006).
The formation of q_E has been shown to depend heavily on the presence of a pH gradient (Goss & Lepetit, 2015), although the exact fluorescence quenching

mechanism is still under investigation. In plants, however, it has been shown that the PsbS protein plays a major role in q_E, as studies have shown that q_E quenching is drastically reduced when PsbS is missing (Li et al. 2002). Zeaxanthin has also been shown to be important for q_E, possibly through interacting with PsbS (Sylak-Glassman et al. 2014).

Zeaxanthin is also involved in a different type of quenching, q_Z (Nilkens et al. 2010), which can be separated from q_E mainly due to the differences in kinetics. q_Z is slower than q_E, occurring on a time scale of 10 – 15 minutes (Nilkens et al. 2010). Since q_Z depends on zeaxanthin, which again depends on the activation of Violaxanthin de-epoxidase, q_Z, just as q_E, is heavily dependent on the presence of a proton gradient.

The most recent models propose that q_E and q_Z in diatoms originate at two different quenching sites both related to the PSII light-harvesting complexes. The fast q_E component has been localized to detached, aggregated PSII light-harvesting complexes (Miloslavina et al. 2009). The zeaxanthin-dependent quenching q_Z, on the other hand, has been localized to the minor PSII light-harvesting complexes CP29, CP26 and CP24, which stay attached to PSII even in conditions where PsbS is active (Nilkens et al. 2010).

The quenching components q_E and q_Z thus have certain similarities, as both are activated by an increased pH gradient across the thylakoid membrane, although through different mechanisms and on different time frames.

Another quenching mechanism, q_T, is assigned to state transitions (discussed in section 1.3.2.1). When PSII-associated light-harvesting complexes dissociate from PSII to migrate to PSI, less fluorescence is emitted by the former PSII-associated light-harvesting antennae, since PSI is more efficient in charge separation than PSII.

The last component traditionally included in the concept of non-photochemical quenching is a slow quenching component, photoinhibitory quenching, or q_I. This mode of quenching occurs over a time frame of several hours, and is thought to reflect light induced damage of D1. As q_I is the slowest fluorescence-quenching component known to date, it has not gained as much attention as the other quenching processes working on shorter time scales. However, recent studies on q_I have produced evidence that what has been thought of as q_I-type

quenching, may involve more than one process (Lambrev et al. 2010; Malnoë, 2018).
Even though not defined as individual modes of quenching like q_E, q_Z, q_T and q_I, other cellular processes could also affect the fluorescence yield on different time scales.

1.3.3.3. Manipulation of the redox state of the plastoquinone pool by oxygen depletion

The redox state of the plastoquinone pool is easily modulated by the availability of oxygen. Both the light-driven oxygen production of PSII, and oxygen consumption by cellular respiration in the dark, thus has an effect on the redox state of the plastoquinone pool, and therefore also on the fluorescence yield.
In darkness, algal cells enclosed in an airtight vessel consume oxygen by mitochondrial respiration. When there is no more oxygen to consume, electrons will accumulate within the mitochondrial electron transport chain (Catalanotti et al. 2013). The mitochondria solve this problem by turning phosphoenolpyruvate into malate in order to generate ATP, and by turning oxaloacetate into malate in order to generate NAD^+, to keep glycolysis going (Kennedy et al. 1992). Malate will thus accumulate in the mitochondria, and it will eventually be transferred to other parts of the cell, such as the chloroplast, via the malate / oxaloacetate shuttle. In the chloroplast, the reducing power of malate can be transferred to the plastoquinone pool by the NADPH dehydrogenase (Ndh) (Mus et al. 2005; Faraloni et al. 2013).
Oxidized plastoquinone is a fluorescence quencher (Vernotte et al. 1979; Haldimann & Tsimilli-Michael, 2005). Therefore, anaerobic conditions will have an effect on chlorophyll fluorescence. In addition, reduction of the plastoquinone pool will also induce a state transition in *Chlamydomonas reinhardtii* (Hohmann-Marriott et al. 2010). The reduction of the plastoquinone pool caused by oxygen depletion therefore has a dual effect on fluorescence. Firstly, the loss of fluorescence quenching, and secondly, the induction of non-photochemical quenching.

1.3.3.4. Manipulation of electron transport chain by inhibitors

Specific inhibitors for different steps of the photosynthetic electron transport chain can be used to manipulate the photosynthetic electron transport chain and hence also have an effect on the observed fluorescence yield.

DCMU

A common inhibitor of the Q_B binding pocket of PSII is 3-(3,4-dichlorophenyl)-1,1-dimethylurea (DCMU) (Metz et al. 1986). Application of DCMU in aerobic conditions and in the presence of light hence results in an oxidized plastoquinone pool. Although cyclic electron transport could still occur and partially reduce the plastoquinone pool, it will not be further reduced with electrons from PSII.

DBMIB

An inhibitor of the Q_0 site of the b_6f complex is 2,5-dibromo-6-isopropyl-3-methyl-1,4-benzoquinone (DBMIB) (Roberts et al. 2004). Application of DBMIB in combination with light results in a completely reduced plastoquinone pool. DBMIB will thus induce the maximum fluorescence yield, as Q_A will be unable to deliver its electron to the plastoquinone pool, and the quenching effect of oxidized plastoquinones is lost.

CCCP

Another chemical that target the regulation of electron transport is carbonylcyanide *m*-chlorophenylhydrazone (CCCP) (Nishio & Whitmarsh, 1993), which acts as an uncoupler by collapsing the proton gradient over the thylakoid membrane. The addition of CCCP will thus not affect electron transport directly, but rather ATP production, which depends on a sustained proton gradient. Application of CCCP also modulates the fluorescence yield by preventing the accumulation of protons in the thylakoid lumen, and thus eliminating q_E and q_Z, which are both dependent on the presence of a proton gradient.

1.3.4. Techniques used for studying chlorophyll fluorescence

1.3.4.1. PAM fluorometry

Pulse Amplitude Modulated (PAM) fluorometry was developed in the 1960s (Schreiber, 1986; Schreiber et al. 1986), and has proved to be an invaluable technique for investigating photosynthetic processes.
When interpreted correctly, fluorescence data collected by PAM fluorometry can provide a large amount of information, especially about processes involved in non-photochemical quenching.
The principle of PAM is based on the fact that excitation captured by a chlorophyll molecule in a plant or an alga can have four possible fates. The excitation can be used to drive photochemistry, it can be quenched by processes involved in photoprotection, it can be used to create a triplet-state chlorophyll, or it can be sent off as fluorescence (Müller et al. 2001). As the rate of fluorescence and triplet-state chlorophyll formation can be assumed to be constant, changes in chlorophyll fluorescence yield are due to non-photochemical quenching or photochemistry (Maxwell & Johnson, 2000). PAM fluorometry in combination with saturating light pulses can distinguish between photochemical and non-photochemical quenching.
A PAM fluorometer continuously probes fluorescence yield by a measuring-light that is too weak to induce photochemistry, and instead probes the ground fluorescence of the system (Schreiber et al. 1986; Maxwell & Johnson, 2000).
In addition, light pulses of high intensity, usually having a duration of 0.8 seconds, are introduced at certain time points. The light intensity of these pulses is high enough to saturate photosynthesis, and for a brief moment during such a light pulse, all reaction centers will be closed (Müller et al. 2001).
When maximum fluorescence is reached during a saturating light pulse, photochemical quenching is briefly turned off, due to the complete reduction of the electron transport chain. Any decrease in this maximal fluorescence level over time is caused by the onset of mechanisms involved in non-photochemical quenching.

At the start of a PAM measurement, when the sample is dark-adapted, processes involved in non-photochemical quenching should not yet be active, so a light pulse given in these conditions provides the absolute maximum possible fluorescence (at least in theory, see paper II).

Actinic light will induce the initiation of non-photochemical quenching, which will cause a lower fluorescence yield during light pulses. Comparing the maximum fluorescence yield over time with the maximum fluorescence obtained in a dark-adapted sample will thus show the development of NPQ. In addition, the maximum and minimum fluorescence yields obtained both at the beginning of and during the measurement, form the basis of a vast amount of calculations of photosynthetic parameters (Maxwell & Johnson, 2000; Nikolaou et al. 2015; Ruban, 2017).

When the actinic light is turned off, the kinetics of the fluorescence recovery can be indicative of different non-photochemical quenching processes. If photoinhibition has taken place, the recovery to the initial maximum fluorescence yield of the dark-adapted samples is slower than the recovery of for example q_E (Figure 9).

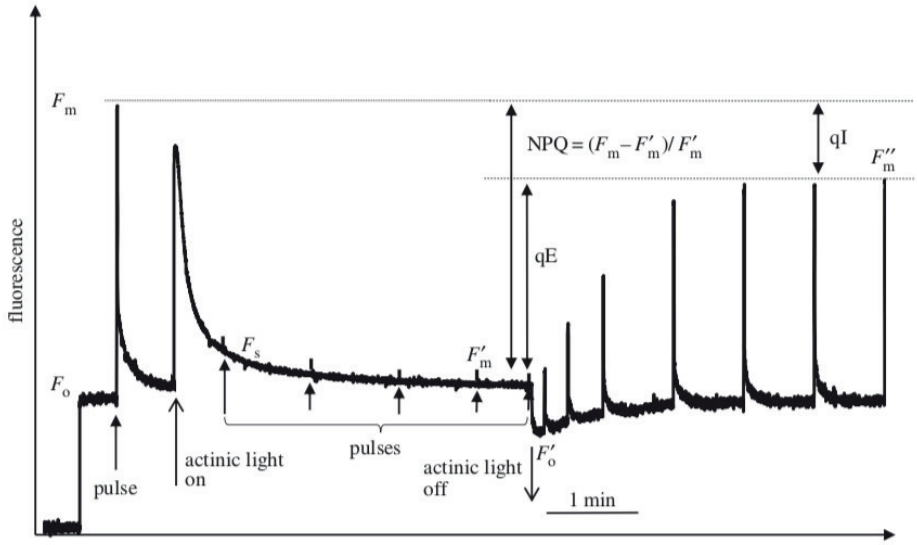

Figure 9: Example of changes in the fluorescence yield during a PAM fluorometry experiment. The overall maximum fluorescence yield (F_m) is obtained from the first bright light pulse applied to a dark-adapted sample. When actinic background light is applied to the sample, the maximum fluorescence obtained during bright light pulses decreases, due to the onset of processes involved in non-photochemical quenching. When actinic background light is switched off, q_E will disappear on a shorter time scale than q_I. (Figure taken from Ruban, 2017)

1.3.4.2. 77 K chlorophyll fluorescence spectroscopy

The assessment of chlorophyll fluorescence at 77 K is a technique that is often used to complement observations made by PAM fluorometry at room temperature. 77 K fluorescence spectroscopy is particularly useful for determining the presence and the kinetics of state transitions (Lamb et al. 2018). Fluorescence emissions by photosynthetic organisms at room temperature mostly consists of fluorescence emitted by PSII (about 90 %). The reason for this is that PSI is a deeper energy trap than PSII (Govindjee, 1995; Wientjes & Croce, 2012). This means that very little energy is lost as fluorescence in the energy transfer between the external antennae complexes of PSI and the PSI core complex itself.

At room temperature, changes in PSII fluorescence can be readily observed, while changes in PSI fluorescence are comparatively small, and are spectrally similar to the fluorescence emitted by PSII.

Lowering the temperature to 77 K makes the PSI and PSII fluorescence more spectrally distinct. Furthermore; at this temperature, electron carriers that are mobile at room temperature become immobile. Electron transport therefore becomes static, as electrons accumulate on the acceptor side of PSII and PSI, and the light that would have been used to fuel charge separation at room temperature, will now be given off as fluorescence.

Lowering the temperature from ~ 20 °C to – 196 °C increases the PSI fluorescence yield by a factor of approximately 20 (Mukerji & Sauer, 1988), and makes the PSI fluorescence comparable in magnitude to the PSII fluorescence. There are minor differences between different organisms, but generally, PSII fluorescence peaks around 685 nm and 695 nm, characteristic of chlorophylls associated within CP43 and CP47, respectively. PSI fluorescence is situated at approximately 720 –730 nm (Lamb et al. 2018). In most organisms, the peak height of fluorescence maxima of PSII and PSI associated chlorophylls relative to each other, can be used to assess the amount of chlorophyll molecules located in the light-harvesting complexes that are associated with PSII and PSI, and can thus be used to assess if a state transition has taken place.

1.4. Metabolic modelling

In the later years, collecting sequence, transcriptome and proteomic data has become both easier and faster, due to the improvement of DNA sequencing methods (Heather & Chain, 2016) and the development of new mass spectrometers and chromatographs. With the increasing availability of biological data, it is more important than ever to be able to put the newly generated data into an analytical framework, and this became the starting point for the development of systems biology as a field.

As the name implies, systems biology aims at putting biological data into a system – to help us see the bigger picture in the jungle of available biological information. The system that is used is usually a mathematical framework.

One of the main approaches of systems biology has been the construction of metabolic models, which aim at describing the metabolism of a cell mathematically, but mathematical models describing for example non-photochemical quenching by using differential equations have also been developed (Zaks et al. 2012).

When gaining increasing amounts of information on
gene – protein associations, and information about which reactions are catalysed by which proteins, the complete (or at least almost complete) metabolism of a cell could be predicted from its sequenced genome. Recently, the number of metabolic reconstructions and the number of newly sequenced genomes has increased at a similar pace (Thiele & Palsson, 2010).

When mathematically modelling a reaction or a set of reactions, this is done on the basis of stoichiometric coefficients and fluxes. The word 'flux' is mainly used in physics, denoting either electric or magnetic forces travelling through a surface on a certain time scale. In metabolic modelling, the word is used to describe the flow through a certain reaction per time unit, or the conversion or production rate of a certain molecule. Fluxes are usually denoted with the Greek letter ν (nu).

An example of a mathematical reconstruction of a set of reactions is given in Figure 10. This particular set of seven reactions and nine metabolites is taken

from the glycolysis / gluconeogenesis. In the example below, every reaction has a corresponding reaction flux, termed v_1 to v_7.

The mini-network in the example could be drawn as a metabolic map (shown in the left part of the figure), or it could be summed up in a tabular form (shown in the right part of the figure), the tabular form being the most convenient when describing large reaction networks containing several thousand reactions.

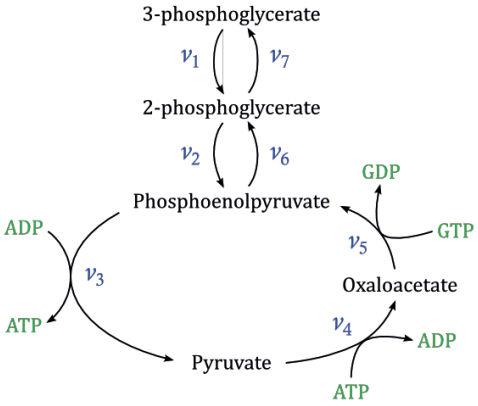

	Rx 1	Rx 2	Rx 3	Rx 4	Rx 5	Rx 6	Rx 7
3-PG	-1	0	0	0	0	0	1
2-PG	1	-1	0	0	0	1	-1
PEP	0	1	-1	0	1	-1	0
Pyr	0	0	1	-1	0	0	0
OxaA	0	0	0	1	-1	0	0
ATP	0	0	1	-1	0	0	0
ADP	0	0	-1	1	0	0	0
GTP	0	0	0	0	-1	0	0
GDP	0	0	0	0	1	0	0

Figure 10: Example of a simple metabolic network made from a part of glycolysis / gluconeogenesis. The metabolic map (left) and the stoichiometric matrix (right) of the example network are shown.

When summarizing a reaction network on a tabular form, as done above, the rows of the table denote metabolites, while the columns denote reactions. The table is then made up by stoichiometric coefficients, showing how many of which molecules that are being consumed or produced in a certain reaction. A negative stoichiometric coefficient denotes consumption while a positive coefficient denotes production. The matrix that arises when summarizing a metabolic network as shown above, is called a stoichiometric matrix, and it can be used to write out individual equations for the change in concentrations over time for all metabolites.

The first row in the stoichiometric matrix above shows the stoichiometric coefficients for 3-phosphoglycerate in all reactions. This particular metabolite is consumed in reaction 1, which is running with a flux v_1, and produced in reaction 7, running with a flux v_7. Keeping in mind that fluxes are time derivatives, the change in concentration over time for 3-phosphoglycerate could thus be described as

$$\frac{d(\text{3-PG})}{dt} = -v_1 + v_7$$

The change in concentration for the other metabolites involved in the reaction network shown above could be written out in a similar manner:

$$\frac{d(\text{2-PG})}{dt} = v_1 - v_2 + v_6 - v_7 \qquad \frac{d(\text{ATP})}{dt} = v_3 - v_4$$

$$\frac{d(\text{PEP})}{dt} = v_2 - v_3 + v_5 - v_6 \qquad \frac{d(\text{ADP})}{dt} = -v_3 + v_4$$

$$\frac{d(\text{Pyr})}{dt} = v_3 - v_4 \qquad \frac{d(\text{GTP})}{dt} = -v_5$$

$$\frac{d(\text{OxaA})}{dt} = v_4 - v_5 \qquad \frac{d(\text{GDP})}{dt} = v_5$$

The set of differential equations that arises when using the reaction fluxes and the stoichiometric coefficients to describe the change in concentration over time for a certain metabolite can again be summarized in matrix form, yielding the following equation set, consisting of a vector of time derivatives of the concentrations, the stoichiometric matrix, and a flux vector:

$$\begin{bmatrix} \dot{A} \\ \dot{B} \\ \dot{C} \\ \dot{D} \\ \dot{E} \\ \dot{F} \\ \dot{G} \\ \dot{H} \\ \dot{I} \end{bmatrix} = \begin{bmatrix} -1 & 0 & 0 & 0 & 0 & 0 & 1 \\ 1 & -1 & 0 & 0 & 0 & 1 & -1 \\ 0 & 1 & -1 & 0 & 1 & -1 & 0 \\ 0 & 0 & 1 & -1 & 0 & 0 & 0 \\ 0 & 0 & 0 & 1 & -1 & 0 & 0 \\ 0 & 0 & 1 & -1 & 0 & 0 & 0 \\ 0 & 0 & -1 & 1 & 0 & 0 & 0 \\ 0 & 0 & 0 & 0 & -1 & 0 & 0 \\ 0 & 0 & 0 & 0 & 1 & 0 & 0 \end{bmatrix} \cdot \begin{bmatrix} v_1 \\ v_2 \\ v_3 \\ v_4 \\ v_5 \\ v_6 \\ v_7 \\ v_8 \\ v_9 \end{bmatrix}$$

Here the nine molecules in the example above have been denoted, A, B, C, …, I, for simplicity.

When modelling an entire cell, which could include several thousand reactions, these systems of differential equations will be increasingly hard to solve. But the equation system above can be simplified.

In the biological world, the concentration of metabolites can certainly fluctuate over time. When describing reactions mathematically, however, one could assume that when the reactions of a metabolic network have been running for a while, the fluxes are stable, and the change in metabolite concentration over time approximates zero. Then the reaction set above could be simplified to

$$\begin{bmatrix} -1 & 0 & 0 & 0 & 0 & 0 & 1 \\ 1 & -1 & 0 & 0 & 0 & 1 & -1 \\ 0 & 1 & -1 & 0 & 1 & -1 & 0 \\ 0 & 0 & 1 & -1 & 0 & 0 & 0 \\ 0 & 0 & 0 & 1 & -1 & 0 & 0 \\ 0 & 0 & 1 & -1 & 0 & 0 & 0 \\ 0 & 0 & -1 & 1 & 0 & 0 & 0 \\ 0 & 0 & 0 & 0 & -1 & 0 & 0 \\ 0 & 0 & 0 & 0 & 1 & 0 & 0 \end{bmatrix} \cdot \begin{bmatrix} v_1 \\ v_2 \\ v_3 \\ v_4 \\ v_5 \\ v_6 \\ v_7 \\ v_8 \\ v_9 \end{bmatrix} = \begin{bmatrix} 0 \\ 0 \\ 0 \\ 0 \\ 0 \\ 0 \\ 0 \\ 0 \\ 0 \end{bmatrix}$$

Or written on a general form:

$$S \cdot v = 0$$

This reduces the original set of differential equations to a set of linear equations, and although this equation set could contain several thousand unknown fluxes, it is easily solved.

This way of modelling reactions mathematically, and the subsequent assumption of steady state, forms the basis for Flux Balance Analysis (FBA) (Orth et al. 2010), which is a common approach for finding values for large sets of reaction fluxes. In large models, there are usually more reactions than metabolites, which will not yield an exact solution for the fluxes, but rather a confined solution space where all sets of fluxes within the solution space are possible solutions (Orth et al. 2010). If this is the case (as it usually is), it is possible to find the set of fluxes that yields the maximum flux for one certain reaction.

Even though cell growth in the real biological world is a complex matter that depends on a multitude of reactions, it is common to include a 'biomass reaction' when modelling a cell mathematically. In the biomass reaction, the most important metabolites a cell needs in order to grow (or to produce biomass) are included as reactants. Usually, this is the reaction that is optimized when using Flux Balance Analysis, as this is a good approximation for the biological world, where the objective of every cell is to grow as fast as their environment allows them to. When optimizing for the biomass reaction, the corresponding reaction flux then yields a growth rate, in biomass produced per time unit.

Building a metabolic model for an entire cell might seem like a daunting task, but in recent years, several step-by-step manuals to model reconstruction have been published (Feist et al. 2009; Thiele & Palsson, 2010). Semi-automated tools that will both annotate a DNA sequence and use that annotation to create a draft reconstruction have also been developed (Henry et al. 2010; Agren et al. 2013). There are several advantages to creating such genome-based metabolic models. Metabolic models have of course been made possible through the rapid increase in biological data available, but that being said, the construction of genome-scale models also represent a great way to structure the vast amounts of new data, and to make it easily available and user-friendly.

Genome-scale metabolic models can also be extremely useful in metabolic engineering approaches (Oberhardt et al. 2009). Genetic engineering has

become common practice to increase the production of useful or valuable chemicals in both bacteria and in yeast, and metabolic models can be used to predict how different gene knockouts will affect the production of a chemical of interest. In 2008, this approach was used on *Saccharomyces cerevisiae* to optimize the production of malate, which is an important industrial chemical that is often used as a building block in chemical synthesis. The malate production was increased to 59 g/l, which was five times higher than all earlier efforts had accomplished (Zelle et al. 2008).

Metabolic models can also be used within the medical field; for example, to study human diseases and the effect of different treatments (Duarte et al. 2007; Lewis et al. 2010).

Recently, the concept of Flux Balance Analysis and constraint-based modelling has been expanded, so transcriptomic data can also be taken into account when optimizing a model (Navid & Almaas, 2012). This approach is ideal for predicting cellular responses to environmental stimuli. It can, for example, be used to predict more accurately than ever the cellular response of a pathogen organism to a toxin.

The first metabolic models were relatively simple models with some hundred metabolites. Over the years, increasingly complex, multi-compartment models with several thousand reactions have been published, even for photosynthetic organisms (Imam et al. 2015; Levering et al. 2016; Loira et al. 2017; Shah et al. 2017).

1.5. Organisms investigated throughout this work

The work presented in this thesis is mainly based on three organisms; the heterokont algae *Nannochloropsis oceanica* and *Phaeodactylum tricornutum*, and the green algal model organism *Chlamydomonas reinhardtii*. These three organisms have been the focus of the investigations of regulation of electron transport using spectroscopic measurements, and of the development of an adjustable chloroplast model.
In the following sections, these three organisms, and the differences between them, will be described in detail.

1.5.1. *Nannochloropsis oceanica*

Nannochloropsis sp. is a heterokont microalga belonging to the class of Eustigmatophyceae. It is a relatively small alga, usually having a diameter of 2 – 4 µm, with cells containing one single chloroplast (Gentile & Blanch, 2001). The alga has gained increasing interest for its ability to produce lipids and high-value chemicals such as long-chain polyunsaturated fatty acids and xanthophylls (Sukenik, 1991; Lubián et al. 2000; Hu et al. 2015).
Nannochloropsis has a unique pigment composition, with violaxanthin and vaucheriaxanthin being the main pigments (Basso et al. 2014; Alboresi et al. 2016; Litvin et al. 2016). The alga also employs minor amounts of canthaxanthin, siphonaxanthin, zeaxanthin and β-carotene. In contrast to many other heterokont algae, *Nannochloropsis* only contains chlorophyll *a* and completely lacks chlorophyll *b* and *c* (Gentile & Blanch, 2001).
In addition to lacking accessory chlorophylls, another peculiarity about *Nannochloropsis* is its unusually high amount of PSI compared to PSII. Plants and green algae usually have a PSI:PSII ratio of 0.53 – 0.67 (Fan et al. 2007), while the PSI:PSII ratio in *Nannochloropsis* is approximately 1.7 (Carbonera et al. 2014).
The light-harvesting complexes of *Nannochloropsis* are called VCPs (Viola- / Vaucheriaxanthin Chlorophyll Proteins) (Carbonera et al. 2014), and are similar

to the three-transmembrane helix light harvesting proteins of red algae and diatoms. It is assumed that each complex contains ~ 3 violaxanthin, ~ 2 vaucheriaxanthin molecules and 10 chlorophyll molecules (Litvín et al. 2016). The light-harvesting complexes of *Nannochloropsis* have been divided into four subtypes; Lhcv, Lhcr, Lhcx and red CLHs (*Chromera velia* like light-harvesting complexes) (Litvín et al. 2016). The main light-harvesting complex in *Nannochloropsis* is the Lhcv type (viola- / vaucheriaxanthin binding light-harvesting complex), which is similar to the Lhcf (fucoxanthin binding light-harvesting complex) complexes found in diatoms. Lhcr complexes are mainly associated with PSI, which is also the case for the red CLHs.

Lhcx are stress response-related light harvesting proteins, and have been found to be similar to the PsbS proteins in higher plants (Litvín et al. 2016).

In higher plants, the light-harvesting complexes associated with PSII usually form trimers (Dubertret et al. 2002). This is not the case in *Nannochloropsis*. *Nannochloropsis* lacks the minor light-harvesting complexes CP24, CP26 and CP29, which in higher plants form docking points between the trimeric light-harvesting complexes and PSII dimers. Trimeric light-harvesting complexes have also so far not been observed in *Nannochloropsis*. It is therefore assumed that the majority of light-harvesting complexes in *Nannochloropsis* exist as monomers linked to PSII (Litvín et al. 2016).

The link between the PSI-associated light-harvesting complexes and PSI are stronger than that between the PSII-associated light-harvesting complexes and PSII (Basso et al. 2014). Usually, PSI in *Nannochloropsis* is strongly linked to five light-harvesting complexes, which form a very efficient energy trap (Alboresi et al. 2017).

Since violaxanthin is one of the most important pigments in *Nannochloropsis*, it might come as no surprise that the xanthophyll cycle is important for photoprotection in this particular alga (Gentile & Blanch, 2001). In *Nannochloropsis*, dissipation of excess excitation energy as heat has been shown to occur in light-harvesting complexes of the Lhcx1 type, via both excitation energy transfer and charge transfer between chlorophyll *a* and zeaxanthin (Park et al. 2019).

State transitions, on the other hand, have not been observed in *Nannochloropsis* thus far. However, studies have shown that the number of light-harvesting complexes associated with PSI in *Nannochloropsis* can range between 5 and 9 light-harvesting complexes (Bína et al. 2017, 1). This indicates that a dynamic adjustment of antenna size between PSII and PSI is a possibility.

Non-photochemical quenching in *Nannochloropsis oceanica* has been found to have two main components; one slow component which seems directly linked to the amount of zeaxanthin present, and one fast component which seems dependent both on a pH gradient, and on the zeaxanthin content (Bína et al. 2017, 2). The fast component is present at increased pH values, and it is assumed that this quenching could be ascribed to light-harvesting complexes of the Lhcx type, and that this quenching component corresponds to the q_E type quenching. The fast quenching component increases with the amount of zeaxanthin (Bína et al. 2017, 2).

It has been demonstrated that the relaxation of NPQ in *Nannochloropsis oceanica* occurs in approximately the same time frame as the conversion of zeaxanthin back to violaxanthin. Studies focusing on *Nannochloropsis gaditana* have shown that two quenching components, one fast and one slow, are also present in this organism. In *N. gaditana*, there are indications that the fast quenching component, related to the presence of Lhcx, is associated with both photosystems, while the zeaxanthin dependent slow quenching is mainly associated with PSII (Chukutsina et al. 2017). Chukutsina and co-workers also observed the redistribution of excitation energy between PSII and PSI.

1.5.2. *Phaeodactylum tricornutum*

Phaeodactylum tricornutum is a model species belonging to the superphylum Heterokontophyta and the class of Bacillariophyceae. It is a pennate diatom found in both coastal and inland waters (Rushforth et al. 1988). Diatoms are a major contributor to the primary production of the oceans, and their fossil remains are also one of the major sources of today's petroleum (Vardi et al. 2009).

A peculiarity about *Phaeodactylum tricornutum* is that it can take three different morphological forms; fusiform, triradiate and oval. Pennate diatoms are usually benthic, but *Phaeodactylum tricornutum* is not a strict benthic species, and can also be found amongst free-floating plankton. It has been suggested that the different morphological forms could be related to where in the water column the diatom can be found, as there are important biochemical differences; for example, in polysaccharide concentration between the morphological forms. Polysaccharide concentration determines density, and due to the differences in polysaccharide compositions between the different morphological forms, it has been proposed that alternating between different forms helps the algae adjust to its environment (Sabir et al. 2018).

The main pigments of *Phaeodactylum tricornutum* are chlorophyll *a*, chlorophyll *c*, and the carotenoids fucoxanthin, diadinoxanthin / diatoxanthin, and lutein (Gundermann & Büchel, 2014). Fucoxanthin is by far the most abundant pigment, and the main light-harvesting complex of *Phaeodactylum* is therefore called Fucoxanthin Chlorophyll Proteins (FCPs) (Guglielmi et al. 2005).

FCPs can be divided into three main groups: (1) Lhcf, which are similar to the Lhcv complexes found in *Nannochloropsis* sp. (Litvín et al. 2016), (2) Lhcr complexes, commonly associated with PSI, and (3) Lhcx complexes, which, as in *Nannochloropsis*, are involved in photoprotection and NPQ (Gundermann & Büchel, 2014). In addition, redCAP proteins (red lineage chlorophyll a/b binding-like proteins) have also been found in *Phaeodactylum* sp. (Sturm et al. 2013).

An increased proton gradient is essential for the onset of NPQ in this organism as well, but here its most important function seems to be the activation of

Diadinoxanthin de-epoxidase, which is the enzyme converting diadinoxanthin into diatoxanthin. Non-photochemical quenching in *Phaeodactylum* thus works differently compared to that in *Nannochloropsis,* where a fast proton-dependent quenching is present (Bína et al. 2017, 2). The relaxation of NPQ in *Phaeodactylum* also occurs on a slower time scale than the decline of the proton gradient, and matches the re-epoxidation of diatoxanthin back to diadinoxanthin by the enzyme Diatoxanthin epoxidase (Goss & Lepetit, 2015). It has been proposed that the pH gradient still is important for NPQ, possibly playing a role in activating the diatoxanthin-dependent quenching (Ruban et al. 2004), which in *Phaeodactylum* is proposed to be mediated by Lhcx complexes (Goss & Lepetit, 2015).

More recent studies have, however, shown the presence of two distinct quenching sites in *Phaeodactylum* Q1 quenching occurs in aggregated oligomeric light-harvesting complexes, which have detached from PSII (Miloslavina et al. 2009), while Q2 quenching is diatoxanthin-dependent quenching mediated by the Lhcx complexes still bound to the core complex.

Since all NPQ in *Phaeodactylum* seems to be diatoxanthin dependent, it has been speculated that the formation of diatoxanthin introduces a conformational change in light-harvesting complexes, which allows certain complexes to detach and form fluorescence quenching aggregates (Goss & Lepetit, 2015). The aggregated, oligomeric light-harvesting complexes have a slightly red-shifted fluorescence (Miloslavina et al. 2009; Herbstová et al. 2015), and have been proposed to be part of the chromatic adaptation occurring in *Phaeodactylum* (Herbstová et al. 2015).

Traditionally, state transitions have been thought of as absent in *Phaeodactylum* (Owens, 1986), but recently, after the finding that light-harvesting complexes detach from PSII and form aggregates, it has been discussed that *Phaeodactylum* may balance excitation energy between PSII and PSI (Fujita & Ohki, 2004).

1.5.3. *Chlamydomonas reinhardtii*

Chlamydomonas reinhardtii is a green alga. It has a diameter of approximately 10 µm, and has emerged as one of the most important and most researched photosynthetic model organisms.

In *Chlamydomonas* sp., the PSII is structured as a dimer that is usually bound to six PSII specific light-harvesting complexes and four minor light-harvesting complexes (including CP26 and CP29) (Drop et al. 2014; Minagawa & Tokutsu, 2015). PSI, on the other hand, operates as a monomer, and is usually bound to 9 PSI-specific light-harvesting complexes (Ünlü at al. 2014; Minagawa & Tokutsu, 2015). However, PSI in *Chlamydomonas* has been observed with up to 11 light-harvesting complexes, each supercomplex containing approximately 215 chlorophyll molecules, 175 chlorophyll *a* molecules, and the rest chlorophyll *b*, which is present in the LHCI antennae (Kargul et al. 2003).

In *Chlamydomonas*, PSII is mainly located in the membranes of the grana stacks, while PSI mainly is located in the stroma lamellae (Haldrup et al. 2001). During light stress and other external conditions that reduce the plastoquinone pool, *Chlamydomonas* carries out a well-observable state transition (Ünlü et al. 2014), with PSII-specific light-harvesting complexes migrating from the grana stacks to re-attach to PSI in the stroma lamellae. In *Chlamydomonas*, state transitions are also accompanied by a shift from linear to cyclic electron transport (Finazzi et al. 2002).

When a state transition occurs in *Chlamydomonas*, around 70 – 80 % of the PSII-associated light-harvesting complexes detach from PSII (Nagy et al. 2014; Ünlü et al. 2014). Initially, it was believed that all the detached PSII-specific light-harvesting complexes would re-attach to PSI, but recent investigations have shown that this is not the case. Only 20 % of the detached light-harvesting complexes re-attach to PSI (Nagy et al. 2014; Ünlü et al. 2014), and it has been proposed that the fraction of light-harvesting complexes that will not re-attach to PSI, forms excitation-quenching complexes, either existing in a free form, or associated with PSII (Nagy et al. 2014).

In *Chlamydomonas*, state transitions are modulated by the redox state of the plastoquinone pool, and involve both the cytochrome b_6f complex and the more

recently discovered Stt7 kinase (Depège et al. 2003) (the mechanism of state transition initiation is explained in depth in section 1.3.2.1).
Even though the main mode of photoprotection in *Chlamydomonas* is state transitions, it was recently discovered that a gene encoding an analogue to violaxanthin de-epoxidase is present in *Chlamydomonas*. This enzyme is present in the chloroplast stroma instead of the thylakoid lumen, and it is similar to the violaxanthin de-epoxidase found in photosynthetic bacteria (Li et al. 2016). *Chlamydomonas* therefore likely uses a combination of q_T and q_E quenching (Wobbe et al. 2016), but q_E only occurs in certain conditions, and the magnitude of the q_E quenching found in *Chlamydomonas* sp. is generally very small compared to that found in other photosynthetic organisms (Finazzi et al. 2006).

2. Aims of the thesis

Heterokont algae contribute significantly to marine primary productivity, and are also considered industrially relevant production platforms for lipids. These key features, however, are not matched by the depth of knowledge concerning fundamental aspects of their photosynthetic processes.

The aim of this thesis has been to gain insights into the regulation of the photosynthetic machinery and lipid metabolism of the heterokont microalgae *Nannochloropsis oceanica* and *Phaeodactylum tricornutum.* For this, a computational model describing chloroplast metabolism was constructed.

A key experimental technique (chlorophyll fluorescence at 77 K) was also reviewed with a focus on heterokont algae. Furthermore, the photosynthetic machinery of the heterokont algae *Nannochloropsis oceanica* and *Phaeodactylum tricornutum* was investigated by spectroscopic techniques.

3. Results and discussion

In this chapter, papers I – V will be presented and discussed.

Paper I

Pathways of lipid metabolism in marine algae, co-expression network, bottlenecks and candidate genes for enhanced production of EPA and DHA in species of Chromista

Alice Mühlroth, Keshuai Li, Gunvor Røkke, Per Winge, Yngvar Olsen, Martin F. Hohmann-Marriott, Olav Vadstein, Atle M. Bones.

Published in Marine Drugs (2013), vol. 11, pp. 4662 – 4697.

Paper I is a review paper focusing on approaches to enhance the synthesis of ω-3 fatty acids in microalgae, which are efficient producers of these lipids. Several ω-3 fatty acids are essential for vertebrates. The membranes of the human brain contain high amounts of both ω-3-fatty acids and ω-6 fatty acids, which make these fatty acids extremely important for both physical and mental health (Plourde & Cunnane, 2007).
The review mainly focuses on how industrial production of the fatty acids eicosapentaenoic acid (EPA) and docosahexaenoic acid (DHA) by microalgae could be increased using genetic approaches. In general, five strategies could be used for genetically increasing the fatty acid content of microalgae. Firstly, the pool of molecules serving as precursors for the fatty acids in question could be increased. Secondly, the reactions involved in β-oxidation, which is a lipid-degrading pathway mainly occurring in peroxisomes, could be inhibited. Thirdly, enzymes involved in biosynthesis of fatty acids could be overexpressed, and as a fourth and fifth approach, fatty acid chain length could be optimized by regulation of thioesterases, and the saturation profile could be controlled by regulation or introduction of desaturases (Hoffman et al. 2008).

The paper reviews genes involved in the different pathways related to the synthesis of EPA and DHA. In order to characterize potential targets for gene knockouts or enzyme modification, a co-expression network was generated, using transcriptomic data from five different experiments. A total of 106 genes were included in the network, all of which are associated with fatty acid metabolism in *Phaeodactylum tricornutum*. The genes included in the co-expression network encode proteins involved in the mitochondrial tricarboxylic acid (TCA) cycle, β-oxidation occurring in peroxisomes, *de novo* synthesis of fatty acids in chloroplasts, and the synthesis of long-chain poly-unsaturated fatty acids (LC-PUFAs) located in the endoplasmic reticulum.
The co-expression network generated for the review revealed that increasing the pool of precursor molecules by over-expression of the proteins responsible for the synthesis of these precursors, is the approach that is likely to have the greatest effect on lipid production in *Phaeodactylum*.
Genes encoding proteins involved in transesterases, elongases and acyltransferases were also found to be possible targets for enhancement of LC-PUFA production.

Contributions:
Alice Mühlroth is the main author of this paper, and wrote most of the manuscript. I contributed to writing the introduction (chapter 1), and I also made figure 4 and 5.

Paper II

The plastoquinone pool of *Nannochloropsis oceanica* is not completely reduced during bright light pulses

Gunvor Røkke, Thor Bernt Melø, Martin Frank Hohmann-Marriott

Published in PLoS One (2017), vol. 12, paper e0175184

Paper II investigates the regulation of electron transport in *Nannochloropsis*, which is known to have a distinct photosynthetic machinery compared to that of green algae and higher plants. *Nannochloropsis* has emerged as a model organism due to its ability to produce and store relatively large amounts of fatty acids that are of interest both as a substrate for biofuel and as a food additive. However, so far the photosynthetic machinery of *Nannochloropsis* is less researched than its ability to produce lipids.

In this paper, we used pulse amplitude modulated (PAM) fluorometry (Schreiber, 1986; Schreiber et al. 1986) to investigate the fluorescence kinetics following bright light pulses.

PAM fluorometry in combination with the saturation pulse method has become a relatively standardized method for studying photosynthetic performance of plants in different environmental conditions. The interpretation of data obtained by PAM fluorometry, however, is highly organism-specific, as we discovered in the work leading up to paper II.

We investigated the photosynthetic performance of *Nannochloropsis* in the presence of actinic background light, in anaerobic conditions, and in the presence of the inhibitor DBMIB. In plants and green algae, these three conditions are all known to reduce the plastoquinone pool, resulting in a characteristic chlorophyll fluorescence transient. However, by interpreting the fluorescence transients in *Nannochloropsis* we conclude that high-intensity light did not result in a complete reduction of the plastoquinone pool in *Nannochloropsis*.

This finding has major implications when using PAM fluorometry in combination with the saturation pulse method to assess different aspects of photosynthetic performance. If the measured maximum fluorescence is not the true maximum fluorescence, this would, for example, lead to a systematic over-assessment of PSII quantum yield.
The finding that bright light pulses are not able to reduce the plastoquinone pool of *Nannochloropsis* has implications for the previously reached conclusion that heterokonts do not carry out state transitions as a part of their photoprotection. The reduction state of the plastoquinone pool has been shown to play a part in the activation of state transitions both in green algae and higher plants. Since the bright light pulses utilized by the saturation pulse method are not able to reduce the plastoquinone pool of *Nannochloropsis*, this might explain why state transitions have never been observed in this organism.

Contributions:
I planned the experiments in collaboration with Martin Hohmann-Marriott, and I performed the experiments. I also developed the necessary tools for data analysis in collaboration with Thor Bernt Melø. I analysed the data, generated the figures, wrote the original draft, and both I, Martin Hohmann-Marriott and Thor Bernt Melø reviewed the final draft of the manuscript.

Paper III

Unique photosynthetic electron transport tuning and excitation distribution in heterokont algae

Gunvor Bjerkelund Røkke, Thor Bernt Melø, Alice Mühlroth, Olav Vadstein, Atle M. Bones, Martin F. Hohmann-Marriott

Published in PLoS One (2019), vol. 14, paper e0209920

The findings presented in paper II led us to take a closer look at the photoprotection mechanisms of *Nannochloropsis*. Since *Nannochloropsis* retains a partly oxidized plastoquinone pool in high-intensity light, we wanted to investigate if this behavior was specific to *Nannochloropsis*, or if it also occurs in other heterokont algae. *Phaeodactylum tricornutum* was therefore included in the study as another heterokont alga where state transitions have not been observed (Owens, 1986).

Phaeodactylum were found to exhibit the same behavior as *Nannochloropsis*. The chlorophyll fluorescence yield found in dark-adapted, aerobic conditions was not the true maximum fluorescence. This led us to conclude that just like *Nannochloropsis*, the plastoquinone pool of *Phaeodactylum* is also not completely reduced by the standard bright light pulses utilized by the saturation pulse method.

In this paper, we also wanted to investigate if state transitions is a mechanism that is part of the photoprotection repertoire in heterokont algae, but knowing that high-intensity light would not lead to a completely reduced plastoquinone pool, we instead exposed the algae to anaerobic conditions, as the combination of anaerobiosis and darkness has been shown to reduce the plastoquinone pool of several organisms.

For both *Nannochloropsis* and *Phaeodactylum*, we observed that the onset of anaerobic conditions led to a decrease in the ratio of PSII-fluorescence to PSI-fluorescence over time. In *Chlamydomonas*, which was included in the study as

well, this shift could also be observed in high-intensity light, which was expected. In *Nannochloropsis* and *Phaeodactylum*, the ratio of PSII-fluorescence to PSI-fluorescence increased in high-intensity light, which was the opposite of the behavior observed in *Chlamydomonas*.

The results from paper III show that the heterokont algae *Nannochloropsis oceanica* and *Phaeodactylum tricornutum* are indeed capable of dynamic partitioning of light energy between PSII and PSI. The mechanisms underlying this light partitioning might be different from the classic state transition of for example *Chlamydomonas reinhardtii*, as the chloroplast architecture is different between green algae and heterokonts. The state transition observed in the heterokont algae therefore might not involve a physical movement of light-harvesting complexes, such as in *Chlamydomonas*, but rather a re-coupling.

In green algae and higher plants, plastoquinone has been shown to act as a sensor molecule, and a reduced plastoquinone pool is required for the onset of state transitions. This also seems to be the case in heterokont algae.

We propose that the regulation of excitation energy in heterokont algae is an adaptation to the changing light-environments they might encounter in the ocean, where the light intensity could exceed the full intensity of sunlight due to the lensing effect of waves.

Contributions:

I planned the experiments in collaboration with Martin Hohmann-Marriott, and performed the experiments with some help from Alice Mühlroth. I developed software tools for analysis of the data in collaboration with Thor Bernt Melø, and I analysed the data, generated figures and wrote the original draft. All co-authors reviewed the original draft of the manuscript prior to submission.

Paper IV

Chlorophyll fluorescence emission spectroscopy of oxygenic organisms at 77 K

Jacob Joseph Lamb, Gunvor Røkke, Martin Frank Hohmann-Marriott

Published in Photosynthetica (2018), vol. 56, pp. 105 – 124

Paper IV is a review focusing on 77 K spectroscopy. The history of the technique is reviewed, and important concepts such as chlorophyll excitation, excitation transfer, and the difference between fluorescence measurements performed at room temperature and at 77 K are explained. Instrumentation and sample preparation is also discussed.
Most of the paper is, however, dedicated to chlorophyll fluorescence characteristics at 77 K in plants, green algae, cyanobacteria, red algae and heterokont algae.

Contributions:
Jacob Joseph Lamb is the main author of this paper, and wrote most of the manuscript. I contributed significantly to writing the section on heterokont algae. I also developed the software for digitizing data from other papers. I digitized the data, and generated all figures except figure 5.

Paper V

An adjustable algal chloroplast plug-and-play model for genome-scale metabolic models

Gunvor Bjerkelund Røkke, Martin Frank Hohmann-Marriott, Eivind Almaas

Manuscript prepared for submission

Paper V focuses on the construction of a metabolic model of a chloroplast, which can be easily coupled to other metabolic models in need of a chloroplast compartment. Our model contains 788 reactions, 764 metabolites, and 774 genes.

The "plug-in" feature of this model is a novel concept, as metabolic models are usually constructed for an entire cell, and not for individual organelles. Even though the metabolism of the chloroplast is relatively conserved, there are minor differences between the chloroplast metabolism of different organisms. The 'plug in' chloroplast has different organism modes, allowing or disabling organism-specific reactions to run. Currently, the chloroplast model could be run both in *Nannochloropsis* mode, *Phaeodactylum* mode and *Chlamydomonas* mode.

A special emphasis and strength of the chloroplast model is a detailed representation of the photosynthetic electron transport chain. This feature allows the user to investigate the regulation of photosynthetic electron transport, and the link between the photosynthetic electron transport and carbon fixation.

Along with the development of the chloroplast model, software tools for working with this novel type of adjustable organelle model have also been developed. Tools have been developed for easily coupling the chloroplast model to another metabolic model, for changing the organism mode of the chloroplast, and for expanding it, either with reactions specific to one of the organisms

currently represented by the model, or by introducing a completely new organism mode.

Contributions:
I planned the chloroplast model in collaboration with Eivind Almaas.
I performed the reconstruction of chloroplast metabolism, developed the software necessary for working with an adjustable compartment model, and wrote the original draft. All co-authors reviewed the final draft of the manuscript.

4. Concluding remarks and future works

One major finding of the work presented in this thesis is that the electron transport and the onset of photoprotection mechanisms is regulated differently in the heterokont algae *Nannochloropsis* and *Phaeodactylum* compared to those in higher plants and green algae. When *Chlamydomonas* is exposed to high-intensity light, the photosynthetic electron transport chain is completely reduced, and photoprotection mechanisms are initiated. In both *Nannochloropsis* and *Phaeodactylum*, high-intensity light seems to decrease the degree of reduction in the plastoquinone pool. In *Nannochloropsis*, a probable explanation for this behaviour is its high PSI:PSII ratio, but for *Phaeodactylum*, this is not presently a satisfactory explanation. Future studies should therefore focus on exploring the mechanisms for this particular feature also in *Phaeodactylum*, by determining its PSI:PSII ratio.

Another major finding is that in contrast to what was previously thought, heterokont algae are capable of dynamic partitioning of excitation energy between PSII and PSI. At first sight, this may look like the state transitions carried out by *Chlamydomonas*, but the mechanism for this dynamic excitation energy partitioning may be fundamentally different in heterokont algae, as their chloroplast structure is different. The thylakoid structure of heterokont algae makes a re-coupling of light-harvesting complexes between the two photosystems more likely than a physical movement of the light-harvesting complexes. The molecular mechanisms that control and facilitate this re-coupling should also be investigated in detail in the future.

Biochemical purification of photosynthetic complexes in combination with single particle electron microscopy techniques could also yield valuable information about the structural features that mediate the re-coupling of light-harvesting complexes between the two photosystems that we determined by using spectroscopic techniques.

This project has also included the construction of a metabolic model describing the metabolism of a chloroplast. This model can switch between different organism modes by enabling or disabling organism-specific reactions, and can also be coupled to another metabolic model in need of a chloroplast. In the

future, the organism-specific parts of the chloroplast metabolism should be made even more detailed, and the model should also be expanded to encompass more organisms than the three microalgae already included.

References

Agren, Rasmus; Liu, Liming; Shoaie, Saeed; Vongsangnak, Wanwipa; Nookaew, Intawat; Nielsen, Jens (2013) The RAVEN toolbox and its use for generating a genome-scale metabolic model for Penecillium chrysogenum. Public Library of Science Computational Biology, vol. 9, e1002980

Alboresi, Alessandro; Le Quiniou, Clotilde; Yadav, Sathish K. N.; Scholz, Martin; Meneghesso, Andrea; Gerotto, Caterina; Simionato, Diana; Hippler, Michael; Boekema, Egbert J.; Croce, Roberta; Morosinotto, Tomas (2016) Concervation of core complex subunits shaped the structure and function of photosystem I in the secondary endosymbiont alga *Nannochloropsis gaditana*. New Phytologist, vol. 213, pp. 714 – 726

Ananyev, Gennady; Gates, Colin; Kaplan, Aaron; Dismukes, Charles (2017) Photosystem II-cyclic electron flow powers exceptional photoprotection and record growth in the microalga *Chlorella ohadii*. Biochimica et Biophysica Acta, vol. 1858, pp. 873 – 883

Arechaga, Ignacio; Butler, P. Jonathan G.; Walker, John E. (2002) Self-assembly of ATP synthase subunit c rings. Federation of European Biochemical Societies letters, vol. 515, pp. 189 – 193

Aslan, Sebnem; Kapdan, Ilgi Karapinar (2006) Batch kinetics of nitrogen and phosphorus removal from synthetic wastewater by algae. Ecological Engineering, vol. 28, pp. 64 – 70

Basso, Stefania; Simionato, Diana; Gerotto, Caterina; Segalla, Anna; Giacometti, Giorgio M.; Morosinotto, Tomas (2014) Characterization of the photosynthetic apparatus of the Eustigmatophycean *Nannochloropsis gaditana*: Evidence of convergent evolution in the supramolecular organization of photosystem I. Biochimca et Biophysica Acta, vol. 1837, pp. 306 – 314

Bedoshvili, Ye. D.; Popkova, T. P.; Likhoshway, Ye. V. (2009) Chloroplast structure of diatoms of different classes. Cell and Tissue Biology, vol. 3, pp. 297 – 310

Ben-Shem, A.; Frolow, F.; Nelson, N. (2003) Crystal structure of plant photosystem I. Nature, vol. 426, pp. 630 – 635Benson, A. A.; Bassham, J. A.; Calvin, M.; Goodale, T. C.; Haas, V. A.; Stepka, W. (1950) The path of carbon in photosynthesis. V. Paper chromatography and radioautography of the products. Journal of the American Chemistry Society, vol. 72, pp. 1710 – 1718

Betsche, Thomas (1983) Aminotransfer from alanine and glutamate to glycine and serine during photorespiration in oat leaves. Plant Physiology, vol. 71, pp. 961 – 965

Betterle, Nico; Ballottari, Matteo; Zorzan, Simone; de Bianchi, Silvia; Cazzaniga, Stefano; Dall'Osto, Luca; Morosinotto, Tomas; Bassi, Roberto (2009) Light-induced dissociation of an antenna hetero-oligomer is needed for non-photochemical quenching induction. The Journal of Biological Chemistry, vol. 284, pp. 15255 – 15266

Bína, David; Herbstová, Miroslava; Gardian, Zdenko; Vácha, František; Litvín, Radek (2016) Novel structural aspect of the diatom thylakoid membrane: lateral segregation of photosystem I under red-enhanced illumination. Scientific Reports, vol. 6, article number 25583

Bína, David; Gardian, Zdenko; Herbstová, Hiroslava; Litvín, Radek (2017, 1) Modular antenna of photosystem I in secondary plastids of red algal origin: a *Nannochloropsis oceanica* case study. Photosynthesis Research, vol. 131, pp. 255 – 266

Bína, David; Bouda, Karel; Litvín, Radek (2017, 2) A two-component nonphotochemical fluorescence quenching in eustigmatophyte algae. Photosynthesis Research, vol. 131, pp. 65 – 77

Blatti, Jillian L.; Michaud, Jennifer; Burkart, Michael D. (2013) Engineering fatty acid biosynthesis in microalgae for sustainable biodiesel. Current Opinion in Chemical Biology, vol. 17, pp. 496 – 505

Bonente, Giulia; Ballottari, Matteo; Truong, Thuy B.; Morosinotto, Tomas; Ahn, Tae K.; Fleming, Graham R.; Niyogi, Krishna K.; Bassi, Roberto (2011) Analysis of LhcSR3, a protein essential for feedback de-excitation in the green alga *Chlamydomonas reinhardtii*. Public Library of Science – Biology, vol. 9, article e1000577

Borowitzka, Michael A. (1995) Microalgae as sources of pharmaceuticals and other biologically active compounds. Journal of Applied Phycology, vol. 7, pp. 3 – 15

Borowitzka, Michael A.; Moheimani, Navid R. (Eds.). (2013). *Algae for biofuel and energy*. Dordrecht, The Netherlands: Springer Science+Business Media.

Boyd, P. W.; Sundby, S.; Pörtner, H.-O. (2014) Cross-chapter box on net primary production in the ocean. In: Field, C. B.; Barros, V. R.; Dokken, D. J.; Mach, K. J.; Mastradrea, M. D., Bilir, T. E.; Ebi, K. L.; Estrada, Y. O.; Genova, R. C.; Girma, B., Kissel, E. S.; Levy, A. N.; MacCracken, S., Mastrandrea, P. R.; White, L. L. (Eds.), *Climate Change 2014: Impacts, adaptation and vulnerability. Part A: Global and sectoral aspects. Contribution of working group II to the fifth assessment report of the intergovernmental panel on climate change.* Cambridge University Press, Cambridge, United Kingdom and New York, NY, USA, pp. 133 – 136

Brugna, M.; Rodgers, S.; Schricker, A.; Montoya, G.; Kazmeier, M.; Nitschke, W.; Sinning, I. (2000) A spectroscopic method for observing the domain

movement of the Rieske iron-sulfur protein. Proceedings of the National Academy of Sciences of the United States of America, vol. 97, pp. 2069 – 2074

Caffarri, S.; Kouril, R.; Kereiche, S.; Boekema, E. J.; Croce, R. (2009) Functional architecture of higher plant photosystem II supercomplexes. The EMBO Journal, vol. 28, pp. 3052 – 3063

Calvin, M.; Benson, A. A. (1949) The path of carbon in photosynthesis IV: The identity and sequence of the intermediates in sucrose synthesis. Science, vol. 109, pp. 140 – 142

Calzadilla, Pablo I.; Zhan, Jiao; Sétif, Pierre; Lemaire, Claire; Solymosi, Daniel; Battchikova, Natalia; Wang, Qiang; Kirilovsky, Diana (2019) The cytochrome b_6f complex is not involved in cyanobacterial state transitions. The Plant Cell, vol. 31, pp. 911 – 931

Carbonera, D.; Agostini, A.; Di Valentin, M.; Gerotto, C.; Basso, S.; Giacometti, G. M.; Morosinotto, T. (2014) Photoprotective sites in the violaxanthin-chlorophyll a binding protein (VCP) from *Nannochloropsis gaditana*. Biochimica et Biophysica Acta, vol. 1837, pp. 1235 – 1246

Catalanotti, Claudia; Yang, Wenqiang; Posewitz, Matthew C.; Grossman, Arthur R. (2013) Fermentation metabolism and its evolution in algae. Frontiers in Plant Science, vol. 4, article 150, pages 1 – 17

Chang, Guifang; Luo, Zhenglin; Gu, Sitian; Wu, Qinghang; Chang, Ming; Wang, Xingguo (2013) Fatty acid shifts and metabolic activity changes of *Schizochytrium* sp. S31 cultured on glycerol. Bioresource Technology, vol. 142, pp. 255 – 260

Chen, Chun-Yen; Zhao, Xin-Qing; Yen, Hong-Wei; Ho, Shih-Hsin; Cheng, Chieh-Lun; Lee, Duu-Jong; Bai, Feng-Wu; Chang, Jo-Shu (2013) Microalgae-based

carbohydrates for biofuel production. Biochemical Engineering Journal, vol. 78, pp. 1 – 10

Chen, Min; Blankenship, Robert E. (2011) Expanding the solar spectrum used by photosynthesis. Trends in Plant Science, vol. 16, pp 427 – 431

Chukutsina, Volha U.; Fristedt, Rikard; Morosinotto, Tomas; Croce, Roberta (2017) Photoprotection strategies of the alga *Nannochloropsis gaditana*. Biochimica et Biophysica Acta – Bioenergetics, vol. 1858, pp. 544 – 552

Cox, Nicholas; Retegan, Marius; Neese, Frank; Pantazis, Dimitrios A.; Boussac, Alain; Lubitz, Wolfgang (2014) Electronic structure of the oxygen-evolving complex in photosystem II prior to O-O bond formation. Science, vol. 345, pp. 804 – 808

Croce, Roberta; Weiss, Saskia; Bassi, Roberto (1999) Carotenoid-binding sites of the major light-harvesting complex II of higher plants. The Journal of Biological Chemistry, vol. 274, pp. 29613 – 29623

Croce, Roberta & Van Amerongen, Herbert (2014) Natural strategies for photosynthetic light harvesting. Nature chemical biology, vol. 10, pp. 492 – 501

Cruz, Jeffrey A.; Salbilla, Brian A.; Kanazawa, Atsuko; Kramer, David M. (2001) Inhibition of plastocyanin to P_{700}^{+} electron transfer in *Chlamydomonas reinhardtii* by hyperosmotic stress. Plant Physiology, vol. 127, pp. 1167 – 1179

Darrouzet, E.; Valkova-Valchanova, M.; Moser, C. C.; Dutton, P. L.; Daldal, F. (2000) Uncovering the [2Fe2S] domain movement in cytochrome bc_1 and its implications for energy conversion. Proceedings of the National Academy of Sciences of the United States of America, vol. 97, pp. 4567 – 4572

De Wijn, Rik; Van Gorkom, Hans J. (2001) Kinetics of electron transfer from Q_A to Q_B in photosystem II. Biochemistry, vol. 40, pp. 11912 – 11922

Demming-Adams, Barbara; Adams, William W. (1996) The role of xanthophyll cycle carotenoids in the protection of photosynthesis. Trends in Plant Science, vol. 1, pp. 21 – 26

Depège, Nathalie; Bellafiore, Stéphane; Rochaix, Jean-David (2003) Role of chloroplast protein kinase Stt7 in LHCII phosphorylation and state transition in *Chlamydomonas*. Science, vol. 299, pp. 1572 – 1575

Derks, Allen; Schaven, Kristin; Bruce, Doug (2015) Diverse mechanisms for photoprotection in photosynthesis. Dynamic regulation of photosystem II excitation in response to rapid environmental change. Biochimica et Biophysica Acta, vol. 1847, pp. 468 – 485

Diner, B.; Mauzerall, D. (1973) Feedback controlling oxygen production in a cross-reaction between two photosystems in photosynthesis. Biochimica et Biophysica Acta, vol. 305, pp. 329 – 352

Dominici, Paola; Caffarri, Stefano; Armenante, Franca; Ceoldo, Stefania; Crimi, Massimo; Bassi, Roberto (2002) Biochemical properties of the PsbS subunit of photosystem II either purified from chloroplast or recombinant. The Journal of Biological Chemistry, vol. 277, pp. 22750 – 22758

Drop, Bartlomiej; Webber-Birungi, Mariam; Yadav, Sathish, K. N.; Filipowicz-Szymanska, Alicja; Fusetti, Fabrizia; Boekema, Egbert J.; Croce, Roberta (2014) Light-harvesting complex II (LHCII) and its supramolecular organization in *Chlamydomonas reinhardtii*. Biochimica et Biophysica Acta, vol. 1837, pp. 63 – 72

Duarte, Natalie C.; Becker, Scott A.; Jamshidi, Neema; Thiele, Ines; Mo, Monica L.; Vo, Thuy D.; Srivas, Rohith; Palsson, Bernhard Ø. (2007) Global reconstruction of the human metabolic network based on genomic and bibliomic data. Proceedings of the National Academy of Sciences of the United States of America, vol. 104, pp. 1777 – 1782

Dubertret, Guy; Gerard-Hirne, Catherine; Trémolières, Antoine (2002) Importance of *trans*-Δ^3-hexadecenoic acid containing phosphatidylglycerol in the formation of the trimeric light-harvesting complex in *Chlamydomonas*. Plant Physiology and Biochemistry, vol. 40, pp. 829 – 836

Erickson, Erika; Wakao, Setsuko; Niyogi, Krishna K. (2015) Light stress and photoprotection in *Chlamydomonas reinhardtii*. The Plant Journal, vol. 82, pp. 449 – 465

Falkowski, P. G.; Katz, M. E.; Knoll, A. H.; Quigg, A.; Raven, J. A.; Schofield O.; Taylor, F. J. R. (2004) The evolution of modern eukaryotic phytoplankton. Science, vol. 305, pp. 354 – 360

Fan, D.-Y.; Hope, A. B; Smith, .P. J.; Jia, H.; Pace, R. J.; Anderson, J. M.; Chow, W. S. (2007) The stoichiometry of the two photosystems in higher plants revisited. Biochimica et Biophysica Acta, vol. 1767, pp. 1064 – 1072

Faraloni, Cecilia; Torzillo, Giuseppe (2013) Xanthophyll cycle induction by anaerobic conditions under low light in *Chlamydomonas reinhardtii*. Journal of applied phycology, vol. 25, pages 1457 – 1471

Feist, Adam M.; Herrgård, Markus J.; Thiele, Ines; Reed, Jennie L.; Palsson, Bernhard Ø. (2009) Nature Reviews. Microbiology, vol. 7, pp. 129 – 143

Finazzi, Giovanni; Furia, Alberto; Barbagallo, Romina Paola; Forti, Giorgio (1999) State transitions, cyclic and linear electron transport and

photophosphorylation in *Chlamydomonas reinhardtii*. Biochimica et Biophysica Acta, vol. 1413, pp. 117 – 129

Finazzi, Giovanni; Rappaport, Fabrice; Furia, Alberto; Fleischmann, Mark; Rochaix, Jean-David; Zito, Francesca; Forti, Giorgio (2002) Involvement of state transitions in the switch between linear and cyclic electron flow in *Chlamydomonas reinhardtii*. EMBO Reports, vol. 3, pp. 280 – 285

Finazzi, Giovanni; Johnson, Giles N.; Dall'Osto, Luca; Zito, Francesca; Bonente, Giulia; Bassi, Roberto; Wollman, Francis-André (2006) Nonphotochemical quenching of chlorophyll fluorescence in *Chlamydomonas reinhardtii*. Biochemistry, vol. 45, pp. 1490 – 1498

Frank, Harry A. Cua, Agnes; Chynwat, Veeradej; Young, Andrew; Gosztola, David; Wasielewski, Michael R. (1994) Photophysics of the carotenoids associated with the xanthophyll cycle in photosynthesis. Photosynthesis Research, vol. 41, pp. 389 – 395

Fujita, Yoshihiko; Ohki, Kaori (2004) On the 710 nm fluorescence emitted by the diatom *Phaeodactylum tricornutum* at room temperature. Plant and Cell Physiology, vol. 45, pp. 392 – 397

Fujita, Yuki; Wakana, Ito; Washiyama, Kento; Shibata, Yutaka (2018) Imaging of intracellular rearrangement of photosynthetic proteins in *Chlamydomonas* cells upon state transition. Journal of Photochemistry & Photobiology, B: Biology, vol. 185, pp. 111 – 116

Gardian, Z.; Bumba, L.; Schrofel, A.; Herbstova, M.; Nebesarova, J.; Vacha, F. (2007) Organisation of photosystem I and photosystem II in red alga *Cyanidium caldarium*: encounter of cyanobacterial and higher plant concepts. Biochimica et Biophysica Acta, vol. 1767, pp. 725 – 731

Gentile, Marie-Pierre; Blanch, Harvey W. (2001) Physiology and xanthophyll cycle activity of *Nannochloropsis gaditana*. Biotechnology and bioengineering, vol. 75, pp. 1 - 12

Gilmore, Adam M.; Mohanty, Narandranath; Yamamoto, Harry Y. (1994) Epoxidation of zeaxanthin and antheraxanthin reverses non-photochemical quenching of photosystem II chlorophyll *a* fluorescence in the presence of trans-thylakoid ΔpH. FEBS Letters, vol. 350, pp. 271 – 274

Gimpel, Javier A.; Nour-Eldin, Hussam H.; Scranton, Melissa A.; Li, Daphne; Mayfield, Stephen P. (2015) Refactoring the six-gene photosystem II core in the chloroplast of the green algae *Chlamydomonas reinhardtii*. American Chemical Society Synthetic Biology, vol. 5, pp. 589 – 596

Gong, Fuyu; Zhu, Huawei; Zhang, Yanping; Li, Yin (2018) Biological carbon fixation: From natural to synthetic. Journal of CO_2 Utilization, vol. 28, pp. 221 – 227

Goss, Reimund; Richter, Michael; Wild, Aloysius (1997) Pigment composition of PSII pigment protein complexes purified by anion exchange chromatography. Identification of xanthophyll cycle pigment binding proteins. Journal of Plant Physiology, vol. 151, pp. 115 – 119

Goss, Reimund; Pinto, Elizabeth Ann; Wilhelm, Christian; Richter, Michael (2006) The importance of a highly active and ΔpH-regulated diatoxanthin epoxidase for the regulation of the PSII antenna function in diadinoxanthin cycle containing algae. Journal of Plant Physiology, vol. 163, pp. 1008 – 1021

Goss, Reimund; Jakob, Torsten (2010) Regulation and function of xanthophyll cycle-dependent photoprotection in algae. Photosynthesis Research, vol. 106, pp. 103 – 122

Goss, Reimund; Lepetit, Bernard (2015) Biodiversity of NPQ. Journal of Plant Physiology, vol. 172, pp. 13 – 32

Govindjee; Papageorgiou, G. (1971) Chlorophyll fluorescence and photosynthesis: fluorescence transients. Photophysiology, vol. 6, pp. 1 – 50

Govindjee (1995) Sixty-three years since Kautsky: Chlorophyll *a* fluorescence. Australian Journal of Plant Physiology, vol. 22, pp. 131 – 160

Govindjee; Shevela, Dmitriy; Björn, Lars Olof (2017) Evolution of the Z-scheme of photosynthesis: a perspective. Photosynthesis Research, vol. 133, pp. 5 – 15

Grossman, Arthur R.; Bartlett, Sue G.; Schmidt, Gregory W.; Mullet, John E.; Chua, Nam-Hai (1982) Optimal conditions for post-translational uptake of proteins by isolated chloroplasts. Journal of Biological Chemistry, vol. 257, pp. 1558 – 1563

Guglielmi, Gérard; Lavaud, Johann; Rousseau, Bernard; Etienne, Anne-Lise; Houmard, Jean; Ruban, Alexander V. (2005) The light-harvesting antenna of the diatom *Phaeodactylum tricornutum*. Evidence for a diadinoxanthin-binding supercomplex. The Federation of European Biochemical Societies Journal, vol. 272, pp. 4339 – 4348

Guihéneuf, Freddy; Stengel, Dagmar B. (2013) LC-PUFA-enriched oil production by microalgae: Accumulation of lipid and triacylglycerols containing *n*-3 LC-PUFA is triggered by nitrogen limitation and inorganic carbon availability in the marine haptophyte *Pavlova lutheri*. Marine Drugs, vol. 11, pp. 4246 – 4266

Gundermann, K.; Büchel, C. (2014). Structure and functional heterogeneity of fucoxanthin-chlorophyll proteins in diatoms. In: Hohmann-Marriott, M. F.

(Ed.): The structural basis of biological energy generation (pp. 27 – 31). Dordrecht, Springer.

Guschina, Irina A.; Harwood, John L. (2006) Lipids and lipid metabolism in eukaryotic algae. Progress in Lipid Research, vol. 45, pp. 160 – 186

Hager, A.; Holocher, K. (1994) Localization of the xanthophyll-cycle enzyme violaxanthin de-epoxidase within the thylakoid lumen and abolition of its mobility by a (light-dependent) pH decrease. Planta, vol. 192, pp. 581 – 589

Haldimann, Pierre; Tsimilli-Michael, Merope (2005) Non-photochemical quenching of chlorophyll *a* fluorescence by oxidized plastoquinone: new evidences based on modulation of the redox state of the endogenous plastoquinone pool in broken spinach chloroplasts. Biochimica et Biophysica Acta, vol. 1706, pp. 239 – 249

Haldrup, Anna; Jensen, Poul Erik; Lunde, Christina; Scheller, Henrik Vibe (2001) Balance of power: a view of the mechanism of photosynthetic state transtions. Trends in Plant Science, vol. 6, pp. 301 – 305

Heather, James M.; Chain, Benjamin (2016) The sequence of sequencers: The history of sequencing DNA. Genomics, vol. 107, pp. 1 – 8

Henry, Christopher S.; DeJongh, Matthew; Best, Aaron A.; Frybarger, Paul M.; Linsay, Ben; Stevens, Rick L. (2010) High-throughput generation, optimization and analysis of genome-scale metabolic models. Nature Biotechnology, vol. 28, pp. 977 – 982

Herbstová, Miroslava; Bína, David; Koník, Peter; Gardian, Zdenko; Vácha, František; Litvín, Radek (2015) Molecular basis of chromatic adaptation in pennate diatom *Phaeodactylum tricornutum*. Biochimica et Biophysica Acta, vol. 1847, pp. 534 – 543

Hoffmann, Mareike; Wagner, Martin; Abbadi, Amine; Fulda, Martin; Feussner, Ivo (2008) Metabolic engineering of ω3-very long chain polyunsaturated fatty acid production by an exclusively acyl-CoA-dependent pathway. Journal of Biological Chemistry, vol. 283, pp. 22352 – 22362

Hohmann-Marriott, Martin F.; Kakizawa, Kenji; Eaton-Rye, Julian J.; Mets, Laurens; Minagawa, Jun (2010) The redox state of the plastoquinone pool directly modulates minimum chlorophyll fluorescence yield in *Chlamydomonas reinhardtii*. Federation of European Biochemical Societies letters, vol. 584, pp. 1021 – 1026

Hohmann-Marriott, Martin F.; Blankenship, Robert E. (2011) Evolution of photosynthesis. Annual Review of Plant Biology, vol. 62, pp. 515 – 548

Hu, Q.; Xiang, W.; Dai, S.; Li, T.; Yang, F.; Jia, Q.; Wang, G.; Wu, H. (2015) The influence of cultivation period on growth and biodiesel properties of microalga *Nannochloropsis gaditana* 1049. Bioresource Technology, vol. 192, pp. 157 – 164

Huang, Wei; Yang, Shi-Jian; Zhang, Shi-Bao; Zhang, Jiao-Lin; Cao, Kun-Fang (2012) Cyclic electron flow plays an important role in photoprotection for the resurrection plant *Paraboea rufescens* under drought stress. Planta, vol. 235, pp. 819 – 828

Huang, Wei; Yang, Ying-Jie; Hu, Hong; Zhang, Shi-Bao (2015) Different roles of cyclic electron flow around photosystem I under sub-saturating and saturating light intensities in tobacco leaves. Frontiers in Plant Science, vol. 6, article 923

Huang, Wei; Yang, Ying-Jie; Hu, Hong; Zhang, Shi-Bao; Cao, Kun-Fang (2016) Evidence for the role of cyclic electron flow in photoprotection for oxygen-evolving complex. Journal of Plant Physiology, vol. 194, pp. 54 – 60

Imam, Saheed; Schäuble, Sascha; Valenzuela, Jacob; de Lomana, Adrián López García; Carter, Warren; Price, Nathan D.; Baliga, Nitin S. (2015) A refined genome-scale reconstruction of *Chlamydomonas* metabolism provides a platform for systems-level analysis. The Plant Journal, vol. 84, pp. 1239 – 1256

Iwai, Masakazu; Takahashi, Yuichiro; Minagawa, Jun (2008) Molecular remodeling of photosystem II during state transitions in *Chlamydomonas reinhardtii*. The Plant Cell, vol. 20, pp. 2177 – 2189

Iwai, Masakazu; Takizawa, Kenji; Tokutsu, Ryutaro; Okamuro, Yuichiro; Minagawa, Jun (2010) Isolation of the elusive supercomplex that drives cyclic electron flow in photosynthesis. Nature, vol. 464, pp. 1210 – 1214

Jagannathan, Bharat; Golbeck, John H. (2009) Understanding of the binding interface between PsaC and the PsaA/PsaB heterodimer in photosystem I. Biochemistry, vol. 48, pp. 5405 – 5416

Jahns, Peter; Latowski, Dariusz; Strzalka, Kazimierz (2009) Mechanism and regulation of the violaxanthin cycle: The role of antenna proteins and membrane lipids. Biochimica et Biophysica Acta, vol. 1787, pp. 3 – 14

Jahns, Peter; Holzwarth, Alfred R. (2012) The role fo the xanthophyll cycle and of lutein in photoprotection of photosystem II. Biochimica et Biophysica Acta, vol. 1817, pp. 182 – 193

Johnson, Giles N. (2011) Physiology of PSI cyclic electron transport in higher plants. Biochimica et Biophysica Acta, vol. 1807, pp. 384 – 389

Johnson, Michael B.; Wen, Zhiyou (2009) Production of biodiesel fuel from the microalga *Schizochytrium limacinum* by direct transesterification of algal biomass. Energy Fuels, vol. 23, pp. 5179 – 5183

Joliot, P.; Joliot A. (1994) Mechanism of electron transfer in the cytochrome b/f complex of algae: evidence for a semiquinone cycle. Proceedings of the National Academy of Sciences of the United States of America, vol. 91, pp. 1034 – 1038

Joshua, Sarah; Mullineaux, Conrad W. (2004) Phycobilisome diffusion is required for light-state transitions in cyanobacteria. Plant Physiology, vol. 135, pp. 2112 – 2119

Karapetyan, Navassard V.; Holzwarth, Alfred R.; Rögner, Matthias (1999) The photosystem I trimer of cyanobacteria:molecular organization, excitation dynamics and physiological significance. Federation of European Biochemical Societies letters, vol. 460, pp. 395 – 400

Kargul, Joanna; Nield, Jon; Barber, James (2003) Three-dimensional reconstruction of a light-harvesting complex I – Photosystem I (LHCI-PSI) supercomplex from the green alga *Chlamydomonas reinhardtii*. The Journal of Biological Chemistry, vol. 278, pp. 16135 – 16141

Kargul, Joanna; Turkina, Maria V.; Nield, Jon; Benson, Sam; Vener, Alexander V.; Barber, James (2005) Light-harvesting complex II protein CP29 binds to photosystem I of *Chlamydomonas reinhardtii* under State 2 conditions. Federation of European Biochemical Societies Journal, vol. 272, pp. 4797 – 4806

Keeling, Patrick J. (2004) Diversity and evolutionary history of plastids and their hosts. American Journal of Botany, vol. 91, pp. 1481 – 1493

Kennedy, Robert A.; Rumpho, Mary E.; Fox, Theodore C. (1992) Anaerobic metabolism in plants. Plant Physiology, vol. 100, pages 1 – 6

Kim, Se-Kwon (Ed.). (2015) *Handbook of marine microalgae*. London, England: Elsevier Academic Press.

Kiss, Anett Z.; Ruban, Alexander V.; Horton, Peter (2009) The PsbS protein controls the organization of the photosystem II antenna in higher plant thylakoid membranes. The Journal of Biological Chemistry, vol. 283, pp. 3972 – 3978

Kodru, Sireesha; Malavath, Tirupathi; Devadasu, Elsinraju; Nellaepalli, Sreedhar; Stirbet, Alexandrina; Subramanyam, Rajagopal; Govindjee (2015) The slow S to M rise of chlorophyll *a* fluorescence reflects transition from state 2 to state 1 in the green alga *Chlamydomonas reinhardtii*. Photosynthesis Research, vol. 125, pp. 219 – 231

Krause, G. H. (1991) Chlorophyll fluorescence and photosynthesis: The basics. Annual Review of Plant Physiology and Plant Molecular Biology, vol. 42, pp. 313 – 349

Kurisu, Genji; Kusunoki, Masami; Katoh, Etsuko; Yamazaki, Toshimasa; Teshima, Keizo; Onda, Yayoi; Kimata-Ariga, Yoko; Hase, Toshiharu (2001) Structure of the electron transfer complex between ferredoxin and ferredoxin-$NADP^+$ reductase. Nature Structural & Molecular Biology, vol. 8, pp. 117 – 121

Kurisu, Genji; Zhang, Huamin; Smith, Janet L.; Cramer, William A. (2003) Structure of the cytochrome b_6f complex of oxygenic photosynthesis: Tuning the cavity. Science, vol. 203, pp. 1009 – 1014

Kuwabara, Tomohiko; Hasegawa, Mika; Kawano, Mitsuko; Takaichi, Shinichi (1999) Characterization of Violaxanthin de-epoxidase purified in the presence of Tween 20: Effects of dithiothreitol and pepstatin A. Plant Cell Physiology, vol. 40, pp. 1119 – 1126

Laisk, Agu; Oja, Vello (2018) Kinetics of photosystem II electron transport: a mathematical analysis based on chlorophyll fluorescence induction. Photosynthesis Research, vol. 136, pp. 63 – 82

Lam, Man Kee & Lee, Keat Teong (2012) Microalgae biofuels: A critical review of issues, problems and the way forward. Biotechnology Advances, vol. 30, pp. 673 – 690

Lamb, Jacob Joseph; Røkke, Gunvor; Hohmann-Marriott, Martin Frank (2018) Chlorophyll fluorescence emission spectroscopy of oxygenic organisms at 77 K. Photosynthetica, vol. 56, pp. 105 – 124

Lambrev, Petar; Nilkens, Manuela; Miloslavina, Yuliya; Jahns, Peter; Holzwarth, Alfred R. (2010) Kinetic and spectral resolution of multiple nonphotochemical quenching components in *Arabidopsis* leaves. Plant Physiology, vol. 152, pp. 1611 – 1642

Lavaud, Johann; Lepetit, Bernard (2013) An explanation for the inter-species variability of the photoprotective non-photochemical chlorophyll fluorescence quenching in diatoms. Biochimica et Biophysica Acta, vol. 1827, pp. 294 – 302

Levering, Jennifer; Broddrick, Jared; Dupont, Christopher L.; Peers, Graham; Beeri, Karen; Mayers, Joshua; Gallina, Alessandra A.; Allen, Andrew E.; Palsson, Bernhard O.; Zengler, Karsten (2016) Genome-scale model reveals metabolic basis of biomass partitioning in a model diatom. Public Library of Science one, vol. 11: e0155038

Lewis, Nathan E.; Schramm, Gunnar; Bordbar, Aarash; Schellenberger, Jan; Andersen, Michael P.; Cheng, Jeffrey K.; Patel, Nilam; Yee, Alex; Lewis, Randall A.; Eils, Roland; Köning, Rainer; Palsson, Bernhard Ø. (2010) Large-scale *in silico* modeling of metabolic interactions between cell types in the human brain. Nature Biotechnology, vol. 28, pp. 1279 – 1285

Li, Xiao-Ping; Phippard, Alba; Pasari, Jae; Niyogi, Krishna K. (2002) Structure-function analysis of photosystem II subunit S (PsbS) in vivo. Functional Plant Biology, vol. 29, pp. 1131 – 139

Li, Xiao-Ping; Gilmore, Adam M.; Caffarri, Stefano; Bassi, Roberto; Golan, Talia; Kramer, David; Niyogi, Krishna K. (2004) Regulation of photosynthetic light harvesting involves intrathylakoid lumen pH sensing by the PsbS protein. The Journal of Biological Chemistry, vol. 279, pp. 22866 – 22874

Li, Zhirong; Peers, Graham; Dent, Rachel M.; Bai, Yong; Yang, Scarlett Y.; Apel, Wiebke; Lionelli, Lauriebeth; Niyogi, Krishna K. (2016) Evolution of an atypical de-epoxidase for photoprotection in the green lineage. Nature Plants, vol. 2, article 16140

Liguori, Nicoletta; Roy, Laura M.; Opacic, Milena; Durand, Grégory; Croce, Roberta (2013) Regulation of light harvesting in the green alga *Chlamydomonas reinhardtii*: The C-terminus of LHCSR is the knob of a dimmer switch. Journal of the American Chemical Society, vol. 135, pp. 18339 – 18342

Litvín, Radek; Bína, David; Herbstová, Miroslava; Gardian, Zdenko (2016) Architecture of the light-harvesting apparatus of the eustigmatophyte alga *Nannochloropsis oceanica*. Photosynthesis Research, vol. 130, pp. 137 – 150

Loira, Nicolás; Mendoza, Sebastian; Cortés, María Paz; Rojas, Natalia; Travisany, Dante; Di Genova, Alex; Gajardo, Natalia; Ehrenfeld, Nicole; Maass, Alejandro (2017) Reconstruction of the microalga *Nannochloropsis salina* genome-scale metabolic model with applications to lipid production. BioMed Central Systems Biology, vol. 11, pp. 66 – 83

Lomoth, Reiner; Magnuson, Ann; Sjödin, Martin; Huang, Ping; Styring, Stenbjörn, Hammarström, Leif (2006) Mimicking the electron donor side of

photosystem II in artificial photosynthesis. Photosynthesis Research, vol. 87, pp. 25 – 40

Lubián, Luis M.; Montero, Olimpio (1998) Excess light-induced violaxanthin cycle activity in *Nannochloropsis gaditana* (Eustigmatophyceae): effect of exposure time and temperature. Phycologia, vol. 37, pp. 16 – 23

Lubián, Luis M.; Montero, Olimpio; Moreno-Garrido, Ignacio; Huertas, Emma; Sobrino, Cristina; González-del Valle, Manuel; Parés, Griselda (2000) *Nannochloropsis* (Eustigmatophyceae) as a source of commercially valuable pigments. Journal of applied phycology, vol. 12, pages 249 – 255

Lubitz, W.; Reijerse, E. J.; Messinger, J. (2008) Solar water-splitting into H_2 and O_2: design principles of PSII and hydrogenases. Energy & environmental science, vol. 1, pages 15 - 31

Lucentini, Jack (2005, June 6). Secondary endosymbiosis exposed. *New Scientist*. Retrieved from https://www.the-scientist.com/research/secondary-endosymbiosis-exposed-48703

MacIntyre, Hugh L.; Kana, Todd M.; Geider, Richard J. (2000) The effect of water motion on short-term rates of photosynthesis by marine phytoplankton. Trends in Plant Science, vol. 5, pp. 12 – 17

Malnoë, Alizée (2018) Photoinhibition of photoprotection of photosynthesis? Update on the (newly termed) sustained quenching component qH. Environmental and Experimental Botany, vol. 154, pp. 123 – 133

Maxwell, Kate; Johnson, Giles N. (2000) Chlorophyll fluorescence – a practical guide. Journal of Experimental Botany, vol. 51, pp. 659 – 668

Mazor, Yuval; Borovikova, Anna; Caspy, Ido; Nelson, Nathan (2017) Structure of the plant photosystem I supercomplex at 2.6 Å resolution. Nature Plants, vol. 3, pp. 1 – 9

McFadden, Geoffrey Ian (2001) Primary and secondary endosymbiosis and the origin of plastids. Journal of Phycology, vol. 37, pp. 951 – 959

Metz, James G.; Pakrasi, Himadri B.; Seibert, Michael; Arntzen, Charles J. (1986) Evidence for a dual function of the herbicide-binding D1 protein in photosystem II. Federation of European Biochemical Societies letters, vol. 205, pp. 269 – 274

Mewes, Heiko; Richter, Michael (2002) Supplementary ultraviolet-B radiation induces a rapid reversal of the diadinoxanthin cycle in the strong light-exposed diatom *Phaeodactylum tricornutum*. Plant Physiology, vol. 130, pp. 1527 – 1535

Miao, Xiaoling; Wu, Qingyu; Yang, Changyan (2004) Fast pyrolysis of microalgae to produce renewable fuels. Journal of Analytical and Applied Pyrolysis, vol. 71, pp. 855 – 863

Miloslavina, Yuliya; Grouneva, Irina; Lambrev, Petar H.; Lepetit, Bernard; Goss, Reimund; Wilhelm, Christian; Holzwarth, Alfred R. (2009) Ultrafast fluorescence study on the location and mechanism of non-photochemical quenching in diatoms. Biochimica et Biophysica Acta, vol. 1787, pp. 1189 – 1197

Minagawa, Jun; Tokutsu, Ryutaro (2015) Dynamic regulation of photosynthesis in *Chlamydomonas reinhardtii*. The Plant Journal, vol. 82, pp. 413 – 428

Mitchell, Peter (1976) Possible molecular mechanisms of the protonmotive function of cytochrome systems. Journal of Theoretical Biology, vol. 62, pp. 327 – 367

Moore, J. M.; Case, D. A.; Chazin, W. J.; Gippert, G. P.; Havel, T. F.; Powls, R.; Wright, P. E. (1988) Three-dimensional solution structure of plastocyanin from the green alga *Scenedesmus obliquus*. Science, vol. 240, pp. 314 – 317

Morris, Jennifer L.; Puttick, Mark N.; Clark, James W.; Edwards, Dianne; Kenrick, Paul; Pressel, Silvia; Wellman, Charles H.; Yang, Ziheng; Schneider, Harald; Donoghue, Philip C. J. (2018) The timescale of early land plant evolution. Proceedings of the National Academy of Sciences of the United States of America, vol. 115, pp. E2274 – E2283

Müh, F.; Glöckner, C.; Hellmich, J.; Zouni, A. (2012) Light-induced quinone reduction in photosystem II. Biochimica et Biophysica Acta, vol. 1817, pp. 44 – 65

Mühlroth, Alice; Li, Keshuai; Røkke, Gunvor; Winge, Per; Olsen, Yngvar; Hohmann-Marriott, Martin F.; Vadstein, Olav; Bones, Atle M. (2013) Pathways of lipid metabolism in marine algae, co-expression network, bottlenecks and candidate genes for enhanced production of EPA and DHA in species of Chromista. Marine Drugs, vol. 11, pp. 4662 – 4697

Mukerji, I; Sauer, K. (1988) Temperature dependent steady state and picosecond kinetic fluorescence measurements of a photosystem I preparation from spinach. Lawrence Berkeley Laboratories, Berkeley, pp. 30

Müller, Patricia; Li, Xiao-Ping; Niyogi, Krishna K. (2001) Non-photochemical quenching. A response to excess light energy. Plant Physiology, vol. 125, pp. 1558 – 1566

Mus, F.; Cournac, L.; Cardettini, V.; Caruana, A.; Peltier, G. (2005) Inhibitor studies on non-photochemical plastoquinone reduction and H2 photoproduction in *Chlamydomonas reinhardtii*. Biochimica et biophysica acta, vol. 1708, pages 322 - 332

Nagao, Ryo; Takahashi, Shuji; Suzuki, Takehiro; Dohmae, Naoshi; Nakazato, Katsuyoshi; Tomo, Tatsuya (2013) Comparison of oligomeric states and polypeptide compositions of fucoxanthin chlorophyll a/c-binding protein complexes among various diatom species. Photosynthesis Research, vol. 117, pp. 281 – 288

Nagy, Gergely; Ünnep, Renáta; Zsiros, Ottó; Tokutsu, Ryutaro; Takizawa, Kenji; Porcar, Linel; Moyet, Lucas; Petroutsos, Dimitris; Garab, Gyözö; Finazzi, Giovanni; Minagawa, Jun (2014) Chloroplast remodelling during state transitions in *Chlamydomonas reinhardtii* as revealed by noninvasive techniques in vivo. Proceedings of the National Academy of Sciences of the United States of America, vol. 111, pp. 5042 – 5047

Naik, S. N.; Goud, Vaibhav V.; Rout, Prasant K.; Dalai, Ajay K. (2010) Production of first and second generation biofuels: A comprehensible review. Renewable and Sustainable Energy Reviews, vol. 14, pp. 578 – 597

Nakamoto, Robert K.; Scanlon, Joanne A. Baylis; Al-Shawi, Marwan K. (2008) The rotary mechanism of the ATP synthase. Archives of Biochemistry and Biophysics, vol. 476, pp. 43 – 50

Navid, Ali; Almaas, Eivind (2012) Genome-level transcription data of *Yersinia pestis* analyzed with a new metabolic constraint-based approach. BioMed Central Systems Biology, vol. 6, pp. 150 – 168

Nawrocki, Wojciech J.; Santabarbara, Stefano; Mosebach, Laura; Wollman, Francis-André; Rappaport, Fabrice (2016) State transitions redistribute rather than dissipate energy between the two photosystems in *Chlamydomonas*. Nature Plants, vol. 2, pp. 1 – 7

Nawrocki, W. J.; Bailleul, B.; Cardol, P.; Rappaport, F.; Wollman, F.-A.; Joliot, P. (2019) Maximal cyclic electron flow rate is independent of PGRL1 in *Chlamydomonas*. Biochimica et Biophysica Acta, vol. 1860, pp. 425 – 432

Nelson, Nathan; Yocum, Charles F. (2006) Structure and function of photosystems I and II. Annual Review of Plant Biology, vol. 57, pp. 521 – 565

Nikolaou, Andreas; Bernardi, Andrea; Meneghesso, Andrea; Bezzo, Fabrizio; Morosinotto, Tomas; Chachuat, Benoit (2015) A model of chlorophyll fluorescence in microalgae integrating photoproduction, photoinhibition and photoregulation. Journal of Biotechnology, vol. 194, pp. 91 – 99

Nilkens, Manuela; Kress, Eugen; Lambrev, Petar; Miloslavina, Yuliya; Müller, Marc; Holzwarth, Alfred R.; Jahns, Peter (2010) Identification of a slowly inducible zeaxanthin-dependent component of non-photochemical quenching of chlorophyll fluorescence generated under steady-state conditions in *Arabidopsis*. Biochimica et Biophysica Acta, vol. 1797, pp. 466 – 475

Nishio, John N.; Whitmarsh, John (1993) Dissipation of the proton electrochemical potential in intact chloroplasts. Plant Physiology, vol. 101, pp. 89 – 96

Oberhardt, Matthew A.; Palsson, Bernhard Ø.; Papin, Jason A. (2009) Applications of genome-scale metabolic reconstructions. Molecular Systems Biology, vol. 5, pp. 1 – 15

Orth, Jeffrey D.; Thiele, Ines; Palsson, Bernhard Ø. (2010) What is flux balance analysis? Nature Biotechnology, vol. 28, pp. 245 – 248

Owens, Thomas G. (1986) Light-harvesting function in the diatom *Phaeodactylum tricornutum*. II: Distribution of excitation energy between the photosystems. Plant Physiology, vol. 80, pp. 739 – 746

Park, Soomin; Steen, Collin J.; Lyska, Dagmar; Fischer, Alexandra L.; Endelman, Benjamin; Iwai, Masakazu; Niyogi, Krishna K.; Fleming, Graham R. (2019) Chlorophyll-carotenoid excitation energy transfer and charge transfer in *Nannochloropsis oceanica* for the regulation of photosynthesis. Proceedings of the National Academy of Sciences of the United States of America, vol. 116, pp. 3385 – 3390

Patil, Vishwanath; Källqvist, Torsten; Olsen, Elisabeth; Vogt, Gjermund; Gislerød, Hans R. (2007) Aquaculture International, vol. 15, pp. 1 – 9

Pfannschmidt, Thomas; Nilsson, Anders; Allen, John F. (1999) Photosynthetic control of chloroplast gene expression. Nature, vol. 397, pp. 625 – 628

Pfündel, Erhard E.; Dilley, Richard A. (1993) The pH dependence of violaxanthin deepoxidation in isolated pea chloroplasts. Plant Physiology, vol. 101, pp. 65 – 71

Plourde, Mélanie; Cunnane, Stephen C. (2007) Extremely limited synthesis of long chain polyunsaturates in adults: implications for their dietary essentiality and use as supplements. Applied Physiology, nutrition, and metabolism, vol. 32, pp. 619 – 634

Pospíšil, Pavel (2009) Production of reactive oxygen species by photosystem II. Biochimica et Biophysica Acta, vol. 1787, pp. 1151 – 1160

Prahl, Scott (2017, June 2). *Chlorophyll a*. Retrieved from http://omlc.org/spectra/PhotochemCAD/html/122.html

Prášil, Ondřej; Kolber, Zbigniew S.; Falkowski, Paul G. (2018) Control of the maximal chlorophyll fluorescence yield by the Q_B binding site. Photosynthetica, vol. 56, pp. 150 – 162

Qin, Xiaochun; Suga, Michihiro; Kuang, Tingyun; Shen, Jian-Ren (2015) Structural basis for energy transfer pathways in the plant PSI-LHCI supercomplex. Science, vol. 348, pp. 989 – 995

Rappaport, Fabrice; Guergova-Kuras, Mariana; Nixon, Peter J.; Diner, Bruce A.; Lavergne, Jérôme (2002) Kinetics and pathways of charge recombination in photosystem II. Biochemistry, vol. 41, pp. 8518 – 8527

Reinhold, Clemens; Niczyporuk, Sylvia; Beran, Karl Christian; Jahns, Peter (2008) Short-term downl-regulation of zeaxanthin epoxidation in *Arabidopsis thaliana* in response to photo-oxidative stress conditions. Biochimica et Biophysica Acta, vol. 1777, pp. 462 – 469

Roberts, A. G.; Bowman, M. K.; Kramer, D. M. (2004) The inhibitor DBMIB provides insight into the functional architecture of the Q_O site in the cytochrome b_6f complex. Biochemistry, vol. 43, pp. 7707 – 7716

Rochaix, Jean-David (2011) Regulation of photosynthetic electron transport. Biochimica et Biophysica Acta, vol. 1807, pp. 375 – 383

Ruban, Alexander V.; Lavaud, Johann; Rousseau, Bernard; Guglielmi, Gerard; Horton, Peter; Etienne, Anne-Lise (2004) The super-excess energy dissipation in diatom algae: comparative analysis with higher plants. Photosynthesis Research, vol. 82, pp. 165 – 175

Ruban, Alexander V. (2017) Quantifying the efficiency of photoprotection. Philosophical Transactions of the Royal Society of London. Series B, Biological Sciences, vol. 372, 20160393

Rushforth, Samuel R.; Johansen, Jeffrey R.; Sorensen, Darwin L. (1988) Occurrence of *Phaeodactylum tricornutum* in the Great Salt Lake, Utah, USA. Great Basin Naturalist, vol. 48, pp. 324 – 326

Sabir, Jamal S. M.; Theriot, Edward C.; Manning, Schonna R.; Al-Malki, Abdulrahman L.; Khiyami, Mohammad A.; Al-Ghamdi, Areej K.; Sabir, Mumdooh J.; Romanovicz, Dwight K.; Hajrah, Nahid H.; El Omri, Abdelfatteh; Jansen, Robert K.; Ashworth, Matt P. (2018) Phylogenetic analysis and a review of the history of the accidental phytoplankter, *Phaeodactylum tricornutum* Bohlin (Bacillariophyceae). Public Library of Science One, vol. 13, e0196744

Schaller, Susann; Latowski, Dariusz; Jemioła-Rzemi, Małgorzatańska; Wilhelm, Christian; Strzałka, Kazimierz; Goss, Reimund (2010) The main thylakoid membrane lipid monogalactosyldiacylglycerol (MGDG) promotes the de-epoxidation of violaxanthin associated with the light-harvesting complex of photosystem II (LHCII). Biochimica et Biophysica Acta, vol. 1797, pp. 414 – 424

Schreiber, Ulrich (1986) Detection of rapid induction kinetics with a new type of high-frequency modulated chlorophyll fluorometer. Photosynthesis Research, vol. 9, pp. 261 – 272

Schreiber, U.; Schliwa, U.; Bilger, W. (1986) Continuous recording of photochemical and non-photochemical chlorophyll fluorescence quenching with a new type of modulation fluorometer. Photosynthesis Research, vol. 10, pp. 51 – 62

Schubert, Hendrik; Sagert, Sigrid; Forster, Rodney Malcolm (2001) Evaluation of the different levels of variability in the underwater light field of a shallow estuary. Helgoland Marine Research, vol. 55, pp. 12 – 22

Schüller, Lisa M.; Schulze, Peter S. C.; Pereira, Hugo; Barreira, Luísa; León, Rosa; Varela, João (2017) Trends and strategies to enhance triacylglycerols and high-value compounds in microalgae. Algal Research, vol. 25, pp. 263 – 273

Schumann, Anika; Goss, Reimund; Jakob, Torsten; Wilhelm, Christian (2007) Investigation of the quenching efficiency of diatoxanthin in cells of *Phaeodactylum tricornutum* (Bacillariophyceae) with different pool sizes of xanthophyll cycle pigments. Phycologia, vol. 46, pp. 113 – 117

Seelert, Holger; Poetsch, Ansgar; Dencher, Norbert A.; Engel, Andreas; Stahlberg, Henning; Müller, Daniel J. (2000) Proton-powered turbine of a plant motor. Nature, vol. 405, pp. 418 – 419

Sétif, Pierre; Fischer, Nicolas; Lagoutte, Bernard; Bottin, Hervé; Rochaix, Jean-David (2002) The ferredoxin docking site of photosystem I. Biochimica et Biophysica Acta, vol. 1555, pp. 204 – 209

Shah, Ab Rauf; Ahmad, Ahmad; Srivastava, Shireesh; Ali, B. M. Jaffar (2017) Reconstruction and analysis of a genome-scale metabolic model of *Nannochloropsis gaditana*. Algal Research, vol. 26, pp. 354 – 364

Shanab, Sanaa M. M.; Mostafa, Soha S. M.; Shalaby, Emad A.; Mahmoud, Ghada I. (2012) Aqueous extracts of microalgae exhibit antioxidant and anticancer activities. Asian Pacific Journal of Tropical Biomedicine, vol. 2, pp. 608 – 615

Shapiguzov, Alexey; Ingelsson, Björn; Samol, Iga; Andres, Charles; Kessler, Felix; Rochaix, Jean-David; Vener, Alexander V.; Goldschmidt-Clermont, Michel (2010) The PPH1 phosphatase is specifically involved in LHCII dephosphorylation and state transitions in *Arabidopsis*. Proceedings of the National Academy of Sciences of the United States of America, vol. 107, pp. 4782 – 4787

Sharma, Kalpesh K.; Schuhmann, Holger; Schenk, Peer M. (2012) High lipid induction in microalgae for biodiesel production. Energies, vol. 5, pp. 1532 – 1553

Shinopoulos, Katherine E.; Brudvig, Gary W. (2012) Cytochrome b_{559} and cyclic electron transfer within photosystem II. Biochimica et Biophysica Acta vol. 1817, pp. 66 – 75

Snellenburg, Joris J.; Wlodarczyk, Lucyna M.; Dekker, Jan P.; Van Grondelle, Rienk; Van Stokkum, Ivo H. M. (2017) A model for the 77K excited state dynamics in *Chlamydomonas reinhardtii* in state 1 and state 2. Biochimica et Biophysica Acta, vol. 1858, pp. 64 – 72

Stock, Daniela; Gibbons, Clyde; Arechaga, Ignacio; Leslie, Andrew G. W.; Walker, John E. (2000) The rotary mechanism of ATP synthase. Current Opinion in Structural Biology, vol. 10, pp. 672 – 679

Sturm, Sabine; Engelken, Johannes; Gruber, Ansgar; Vugrinec, Sascha; Kroth, Peter G.; Adamska, Iwona; Lavaud, Johann (2013) A novel type of light-harvesting antenna protein of red algal origin in algae with secondary plastids. BioMed Central Evolutionary Biology, vol. 13, pp. 159 – 173

Sukenik, A. (1991) Ecophysiological conciderations in the optimization of eicosapentaenoic acid production by *Nannochloropsis* sp. (Eustigmatophyceae). Bioresource technology, vol. 35, pages 263 – 269

Sylak-Glassman, Emily J.; Malnoë, Alizée; De Re, Eleonora; Brooks, Matthew D.; Fischer, Alexandra Lee; Niyogi, Krishna K.; Fleming, Graham R. (2014) Distinct roles of the photosystem II protein PsbS and zeaxanthin in the regulation of light harvesting in plants revealed by fluorescence lifetime snapshots. Proceedings of the National Academy of Sciences of the United States of America, vol. 111, pp. 17498 – 17503

Takahashi, Hiroko; Iwai, Masakazu; Takahashi, Yuichiro; Minagawa, Jun (2006) Identification of the mobile light-harvesting complex II polypeptides for state transitions in *Chlamydomonas reinhardtii*. Proceedings of the National Academy of Sciences of the United States of America, vol. 103, pp. 477 – 482

Takahashi, Shunichi; Bauwe, Hermann; Badger, Murray (2007) Impairment of the photorespiratory pathway accelerates photoinhibition of photosystem II by suppression of repair but not acceleration of damage processes in *Arabidopsis*. Plant Physiology, vol. 144, pp. 487 – 494

Takaichi, Shinichi; Shimada, Keizo (1992) [35] Characterization of carotenoids in photosynthetic bacteria. Methods in Enzymology, vol. 213, pp. 374 – 485

Thiele, Ines; Palsson, Bernhard Ø. (2010) A protocol for generating a high-quality genome-scale metabolic reconstruction. Nature Protocols, vol. 5, pp. 93 – 121

Tikhonov, Alexander N. (2014) The cytochrome b_6f complex at the crossroad of photosynthetic electron transport pathways. Plant Physiology and Biochemistry, vol. 81, pp. 163 – 183

Tymoczko, John L.; Berg, Jeremy M.; Stryer, Lubert (2011). *Biochemistry: A short course, 2nd edition*. W. H. Freeman & Co. Ltd.

Umena, Y.; Kawakami, K.; Shen, J.-R.; Kamiya, N. (2011) Crystal structure of oxygen-evolving photosystem II at a resolution of 1.9 Å. Nature, vol. 473, pp. 55 – 60

Ünlü, Caner; Drop, Bartlomiej; Croce, Roberta; Van Amerongen, Herbert (2014) State transitions in *Chlamydomonas reinhardtii* strongly modulate the functional size of photosystem II but not of photosystem I. Proceedings of

the National Academy of Sciences of the United States of America, vol. 111, pp. 3460 – 3465

Van Amerongen, Herbert; Van Grondelle, Rienk (2001) Understanding the energy transfer function of LHCII, the major light-harvesting complex of green plants. Journal of Physical Chemistry, vol. 105, pp. 604 – 617

Vanthoor-Koopmans, Marieke; Wijffels, Rene H.; Barbosa, Maria J.; Eppink, Michel H. M. (2013) Biorefinery of microalgae for food and fuel. Bioresource Technology, vol. 135, pp. 142 – 149

Vardi, Assaf; Thamatrakoln, Kimberlee; Bidle, Kay D.; Falkowski, Paul G. (2009) Diatom genomes come of age. Genome Biology, vol. 9, pp. 243 – 249

Vernotte, C.; Etienne, A. L.; Briantais, J.-M. (1979) Quenching of the system II chlorophyll fluorescence by the plastoquinone pool. Biochimica et Biophysica Acta, vol. 545, pp. 519 – 527

Vieler, Astrid; Wu, Guangxi; Tsai, Chia-Hong; Bullard, Blair; Cornish, Adam J.; Harvey, Christopher; …; Benning, Christoph (2012) Genome, functional gene annotation, and nuclear transformation of the heterokont oleaginous alga *Nannochloropsis oceanica* CCMP1779. Public Library of Science Genetics, vol. 8, e1003064

Wientjes, Emilie; Croce, Roberta (2012) PMS: Photosystem I electron donor or fluorescence quencher. Photosynthesis Research, vol. 111, pp. 185 – 191

Wikström, Mårten; Krab, Klaas (1986) The semiquinone cycle. A hypothesis of electron transfer and proton translocation in cytochrome *bc*-type complexes. Journal of Bioenergetics and Biomembranes, vol. 18, pp. 181 – 193

Wobbe, Lutz; Bassi, Roberto; Kruse, Olaf (2016) Multi-level light capture control in plants and green algae. Trends in Plant Science, vol. 21, pp. 55 – 68

Wollman, Francis-André (2001) State transitions reveal the dynamics and flexibility of the photosynthetic apparatus. The EMBO Journal, vol. 20, pp. 3623 – 3630

Yamori, Wataru; Shikanai, Toshiharu (2016) Physiological functions of cyclic electron transport around photosystem I in sustaining photosynthesis and plant growth. Annual Review of Plant Biology, vol. 67, pp. 81 – 106

Yeates, Todd O.; Wheatley, Nicole M. (2017) Putting the RuBisCO pieces together. Science, vol. 358, pp. 1253 – 1254

Yoon, Hwan Su; Hackett, Jeremiah D.; Ciniglia, Claudia; Pinto, Gabriele; Bhattacharya, Debashish (2004) A molecular timeline for the origin of photosynthetic eukaryotes. Molecular Biology and Evolution, vol. 21, pp. 809 – 818

Zaks, Julia; Amarnath, Kapil; Kramer, David M.; Niyogi, Krishna K.; Fleming, Graham R. (2012) A kinetic model of rapidly reversible nonphotochemical quenching. Proceedings of the National Academy of Sciences of the United States of America, vol. 109, article number 39

Zelle, Rintze M.; De Hulster, Erik; Van Winden, Wouter A.; De Waard, Pieter; Dijkema, Cor; Winkler, Aaron A.; Geertman, Jan-Maarten A.; Van Dijken, Johannes P.; Pronk, Jack T.; Van Maris, Antonius J. A. (2008) Malic acid production by *Saccharomyces cerevisiae*: Engineering of pyruvate carboxylation, oxaloacetate reduction, and malate export. Applied and Environmental Microbiology, vol. 74, pp. 2766 – 2777

Öqvist, Gunnar; Huner, Norman, P. A. (2003) Photosynthesis of overwintering evergreen plants. Annual Review of Plant Biology, vol. 54, pp. 329 – 355

Paper I

Mar. Drugs **2013**, *11*, 4662-4697; doi:10.3390/md11114662

OPEN ACCESS

marine drugs

ISSN 1660-3397

www.mdpi.com/journal/marinedrugs

Review

Pathways of Lipid Metabolism in Marine Algae, Co-Expression Network, Bottlenecks and Candidate Genes for Enhanced Production of EPA and DHA in Species of Chromista

Alice Mühlroth [1], Keshuai Li [1], Gunvor Røkke [2], Per Winge [1], Yngvar Olsen [1], Martin F. Hohmann-Marriott [2], Olav Vadstein [2] and Atle M. Bones [1,*]

[1] Department of Biology, Norwegian University of Science and Technology, Trondheim 7491, Norway; E-Mails: alice.muehlroth@ntnu.no (A.M.); keshuai.li@ntnu.no (K.L.); per.winge@ntnu.no (P.W.); yngvar.olsen@ntnu.no (Y.O.)

[2] Department of Biotechnology, Norwegian University of Science and Technology, Trondheim 7491, Norway; E-Mails: gunvor.røkke@ntnu.no (G.R.); martin.hohmann-marriott@ntnu.no (M.F.H.-M.); olav.vadstein@ntu.no (O.V.)

* Author to whom correspondence should be addressed; E-Mail: atle.bones@bio.ntnu.no; Tel.: +47-7359-8692; Fax: +47-7359-6100.

Received: 24 September 2013; in revised form: 5 November 2013 / Accepted: 7 November 2013 / Published: 22 November 2013

Abstract: The importance of *n*-3 long chain polyunsaturated fatty acids (LC-PUFAs) for human health has received more focus the last decades, and the global consumption of *n*-3 LC-PUFA has increased. Seafood, the natural *n*-3 LC-PUFA source, is harvested beyond a sustainable capacity, and it is therefore imperative to develop alternative *n*-3 LC-PUFA sources for both eicosapentaenoic acid (EPA, 20:5*n*-3) and docosahexaenoic acid (DHA, 22:6*n*-3). Genera of algae such as *Nannochloropsis*, *Schizochytrium*, *Isochrysis* and *Phaedactylum* within the kingdom Chromista have received attention due to their ability to produce *n*-3 LC-PUFAs. Knowledge of LC-PUFA synthesis and its regulation in algae at the molecular level is fragmentary and represents a bottleneck for attempts to enhance the *n*-3 LC-PUFA levels for industrial production. In the present review, *Phaeodactylum tricornutum* has been used to exemplify the synthesis and compartmentalization of *n*-3 LC-PUFAs. Based on recent transcriptome data a co-expression network of 106 genes involved in lipid metabolism has been created. Together with recent molecular biological and metabolic studies, a model pathway for *n*-3 LC-PUFA synthesis in *P. tricornutum* has been proposed, and is compared to industrialized species of Chromista. Limitations of the *n*-3 LC-PUFA synthesis by enzymes such as thioesterases, elongases, acyl-CoA

synthetases and acyltransferases are discussed and metabolic bottlenecks are hypothesized such as the supply of the acetyl-CoA and NADPH. A future industrialization will depend on optimization of chemical compositions and increased biomass production, which can be achieved by exploitation of the physiological potential, by selective breeding and by genetic engineering.

Keywords: *Phaeodactylum tricornutum*; long chain polyunsaturated fatty acid synthesis; metabolic engineering; elongases; desaturases; acyl-CoA synthetases; acyltransferases

---

Fatty Acid Nomenclature and Abbreviations

ADA, adrenic acid (22:4*n*-6); ALA, α-linolenic acid (18:3*n*-3); ARA, arachidonic acid (20:4*n*-6); DGLA, dihomo-γ-linolenic acid (20:3*n*-6); DHA, docosahexaenoic acid (20:6*n*-3); DPA, docosapentaenoic acid (22:5*n*-3); EDA, eicosadienoic acid (20:2*n*-6); EPA, eicosapentaenoic acid (20:5*n*-3); ETA, eicosatetraenoic acid (20:4*n*-3); ETrA, eicosatrienoic acid (20:3*n*-3); FA(s), fatty acid(s); GLA, γ-linolenic acid (18:3*n*-6); HAD, hexadecadienoic acid (16:2*n*-4); HTA, hexadecatrienoic acid (16:3*n*-4); LA, linoleic acid (18:2*n*-6); LC-PUFA(s), long chain polyunsaturated fatty acid(s), >C20; MA, myristic acid (14:0); OA, oleic acid (18:1*n*-9); PA, Palmitic acid (16:0); POA, Palmitoleic acid (16:1*n*-7); PONA, palmitolenic acid (16:2*n*-7); PUFA(s), polyunsaturated fatty acid(s), >C18; SA, stearic acid (18:0); STA, stearidonic acid (18:4*n*-3); THA, tetracosahexaenoic acid (24:6*n*-3).

1. Introduction

Long chain polyunsaturated *n*-3 fatty acids (LC-PUFAs) are of increasing interest, due to their many positive effects for human health and their use as feed for fish farming. Until now, seafood has been the main source of *n*-3 LC-PUFAs; however, as seafood harvesting is at peak production, alternative sustainable sources for *n*-3 LC-PUFAs should be developed. Most fishes cannot produce *n*-3 LC-PUFAs themselves, but are channelled up the marine food chain, with microalgae as the primary producers [1]. Therefore, it is not surprising that marine microalgae have been targeted as potential candidates for industrial production of *n*-3 LC-PUFAs such as eicosapentaenoic acid (EPA, 20:5*n*-3) and docosahexaenoic acid (DHA, 22:6*n*-3) [2–5].

Many of the *n*-3 LC-PUFA-producing algae belong to the Chromista kingdom, a diverse group of microorganisms that includes divisions like cryptomonads, haptophytes and heterokonts [6]. The classification is based on the hypothesis that chloroplasts of all Chromista arose from a single secondary endosymbiotic event between a eukaryote and a red alga-like organism [6,7]. Interestingly, the heterotrophic thraustochytrid, also belonging to Chromista, have lost their photosynthetic capacity but have retained a vestigial chloroplast and their ability to synthesize and store *n*-3 LC-PUFAs, as chloroplasts are the site of lipid synthesis in alga.

At present, mostly thraustochytrids like *Schizochytrium* spp. are used in industrial-scale *n*-3 LC-PUFA production as they can reach a DHA content of 43% (cell dry weight) and have a

productivity of up to 7.2 g of DHA per liter of culture and per day [8,9]. The close relationship between the thraustochytrids and photosynthetic microalgae of the Chromista kingdom suggests a high potential for these microalgae as an alternative *n*-3 LC-PUFA source in the future. Additionally, algae have advantages such as consuming carbon dioxide, growing in salt water on marginal land and thereof no compete with the agriculture industry or freshwater use [10]. The major genera of commercial microalgae are to date Chromista [11–13]. EPA-producing heterokonts include the photoautotrophic commercial-used *Nannochloropsis* spp. [14], *Monodus subterraneus* [15], *Nitzschia* spp. [16] and the model diatom *Phaeodactylum tricornutum* [17]. Whereas DHA-producers include *Isochrysis galbana* [11,18] and the thraustochytrids *Aurantochytrium* spp. [19], *Thraustochytrium* spp. [11,12], and *Schizochytrium* spp. [20]. The amount of *n*-3 LC-PUFAs produced by these organisms depends on the environmental conditions. Exposing the algae to environmental stresses such as nitrate starvation [17], increased salinity [20], changes in light intensity [15] or variations in the amount and composition of carbon [14,20] can increase both lipid synthesis and accumulation and also the composition of *n*-3 LC-PUFAs themselves. Several recent reviews have dealt with this topic for different algae [9,21–25]. For instance, the eustigmatophyceae *Nannochloropsis* has under mild growth conditions an EPA content of 1.6% of cell dry weight, while subjecting *Nannochloropsis oceanica* to high light and N-limitation an EPA content of 2.6% (cell dry weight) can be reached [14,18,26]. However, the low production of *n*-3 LC-PUFAs per culture volume and day, mainly due to low biomass density, makes photosynthetic production of *n*-3 LC-PUFA not profitable at present [13].

To improve the *n*-3 LC-PUFAs or the lipid bodies, triacylglycerides (TAGs), productivity in algae two main strategies exist; (1) Increase the content of desired lipids per unit of biomass and (2) Increase the biomass density of the given strain to maximize biomass per culture volume or area. Optimization of growth conditions that increase *n*-3 LC-PUFAs is challenging, as LC-PUFAs and TAGs accumulate under abiotic stress, which in turn decreases the biomass yield. Besides optimizing physical growth conditions approaches such as selection/breeding and metabolic engineering can be used to enhance the lipid yield. These high level skill approaches have advantages and disadvantages, while genetic engineering requires significant resources in establishing a suitable transformation of functional plasmids, selection processes require a sustainable breeding and selecting program [21,22]. A combination of approaches like metabolic engineering and selective breeding have been shown to be successful in plants by genetic engineering of *n*-3 LC-PUFAs and classical mutation strategies to bypass bottlenecks [23–25]. Successful approaches must be based on identification of genetic drivers influencing both qualitative and quantitative aspects of the lipid metabolism in Chromista. Even though genetic drivers are applicable for different approaches, we will in this review focus on the metabolic engineering approach because it has been discussed by Khozin-Goldberg *et al.* (2011) as a strategy to obtain a high yield of *n*-3 LC-PUFA by microalgae and reviews focused on engineering of lipid metabolism in algae with emphasis on TAG accumulation [22,27–30].

In this review, we address the synthesis and compartmentalization of *n*-3 LC-PUFAs in Chromista by mapping the lipid metabolism for the model diatom *P. tricornutum*. Genomic data have been analyzed and a co-expression network has been assembled. Several pathways have been predicted and candidate genes and bottlenecks were identified in order to find strategies for improve the *n*-3 LC-PUFAs in commercially used Chromista such as *Nannochloropis* or *Isochrysis*. In doing so, we

have identified and compared parts of the known EPA and DHA pathways of biotechnological important Chromista species which differ from the lipid pathway of *P. tricornutum*.

2. Long Chain Polyunsaturated Fatty Acids (LC-PUFAs) for Human Health

Linoleic acid (LA, 18:2*n*-6) and α-linolenic acid (ALA, 18:3*n*-3) are essential fatty acids (FAs) for vertebrates [31,32] and are precursors for the LC-PUFA of the *n*-6 group arachidonic acid (ARA, 20:4*n*-6) and of the *n*-3 group EPA and DHA. Humans have the capability to synthesize EPA (20:5*n*-3) and DHA (22:6*n*-3) from ALA (18:3*n*-3), but the capacity is too low to provide sufficient amounts of these *n*-3 LC-PUFAs for maintenance of mental and cardiovascular health [33,34]. Some fresh water and diadromous fish species may survive on diets containing only C18 PUFA, whereas marine fish have a strict requirement for long chain PUFAs that e.g. play important roles in osmoregulation for animals in different aquatic environments [32]. ARA (20:4*n*-6), EPA (20:5*n*-3) and DHA (22:6*n*-3) are also required for normal growth, development of specific and nonspecific immunity, and stress tolerance of marine fish, especially at early stages [35–37].

The membranes of the brain contain high amounts of ARA (20:4*n*-6) and DHA (22:6*n*-3) in the phospholipids, and are important for optimal visual and cognitive development and functioning. Fish larvae and human infants have high requirement of LC-PUFA, probably due to an immature digestive/absorptive system and the need for fast growth and development, especially for neural and visual tissues [38]. The beneficial health effects of *n*-3 FAs, particularly *n*-3 LC-PUFAs, have been extensively studied [13,39–41]. Positive effects include anti-viral, anti-bacterial and anti-fungal effects [42,43]. These benefits appear to be related to the alternations of fluidity in membrane phospholipids composition and function, gene expression and eicosanoid production [44]. In general, it is recommended to increase the dietary *n*-3 FAs intake for the human population, but the recommendations vary in different countries because of different dietary background and cultural traditions [45,46]. For instance, the American Dietetic Association recommends 500 mg/day of EPA + DHA [47], whereas the Norwegian authorities propose 250 mg/day of EPA + DHA for older children and adults and 0.5 E% (percent of total energy intake) of total *n*-3 FAs, 0.10 g/day of DHA (22:6*n*-3) for infants and small children (6–24 months) [48]. Beside the absolute amount of PUFAs that is required, the ratio of *n*-6/*n*-3 FAs is considered to be very important for development and health of both humans and fish. EPA (20:5*n*-3) and ARA (20:4*n*-6) are precursors for the synthesis of hormones named eicosanoids which are involved in many cell regulatory functions. EPA-derived eicosanoids have potent anti-angiogenic effects, whereas ARA-derived metabolites have pro-angiogenic effects. Because EPA (20:5*n*-3) and ARA (20:4*n*-6) compete for the common enzymes, cyclooxygenases, lipooxygenases, and cytochrome P450, the ratio between *n*-6 and *n*-3 FAs seems to determine the ratio of the respective enzymatic products, EPA (20:5*n*-3) and ARA (20:4*n*-6) derived eicosanoids [44,49,50]. The ratio of *n*-6/*n*-3 FAs in typical Western diets is 15/1–16.7/1, whereas it is suggested that humans evolved on a diet with a ratio close to 1 [40]. A ratio of *n*-6/*n*-3 of 4:1 or less seems to reduce the risk of many chronic diseases, such as cardiovascular disease, colorectal cancer, breast cancer and asthma [40].

An overview of the content of *n*-6 and *n*-3 PUFAs in different organisms and food sources reveals that the *n*-6/*n*-3 ratios of commonly farmed and wild fish species in Norway and frequently used

marine microalgae is in general very low (<1:2), whereas the ratio in red meat, chicken and plant oils is high (>4:1; Figure 1). A high percentage of *n*-3 FAs, e.g., >20%, is only found in marine organisms, and none of the marine organisms contain >15% *n*-6 FAs.

Figure 1. *n*-6 fatty acids (%) *versus* *n*-3 fatty acids (%) in different food sources and microalgae [51–56].

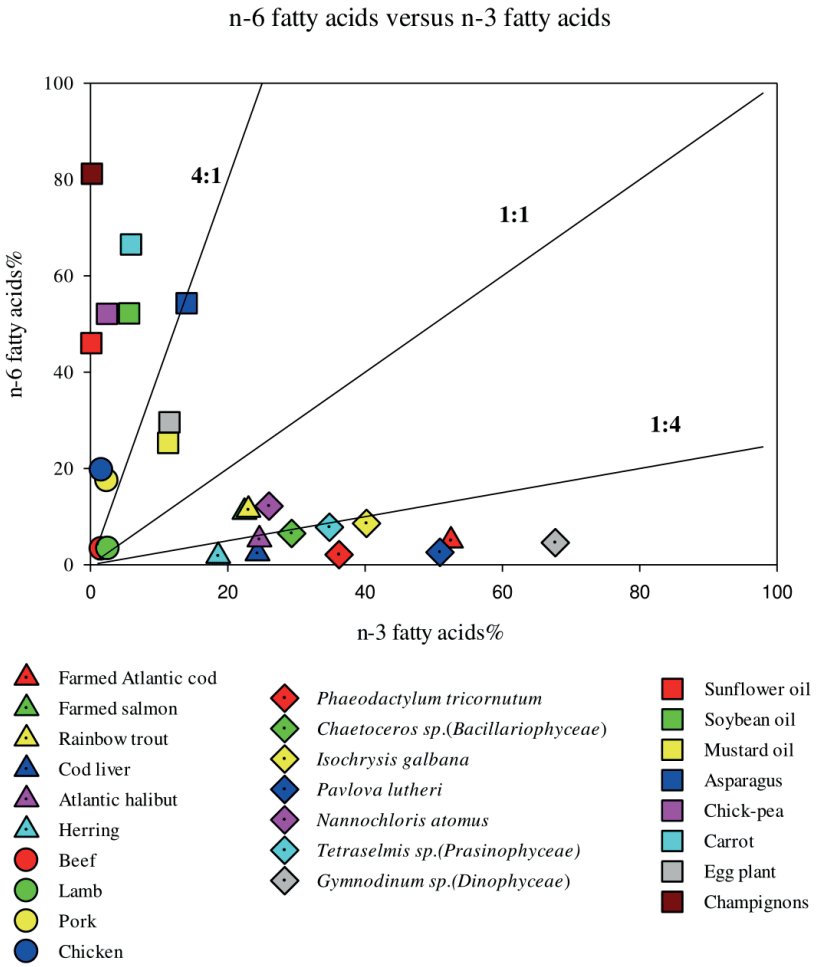

3. LC-PUFA Sources and the Need for Alternatives

The main source of *n*-3 LC-PUFAs for human consumption is currently marine fish and in particular the fish oils of fat fish. The world capture fisheries have remained stable since 1990, whereas aquaculture production has increased strongly [57]. The global production of fish oil decreased from 1.6 million tons in the late 1980s to 1 million tons in 2012, of which about 7% was used for human consumption and about 88% was used for aquaculture [48]. During the last decades, the aquaculture industry has started to replace fish oil and fish meal with plant seed meals and

vegetable oils in order to secure growth in the production [58,59]. Studies suggest that salmonids and gilthead sea bream can be grown with 100% of blended vegetable oils, without any serious effect on growth rates [60,61]. However, the EPA (20:5*n*-3) and DHA (22:6*n*-3) levels in the flesh of the fish fed were reduced by feeding high levels of vegetable oils, and the beneficial effects of fish consumption to the human consumer is therefore reduced [32]. Meanwhile, the positive health effects of the *n*-3 PUFAs, especially EPA (20:5*n*-3) and DHA (22:6*n*-3) have become widely accepted, and the human consumption for *n*-3 PUFAs in various products is increasing. Fortified foods (milk, yogurt, eggs and breads) and dietary supplements (cod liver oil, fish oil capsules) with oils that are rich in EPA (20:5*n*-3) and DHA (22:6*n*-3) have become widely used [62]. As traditional fisheries cannot increase in size, there is a search for alternative *n*-3 LC PUFA sources for the future expansion of both marine aquaculture and human consumptions. Proposed alternatives are large stocks of herbivore copepods, krill in the world's oceans and microalgae [34,58].

4. Chromista and Their LC-PUFA Content and Function

Chromista include promising candidate species for commercial production of *n*-3 LC-PUFA but a deeper understanding of the synthesis, composition and function of fatty acids (FAs) in algae is needed for a knowledge-based future industrial production. In general, saturated and monounsaturated FAs are predominant in the FA profile of Chromista, and with a minor amount of ARA (20:4*n*-6) and a high level of one *n*-3 LC-PUFA, EPA (20:5*n*-3) and DHA (22:6*n*-3). The total FA composition is highly variable from species to species. In this section an overview of LC-PUFA occurrence in Chromista cells and the function of LC-PUFAs will be given.

LC-PUFAs in Chromista are mainly associated with the membranes or found in the storage compartments as TAGs. Membrane systems in algae can be divided into the photosynthetic active thylakoid membrane and the structural membranes surrounding compartments for example the chloroplast or the endoplasmic reticulum (ER). In membrane lipids, PUFAs are esterified to glycerol and further processed to produce polar lipids.

In both the thylakoid and the non-photosynthetic membrane, the betaine-type glycerolipids (e.g., diacylglyceryltrimethylhomoserine (DGTS), diacylglycerylhydroxy-methyltrimethylalanine (DGTA) and diacylglycerylcarboxyhydroxymethylcholine (DGCC)) and the phosphoglycerides (e.g., phosphatidylcholine (PC) and phosphatidylethanolamine (PE)) are present [63]. The special component of the photosynthetic membrane is phosphatidylglycerol (PG) [27]. In all eukaryotic photosynthetic organisms, PGs contain an uncommon Δ^3-trans hexadecenoic acid (16:1(3-t)) at their *sn*-2 position. PG-16:1(3-t) plays an important role in the LHCII trimerisation process and in the function of the photosystem [64]. The major components of the photosynthetic membrane are the glycosylglycerides, which are mainly uncharged polar lipids and far more abundant than phosphoglycerides. The glycosylglycerides vary in abundance from species to species [65]. Apparently diatoms possess negatively charged galactosylglycerides because of their higher levels of anionic sulphoquinovosyldiacylglycerol (SQDG) than land plants [66]. Monogalactosyldiacylglycerol (MGDG) and digalactosyldiacylglycerol (DGDG) are neutral lipids and contain either one or two galactose molecules linked to the *sn*-3 position of the 1,2-diacyl-*sn*-glycerol moiety [27]. Thus, FAs occupy the *sn*-1 and *sn*-2 positions, and the FA composition at these positions can be highly variable.

Examples of PUFA distribution in different Chromista such as *N. oculata*, *P. tricornutum*, *Pavlova lutheri* and *M. subterraneus* under different environmental conditions are given in Figure 2. Figure 2 shows obvious differences in FA composition, for instance, *Pavlova lutheri* sustain high amount of DHA (22:6*n*-3), whereas *P. tricornutum* mostly contains EPA (20:5*n*-3).

Figure 2. Content of LC-PUFAs of different lipid classes in selected Chromistans under different environmental conditions. Due to the experimental setups of the referred papers, not all lipid classes of the organisms could be assembled. *Monodus subterraneus* [67], *N. oculata* [68], *Pavlova lutheri* [69], *P. tricornutum* [70]. Blue: ARA (20:4*n*-6); red: EPA (20:5*n*-3); green: DHA (22:6*n*-3). MGDG: monogalactosyldiacylglycerol; NL: neutral lipids; DGCC: diacylglycerylcarboxyhydroxymethylcholine; DGDG: digalactosyldiacylglycerol; DGGA: diacylglyceryl glucuronide; DGTS: diacylglyceryl trimethylhomoserine; DGTA: diacylglycerylhydroxymethyl-trimethylalanine; SQDG: sulfoquinovosyldiacylglycerol; PC: phosphatidylcholine; PE: phosphatidylethanolamine; PG: phosphatidylglycerol.

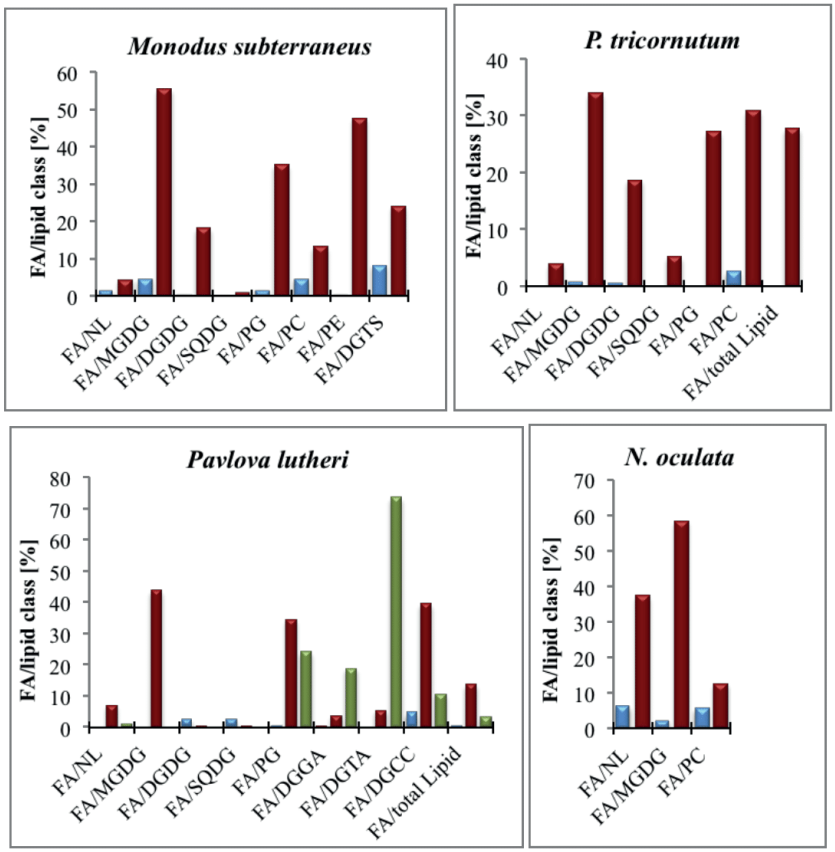

Some diatoms, for instance, *P. tricornutum* and *Thalassiosira weissflogii*, contain *n*-3 LC-PUFA primarily in C20/C16 and C18/C16 forms of MGDG and DGDG; whereas the pennate diatom *Navicula perminuta* produce only C18/C16 and C18/C18 forms [71]. In plants, the FA combination of the galactosylglycerides can be traced back to their biosynthetic pathways; the so-called eukaryotic molecular species (C18/C18) of galactosylglycerides are synthesized outside the chloroplast in the eukaryotic pathway and the prokaryotic molecular species (C18/C16) are synthesized plastidial via the prokaryotic pathway [72]. Whereas in plants, clear separation of the galactosylglyceride origin is given, in algae most C20 FAs are synthesized outside of the chloroplast and are present in both molecular species of galactosylglycerides: the eukaryotic-like (C20/C20, C18/C18) and the prokaryotic-like (C18/C16, C20/C16) species [67,73]. Therefore, in algae it is suggested to refer to species of galactosylglycerides as "C20/C20" or "C20/MLC" (MLC = medium to long chain) rather than to eukaryotic- and prokaryotic-like molecular species [67]. In Chromista, the biological function of different combinations of FAs in galactosylglycerides remains unclear, but it will certainly affect the overall PUFA distribution and composition of the cell. However, some observations in other algae may be relevant. For instance in the red algae *Porphyridium curentum* a shift to lower temperatures decreases C20/C20 MGDG and increases C20/C16 MGDG [74]. This observation may be interpreted as a response to adjust the membrane fluidity of photosynthetic membranes. PUFAs in membranes are also important for adjusting membrane fluidity during shifts in salinity and light intensity [75]. It has been shown that a temperature-shift from 25 to 10 °C will enhance the proportion of PUFAs, especially EPA, by 120% in *P. tricornutum* [76].

TAGs are another but less likely *n*-3 LC-PUFA source in oleaginous algae. Most algae accumulate saturated and monounsaturated FAs in the TAGs under certain stress conditions such as P- and N-limitation and cell division arrest [77,78]. For example, in the eustigmatophyceae *N. oceanica* TAG accumulation increases while the EPA amount declines by 30% during N-deprivation [79]. Contrary to this, an increase in TAGs and incorporation of EPA in TAGs was observed in the diatom *T. pseudomonas* in the stationary growth phase [77]. TAGs are collected in lipid bodies in the cytoplasma and belong to the neutral or non-polar lipids together with, e.g., waxes, free FAs, and sterols [29]. Sukenik *et al.* (1991) proposed that TAG accumulation occurs in non-stress conditions during the day when cell division is at rest in order maximize harvest of photons and CO_2 fixation [4]. The energy stored in TAG can be used to supply energy and reduced carbon in the dark phase. TAGs serve as a sink for excess electrons and bind and accumulate reduced carbon. Imbalance of the cellular C:N ratio, which occurs for example under N-limitation, leads to a rearrangement of the molecular pools. Whether carbohydrates or lipids are used as carbon/energy storage is dependent on the algae strain, the photosynthetic activity and environmental conditions [80,81]. In some algae, the major carbohydrate storage is the glucose polymer chrysolaminarin, which is used in heterokons such as the diatoms *Nitzschia sigmoida* and *Melosira varians* [82,83]. When cell division is not possible, the conversion of light energy into reduced carbon components, *i.e.*, fatty acids provides a useful mechanism to convert energy harvested by the photosynthetic machinery. The reduction of CO_2 to the redox state of carbohydrates requires 2 mol of NADPH and ~3 mol of ATP, whereas the reduction of CO_2 to the redox state of saturated fatty acids requires ~3 mol NADPH and ~4 mol ATP [84]. In addition to carbon and energy storage, the FA moieties of the lipid bodies are required for both the synthesis and the remodeling of PUFA rich thylakoid membranes [29].

PUFAs in algae possess several specific functions. One known function is to scavenge reactive oxygen, which interacts with the double bonds of the PUFA. This process, called lipid peroxidation, may play a role as an intermediate in cell signaling pathways [85]. Polar lipids such as inositol lipids or sphingolipids are also involved in such pathways [65]. Because LC-PUFAs are enriched in galactosylglycerides such as SQDG and M/DGDG in the thylakoid membranes, it is assumed that they contribute to the photosynthetic function of algae. For instance, studies of the green algae *Chlamydomondas reinhardtii* showed the importance of the glycosylglyceride SQDG for maintaining photosystem II functionality during environmental changes (e.g., temperature), and thus indicates, as well, a role of PUFAs in maintaining the photosynthetic machinery [75].

Advances in utilizing environmental factors to increase *n*-3 LC-PUFA in Chromista have been made, but in many cases the mechanisms behind this physiological plasticity, including regulation at the transcriptional level, are not understood. Information gained on the molecular level, could allow adaptation of algae, by selective breeding, metabolic engineering and physiological studies, as a *n*-3 producer on an industrial scale.

5. Eicosapentaenoic Acid (EPA, 20:5*n*-3) Synthesis in *Phaedoactylum tricornutum*

There are many studies of lipid accumulation in algae but there is still limited knowledge on the molecular mechanisms and the transcriptional regulations of the lipid metabolism. To exemplify the *n*-3 LC-PUFA synthesis and to find bottlenecks of the pathway, the model organism *P. tricornutum* has been used to assemble recent knowledge and to point out genetic drivers. For a better evaluation of the involvement of TCA cycle intermediates in the FA synthesis, studies of different Chromista have been included in the following section.

Phaedactylum tricornutum is one of the diatoms best studied at the molecular level. This is due to the sequencing of the 27.45 Mb genome in 2008 [86]. Several studies have been published that have used transcriptomics (microarrays, RNAseq) in combination with metabolomics and related them to physiological/biochemical responses of the photosynthetic system, the lipid metabolism and the carbon flux network [17,87–89]. It has been shown that *P. tricornutum* tends to reduce carbohydrate content and increase lipid content under nitrogen starvation compared to non-nutrition limitation, indicating a metabolic switch to lipid accumulation [80,90]. To get more insights into the transcriptional regulation of genes involved in the FA metabolism we performed a co-expression study based on assembled microarray data available on the Gene Expression Omnibus (GEO), NCBI, from the model organism *P. tricornutum*. The unweighted co-expression network (see Figure 3) identified 106 genes that encode enzymes coupled to the FA metabolism and the tricarboxylic acid (TCA) cycle. DiatomCyc [91] and Kyoto Encyclopedia of Genes and Genomes [92] were used for identification of the co-expression cluster, for biochemical pathway analysis, and for protein identification. In the following paragraphs, the genes identified in the *n*-3 LC-PUFAs synthesis and the co-expression cluster (Figure 3) will be discussed. An overview of the primary lipid metabolism in most Chromista, including synthesis of FAs, TAGs and *n*-3 LC-PUFAs, required cofactors, and the end products are presented in Figure 4.

Figure 3. Co-expression network of 106 genes associated to the FA metabolism in *P. tricornutum*. The co-expression network can visually be divided into two subclusters. Subcluster 1 (blue, left square) contains mainly genes of the mitochondrial TCA cycle and β-oxidation. Subcluster 2 (red, right square) includes genes of the plastidial-located *de novo* FA synthesis and the endoplasmatic *n*-3 LC-PUFA biosynthesis. Color code: TAG biosynthesis (light purple); TCA cycle (red); ACCase (acetyl-CoA carboxylase); *de novo* FA and HTA (16:3*n*-4) synthesis (light blue); Predicted elongases and desaturases (dark blue); Predicted EPA pathway (turquoise); Acetyl-CoA precursors and transporter (light red); Acyl-CoA synthetases, ATpase4 (gray); Mitochondrial or peroxisomal located β-oxidation and FA elongation (yellow); Kennedy pathway, phospholipid-, glycerolipids, sphingolipid and sterol biosynthesis (green); Ca^{2+}-dependent lipid-binding protein, amid hydrolase, DHHC palmitoyltransferase, serine incorporator, ATP-binding protein (ABC) transporter (purple). Shapes in the cluster indicate the localization of enzymes encoded by the gene: Triangle, mitochondria; Square, chloroplast; Diamond, peroxisome; Circle, no prediction. Transcription data of five microarray datasets from *P. tricornutum* submitted to GEO, NCBI (GSE12015, GSE17237, GSE31131, GSE42039 and GSE42514; [93–97]) were used to construct based on log2 expression ratios from the experiments, an unweighted co-expression network by using Cytoscape (version 2.8.3) and the force directed drawing algorithm [98]. The network represents 106 genes related to lipid metabolism with similar transcriptional profiles and includes 311 calculated gene-pairs with Pearson correlation values $r > 0.85$.

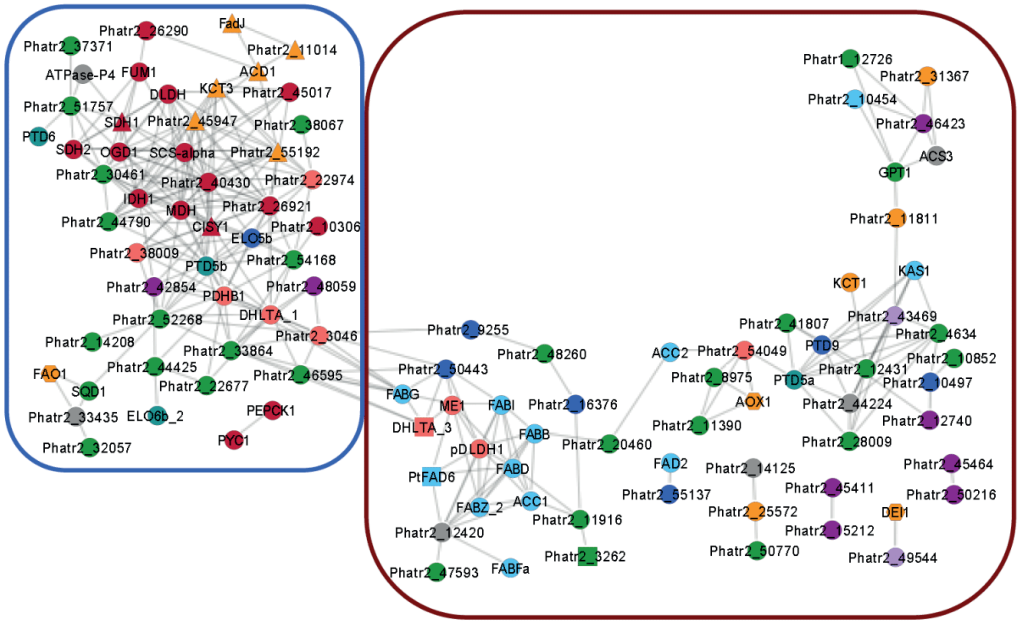

Figure 4. Simplified overview of the compartments, the main pathways and the metabolites in most Chromista; calvin cycle, fatty acid synthesis, tricarboxylic acid cycle, polyunsaturated FA pathway, β-oxidation and lipid synthesis shown in black arrows. Involved enzymes are shown in red: ACCase, acetyl-CoA carboxylase; ACS, Acyl-CoA synthetase, ACP, acyl carrier protein; CoA, coenzyme A; ATP:CL, ATP-citrat lyase; ENR, enoyl-ACP reductase; FAT, fatty acyl-ACP thioesterase; HD, 3-hydroxyacyl-ACP dehydratase; KAR, 3-ketoacyl-ACP reductase; KAS, 3-ketoacyl-ACP synthase; LACS, long chain acyl CoA synthetase; MAT, malonyl-CoA:ACP transacylase; ME, malic enzyme; PDC, pyruvate dehydrogenase complex; PUFA, polyunsaturated fatty acid; TAG, triacylglyceride; TCA, tricarboxylic acid. Different MEs possess different localizations (plastidial, mitochondrial). For simplicity, ME is placed in the cytosol. Modified after [22,65,99].

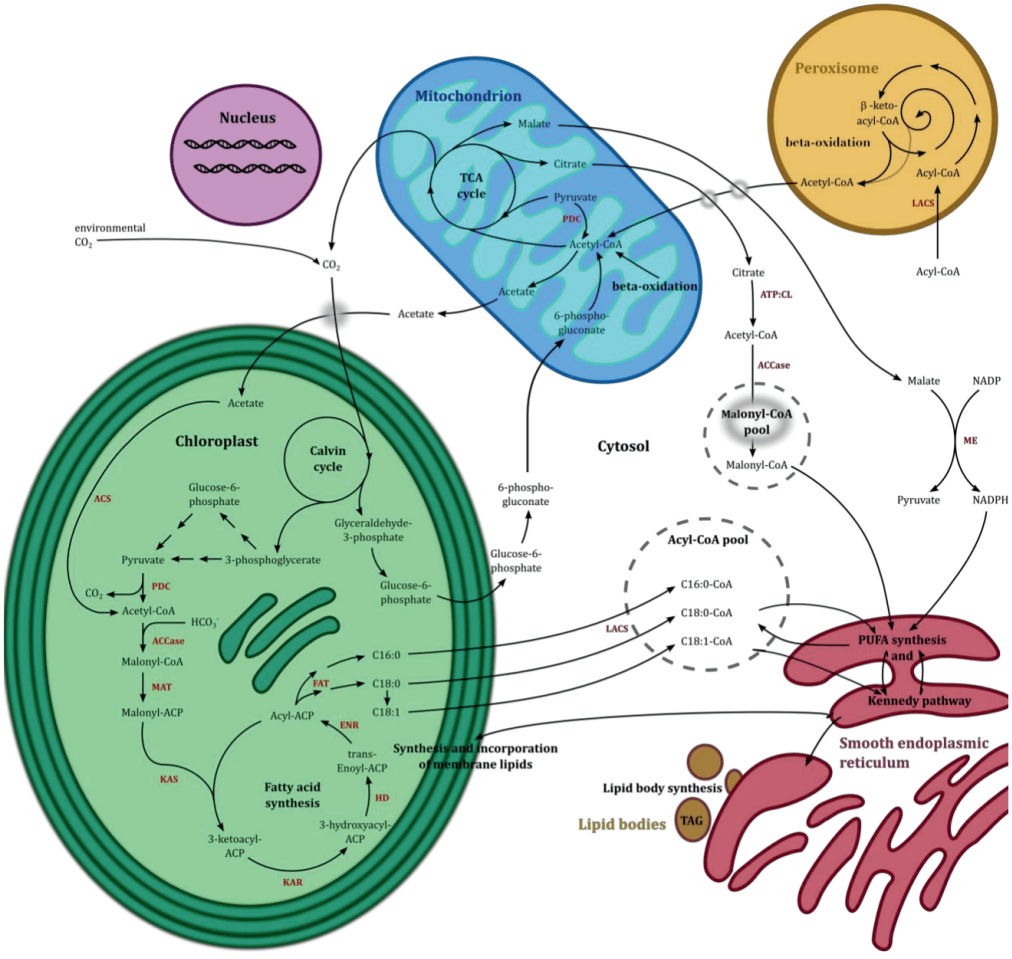

5.1. The TCA Cycle and β-Oxidation

To supply the cell with energy and reduced carbon, pyruvate is converted to acetyl-CoA, which enters the TCA cycle to form ATP and carbon skeletons for the anabolic pathways. In *P. tricornutum* the genes encoding enzymes of the TCA cycle show a diurnal regulation pattern when the algae are grown in a day/night cycle [97]. An increased activity of the TCA genes at the beginning of the dark period and co-regulation with genes coupled to cell division suggests that the TCA cycle provide energy for the cell division processes [97]. During the day when cells received their energy via photosynthesis, the TCA cycle associated genes exhibited limited regulation [97]. Figure 4 illustrates that acetyl-CoA is the precursor for both the TCA cycle and the FA synthesis, and that the intermediates of the TCA cycle can be precursors and cofactors in the FA synthesis. Because of this versatile role, the genes of the TCA cycle were included in the cluster analysis. The cluster analysis reveals that the TCA cycle genes had a high degree of co-expression with genes coupled with the FA metabolism. By visual inspection, the cluster can be divided into two subclusters (see Figure 3). Also, genes encoding for mitochondrial enzymes involved in both the FA elongation (C4 < *n* < C16) and the β-oxidation are in this cluster. Whereas oxidation of FA in algae can take place in the mitochondria and the peroxisome, Subcluster 1 represents mostly genes encoding enzymes of the mitochondrial β-oxidation (*ACD1*, *FadJ*, *Phatr2_55192* (enoyl-CoA hydratase), *Phatr2_45947* (3-ketoacyl-CoA thiolase) and *KCT3*). A tight co-regulation between genes coupled to the β-oxidation and the TCA cycle as shown in the cluster is likely, and it has been suggested that oxidation of FAs most likely provides the TCA cycle with acetyl-CoA during dark periods without photosynthetic activity [97]. Malate represents an intermediate of the TCA cycle and can deliver CO_2 for the plastidial Ribulose-1,5-bisphosphate carboxylase (Rubisco) by the activity of the malic enzymes (ME) [100]. The NAD(P)-dependent ME catalyzes the conversion of malate to pyruvate and provides NAD(P)H for the cell. The irreversible decarboxylation products NAD(P)H and pyruvate can be utilized in the FA synthesis. An overexpression of ME in fungus and yeast species increases the accumulation of lipids [101]. Availability of NADPH can increase the reaction velocity of NADPH-requiring enzymes involved in FA synthesis such as acetyl-CoA carboxylase (ACCase) and ATP citrate lyase (ATP:CL) (Figure 4). FA synthesis is an energy demanding process due to the activity of elongases and desaturases. For instance, the formation of a C18 FA requires 54 NADPH from oxygenic photosynthesis [17]. Biochemical studies with the eustigmatophyceae *N. salina*, grown in batch and continuous cultures, indicated that lipid accumulation is controlled by the availability of NADPH [99]. Transcriptomic studies in N-depleted cells of *P. tricornutum* showed strong up-regulation of the gene producing a predicted plastidial NADP-dependent ME (*Phatr2_51970*) [17]. Such findings indicate that the ME genes are involved in lipid synthesis of *P. tricornutum*. Overexpression of the *Phatr2_51970* may be one avenue to provide electrons which can be channeled into FA synthesis. Mitochondrial malate can also be converted in the mitochondrion or cytosol into pyruvate [99,100]. Therefore, predicted mitochondrial NAD(P)-dependent ME are encoded by *Phatr2_27477* and *ME1* (*Phatr2_54082*), the latter being part of Subcluster 1.

Another intermediate of the TCA cycle serving as a precursor for the *n*-3 LC-PUFA synthesis is citrate. Kinetic profiles and activity studies have revealed that the eustigmatophyceae *N. salina* is able

to convert sugar via citrate to lipids [99]. A high activity of ATP-citrate lyase (ATP:CL), encoded by *ACL*, may provide acetyl-CoA for the FA synthesis.

Mixotrophic grown cultures of heterokonts such as *Nannochloropsis* sp., *Dictyopteris membranacea*, *Navicula saprophila* and *P. tricornutum* can incorporate acetate directly into lipids [87,102–104]. The acetyl-CoA synthetase (ACS) converts acetate to plastidial acetyl-CoA (Figure 4). In *Nannochloropsis* sp., the acetate uptake is light-dependent. In [^{14}C]-acetate labeling studies more than half of the acetate was incorporated into long chain FAs and PC [14,103]. When acetate is abundant in mixotrophic conditions, the lipid levels and subsequently the EPA levels increased by 25% in *N. saprophila* (phototrophic conditions: 27.2 and mixotrophic; 34.6 mg EPA/g biomass) [102].

To conclude, our data shows that the genes of the TCA cycle are co-expressed with the genes of the FA synthesis and may therefore be targeted to improve lipid production.

5.2. De Novo *Fatty Acid Synthesis and Hexadecatrienoic Acid Synthesis*

The *de novo* FA synthesis and further processing of one of the most abundant FA in *P. tricornutum*, hexadecatrienoic acid (16:3*n*-4), takes place in the plastid [105]. Thus, acetyl-CoA is the starting point for the FA synthesis in the chloroplast and the ER. Plastidial and cytosolic acetyl-CoA can be provided by the conversion of pyruvate, citrate or acetate. Acetyl-CoA in turn is then converted by the acetyl-CoA carboxylase (ACCase) to malonyl-CoA. In eukaryotes, the ACCase possesses three functional domains; one *N*-terminal biotin carboxylase, one central acetyl-CoA carboxylase and one C-terminal α-carboxyltransferase domain (α-CT). In most plants, the ACCase has an additional chloroplast-encoded subunit, the β-carboxyltransferase (β-CT). To our knowledge, this subunit has not been reported in Chromista which all have homomeric ACCases. The three domains of the homomeric ACCase are located on a multifunctional polypeptide encoded by a nuclear gene [106]. The diatoms *T. pseudonana* and *P. tricornutum* contain two homomeric ACCases, one in the plastid (*ACC1*) and the other in the cytosol (*ACC2*) [106]. The haptophyte *I. galbana*, in turn, has only one plastidial homomeric ACCase. In plants and maybe also in Chromista, the plastidial ACCase (*ACC1*) converts malonyl-CoA for the *de novo* FA synthesis, whereas the cytosolic ACCase (*ACC2*) generates a malonyl-CoA pool as intermediates for the FA elongation [107]. In the co-expression network, both genes are present in Subcluster 2. Although the ACCase is an important enzyme in *de novo* FA synthesis, increased expression of the plastidial ACCase gene *acc1* of the diatoms *Cyclotella cryptica* and *N. saprophila* did not result in increased FA content, indicating inhibition of regulatory processes within the FA synthesis [108,109].

P. tricornutum possesses the type II fatty acid synthase (FAS) with discrete, monofunctional enzymes encoded by distinct genes [110]. In the FA biosynthesis pathway, malonylation of malonyl-acyl carrier protein (malonyl-ACP) is carried out by malonyl-CoA:ACP transacylase encoded by *FABD*. Malonyl-ACP is used in the cyclic condensation reactions to extend the acyl group to middle chain length fatty acids (<C18) in the prevalent, plastidial *de novo* FA synthesis [111,112]. The prolonged acyl-ACP is released for further processing by an acyl-ACP thioesterase located in the chloroplast envelope. This thioesterase (TE) has not been characterized in *P. tricornutum*.

Figure 5. Overview of FA and LC-PUFA synthesis in *P. tricornutum.* Shown are the hypothetical *de novo* fatty acid synthesis (FAS) and the HTA (16:3*n*-4) synthesis plastidial (green) and the EPA (20:5*n*-3) synthesis at the ER membrane (blue) with further incorporation at the *sn*-1 and *sn*-2 position of glycosylglycerides (in plastid or Kennedy pathway in ER). Purple: Long chain acyl-coenzyme A (CoA) synthetases (LACS), lysophospholipid acyltransferases (LPLAT), acyl-CoA:glycerol-3-phosphate acyltransferase (GPAT) and acyl-CoA:lysophosphatidic acyltransferase (LPAAT), phosphatidic acid phosphatase (PAP), elongases (Elo) and desaturases (ΔD or ωD); Red: putative genes, enzymes encoded by genes that have been identified are marked in bold. The other genes are predicted for EPA synthesis from transcriptional data. The co-factors for the desaturases are not indicated. At the ER, the FA are available as acyl-CoA or linked to a glycerol-backbone such as PC indicated by F. MGDG is indicated by a glycerol-backbone with a framed G. Before and after elongation, the FA has to be de-linking and re-linking from the glycerol-backbone indicated with two consecutive arrows. Question marks indicate that the reaction and the involved enzymes are not predicted. Modified after [28,113].

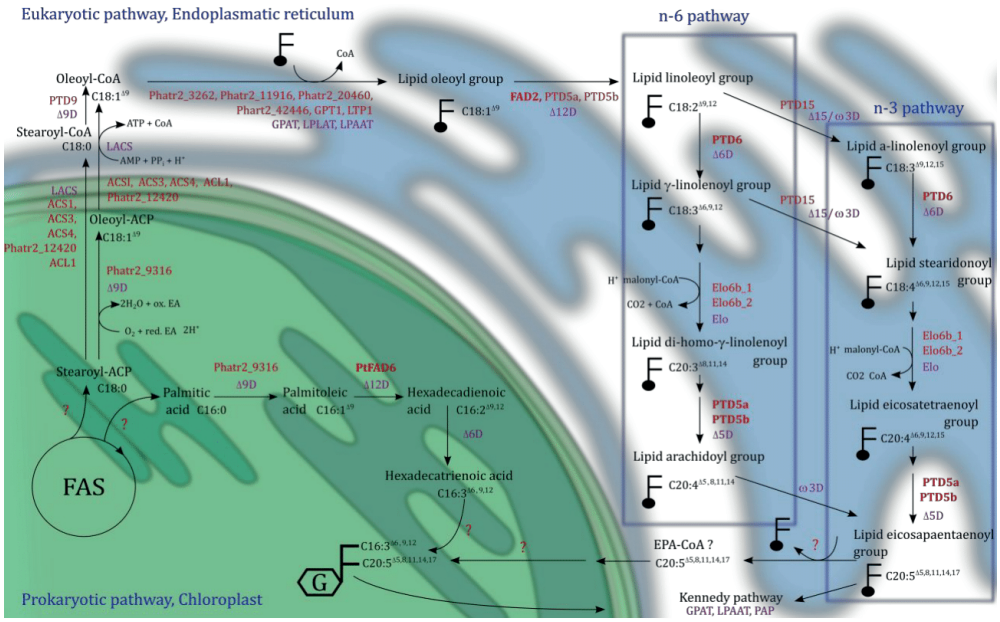

In the presence of oxygen, desaturases can saturate FAs into unsaturated FAs. Two types of desaturases can be distinguished; (1) The front-end desaturase contains an *N*-terminal cytochrom b5-domain and inserts the new double bond between the FA carboxyl group and a possible existing double bond. (2) The ω6/ω3 desaturase inserts a new double bond between the FA methyl end and a pre-existing double bond [114]. An example for an identified front-end desaturase in *P. tricornutum* is the high substrate specific plastidial-located Δ12 desaturase, PtFAD6, synthesizes palmitoleic acid (POA, 16:1*n*-7) to hexadecadienoic acid (HAD, 16:2*n*-4), indicated in Figure 5 [105]. Figure 5 shows

the synthesis of FA in *P. tricornutum*, especially the putative EPA (20:5*n*-3) and HTA (16:*3n*-4) pathway and genes, which have been either identified or predicted to be involved in these pathways.

Ten out of 12 genes involved in the *de novo* FA and HTA synthesis show a tight co-regulation in Subcluster 2. In the day/night cycle study, these genes as well as *Phatr2_9316* and *Phatr2_50443* showed a strong co-regulation pattern [97]. The maximum expression level of these genes in the beginning of the light period indicates that the FA synthesis uses electrons generated by the photosynthetic machinery. Throughout the day, when energy is needed in other processes, genes coupled to the FA synthesis are downregulated. In the beginning of the light period no neutral lipids were detected [97]. This may support the suggestion that increased availability of NADPH could lead to higher synthesis of FAs.

5.3. Acyl-CoA Activator and EPA Synthesis

FA synthesis, membrane glycerolipid synthesis, and β-oxidation require the FA to be present in the acyl-CoA form [115]. The acyl-coenzyme A (CoA) synthetases (ACS) regulate in each compartment the internal acyl-CoA pools by esterification of FAs to CoA. The localization of the pools is maintained due to acyl-CoAs not being able to cross the intracellular membranes [116]. In *P. tricornutum* genes encoding, five long chain acyl-CoA synthetases (LACS) have been predicted (*ACS1*, *ACS3*, *ACS4*, *ACL1* and *Phatr2_12420*). The ATP citrate lyase *ACL1* contains a predicted peroxisomal targeting signal, whereas the other LACS genes exhibit no predicted transmembrane domain, and their localizations are unclear. To our knowledge, the predicted LACSs of *P. tricornutum* have not been functionally characterized.

The cytosolic acyl-CoA pool provides C18 FAs for the extra-chloroplastic EPA synthesis. During the EPA synthesis, the characterized membrane-bound desaturases PTD5, PTD6 and FAD2 appear to be located in the ER membrane and facing the cytosol (Figure 5) [113]. Desaturation of stearic acid (SA, 18:0) to oleic acid (OA, 18:1*n*-9) can take place through a Δ9 desaturase in the chloroplast or the cytosol in *P. tricornutum*. In the plastid, the stearoyl-ACP Δ9 desaturase (*Phatr2_9316*) could convert the reaction, whereas the ER-bound Δ9 desaturase PTD9 may be responsible for the endoplasmatic desaturation by utilizing acyl-CoA as the substrate. Transport of either SA (18:0) or OA (18:1*n*-9) into the cytosol and subsequent activation by the ACSs is necessary. Except the Δ9 desaturase *Phatr2_9316*, ER-located desaturases utilize acyl-lipids (FAs linked to the glycerol-backbone PC) as substrates [28,70,113]. In addition to the chemical character of the glycerol-backbone, the *sn*-position at the molecule also influences desaturation, *i.e.*, the PTD5 and PTD6 had the highest desaturation activity toward the *sn-2* position at PC. However, the Δ12 desaturase FAD2, encoded by *FAD2*, desaturates different glycerol-backbones such as PC and MGDG with similar efficiency [113]. FAD2 possesses high substrate specificity towards OA (18:1*n*-9) (50% conversion) [105]. The acyltransferases residing in the ER are required for the esterification of FAs to the desired *sn*-position of the glycerol-backbone. Most likely the acyltransferases involved in the *n*-3 LC-PUFA synthesis are similar to those in plants (lysophospholipid acyltransferases (LPLAT), acyl-CoA:glycerol-3-phosphate acyltransferase (GPAT) and acyl-CoA:lysophosphatidic acyltransferase (LPAAT)) [117,118]. The latter two represent enzymes of the Kennedy pathway in the ER [119]. One candidate LPLAT (encoded by *Phatr2_20460*) and a LPAAT (encoded by *Phatr2_45551*) have been found in

P. tricornutum, as well as several GPATs; *GPT1*, *LTP1*, *Phatr2_3262*, *Phatr2_11916*, *Phatr2_42446*. Acyltransferases in microalgae are not well characterized. Therefore, it is uncertain to what extend they control the lipid composition by substrate specificity and relative activity, but a high influence in *n*-3 LC-PUFA synthesis is predicted [118,120].

In *P. tricornutum* EPA is most likely synthesized via a combination of the *n*-6 and *n*-3 pathway [105]. According to Domergue *et al.* (2003), PTD6 converts linoleoyl-PC (18:2*n*-6) to the γ-linolenoyl-PC (GLA, 18:3*n*-6), which then is catalyzed to stearidonoyl-PC (STA, 18:4*n*-3) by a Δ15/ω3 desaturase [121]. To be elongated, the FA has to be transferred from the acyl-glycerol-backbone to the acyl-CoA form and afterwards esterified back to the glycerol-backbone by lipase and acyltransferases activities, respectively. Due to the substrate preference of elongases and the need of malonyl-CoA and NADPH, elongases are generally limiting factors in pathway fluxes [25]. The Δ6 elongases in *P. tricornutum* encoded by *ELO6b_1* and *ELO6b_2* are utilizing acyl-CoA as substrate and prolong stearidonoyl-PC (STA, 18:4*n*-3) to eicosatetraenoyl-PC (ETA, 20:4*n*-3). The last desaturation step through the PTD5 desaturase leads to formation of eicosapentaenoyl-PC (EPA, 20:5*n*-3) [121]. Five genes predicted to be involved in the EPA pathway (*FAD2*, *PTD6*, *PTD5b*, *PTD5a*, *ELO6b_2*) have highly co-regulated expression patterns (Figure 3). An alternative *n*-3 pathway involving a Δ9 elongase and Δ8 desaturase was suggested by Arao T. *et al.* (1994) after a ^{14}C-FA pulse-chase experiment [122]. In this pathway, ALA (18:3*n*-3) is elongated to eicosatrienoic acid (ETrA, 20:3*n*-3) and further desaturated to ETA (20:4*n*-3), which then is desaturated by PTD5 to EPA (20:5*n*-3). Enzymes involved in this Δ9 elongase and Δ8 desaturase pathway are not identified in *P. tricornutum*, but might be among the elongases and desaturases predicted in Table 1.

Table 1. Predicted elongases and desaturases in *P. tricornutum* shown with gene number, enzyme name and predicted annotation. Information collected from NCBI, Diatomcyc and KEGG.

Gene Number	*Enzyme Name*	*Annotation*	**Present in Cluster (Figure 3)**
Elongases predicted to be membrane bound			
Phatr2_16376	-	Long chain fatty acid elongase	√
Phatr2_9255	-	Polyunsaturated fatty acid elongase	√
Phatr2_49867	-	Long chain fatty acid elongase	
Phatr2_34485	Elo5b	Long chain fatty acid elongases, membrane bound	√
Phatr2_25360	-	Probably a short-chain dehydrogenase/reductase	
Desaturases predicted to be microsomal or membrane bound			
Phatr2_55137	-	Fatty acid desaturase	√
Phatr2_50443	-	Fatty acid desaturase, cytochrome b5 motif	√
Phatr2_46275	-	Fatty acid desaturase, putative	
Phatr2_44622	-	Fatty acid desaturase	
Phatr2_22510	-	Fatty acid desaturase, cytochrome b5 motif	

P. tricornutum possesses diverse pathways for EPA synthesis but with few characterized enzymes. The complexity of the pathway originates from the elongation and desaturation steps and the substrate specificities of the associated enzymes which have to switch between the acyl-CoA and acyl-glycerol-backbone pools.

5.4. EPA Incorporation into Galactosylglycerides and Triacylglycerides

After elongation and desaturation, EPA is incorporated into the membrane. Although the final location of EPA is to be incorporated into a lipid class, different paths can be perceived as dependent on whether EPA is available as a free FA or linked to a glycerol-backbone. Preferences for the EPA trafficking require further investigation, because it is a complex process. This is especially the case in algae like Chromista where the chloroplasts have four membranes. Free EPA will be linked to PE, PC or DGTS molecules, and then processed through the Kennedy pathway or imported into the plastid and incorporated into glycolipids [123,124]. In the Kennedy pathway, GPAT performs the initial step by adding acyl-CoA to the *sn*-1 position of the glycerol-3-phosphate [119]. The lysophosphatidic acid (LPA) formed is converted by lysophosphatidate acyltransferase (LPAAT) into phosphatidic acid (PA) by adding a second FA to the *sn*-2 position. Diacylglycerol (DAG) is formed by dephosphorylation of the *sn*-3 position through the activity of phosphatidic acid phosphatase (PAP) [119]. PA and DAG as well as other phospholipids can act as precursors for the production of sulfolipids and galactosylglycerides [29]. The incorporation of EPA in sulfolipids is processed by sulfolipid sulfoquinovosyldiacylglycerol synthase (SQD2). MGD and DGD synthases, which also mediate remodeling of membrane lipids in plants, catalyze the final step to synthesize MGDG and DGDG [125]. Several putative genes involved in phospholipid, sulfolipid and galactosylglyceride synthesis as well as in the Kennedy pathway are co-expressed within the cluster *(Phatr2_20460*, *Phatr2_12431*, *Phatr2_33864*, *SQD1*, *Phatr2_33864*, *Phatr2_11390*, *Phatr2_54168*, *Phatr2_14125*). Additionally, three genes encoding glycerol-3-phosphate dehydrogenases are also expressed within the cluster (*Phatr2_12726*, *Phatr2_38067*, *Phatr2_8975*). The glycerol-3-phosphate dehydrogenases produce glycerol-3-phosphate from an intermediate of the glycolysis.

TAGs in *P. tricornutum* are a second EPA pool that is not commonly found in all algae. TAG accumulation mostly occurs under sub-optimal environmental conditions. It is generally assumed that only small amounts of EPA are incorporated into TAGs via synthesis of EPA. Remodeling of FAs from membranes is the main contributor of EPA in TAG [87]. Alternative pathways to convert membrane lipids to TAGs have been shown in both eukaryotes and prokaryotes, and involve phospholipase and phospholipid/diacylglycerol acyltransferase (PDAT). Mus *et al.* (2013) showed that the expression of a PDAT and/or a putative phospholipases increased in *P. tricornutum* under nitrogen starvation, and remodeling of lipid classes such as PC, PE or galactosylipids contributed to lipid accumulation [87]. To regulate EPA production, it is important to understand the mechanisms that determine in what lipid fraction EPA is present. EPA is not present as a free FA but is either incorporated in the membranes or accumulated in TAG.

5.5. Genetic Drivers for n-*3 LC-PUFA Synthesis*

It is important to identified genetic drivers for increased *n*-3 LC-PUFA synthesis as they can be used in different optimization approaches such as selective breeding, conditioning and metabolic engineering to enhance the *n*-3 LC-PUFA production in Chromista. Genetic transformation methods based on overexpression and knockdown techniques are already developed for *P. tricornutum* [126,127]. Thus, metabolic engineering approaches may be pursued to increase the amount of EPA (20:5*n*-3).

According to Hoffman *et al.* (2008), five main strategies are applicable for engineering of the FA synthesis in both plants and yeast; (1) Increasing the precursor pool, (2) Inhibition of β-oxidation or lipase hydrolysis, (3) Overexpression of FA biosynthetic enzymes, (4) Regulation of thioestarase (TE) for optimizing the FA chain length, and (5) Regulation or introduction of desaturases to control the saturation profile [25].

Following these strategies in *P. tricornutum*, several target genes can be identified partly from the co-expression cluster and from the literature. Strategy 1 has a wide range of targets. Increasing availability of NADPH by overexpression of the ME produced by *Phatr2_51970* might be suitable to provide reduction equivalents for FA synthesis [17]. Overexpressing acetyl-CoA by *ACL* (ATP:CL) and *Phatr2_22974* (acetyl-CoA synthetase) may establish a larger acetyl-CoA pool in the plastid and the cytosol, respectively [22,99]. A larger precursor-pool may also require an increase in transporters, such as the putative plastidal sodium-dependent pyruvate transporter (*Phatr2_3046*) and the acetyl-CoA transporter (*Phatr2_54049*). Both these transporters show co-expression in Subcluster 2 (Figure 3). Also, a possible bottleneck in *n*-3 LC-PUFA synthesis is the qualitative and quantitative acyl-CoA pool. The acyl-CoA pool in turn is dependent on the activity of LACSs regulating the activation of free FAs. In order to provide a suitable acyl-CoA pool the specific activities of LACSs from *P. tricornutum* have to be characterized. Potential targets are the putative *ACS3* and *Phatr2_12420*, which are co-regulated in the Subcluster 2 (Figures 3 and 5). Several ACS in different Chromista have been isolated and characterized already [128]. When a LACS from *N. oculata* was expressed in a LACS-deficient *Saccaromyces cerevisiae* strain, it showed high activity for long chain FA such as eicosadienoic acid (EDA, 20:2*n*-6), LA (18:2*n*-6), SA (18:0) and middle chain unsaturated FA [129]. Reverse transcription-PCR analysis of two LACSs from *Thalassiosira pseudonana* encoded by *TplacsA* and *TplacsI* appeared to be constitutively expressed during cell cultivation [130]. Co-expression of *TplacsI* in a yeast deletion strain (faa4D) TpLACSA showed a broad substrate specificity by inducing the formation of several PUFAs (18:3*n*-6, 18:4*n*-3, 20:4*n*-6, 20:5*n*-3, 22:6*n*-3), but with highest activity towards DHA (22:6*n*-3). The TpLACSA has been shown to be active during the incorporation of DHA in TAGs [130]. Due to their high substrate specificity, LACS are after identification suitable target genes for increasing the synthesis of PUFAs [109]. Overexpression of TpLACSA from *T. pseudonana* might improve the incorporation and production of *n*-3 LC-PUFAs in *P. tricornutum*.

Genes of the β-oxidation pathway are suitable targets for creating knockdown mutants (Strategy 2), but complete elimination of the lipid degradation path may lead to negative effects on the growth and the health of the cell [22,131]. For example, in *Arabidopsis thaliana* the gene-knockouts of both peroxisomal LACS involved in β-oxidation resulted in an alteration of the FA composition, (an increase of monounsaturated long chain FA) and growth inhibition, which was compensated by supply of an external carbon source [131]. Most genes in β-oxidation of *P. tricornutum* are single copy genes. Therefore, knockouts of peroxisomal or mitochondrial localized genes such as *ACD1* and *FAO1* would probably be lethal and strategies of inhibiting β-oxidation might not be suited for *P. tricornutum*. Initial activation of β-oxidation in plants and yeast involves import of FA into the peroxisome by an ATP-binding cassette (ABC) transporter and activation of these FAs by ACSs [131,132]. A similar system of peroxisomal transport and the activation of FAs might also exist in *P. tricornutum* via the

peroxisomal located LACS encoded by *ACL1* and an ABC transporter. LACS as well as an ABC transporter (encoded by *Phatr2_15212*) are co-regulated in the cluster (Figure 3).

If other strategies are used, overexpression of genes in type II FAS (Strategy 3) is probably not required in *P. tricornutum* for increasing *n*-3 LC-PUFA synthesis, because if enough energy and precursors are supplied, an upregulation of genes encoding enzymes involved in *de novo* FA synthesis might occur naturally. For instance, in the beginning of the light period, the FA synthesis is upregulated to serve as a sink for excess electrons [97].

In Strategy 4, the feedback inhibitions caused by long chain fatty acyl-ACPs can be suppressed by overexpression of acyl-ACP TE [109,133]. Overexpression of the acyl-ACP TE with specificity for long chain FAs (18:0, 18:1) may improve the *n*-3 LC-PUFA synthesis. A positive effect of TEs on FA compositions was shown by overexpression of acyl-ACP TE specific for shorter chain FA from plants in *P. tricornutum*, resulting in an increase of saturated FAs for TAG assembling [109]. Gong *et al.* (2011) characterized a 4-hydroxybenzoyl-CoA thioesterase PtTE (*Phart2_33198*) from *P. tricornutum*, with an *N*-terminal mitochondrial targeting peptide [134]. Overexpression in *Escherichia coli* showed activity for C18:1-ACP and lower activity for saturated FAs (16:0, 18:0). Overexpression of *Phart2_33198* (PtTE) in *P. tricornutum* increased the total FA content up to 72%. While PA (16:0) and POA (16:1*n*-7) showed a higher content, EPA (20:5*n*-3) showed only a minor increase [134]. So far no plastidial acyl-ACP TE involved in *n*-3 LC-PUFA synthesis has been identified.

Strategy 5 is based on the regulation and overexpression of desaturases to change the FA profile. Desaturases and elongases from *P. tricornutum* that are not functionally characterized or predicted to be involved in a specific pathway are listed in Table 1 and represent potential targets for identification and later on overexpression. Targets for modifying desaturation activity may be *Phatr2_50443* and *Phatr2_55137*. Interestingly, *P. tricornutum* possesses only one ER acyl-CoA Δ9 desaturase and one plastidial acyl-ACP Δ9 desaturase (Figure 5), whereas in the diatom *Fistulifera* sp., six Δ9 desaturases have been functionally characterized [135]. Four desaturases showed acyl-CoA- and two acyl-ACP dependent Δ9 desaturation activity for C16 and/or C18 FAs, indicating that this diatom has more genes for a possible sustainable FA synthesis [135]. Putative FA elongases encoded by *Phatr2_9255* and *Phatr2_16376* indicated by co-expression in the cluster are additional potential targets (Table 1 and Figure 3). In general, the rate-limiting factor of PUFA production in transgenic plants are acyl-CoA dependent elongases, because of the inefficient exchange of acyl molecules back and forth between the desaturation and elongation steps [25]. An advantage would be if the *n*-3 LC-PUFA pathway possesses acyl-CoA-dependent Δ6 and Δ5 desaturases, similar to mammalian desaturases. However, such acyl-CoA-dependent Δ6 and Δ5 desaturases have only been identified in green algae species, and successfully expression resulting in an increase of the *n*-3 LC-PUFA level has only been seen in plants [25,136].

Regulation of the transesterification steps might be an alternative target for overcoming the elongation bottleneck and could be consider as an additional strategy to the strategy of Hoffmann *et al.* (2008) [25]. Overexpression of genes encoding high substrate specific acyltransferases would lead to a higher esterification rate of acyl-donor to a specific *sn*-position of the glycerol-3-phosphate or the PC. The two ER-localized enzymes of the Kennedy pathway (GPAT and LPAAT) and the LPLAT are responsible for the incorporation of activated FAs into membrane lipids, or precursors of membrane lipids [117,118]. Recently, it was shown that an ER-membrane bound TpGPAT from the marine

diatom *T. pseudonana* affected FA composition and accumulation in triacylglycerides and phospholipids by overexpression in a GPAT-deficient yeast strain [128]. In the lipid profile, the amount of PA (16:0) in triacylglycerides and phospholipids increased by 18% and 12%, respectively, whereas monounsaturated FA were reduced. *In vitro* enzyme tests showed that TpGPAT has a high preference towards PA (16:0) and a lower towards ARA (20:4*n*-6) as acyl-donor for esterification of the *sn*-1 position of the glycerol-3-phosphate [128]. Two GPATs of the thraustochytrid *T. aureum*, which were isolated and expressed in plants, exhibited high substrate specificity for the esterification of glycerol-3-phosphate with LC-PUFAs (20:3*n*-6, 20:4*n*-3, 20:5*n*-3, 22:6*n*-3) [137]. Whereas GPATs link FAs to glycerol-3-phosphates backbones, radiolabeling studies of flaxseed indicated that LPAAT links C18 FA to the *sn*-2 position of PC [117,118]. Heterologous LPAATs activities of the eustigmatophyceae *N. oculata* were also measured in plants, and they showed high substrate specificity towards C18 FA or C20 FA [137]. This finding shows that diverse acyltransferases such as the LPAAT and GPAT are probably required in EPA synthesis in *P. tricornutum* for the esterification of EPA to the *sn*-2 position of PC [113]. Also, the lysophosphatidylcholine acyltransferase (LPCAT), belonging to the group of LPLATs, may be involved in esterification steps, because LPCAT in plants converts the acyl-group to either the *sn*-1 or the *sn*-2 position of a PC [118]. LPLATs in plants are part of the so-called acyl-editing, which shuffles FAs between the PC-pool and the DAG-pool, by activities of acyltransferases and phospholipases [138]. In plants, acyl-editing mechanisms are very complex and are possible bottlenecks in the FA synthesis [139]. In the co-expression network (Figure 3), several genes are present and identified as enzymes potentially involved in acyl-editing (*Phatr2_32057*, *Phatr2_33864*, see acyltransferase mentioned in Section 5.3) and so in the EPA pathway of *P. tricornutum*.

To conclude, possible genetic driver such as precursors, cofactors, acyl-CoA dependent elongases, LACSs, lipases and acyltransferases have been identified in *P. tricornutum*, and thus show potential as targets for several approaches. Furthermore, the strategies/genetic drivers above can be used to modify *n*-3 LC-PUFA synthesis in commercial approached Chromista, such as *Nannochloropis* or *Isochrysis*.

6. EPA Synthesis in Other Chromista

The EPA synthesis in Chromista differs depending on enzyme affinities for glycerol-backbones and desaturation positions. For instance, most eustigmatophyceae are overall identical to *P. tricornutum*, and synthesize EPA (20:5*n*-3) in ER before incorporation into the galactosylglycerides in the plastid. But in small details eustigmatophyceae species also differ to *P. tricornutum* because they preferable synthesize EPA (20:5*n*-3) via the *n*-6 pathway by a ω3 desaturase activity converting ARA (20:4*n*-6) to EPA (20:5*n*-3) [67,103]. In the eustigmatophyceae *Nannochloropsis* sp. and *M. subterraneus*, it is predicted that this conversion step involves Δ17 desaturase activity, but this is not yet confirmed [67,103]. Eustigmatophyceae are important algae in industrial production today, and the genus *Nannochloropsis* (including six different species) is most promising because of their growth rate, their robustness and their haploid genome which is easy to engineer [140–144]. The major FAs in *Nannochloropsis* species are POA (16:1*n*-7) followed by EPA (20:5*n*-3) and PA (16:0) [77,99,145]. So far, two Δ12 desaturases, two Δ9 desaturases, one ω3 desaturase and several elongases have been shown to be involved in the synthesis of the main FAs in *Nannochloropsis* [146,147]. The

characteristics of the desaturases and the elongases were shown by activity studies and overexpression of target genes under regulation of different promoters, which were inserted into the genome via homologous recombination [146]. Two Δ9 desaturases showed to be involved in the synthesis of one of the main FAs of *Nannochloropsis*, POA (16:1*n*-7), by detection of high substrate activity towards PA-CoA (16:0) and PA (16:0) linked to a glycerol-backbone [146]. Contrary to Δ9 desaturases, the two Δ12 desaturases showed different activities. One desaturase is indicated to be involved in the plastidial unsaturation of C16 FAs, and the other Δ12 desaturase likely has OA (18:1*n*-9) as substrate and is probably involved in the EPA synthesis. The ω3 desaturase involved in EPA synthesis showed high substrate preferences towards ARA (20:4*n*-6) and LA (18:2*n*-6) [146]. Overexpression of the ω3 desaturase in *Nannochloropsis* resulted in a large increase of the EPA/ARA ratio, and a small increase of ALA (18:3*n*-3) [146]. *In vivo* ^{14}C-C18:1-CoA radiolabeling studies showed C18 FAs desaturation by Δ6 and Δ5 desaturases when the FA was attached to the *sn*-2 position of PC, which is similar to in *P. tricornutum*. In contrast to *P. tricornutum*, positional analysis of labeled lipids indicated acyltransferase activities linking ^{14}C-C20:4-CoA to the *sn*-1 and *sn*-2 position of PE [103,148]. Concomitantly, other lipids such as the betaine lipid DGTS and TAG were labeled to a small degree. Also, the acyl moieties C16/C18 PC, C20/C20 PE and C20/C16, C20/C14 DGTS were produced. Consequently, the apparent source of MGDGs is the ER-located acyl-PEs by being converted into DAG and imported into the plastid. Molecular species of DGDGs use DGTS as precursor which has EPA attached at the *sn*-1 position [67].

Whereas most algae utilize PC to assemble glycolipids and synthesize *n*-3 LC-PUFAs, it has been shown that *Nannochloropsis* sp. and *M. subterraneus* utilize PC, PE and DGTS. Conversely, the brown algae *D. membranacea* has complete absence of PC, and the betaine lipid diacylglyceroltrimethylalanine (DGTA) seems to have the role of the PC and therefore plays a key role in the EPA and galactosylglyceride synthesis in *D. membranacea* [104]. DGTA is somewhat neglected when it comes to lipid metabolism, but it seems to be more important for the PUFA synthesis of some species to have a higher abundance of betaine lipids than previously thought [104,149].

Recently, eustigmatophyceae are of more interest which is reflected in the research making progress by identifying genes that encode enzymes involved in the EPA synthesis. Still, no transcriptome data are available and so the lack of characterized genes hampers the manipulation of the Section 5.5 identified genetic drivers.

7. DHA Synthesis in Other Chromista

Besides EPA (20:5*n*-3), DHA (20:6*n*-3) is the other high-valuable *n*-3 LC-PUFA which can be found in several Chromista species. These species possess specific Δ5 elongase and Δ4 desaturase activities for the consecutive steps of converting EPA (20:5*n*-3) into DHA (22:6*n*-3). Unlike mammals and fish, Chromista do not produce DHA via the Sprecher pathway by shortening tetracosahexaenoic acid (THA, 24:6*n*-3) in the β-oxidation pathway [150]. Chromista possess a simpler pathway to synthesize DHA (22:6*n*-3). This makes Chromista favorable DHA producers and their enzymes more interesting for metabolic engineering. The main DHA producers among Chromista are the three genera of thraustochytrids (*Thraustochytrium* sp. and *Schizochytrium*, *Aurantiochytrium*) that accumulate high DHA amounts in TAGs under nitrogen depletion [13]. Interestingly, the heterotrophic thraustochytrid

Schizochytrium sp. (genera renamed to *Aurantiochytrium*) possesses an alternative anaerobic polyketide synthase pathway (PKS) for the *n*-3 LC-PUFA synthesis [151]. A large multifunctional enzyme complex carries out the multitude of individual reactions, utilizing malonyl-CoA and producing free *n*-3 LC-PUFAs [151]. The major free FAs DPA (22:5*n*-6) and DHA (22:6*n*-3) are then activated to acyl-CoA and incorporated into TAGs [152]. To convert the major saturated components of TAGs (14:0 and 16:0), *Aurantiochytrium* additionally contains additionally a short-chain FAS complex [153]. Different from the type II fatty acid synthase (FAS) of *P. tricornutum*, the FAS of *Aurantiochytrium* is a type I FAS synthesized from one or two polypeptides [110]. The synthesized free FAs and the absence of genes homologous to a type II TE may indicate integration of TE activity into the synthase [152]. Because PKS does not require aerobic desaturation, the pathway is energetically favorable compared to the membrane-bond desaturases and elongases [27]. However, it was shown that ATP:CL and ME play key roles in the lipid assembling in *Schizochytrium* sp. S31, by providing acetyl-CoA and NADPH to the FAS and the PKS [154]. The energetically favorable pathway for DHA/*n*-3 LC-PUFA production is not the only pathway in thraustochytrids. *T. aureum* for instance is capable of synthesizing *n*-3 LC-PUFAs through the standard *n*-3 LC-PUFA pathway. Δ5 and Δ12 desaturase activity was detected in the PUFA pathway, indicating that either acyl-CoA substrates are used or acyl-edition occurs after desaturation [155]. A gene-knockdown mutant deficient in Δ12 desaturase showed a change in FA composition, but maintained high production of DHA via the PKS pathway [155]. This indicates that DHA (22:6*n*-3) is synthesized in the PKS pathway, whereas GLA (18:3*n*-6) and EPA (20:5*n*-3) are synthesized in the common PUFA pathway. Further studies on *Thraustochytrium* sp. identified two genes for elongases (*tselo1* and *tselo2*) and a Δ4 desaturase encoding gene to be enzyme is involved in LC-PUFA/DHA synthesis [156,157]. PCR-based gene identification studies revealed that many species within *Thraustochytrium* sp. and *Schizochytrium*, but not *Aurantiochytrium*, possess Δ4 desaturates and Δ5 elongases [158].

Several desaturases in Chromista are characterized, such as the Δ4 desaturase of the haptophyta *I. galbana* or *P. lutheri* [159]. The DHA-producing haptophyta *P. lutheri* contain STA (18:4*n*-3), EPA (20:5*n*-3) and DHA (22:6*n*-3) as the main FAs. *P. lutheri* contain no PC, but have instead betaine lipids (DGCC, DGAT, see Figure 2) [69]. DGCC is the glycerol-backbone for both the transfer of FAs in the plastid and the synthesis of MGDG [69]. Radiolabeling studies indicated that the main common LC-PUFA pathway started at PA (16:0), and involves possibly the *n*-6 pathway with the intermediates DGLA (20:3*n*-6) and ARA (20:4*n*-6) [160]. Through labeling of ^{14}C-20:3*n*-6, most radioactivity was detected in EPA (64%–67%) and DHA (9%–21%), which indicate a desaturase that converted either ETA (20:4*n*-3) or ARA (20:4*n*-6) to EPA (20:5*n*-3) [160]. Based on studies in the red algae *P. cruentum* and the freshwater eustigmatophyceae *M. subterraneus*, Δ17 desaturase activity has been proposed in *P. lutheri* [73]. No clear evidence of a Δ17 desaturase in *M. subterraneus* exists; however, such an activity exists in the chloroplast of the red algae *P. cruentum* [73,160]. After lipid-linked ARA (20:4*n*-6) is transported into the chloroplast, it is further desaturated to EPA (20:5*n*-3) and incorporated into galactosylglycerides [73]. The identified Δ5 elongase and Δ4 desaturase encoded by *pavELO* and *Pldes1* can prolong EPA (20:5*n*-3) to DHA (22:6*n*-3) in *P. lutheri* [161]. The gene *pavELO* possesses a unique substrate specificity towards C20 FA (EPA (20:5*n*-3) and ARA (20:4*n*-6)) expressed in yeast. Also, the Δ4 desaturase (encoded by *Pldes1*) showed desaturation activity for generating adrenic acid (ADA, 22:4*n*-6) and DPA (22:5*n*-3) [162].

When it comes to industrial DHA-production strains of Chromista, two different pathways—the PKS and the common PUFA synthesis—are suggested to synthesis DHA (22:6*n*-3). In the genus thraustochytrids similarities to desaturases and elongases in other Chromista were identified, but it is still unknown which pathway thraustochytrids utilize for DHA synthesis.

8. Conclusions

Species within Chromista are promising candidates for sustainable production of high-value PUFAs, with different species providing different opportunities and challenges. As the quest for PUFA is increasing, comparative studies will provide exciting advances in our basic knowledge of the metabolism of this group of organisms. This review reflects that the knowledge on biochemistry of lipids and genetic regulation of the FA and lipid synthesis is evolving rapidly, and will continue to do so in the coming years.

Biosynthesis of PUFAs in Chromista has mainly been studied by biochemical/metabolic studies including FA composition analysis, desaturation/elongation activity measurements, pulse-chase radiolabeling and inhibitor studies [28]. In this review, the diatom *P. tricornutum* has been used to exemplify the complexity of *n*-3 LC-PUFA synthesis in Chromista. Full genome sequences, biochemical analysis, and the fact that recent studies demonstrate that homologous recombination is feasible in the challenging diploid genome of *P. tricornutum* makes this diatom a good model organism [86,163]. However, industrial application of *P. tricornutum* is unlikely [22]. Possible bottlenecks in *P. tricornutum* synthesis of *n*-3 LC-PUFAs were identified with the help of a co-expression network study of genes coding for proteins involved in lipid synthesis. Our analysis points to enzymes producing precursors and cofactors (acetyl-CoA pool and NADPH) for the *n*-3 LC-PUFAs synthesis as suitable targets for further improvements in *n*-3 LC-PUFA content by using different approaches such as selective breeding, environmental conditioning and genetic engineering. Other key players in *n*-3 LC-PUFAs synthesis are TE, acyl-CoA-dependent elongases, LACSs and acyltransferases. This knowledge was compared with knowledge from Chromista species with greater interest for industrial applications. In general, genetic drivers could be identified but most genes encoding the genetic drivers are still uncharacterized in *P. tricornutum* and in most Chromista. This hampers the application of, for example, genetic engineering. However, with 15 sequenced available genomes of algae, a new era has started that will result in a rapid improvement of our understanding of transcriptional lipid metabolism and gives us the opportunity to characterize the identified genetic drivers [91,106]. Genetic transformation has been shown to be successful in more than 30 strains of algae, and expression stability can be controlled by endogenous promoters, species-specific codon usage and intron sequences [22]. Currently, most commercial interest for engineering lipid metabolism is on the *Nannochloropsis* genus, which under nitrogen starvation can accumulate more than 55% of cell dry weight as FA with >5% in the form of EPA [145]. The established homologous recombination technique for the haploid genome is a powerful tool to drive lipid research in this organism and also to introduce genes for DHA production in this heterokont [140–144]. Furthermore, it has been shown in *Nannochloropsis* and *Pavlova* that genetic breeding can yield to a higher lipid or *n*-3 LC-PUFA content, respectively [164–166]. With the knowledge of the genetic drivers and the biochemical

pathway, selective breeding can be improved by easier selection of triggers for creating a genetic bottleneck that selects for cells with a high capacity for lipid production.

It seems clear that manipulation of, for instance, elongases and acyltransferase can lead to a higher *n*-3 LC-PUFA content in biologically interesting Chromista, as it has been shown in the patents of the species of *Nannochloropsis* [146,147]. However, it remains to be seen at which point the algal physiology may be limiting for that approach. Therefore, a combination of approaches such as metabolic engineering, conditioning and selection may be more suitable for both increasing the biomass density and increasing the *n*-3 LC-PUFA content in the biomass.

The intake of *n*-3 LC-PUFAs is a dietary requirement for humans for healthy cognitive development in infants, as well as reducing the risk of chronic diseases for adults. As the need for a sustainable *n*-3 LC-PUFA source increases proportionally to the increase in global populations, more research is required in alternative biological sources, therefore providing a potential long-term source of *n*-3 PUFAs. Even though much research has to be done on the physiological and molecular levels, Chromista are a promising long-term alternative source of *n*-3 LC-PUFAs for humans and fish feed.

Acknowledgments

We thank Jaques Joseph Lamb, Daniel Frosch, Leila Alipanah and members of the Cell, Molecular Biology and Genomics Group at NTNU for input on the manuscript. The Strategic Marine Program at NTNU provided financial support to AM, KL and GR.

Conflicts of Interest

The authors declare no conflict of interest.

References

1. Kelly, P.B.; Reiser, R.; Hood, D.W. The origin of the marine polyunsaturated fatty acids. Composition of some marine plankton. *J. Am. Oil Chem. Soc.* **1959**, *36*, 104–106.
2. Yaguchi, T.; Tanaka, S.; Yokochi, T.; Nakahara, T.; Higashihara, T. Production of high yields of docosahexaenoic acid by *Schizochytrium* sp. strain SR21. *J. Am. Oil Chem. Soc.* **1997**, *74*, 1431–1434.
3. Yongmanitchai, W.; Ward, O.P. Growth of and omega-3 fatty acid production by *Phaeodactylum tricornutum* under different culture conditions. *Appl. Environ. Microbiol.* **1990**, *57*, 419–425.
4. Sukenik, A. Ecophysiological considerations in the optimization of eicosapentaenoic acid production by *Nannochloropsis* sp. (Eustigmatophyceae). *Bioresour. Technol.* **1991**, *35*, 263–269.
5. Wan, C.; Bai, F.-W.; Zhao, X.-Q. Effects of nitrogen concentration and media replacement on cell growth and lipid production of oleaginous marine microalga *Nannochloropsis oceanica* DUT01. *Biochem. Eng. J.* **2013**, *78*, 32–38.
6. Cavalier-Smith, T. Kingdoms protozoa and chromista and the eozoan root of the eukaryotic tree. *Biol. Lett.* **2010**, *6*, 342–345.

7. Cavalier-Smith, T. Principles of protein and lipid targeting in secondary symbiogenesis: euglenoid, dinoflagellate, and sporozoan plastid origins and the eukaryote family tree. *J. Eukaryot. Microbiol.* **1999**, *46*, 347–366.
8. Chang, G.; Luo, Z.; Gu, S.; Wu, Q.; Chang, M.; Wang, X. Fatty acid shifts and metabolic activity changes of *Schizochytrium sp.* S31 cultured on glycerol. *Bioresour. Technol.* **2013**, *142*, 255–260.
9. Ward, O.P.; Singh, A. Omega-3/6 fatty acids: Alternative sources of production. *Process Biochem.* **2005**, *40*, 3627–3652.
10. Hu, Q.; Sommerfeld, M.R.; Jarvis, E.; Ghirardi, M.; Posewitz, M.; Seibert, M.; Darzins, A. Microalgal triacylglycerols as feedstocks for biofuel production: Perspectives and advances. *Plant J.* **2008**, *54*, 521–639.
11. Adarme-Vega, T.C.; Lim, D.K.; Timmins, M.; Vernen, F.; Li, Y.; Schenk, P.M. Microalgal biofactories: A promising approach towards sustainable omega-3 fatty acid production. *Microb. Cell Fact.* **2012**, *11*, 96.
12. Barclay, W.R. Method of aquaculture comprising feeding microflora having a small cell aggregate size. US Patent 5,688,500, 18 November 1997.
13. Martins, D.A.; Custodio, L.; Barreira, L.; Pereira, H.; Ben-Hamadou, R.; Varela, J.; Abu-Salah, K.M. Alternative sources of *n*-3 long-chain polyunsaturated fatty acids in marine microalgae. *Mar. Drugs* **2013**, *11*, 2259–2281.
14. Hu, H.; Gao, K. Optimization of growth and fatty acid composition of a unicellular marine picoplankton, *Nannochloropsis* sp., with enriched carbon sources. *Biotechnol. Lett.* **2003**, *25*, 421–425.
15. Lu, C.; Rao, K.; Hall, D.; Vonshak, A. Production of eicosapentaenoic acid (EPA) in *Monodus subterraneus* grown in a helical tubular photobioreactor as affected by cell density and light intensity. *J. Appl. Phycol.* **2001**, *13*, 517–522.
16. Wen, Z.-Y.; Chen, F. Production potential of eicosapentaenoic acid by the diatom *Nitzschia laevis*. *Biotechnol. Lett.* **2000**, *22*, 727–733.
17. Yang, Z.-K.; Niu, Y.-F.; Ma, Y.-H.; Xue, J.; Zhang, M.-H.; Yang, W.-D.; Liu, J.-S.; Lu, S.-H.; Guan, Y.; Li, H.-Y. Molecular and cellular mechanisms of neutral lipid accumulation in diatom following nitrogen deprivation. *Biotechnol. Biofuels* **2013**, *6*, 67.
18. Fidalgo, J.P.; Cid, A.; Torres, E.; Sukenik, A.; Herrero, C. Effects of nitrogen source and growth phase on proximate biochemical composition, lipid classes and fatty acid profile of the marine microalga *Isochrysis galbana*. *Aquaculture* **1998**, *166*, 105–116.
19. Taoka, Y.; Nagano, N.; Okita, Y.; Izumida, H.; Sugimoto, S.; Hayashi, M. Influences of culture temperature on the growth, lipid content and fatty acid composition of *Aurantiochytrium* sp. strain mh0186. *Mar. Biotechnol.* **2009**, *11*, 368–374.
20. Yokochi, T.; Honda, D.; Higashihara, T.; Nakahara, T. Optimization of docosahexaenoic acid production by *Schizochytrium limacinum* SR21. *Appl. Microbiol. Biotechnol.* **1998**, *49*, 72–76.
21. Chepurnov, V.A.; Mann, D.G.; von Dassow, P.; Vanormelingen, P.; Gillard, J.; Inze, D.; Sabbe, K.; Vyverman, W. In search of new tractable diatoms for experimental biology. *BioEssays* **2008**, *30*, 692–702.

22. Radakovits, R.; Jinkerson, R.E.; Darzins, A.; Posewitz, M.C. Genetic engineering of algae for enhanced biofuel production. *Eukaryot. Cell* **2010**, *9*, 486–501.
23. Graham, I.A.; Larson, T.; Napier, J.A. Rational metabolic engineering of transgenic plants for biosynthesis of omega-3 polyunsaturates. *Curr. Opin. Biotechnol.* **2007**, *18*, 142–147.
24. Drexler, H.; Spiekermann, P.; Meyer, A.; Domergue, F.; Zank, T.; Sperling, P.; Abbadi, A.; Heinz, E. Metabolic engineering of fatty acids for breeding of new oilseed crops: Strategies, problems and first results. *J. Plant Physiol.* **2003**, *160*, 779–802.
25. Hoffmann, M.; Wagner, M.; Abbadi, A.; Fulda, M.; Feussner, I. Metabolic engineering of omega 3-very long chain polyunsaturated fatty acid production by an exclusively acyl-CoA-dependent pathway. *J. Biol. Chem.* **2008**, *283*, 22352–22362.
26. Sharma, K.K.; Schuhmann, H.; Schenk, P.M. High lipid induction in microalgae for biodiesel production. *Energies* **2012**, *5*, 1532–1553.
27. Harwood, J.L.; Guschina, I.A. The versatility of algae and their lipid metabolism. *Biochimie* **2009**, *91*, 679–684.
28. Guschina, I.A.; Harwood, J.L. Lipids and lipid metabolism in eukaryotic algae. *Prog. Lipid Res.* **2006**, *45*, 160–186.
29. Khozin-Goldberg, I.; Cohen, Z. Unraveling algal lipid metabolism: Recent advances in gene identification. *Biochemie* **2011**, *93*, 91–100.
30. Liu, B.S.; Benning, C. Lipid metabolism in microalgae distinguishes itself. *Curr. Opin. Biotechnol.* **2013**, *24*, 300–309.
31. Das, U.N. Essential fatty acids—A review. *Curr. Pharm. Biotechnol.* **2006**, *7*, 467–482.
32. Tocher, D.R. Fatty acid requirements in ontogeny of marine and freshwater fish. *Aquac. Res.* **2010**, *41*, 717–732.
33. Plourde, M.; Cunnane, S.C. Extremely limited synthesis of long chain polyunsaturates in adults: Implications for their dietary essentiality and use as supplements. *Appl. Physiol. Nutr. Metab.* **2007**, *32*, 619–634.
34. Khozin-Goldberg, I.; Iskandarov, U.; Cohen, Z. LC-PUFA from photosynthetic microalgae: Occurrence, biosynthesis, and prospects in biotechnology. *Appl. Microbiol. Biotechnol.* **2011**, *91*, 905–915.
35. Bell, J.G.; McEvoy, L.A.; Estevez, A.; Shields, R.J.; Sargent, J.R. Optimising lipid nutrition in first-feeding flatfish larvae. *Aquaculture* **2003**, *227*, 211–220.
36. Harel, M.; Koven, W.; Lein, I.; Bar, Y.; Behrens, P.; Stubblefield, J.; Zohar, Y.; Place, A.R. Advanced DHA, EPA and ArA enrichment materials for marine aquaculture using single cell heterotrophs. *Aquaculture* **2002**, *213*, 347–362.
37. Li, Q.; Ai, Q.; Mai, K.; Xu, W.; Zheng, Y. A comparative study: Invitro effects of EPA and DHA on immune functions of head-kidney macrophages isolated from large yellow croaker (*Larmichthys crocea*). *Fish Shellfish Immunol.* **2013**, *35*, 933–940.
38. Kuratko, C.N.; Barrett, E.C.; Nelson, E.B.; Salem, N., Jr. The relationship of docosahexaenoic acid (DHA) with learning and behavior in healthy children: A review. *Nutrients* **2013**, *5*, 2777–2810.

39. Kremmyda, L.S.; Tvrzicka, E.; Stankova, B.; Zak, A. Fatty acids as biocompounds: Their role in human metabolism, health and disease-a review. Part 2: Fatty acid physiological roles and applications in human health and disease. *Biomed. Pap. Med. Fac. Univ. Palacky Olomouc. Czech. Repub.* **2011**, *155*, 195–218.
40. Simopoulos, A.P. The importance of the ratio of omega-6/omega-3 essential fatty acids. *Biomed. Pharmacother.* **2002**, *56*, 365–379.
41. Sinn, N.; Milte, C.M.; Street, S.J.; Buckley, J.D.; Coates, A.M.; Petkov, J.; Howe, P.R.C. Effects of *n*-3 fatty acids, EPA v. DHA, on depressive symptoms, quality of life, memory and executive function in older adults with mild cognitive impairment: A 6-month randomised controlled trial. *Br. J. Nutr.* **2012**, *107*, 1682–1693.
42. Das, U.N. Essential fatty acids in health and disease. *J. Assoc. Physicians India* **1999**, *47*, 906–911.
43. Ormarsson, O.T.; Geirsson, T.; Bjornsson, E.S.; Jonsson, T.; Moller, P.H.; Loftsson, T.; Stefansson, E. Clinical trial: marine lipid suppositories as laxatives. *Mar. Drugs* **2012**, *10*, 2047–2054.
44. Riediger, N.D.; Othman, R.A.; Suh, M.; Moghadasian, M.H. A systemic review of the roles of *n*-3 fatty acids in health and disease. *J. Am. Diet. Assoc.* **2009**, *109*, 668–679.
45. Hibbeln, J.R.; Nieminen, L.R.G.; Blasbalg, T.L.; Riggs, J.A.; Lands, W.E.M. Healthy intakes of *n*-3 and *n*-6 fatty acids: estimations considering worldwide diversity. *Am. J. Clin. Nutr.* **2006**, *83*, 1483S–1493S.
46. Kris-Etherton, P.M.; Grieger, J.A.; Etherton, T.D. Dietary reference intakes for DHA and EPA. *Prostag. Leukotr. Ess.* **2009**, *81*, 99–104.
47. Kris-Etherton, P.M.; Innis, S. Position of the American dietetic association and dietitians of Canada: Dietary fatty acids. *J. Am. Diet. Assoc.* **2007**, *107*, 1599–1611.
48. Norwegian Scientific Committee for Food Safety (VKM). *Evaluation of Negative and Positive Health Effects of* N*-3 Fatty Acids as Constituents of Food Supplements and Fortified Foods*; VKM: Oslo, Norway, 2011.
49. Sargent, J.; McEvoy, L.; Estevez, A.; Bell, G.; Bell, M.; Henderson, J.; Tocher, D. Lipid nutrition of marine fish during early development: Current status and future directions. *Aquaculture* **1999**, *179*, 217–229.
50. Kang, J.X.; Liu, A. The role of the tissue omega-6/omega-3 fatty acid ratio in regulating tumor angiogenesis. *Cancer Metastasis Rev.* **2013**, *32*, 201–210.
51. Seafood data. Available online: http://www.nifes.no/index.php?page_id=164&lang_id=2 (accessed on 28 August 2013).
52. Reitan, K.I.; Rainuzzo, J.R.; Olsen, Y. Effect of nutrient limitation on fatty acid and lipid content of marine microalgae. *J. Phycol.* **1994**, *30*, 972–979.
53. Enser, M.; Hallett, K.; Hewitt, B.; Fursey, G.A.J.; Wood, J.D. Fatty acid content and composition of English beef, lamb and pork at retail. *Meat Sci.* **1996**, *42*, 443–456.
54. Carnevale de Almeida, J.; Perassolo, M.S.; Camargo, J.L.; Bragagno, N.; Gross, J.L. Fatty acid composition and cholesterol content of beef and chicken meat in Southern Brazil. *Rev. Bras. Cienc. Farm.* **2006**, *42*, 109–117.

55. Chowdhury, K.; Banu, L.A.; Khan, S.; Latif, A. Studies on the Fatty Acid Composition of Edible Oil. *Bangladesh J. Sci. Ind. Res.* **2007**, *42*, 311–316.
56. Vidrih, R.; Filip, S.; Hribar, J. Content of Higher Fatty Acids in Green Vegetables. *Czech J. Food Sci.* **2009**, *27*, S125–S129.
57. FAO Fisheries and Aquaculture Department. *The State of World Fisheries and Aquaculture*; Food and Agriculture Organization of the United Nations: Rome, Italy, 2012.
58. Olsen, Y. Resources for fish feed in future mariculture. *Aquacult. Environ. Interact.* **2011**, *1*, 187–200.
59. Nasopoulou, C.; Zabetakis, I. Benefits of fish oil replacement by plant originated oils in compounded fish feeds. A review. *LWT-Food Sci. Technol.* **2012**, *47*, 217–224.
60. Torstensen, B.E.; Bell, J.G.; Rosenlund, G.; Henderson, R.J.; Graff, I.E.; Tocher, D.R.; Lie, O.; Sargent, J.R. Tailoring of Atlantic salmon (*Salmo salar* L.) flesh lipid composition and sensory quality by replacing fish oil with a vegetable oil blend. *J. Agric. Food Chem.* **2005**, *53*, 10166–10178.
61. Benedito-Palos, L.; Navarro, J.C.; Sitja-Bobadilla, A.; Bell, J.G.; Kaushik, S.; Perez-Sanchez, J. High levels of vegetable oils in plant protein-rich diets fed to gilthead sea bream (*Sparus aurata* L.): Growth performance, muscle fatty acid profiles and histological alterations of target tissues. *Br. J. Nutr.* **2008**, *100*, 992–1003.
62. Tur, J.A.; Bibiloni, M.M.; Sureda, A.; Pons, A. Dietary sources of omega 3 fatty acids: Public health risks and benefits. *Br. J. Nutr.* **2012**, *107*, S23–S52.
63. Dembitsky, V.M. Betaine ether-linked glycerolipids: Chemistry and biology. *Prog. Lipid Res.* **1996**, *35*, 1–51.
64. Loll, B.; Kern, J.; Saenger, W.; Zouni, A.; Biesiadka, J. Lipids in photosystem II: Interactions with protein and cofactors. *Biochim. Biophys. Acta* **2007**, *1767*, 509–519.
65. Guschina, I.A.; Harwood, J.L. Algal lipids and their metabolism. In *Developments in Applied Phycology 5, Algae for Biofuels and Energy*; Moheimani, N.R., Borowitzka, M.A., Eds.; Springer Science+Business Media Dordrecht: Dordrecht, The Netherlands, 2013; pp. 17–36.
66. Lepetit, B.; Goss, R.; Jakob, T.; Wilhelm, C. Molecular dynamics of the diatom thylakoid membrane under different light conditions. *Photosyn. Res.* **2012**, *111*, 245–257.
67. Khozin-Goldberg, I.; Didi-Cohen, S.; Shayakhmetova, I.; Cohen, Z. Biosynthesis of eicosapentaenoic acid (EPA) in the freshwater eustigmatophyte *Monodus subterraneus* (Eustigmatophyceae). *J. Phycol.* **2002**, *38*, 745–756.
68. Hodgson, P.A.; Henderson, R.J.; Sargent, J.R.; Leftley, J.W. Patterns of variation in the lipid class and fatty acid composition of *Nannochloropsis oculata* (Eustigmatophyceae) during batch culture. *J. Appl. Phycol.* **1991**, *3*, 169–181.
69. Eichenberger, W.; Gribi, C. Lipids of *Pavlova lutheri*: Cellular site and metabolic role of DGCC. *Phytochemistry* **1997**, *45*, 1561–1567.
70. Arao, T.; Kawaguchi, A.; Yamada, M. Positional distribution of fatty-acids in lipids of the marine diatom *Phaeodactylum tricornutum*. *Phytochemistry* **1987**, *26*, 2573–2576.
71. Dodson, V.J.; Dahmen, J.L.; Mouget, J.-L.; Leblond, J.D. Mono- and digalactosyldiacylglycerol composition of the marennine-producing diatom, *Haslea ostrearia*: Comparison to a selection of pennate and centric diatoms. *Phycol. Res.* **2013**, *61*, 199–207.

72. Roughan, P.G.; Slack, C.R. Cellular organization of glycerolipid metabolism. *Plant Physiol.* **1982**, *33*, 97–132.
73. Khozin, I.; Adlerstein, D.; Bigongo, C.; Heimer, Y.M.; Cohen, Z. Elucidation of the biosynthesis of eicosapentaenoic acid in the microalga *Porphyridium cruentum* (II. studies with radiolabeled precursors). *Plant Physiol.* **1997**, *114*, 223–230.
74. Khozin-Goldberg, I.; Yu, H.Z.; Adlerstein, D.; Didi-Cohen, S.; Heimer, Y.M.; Cohen, Z. Triacylglycerols of the red microalga *Porphyridium cruentum* can contribute to the biosynthesis of eukaryotic galactolipids. *Lipids* **2000**, *35*, 881–889.
75. Sato, N.; Aoki, M.; Maru, Y.; Sonoike, K.; Minoda, A.; Tsuzuki, M. Involvement of sulfoquinovosyl diacylglycerol in the structural integrity and heat-tolerance of photosystem II. *Planta* **2003**, *217*, 245–251.
76. Jiang, H.M.; Gao, K.S. Effects of lowering temperature during culture on the production of polyunsaturated fatty acids in the marine diatom *Phaeodactylum tricornutum* (Bacillariophyceae). *J. Phycol.* **2004**, *40*, 651–654.
77. Tonon, T.; Harvey, D.; Larson, T.R.; Graham, I.A. Long chain polyunsaturated fatty acid production and partitioning to triacylglycerols in four microalgae. *Phytochemistry* **2002**, *61*, 15–24.
78. Khozin-Goldberg, I.; Cohen, Z. The effect of phosphate starvation on the lipid and fatty acid composition of the fresh water eustigmatophyte *Monodus subterraneus*. *Phytochemistry* **2006**, *67*, 696–701.
79. Pal, D.; Khozin-Goldberg, I.; Cohen, Z.; Boussiba, S. The effect of light, salinity, and nitrogen availability on lipid production by *Nannochloropsis* sp. *Appl. Microbiol. Biotechnol.* **2011**, *90*, 1429–1441.
80. Palmucci, M.; Ratti, S.; Giordano, M. Ecological and evolutionary implications of carbon allocation in marine phytoplankton as a function of nitrogen availability: A fourier transform infrared spectroscopy approach. *J. Phyciol.* **2011**, *47*, 313–323.
81. Markou, G.; Angelidaki, I.; Georgakakis, D. Microalgal carbohydrates: An overview of the factors influencing carbohydrates production, and of main bioconversion technologies for production of biofuels. *Appl. Microbiol. Biotechnol.* **2012**, *96*, 631–645.
82. Obata, T.; Fernie, A.R.; Nunes-Nesi, A. The Central Carbon and Energy Metabolism of Marine Diatoms. *Metabolites* **2013**, *3*, 325–346.
83. Beattie, A.; Hirst, E.L.; Percival, E. Studies on the metabolism of the chrysophyceae. Comparative structural investigations on leucosin (chrysolaminarin) separated from diatoms and laminarin from the brown algae. *Biochem. J.* **1961**, *79*, 531–537.
84. Wilhelm, C.; Jakob, T. From photons to biomass and biofuels: evaluation of different strategies for the improvement of algal biotechnology based on comparative energy balances. *Appl. Microbiol. Biotechnol.* **2011**, *92*, 909–919.
85. Wang, K.S.; Chai, T.-J. Reduction in omega-3 fatty acids by UV-B irradiation in microalgae. *J. Appl. Phycol.* **1994**, *6*, 415–421.
86. Bowler, C.; Allen, A.E.; Badger, J.H.; Grimwood, J.; Jabbari, K.; Kuo, A.; Maheswari, U.; Martens, C.; Maumus, F.; Otillar, R.P.; *et al.* The *Phaeodactylum* genome reveals the evolutionary history of diatom genomes. *Nature* **2008**, *456*, 239–244.

87. Mus, F.; Toussaint, J.P.; Cooksey, K.E.; Fields, M.W.; Gerlach, R.; Peyton, B.M.; Carlson, R.P. Physiological and molecular analysis of carbon source supplementation and pH stress-induced lipid accumulation in the marine diatom *Phaeodactylum tricornutum*. *Appl. Microbiol. Biotechnol.* **2013**, *97*, 3625–3642.
88. De Martino, A.; Bartual, A.; Willis, A.; Meichenin, A.; Villazan, B.; Maheswari, U.; Bowler, C. Physiological and molecular evidence that environmental changes elicit morphological interconversion in the model diatom *Phaeodactylum tricornutum*. *Protist* **2011**, *162*, 462–481.
89. Valenzuela, J.; Mazurie, A.; Carlson, R.P.; Gerlach, R.; Cooksey, K.E.; Peyton, B.M.; Fields, M.W. Potential role of multiple carbon fixation pathways during lipid accumulation in *Phaeodactylum tricornutum*. *Biotechnol. Biofuels* **2012**, *5*, 40.
90. Gardner, R.D.; Cooksey, K.E.; Mus, F.; Macur, R.; Moll, K.; Eustance, E.; Carlson, R.P.; Gerlach, R.; Fields, M.W.; Peyton, B.M. Use of sodium bicarbonate to stimulate triacylglycerol accumulation in the chlorophyte *Scenedesmus* sp. and the diatom *Phaeodactylum tricornutum*. *J. Appl. Phycol.* **2012**, *24*, 1311–1320.
91. Fabris, M.; Matthijs, M.; Rombauts, S.; Vyverman, W.; Goossens, A.; Baart, G.J. The metabolic blueprint of *Phaeodactylum tricornutum* reveals a eukaryotic Entner-Doudoroff glycolytic pathway. *Plant J.* **2012**, *70*, 1004–1014.
92. Kanehisa, M.; Goto, S.; Sato, Y.; Furumichi, M.; Tanabe, M. KEGG for integration and interpretation of large-scale molecular data sets. *Nucl. Acids Res.* **2012**, *40*, D109–D114.
93. Brembu, T.; Jorstad, M.; Winge, P.; Valle, K.C.; Bones, A.M. Genome-Wide profiling of responses to cadmium in the diatom *Phaeodactylum tricornutum*. *Environ. Sci. Technol.* **2011**, *45*, 7640–7647.
94. Nymark, M.; Valle, K.C.; Brembu, T.; Hancke, K.; Winge, P.; Andresen, K.; Johnsen, G.; Bones, A.M. An integrated analysis of molecular acclimation to high light in the marine diatom *Phaeodactylum tricornutum*. *PLoS One* **2009**, *4*, e7743.
95. Nymark, M.; Valle, K.C.; Hancke, K.; Winge, P.; Andresen, K.; Johnsen, G.; Bones, A.M.; Brembu, T. Molecular and photosynthetic responses to prolonged darkness and subsequent acclimation to re-illumination in the diatom *Phaeodactylum tricornutum*. *PLoS One* **2013**, *8*, e58722.
96. Sapriel, G.; Quinet, M.; Heijde, M.; Jourdren, L.; Tanty, V.; Luo, G.Z.; Le Crom, S.; Lopez, P.J. Genome-Wide transcriptome analyses of silicon metabolism in *Phaeodactylum tricornutum* reveal the multilevel regulation of silicic acid transporters. *PLoS One* **2009**, *4*, e7458.
97. Chauton, M.S.; Winge, P.; Brembu, T.; Vadstein, O.; Bones, A.M. Gene regulation of carbon fixation, storage, and utilization in the diatom *Phaeodactylum tricornutum* acclimated to light/dark cycles. *Plant Physiol.* **2013**, *161*, 1034–1048.
98. Shannon, P.; Markiel, A.; Ozier, O.; Baliga, N.S.; Wang, J.T.; Ramage, D.; Amin, N.; Schwikowski, B.; Ideker, T. Cytoscape a software envirnoment for inetgrated models of biomolecular interaction networks. *Genome Res.* **2003**, *13*, 2498–2504.
99. Bellou, S.; Aggelis, G. Biochemical activities in *Chlorella* sp. and *Nannochloropsis salina* during lipid and sugar synthesis in a lab-scale open pond simulating reactor. *J. Biotechnol.* **2012**, *164*, 318–329.

100. Kroth, P.G.; Chiovitti, A.; Gruber, A.; Martin-Jezequel, V.; Mock, T.; Parker, M.S.; Stanley, M.S.; Kaplan, A.; Caron, L.; Weber, T.; *et al.* A model for carbohydrate metabolism in the diatom *Phaeodactylum tricornutum* deduced from comparative whole genome analysis. *PLoS One* **2008**, *3*, e1426.
101. Zhang, Y.; Adams, I.P.; Ratledge, C. Malic enzyme: The controlling activity for lipid production? Overexpression of malic enzyme in *Mucor circinelloides* leads to a 2.5-fold increase in lipid accumulation. *Microbiology* **2007**, *153*, 2013–2025.
102. Kitano, M.; Matsukawa, R.; Karube, I. Enhanced eicosapentaenoic acid production by *Navicula saprophila*. *J. Appl. Phycol.* **1998**, *10*, 101–105.
103. Schneider, J.C.; Roessler, P. Radiolabeling Studies of Lipids and Fatty-Acids in *Nannochloropsis* (Eustigmatophyceae), an Oleaginous Marine Alga. *J. Phycol.* **1994**, *30*, 594–598.
104. Hofmann, M.; Eichenberger, W. Radiolabelling studies on the lipid metabolism in the marine brown alga *Dictyopteris membranacea*. *Plant Cell Physiol.* **1998**, *39*, 508–515.
105. Domergue, F.; Spiekermann, P.; Lerchl, J.; Beckmann, C.; Kilian, O.; Kroth, P.G.; Boland, W.; Zähringer, U.; Heinz, E. New insight into *Phaeodactylum tricornutum* fatty acid metabolism. Cloning and functional characterization of plastidial and microsomal Δ12-fatty acid sesaturases. *Plant Physiol.* **2003**, *131*, 1648–1660.
106. Huerlimann, R.; Heimann, K. Comprehensive guide to acetyl-carboxylases in algae. *Crit. Rev. Biotechnol.* **2013**, *33*, 49–65.
107. Nikolau, B.J.; Ohlrogge, J.B.; Wurtele, E.S. Plant biotin-containing carboxylases. *Arch. Biochem. Biophys.* **2003**, *414*, 211–222.
108. Dunahay, T.G.; Jarvis, E.E.; Dais, S.S.; Roessler, P.G. Manipulation of microalgal lipid production using genetic engineering. *Appl. Biochemi. Biotechnol.* **1996**, *57*, 223–231.
109. Radakovits, R.; Eduafo, P.M.; Posewitz, M.C. Genetic engineering of fatty acid chain length in *Phaeodactylum tricornutum*. *Metab. Eng.* **2011**, *13*, 89–95.
110. Ryall, K.; Harper, J.T.; Keeling, P.J. Plastid-derived Type II fatty acid biosynthetic enzymes in chromists. *Gene* **2003**, *313*, 139–148.
111. Harwood, J.L.; Guschina, I.A. Regulation of lipid synthesis in oil crops. *FEBS Lett.* **2013**, *587*, 2079–2081.
112. Subrahmanyam, S.; Cronan, J.E. Overproduction of a functional fatty acid biosynthetic enzyme blocks fatty acid synthesis in Escherichia coli. *J. Bacteriol.* **1998**, *180*, 4596–4602.
113. Domergue, F.; Abbadi, A.; Ott, C.; Zank, T.K.; Zahringer, U.; Heinz, E. Acyl carriers used as substrates by the desaturases and elongases involved in very long-chain polyunsaturated fatty acids biosynthesis reconstituted in yeast. *J. Biol. Chem.* **2003**, *278*, 35115–35126.
114. Sperling, P.; Heinz, E. Desaturases fused to their electron donor. *Eur. J. Lipid Sci. Technol.* **2001**, *103*, 158–180.
115. Groot, P.H.; Scholte, H.R.; Hulsmann, W.C. Fatty acid activation: specificity, localization, and function. *Adv. Lipid Res.* **1976**, *14*, 75–126.
116. Fulda, M.; Shockey, J.; Werber, M.; Wolter, F.P.; Heinz, E. Two long-chain acyl-CoA synthetases from *Arabidopsis thaliana* involved in peroxisomal fatty acid beta-oxidation. *Plant J.* **2002**, *32*, 93–103.

117. Sørensen, B.M.; Furukawa-Stoffer, T.L.; Marshall, K.S.; Page, E.K.; Mir, Z.; Forster, R.J.; Weselake, R.J. Storage lipid accumulation and acyltransferase action in developing flaxseed. *Lipids* **2005**, *40*, 1043–1049.
118. Snyder, C.S.; Yurchenko, O.P.; Siloto, R.M.P.; Chen, X.; Liu, Q.; Mietkiewska, E.; Weselake, R.J. Acyltransferase action in the modification of seed oil biosynthesis. *New Biotechnol.* **2009**, *26*, 11–14.
119. Kennedy, E.P. Biosynthesis of complex lipids. *Fed. Proc.* **1961**, *20*, 934–940.
120. Wendel, A.A.; Lewin, T.M.; Coleman, R.A. Glycerol-3-phosphate acyltransferases: Rate limiting enzymes of triacylglycerol biosynthesis. *Biochim. Biophys. Acta Mol. Cell. Biol. Lipids* **2009**, *1791*, 501–506.
121. Domergue, F.; Lerchl, J.; Zahringer, U.; Heinz, E. Cloning and functional characterization of *Phaeodactylum tricornutum* front-end desaturases involved in eicosapentaenoic acid biosynthesis. *Eur. J. Biochem.* **2002**, *269*, 4105–4113.
122. Arao, T.; Yamada, M. Biosynthesis of Polyunsaturated Fatty-Acids in the Marine Diatom, *Phaeodactylum tricornutum*. *Phytochemistry* **1993**, *35*, 1177–1181.
123. Yongmanitchai, W.; Ward, O.P. Positional distribution of fatty acids, and molecular species of polar lipids, in the diatom *Phaeodactylum tricornutum*. *J. Gen Microbiol.* **1993**, *139*, 465–472.
124. Joyard, J.; Ferro, M.; Masselon, C.; Seigneurin-Berny, D.; Salvi, D.; Garin, J.; Rolland, N. Chloroplast proteomics highlights the subcellular compartmentation of lipid metabolism. *Prog. Lipid Res.* **2010**, *49*, 128–158.
125. Kobayashi, K.; Awai, K.; Nakamura, M.; Nagatani, A.; Masuda, T.; Ohta, H. Type-B monogalactosyldiacylglycerol synthases are involved in phosphate starvation-induced lipid remodeling, and are crucial for low-phosphate adaptation. *Plant J.* **2009**, *57*, 322–331.
126. De Riso, V.; Raniello, R.; Maumus, F.; Rogato, A.; Bowler, C.; Falciatore, A. Gene silencing in the marine diatom *Phaeodactylum tricornutum*. *Nucleic Acids Res.* **2009**, *37*, e96.
127. Siaut, M.; Heijde, M.; Mangogna, M.; Montsant, A.; Coesel, S.; Allen, A.; Manfredonia, A.; Falciatore, A.; Bowler, C. Molecular toolbox for studying diatom biology in *Phaeodactylum tricornutum*. *Gene* **2007**, *406*, 23–35.
128. Xu, J.Y.; Zheng, Z.F.; Zou, J.T. A membrane-bound glycerol-3-phosphate acyltransferase from *Thalassiosira pseudonana* regulates acyl composition of glycerolipids. *Botany* **2009**, *87*, 544–551.
129. Zhang, L.; Ma, X.L.; Yang, G.P.; Zhu, B.H.; Han, J.C.; Yu, W.G.; Pan, K.H. Isolation and characterization of a long-chain acyl-coenzyme A synthetase encoding gene from the marine microalga *Nannochloropsis oculata*. *J. Appl. Phycol.* **2012**, *24*, 873–880.
130. Tonon, T.; Qing, R.; Harvey, D.; Li, Y.; Larson, T.R.; Graham, I.A. Identification of a long-chain polyunsaturated fatty acid acyl-coenzyme A synthetase from the diatom *Thalassiosira pseudonana*. *Plant. Physiol.* **2005**, *138*, 402–408.
131. Fulda, M.; Schnurr, J.; Abbadi, A.; Heinz, E.; Browse, J. Peroxisomal Acyl-CoA synthetase activity is essential for seedling development in *Arabidopsis thaliana*. *Plant Cell* **2004**, *16*, 394–405.

132. Hettema, E.H.; van Roermund, C.W.; Distel, B.; van den Berg, M.; Vilela, C.; Rodrigues-Pousada, C.; Wanders, R.J.; Tabak, H.F. The ABC transporter proteins Pat1 and Pat2 are required for import of long-chain fatty acids into peroxisomes of *Saccharomyces cerevisiae*. *EMBO J.* **1996**, *15*, 3813–3822.
133. Gong, Y.; Zhang, J.; Guo, X.; Wan, X.; Liang, Z.; Hu, C.J.; Jiang, M. Identification and characterization of PtDGAT2B, an acyltransferase of the DGAT2 acyl-coenzyme A: diacylglycerol acyltransferase family in the diatom Phaeodactylum tricornutum. *FEBS Lett.* **2013**, *587*, 481–487.
134. Gong, Y.; Guo, X.; Wan, X.; Liang, Z.; Jiang, M. Characterization of a novel thioesterase (PtTE) from *Phaeodactylum tricornutum*. *J. Basic Microbiol.* **2011**, *51*, 666–672.
135. Muto, M.; Kubota, C.; Tanaka, M.; Satoh, A.; Matsumoto, M.; Yoshino, T.; Tanaka, T. Identification and functional analysis of delta-9 desaturase, a key enzyme in PUFA synthesis, isolated from the oleaginous diatom *Fistulifera*. *PLoS One* **2013**, *8*, e73507.
136. Petrie, J.R.; Shrestha, P.; Mansour, M.P.; Nichols, P.D.; Liu, Q.; Singh, S.P. Metabolic engineering of omega-3 long-chain polyunsaturated fatty acids in plants using an acyl-CoA Δ6-desaturase with omega 3-preference from the marine microalga *Micromonas pusilla*. *Metab. Eng.* **2010**, *12*, 233–240.
137. Senger, T.; Marty, L.; Stymne, S.; Lindberg Yilmaz, J.; Napier, J.A.; Sayanova, O.; Haslam, R.; Noemi, R.L. Acyltransferases and uses therof in fatty acid production. US Patent 20,120,060,242 A1, 29 December 2011.
138. Bates, P.D.; Ohlrogge, J.B.; Pollard, M. Incorporation of newly synthesized fatty acids into cytosolic glycerolipids in pea leaves occurs via acyl editing. *J. Biol. Chem.* **2007**, *282*, 31206–31216.
139. Hu, Z.; Ren, Z.; Lu, C. The phosphatidylcholine diacylglycerol cholinephosphotransferase is required for efficient hydroxy fatty acid accumulation in transgenic *Arabidopsis*. *Plant Physiol.* **2012**, *158*, 1944–1954.
140. Pan, K.; Qin, J.; Li, S.; Dai, W.; Zhu, B.; Jin, Y.; Yu, W.; Yang, G.; Li, D. Nuclear monoploidy and asexual propagation of *Nannochloropsis oceanica (Eustigmatophyceae)* as revealed by its genome sequence. *J. Phyciol.* **2011**, *47*, 1425–1432.
141. Radakovits, R.; Jinkerson, R.E.; Fuerstenberg, S.I.; Tae, H.; Settlage, R.E.; Boore, J.L.; Posewitz, M.C. Draft genome sequence and genetic transformation of the oleaginous alga *Nannochloropis gaditana*. *Nat. Commun.* **2012**, *3*, 686.
142. Kilian, O.; Vick, B. Homologous recombination in an algal nuclear genome. US Patent 20,110,091,977 A1, 21 April 2011.
143. Jinkerson, R.E.; Radakovits, R.; Posewitz, M.C. Genomic insights from the oleaginous model alga *Nannochloropsis gaditana*. *Bioengineered* **2013**, *4*, 37–43.
144. Vieler, A.; Wu, G.; Tsai, C.H.; Bullard, B.; Cornish, A.J.; Harvey, C.; Reca, I.B.; Thornburg, C.; Achawanantakun, R.; Buehl, C.J.; *et al.* Genome, functional gene annotation, and nuclear transformation of the heterokont oleaginous alga *Nannochloropsis oceanica* CCMP1779. *PLoS Genet.* **2012**, *8*, e1003064.

145. Bondioli, P.; Bella, L.D.; Rivolta, G.; Zittelli, G.C.; Bassi, N.; Rodolfi, L.; Casini, D.; Prussi, M.; Chiaramonti, D.; Tredici, M.R. Oil production by the marine microalgae *Nannochloropsis* sp. F&M-M24 and *Tetraselmis suecica* F&M-M33. *Bioresour. Technol.* **2012**, *114*, 567–572.
146. Kilian, O.; Vick, B. Algal desaturases. Patent US8440805B2, 14 May 2013.
147. Kilian, O.; Vick, B. Algal elongases. Patent US2012/0277418A1, 1 November 2012.
148. Schneider, J.C.; Roessler, P.G. A novel acyltransferase activity in an oleaginous alga. *Plant Lipid Meta.* **1995**, 105–107.
149. Kato, M.; Sakai, M.; Adachi, K.; Ikemoto, H.; Sano, H. Distribution of betaine lipids in marine algae. *Phytochemistry* **1996**, *42*, 1341–1345.
150. Sprecher, H. Metabolism of highly unsaturated *n*-3 and *n*-6 fatty acids. *Biochim. Biophys. Acta Mol. Cell. Biol. Lipids* **2000**, *1486*, 219–231.
151. Metz, J.G.; Roessler, P.; Facciotti, D.; Levering, C.; Dittrich, F.; Lassner, M.; Valentine, R.; Lardizabal, K.; Domergue, F.; Yamada, A.; *et al.* Production of polyunsaturated fatty acids by polyketide synthases in both prokaryotes and eukaryotes. *Science* **2001**, *293*, 290–293.
152. Metz, J.G.; Kuner, J.; Rosenzweig, B.; Lippmeier, J.C.; Roessler, P.; Zirkle, R. Biochemical characterization of polyunsaturated fatty acid synthesis in *Schizochytrium*: release of the products as free fatty acids. *Plant Physiol. Biochem.* **2009**, *47*, 472–478.
153. Hauvermale, A.; Kuner, J.; Rosenzweig, B.; Guerra, D.; Diltz, S.; Metz, J.G. Fatty acid production in *Schizochytrium* sp.: Involvement of a polyunsaturated fatty acid synthase and a type I fatty acid synthase. *Lipids* **2006**, *41*, 739–747.
154. Chang, G.; Gao, N.; Tian, G.; Wu, Q.; Chang, M.; Wang, X. Improvement of docosahexaenoic acid production on glycerol by *Schizochytrium* sp. S31 with constantly high oxygen transfer coefficient. *Bioresour. Technol.* **2013**, *142*, 400–406.
155. Matsuda, T.; Sakaguchi, K.; Hamaguchi, R.; Kobayashi, T.; Abe, E.; Hama, Y.; Hayashi, M.; Honda, D.; Okita, Y.; Sugimoto, S.; *et al.* Analysis of Δ12-fatty acid desaturase function revealed that two distinct pathways are active for the synthesis of PUFAs in *T. aureum* ATCC 34304. *J. Lipid Res.* **2012**, *53*, 2806–2806.
156. Ohara, J.; Sakaguchi, K.; Okita, Y.; Okino, N.; Ito, M. Two fatty acid elongases possessing C18-Δ6/C18-Δ9/C20-Δ5 or C16-Δ9 elongase activity in *Thraustochytrium* sp. ATCC 26185. *Marine Biotechnol.* **2013**, *15*, 476–486.
157. Qiu, X.; Hong, H.P.; MacKenzie, S.L. Identification of a Δ4 fatty acid desaturase from T*hraustochytrium sp.* involved in the biosynthesis of docosahexanoic acid by heterologous expression in *Saccharomyces cerevisiae* and *Brassica juncea*. *J. Biol. Chem.* **2001**, *276*, 31561–31566.
158. Nagano, N.; Sakaguchi, K.; Taoka, Y.; Okita, Y.; Honda, D.; Ito, M.; Hayashi, M. Detection of genes Involved in fatty acid elongation and desaturation in thraustochytrid marine eukaryotes. *J. Oleo Sci.* **2011**, *60*, 475–481.
159. Shi, T.L.; Yu, A.Q.; Li, M.; Ou, X.Y.; Xing, L.J.; Li, M.C. Identification of a novel C22-Δ4-producing docosahexaenoic acid (DHA) specific polyunsaturated fatty acid desaturase gene from *Isochrysis galbana* and its expression in *Saccharomyces cerevisiae*. *Biotechnol. Lett.* **2012**, *34*, 2265–2274.

160. Guihéneuf, F.; Ulmann, L.; Mimouni, V.; Tremblin, G. Use of radiolabeled substrates to determine the desaturase and elongase activities involved in eicosapentaenoic acid and docosahexaenoic acid biosynthesis in the marine microalga *Pavlova lutheri*. *Phytochemistry* **2013**, *90*, 43–49.
161. Pereira, S.L.; Leonard, A.E.; Huang, Y.S.; Chuang, L.T.; Mukerji, P. Identification of two novel microalgal enzymes involved in the conversion of the omega3-fatty acid, eicosapentaenoic acid, into docosahexaenoic acid. *Biochem. J.* **2004**, *384*, 357–366.
162. Tonon, T.; Harvey, D.; Larson, T.R.; Graham, I.A. Identification of a very long chain polyunsaturated fatty acid Δ4-desaturase from the microalga *Pavlova lutheri*. *FEBS Lett.* **2003**, *553*, 440–444.
163. Daboussia, F.; Collinb, S.; Leduca, S.; Cavareca, L.; Marechala, A.; Falciatorec, A.; Laeufferb, F.; Fourageb, L.; Duchateaua, P. Diatoms genome engineering using targeted nucleases approaches. In *The Molecular Life of Diatoms*; EMBO Workshop: Paris, France, 2013.
164. Doan, T.T.Y.; Obbard, J.P. Enhanced intracellular lipid in *Nannochloropsis* sp. via random mutagenesis and flow cytometric cell sorting. *Algal Res.* **2012**, *1*, 17–21.
165. Chaturvedi, R.; Uppalapati, S.R.; Alamsjah, M.A.; Fujita, Y. Isolation of quizalofop-resistant mutants of *Nannochloropsis oculata* (Eustigmatophyceae) with high eicosapentaenoic acid following *N*-methyl-*N*-nitrosourea-induced random mutagenesis. *J. Appl. Phycol.* **2004**, *16*, 135–144.
166. Meireles, L.A.; Guedes, A.C.; Malcata, F.X. Increase of the yields of eicosapentaenoic and docosahexaenoic acids by the microalga *Pavlova lutheri* following random mutagenesis. *Biotechnol. Bioeng.* **2003**, *81*, 50–55.

Appendix: Definitions and Abbreviations

Acetyl-CoA carboxylase (ACCase): Catalyzation of acetyl-CoA to malonyl-CoA in the chloroplast and the cytosol.

Acyl-CoA synthetase (ACS): Substrate specific esterification of a FA to a glycerol-backone (see Kennedy pathway).

Acyl-editing: Shuffling the FAs between the PC-pool and the DAG-pool by activities of acyltransferases; phospholipid/diacylglycerol acyltransferase (PDAT), lysophospholipid acyltransferases (LPLAT) and phospholipases.

ATP-citrate lyase (ATP:CL): Synthesis of citrate to acetyl-CoA.

Betaine-type glycerolipids: Membrane compartments; diacylglyceryltrimethylhomoserine (DGTS), diacylglyceryl glucuronide (DGGA), diacylglycerylhydroxymethyltrimethylalanine (DGTA), diacylglycerylcarboxyhydroxymethylcholine (DGCC).

Galactosylglycerides: Membrane compartments; eukaryotic and prokaryotic species of Monogalactosyldiacylglycerol (1,2-diacyl-3-*O*-(β-D-galactopyranosyl)-*sn* glycerol, MGDG), digalactosyldiacylglycerol (1,2-diacyl-3-*O*-(α-D-galactopyranosyl)-(1→6)-*O*-β galactopyranosyl *sn*-glycerol, DGDG).

Glycosylglycerides: Represent in the thylakoid and the non-photosynthetic membrane; MGDG, DGDG and sulphoquinovosyldiacylglycerol (1,2-diacyl-3-*O*-(6-deoxy-6-sulfo-a-D-glucopyranosyl)-*sn* glycerol, SQDG).

Fatty acid synthase (FAS): Synthesize malonyl-ACP to short chain FAs in several condensation steps, type I FAS: FAS synthesized from one or two polypeptides, type II FAS: discrete, monofunctional enzymes encoded by distinct genes.

Fatty acyl-ACP thioesterase (FAT): Releases free FAs from acyl-ACPs, synthesized from de novo fatty acid biosynthesis.

Kennedy pathway: Esterification of glycerol-3-phosphate by acyl-CoA:glycerol-3-phosphate acyltransferase (GPAT). The formed lysophosphatidic acid (LPA) is converted by acyl-CoA:lysophosphatidic acyltransferase (LPAAT) into phosphatidic acid (PA) by adding a second FA to the *sn*-2 position. Dephosphorylation of the *sn*-3 position forms through the phosphatidic acid phosphatase (PAP) activity. Diacylglycerol (DAG) is formed which can be synthesis to TAG.

Long chain acyl CoA synthetase (LACS): Activation of FA by esterification to coenzyme A.

Malic enzyme (ME): Possess different localizations (plastidial, mitochondrial), synthesize malate and NAD(P) to pyruvate and NAD(P)H.

Phosphoglycerides: Membrane compartments; phosphatidylcholine (PC), phosphatidylglycerol (PG), phosphatidylethanolamine (PE).

Polyketide synthase (PKS): Multi-domain enzymes or enzyme complexes that synthesize PUFAs while being attached to ACP-domains.

Pyruvate dehydrogenase complex (PDC): Complex of three enzymes transforming pyruvate into acetyl-CoA by a process called pyruvate decarboxylation.

Thioesterase (TE): Hydrolyze thioester bonds.

Triacylglycerides (TAGs): Lipid storage compartments in algae, three FAs are esterificated to a glycerol.

Paper II

PLOS ONE

RESEARCH ARTICLE

The plastoquinone pool of *Nannochloropsis oceanica* is not completely reduced during bright light pulses

Gunvor Røkke[1], Thor Bernt Melø[2], Martin Frank Hohmann-Marriott[1]*

1 Department of Biotechnology, Norwegian University of Science and Technology, Trondheim, Norway,
2 Department of Physics, Norwegian University of Science and Technology, Trondheim, Norway

* martin.hohmann-marriott@ntnu.no

Citation: Røkke G, Melø TB, Hohmann-Marriott MF (2017) The plastoquinone pool of *Nannochloropsis oceanica* is not completely reduced during bright light pulses. PLoS ONE 12(4): e0175184. https://doi.org/10.1371/journal.pone.0175184

Editor: Rajagopal Subramanyam, University of Hyderabad School of Life Sciences, INDIA

Received: January 5, 2017

Accepted: March 21, 2017

Published: April 12, 2017

Data Availability Statement: The raw data is uploaded to Dryad: doi:10.5061/dryad.vb724.

Funding: The Faculty of Natural Sciences (https://www.ntnu.no/nv) at the Norwegian University of Science and Technology (NTNU) founded the PhD position (G.R). Grant number is not available. The funder had no role in study design, data collection and analysis, decision to publish, or preparation of the manuscript.

Competing interests: The authors have declared that no competing interests exist.

Abstract

The lipid-producing model alga *Nannochloropsis oceanica* has a distinct photosynthetic machinery. This organism possesses chlorophyll *a* as its only chlorophyll species, and has a high ratio of PSI to PSII. This high ratio of PSI to PSII may affect the redox state of the plastoquinone pool during exposure to light, and consequently may play a role in activating photoprotection mechanisms. We utilized pulse-amplitude modulated fluorometry to investigate the redox state of the plastoquinone pool during and after bright light pulses. Our data indicate that even very intense (5910 μmol photons $s^{-1}m^{-2}$ of blue light having a wavelength of 440 nm) light pulses of 0.8 second duration are not sufficient to completely reduce the plastoquinone pool in *Nannochloropsis*. In order to achieve extensive reduction of the plastoquinone pool by bright light pulses, anaerobic conditions or an inhibitor of the photosynthetic electron transport chain has to be utilized. The implication of this finding for the application of the widely used saturating pulse method in algae is discussed.

Introduction

Pulse Amplitude Modulated (PAM) fluorometry has proven a valuable technique for studying the photosynthetic performance of plants and algae *in situ* [1, 2].

A PAM fluorometer assesses variable chlorophyll fluorescence by applying very weak measuring light pulses that ideally do not induce photosynthesis. The fluorescence induced by these low energy light pulses can be electronically isolated from the fluorescence induced by other light sources. Consequently, the fluorescence signal obtained by a PAM fluorometer is easily interpreted and independent of applied light sources, which could include photosynthetically active light or additional saturating light pulses. Sophisticated PAM fluorometry techniques have been developed that allow for the assessment of photosynthetic performance and for the characterization of different mechanisms that modulate chlorophyll fluorescence.

Modulation of chlorophyll fluorescence

The main modulator of chlorophyll fluorescence is the redox state of Q_A, a plastoquinone that is the first stable electron acceptor of Photosystem II (PSII). From Q_A the electron passes to

Abbreviations: DBMIB, 2,5-dibromo-3-methyl-6-isopropylbenzoquinone; LHCII, Light Harvesting Complex II; NPQ, Non-photochemical Quenching; PAM, Pulse Amplitude Modulation; PQ, Plastoquinone; PSI, Photosystem I; PSII, Photosystem II; PTOX, Plastid terminal oxidase.

Q_B, which is a PSII-associated member of the plastoquinone pool. If Q_A is oxidized, excitation energy captured in the light harvesting complexes associated with PSII (LHCII) is efficiently used for charge separation, and the fluorescence emission will thus be low [3]. However, if Q_A is already reduced, and therefore unable to accept an electron, excitation energy captured by chlorophylls in the light harvesting complexes will be given off as fluorescence.

A second mechanism that modulates the fluorescence yield is state transitions. If an alga or a plant receives an unusually high amount of light energy, electrons can accumulate in the electron transport chain leading to the generation of reactive oxygen species. In order to avoid the production of reactive oxygen species, some plants and algae are able to move some of their light harvesting complexes (LHCs), which are usually associated with PSII to Photosystem I (PSI). This re-balances the photosynthetic electron transport chain, as fewer electrons are generated by PSII and more electrons are being disposed of by PSI. While state transitions have been established in plants [4] and certain algae [5], state transitions are not thought to be a major contributor to modulating fluorescence in heterokont algae, such as *Nannochloropsis*.

State transitions can also be induced by oxygen depletion [6, 7]. When cells are deprived of oxygen, which is their usual mitochondrial terminal electron acceptor, they will no longer be able to re-oxidise NADH to NAD^+ [8]. Consequently, electrons will accumulate within the cell, and eventually also reduce the PQ pool.

A third mechanism that modulates fluorescence is the conversion of certain pigments within the light harvesting complexes, enabling them to dissipate excitation as heat. Violaxanthin, which is a light harvesting xanthophyll pigment, can be converted via antheraxanthin into zeaxanthin, which is efficient in converting excess excitation energy into heat. This protective pathway is termed the xanthophyll cycle, and has been demonstrated in plants and green algae. It is also thought of as a major modulator of fluorescence in heterokont algae [9].

An additional, often neglected fluorescence modulating mechanism is the decrease in chlorophyll fluorescence yield occurring when oxidised plastoquinones interact with chlorophyll *a* molecules. This type of fluorescence modulation was termed "non-photochemical quenching of chlorophyll *a* by oxidised plastoquinone" by Haldimann and Tsimilli-Michael in 2005 [10], and was first described by Vernotte et al. in 1979 [11]. The effect of this quenching mechanism can be observed in conditions that reduce the plastoquinone pool, such as anaerobic conditions [12].

Photochemical vs. non-photochemical quenching

A decrease in fluorescence is often termed "fluorescence quenching", indicating that the energy captured by the light harvesting complexes is dissipated by other means than via emitting fluorescence. If excitation energy is utilized by PSII to perform a charge separation, a "photochemical quench", mainly modulated by the availability of oxidized Q_A, is present. A decrease in the chlorophyll fluorescence yield that is not caused by photochemistry is called non-photochemical quenching (NPQ) as a collective term. Both state-transition-dependent quenching and xanthophyll-cycle-dependent quenching are established types of non-photochemical quenching.

The saturating light pulse method

The saturating light pulse method is an experimental approach that has been devised to determine the amount of photochemical quenching. This approach uses saturating light pulses that have been shown to completely reduce the PQ pool in plants and green algae. In this condition, no electron acceptors are available for Q_A, and consequently every Q_A will be reduced, thus eliminating all photochemical quenching. For work in plants and green algae a standard

nomenclature for different fluorescence levels has been adopted. The maximum fluorescence yield that can be achieved during a bright light pulse is termed F_m. In contrast, the lowest possible fluorescence yield, F_0 (both F_m and F_0 are defined in dark, aerobic conditions), is the ground fluorescence of the light harvesting complexes of the system recorded in measuring light, which is weak enough to not cause any reduction of Q_A. During measuring light, the PQ pool stays largely oxidized.

The saturating light pulse method is also able to assess non-photochemical quenching. For this purpose, a reference condition is chosen where non-photochemical quenching is absent. In plants and algae, this is the case in dark and oxygenated conditions, where light harvesting complexes have been shown to be associated with PSII, and the xanthophyll cycle is not engaged. After exposure to light or other conditions known to modulate chlorophyll fluorescence, the decrease in chlorophyll fluorescence induced by saturating light pulses is interpreted as NPQ.

The saturation pulse method has also been applied to heterokont algae, such as *Phaeodactylum* [13, 14] or *Nannochloropsis* [15]. However, the suitability of applying this method in *Nannochloropsis* has not been tested in detail.

Saturation pulse method in *Nannochloropsis*

In this report, we investigate if the saturation pulse method can be applied to the heterokont alga *Nannochloropsis*. This alga has emerged as a model organism due to its ability to produce triacylglycerols and ω3-fatty acids [16, 17], as well as pigments and antioxidants [18].

The photosynthetic machinery of *Nannochloropsis* is similar to other heterokont algae. However, some *Nannochloropsis*-specific features in the pigmentation and photosystem ratio have been recognized. Unlike many other heterokont algae, which utilize both chlorophyll *a* and *c* in their light harvesting complexes, *Nannochloropsis* only possesses chlorophyll *a* [19]. Also, contrary to green algae and plants, where the ratio between PSI and PSII has been shown to lie between 0.53–0.67 [20], the PSI to PSII ratio in *Nannochloropsis* is about 1.7 [21]. This high ratio of PSI to PSII may make it difficult to fully reduce the PQ pool by bright light pulses used in the saturating light pulse method.

Materials and methods

Preparation of cell cultures

Nannochloropsis oceanica CCMP1779 obtained from the National Center for Marine Algae and Microbiota (NCMA) was utilized in the study. Pre-cultures were incubated at 18˚C and a light intensity of 200 μmol photons $m^{-2}s^{-1}$. In all liquid cultures, f/2 medium was utilized [22].

For experiments, cultures with cells in the exponential growth phase were harvested and concentrated to a chlorophyll concentration of 40 μg Chl *a*/ml.

The samples were dark acclimated for three hours prior to starting PAM measurements.

Chlamydomonas reinhardtii was included in certain measurements. The strain CC-4532 mt- obtained from the *Chlamydomonas* Resource Center at the University of Minnesota was utilized. TrisAcPO$_4$ (TAP) medium was utilized for the liquid *Chlamydomonas* cultures. The pre-cultures of *C. reinhardtii* were incubated in the same conditions as the pre-cultures of *Nannochloropsis*, and a chlorophyll *a* concentration of 40 μg/ml was used for experiments. *Chlamydomonas* samples were dark-acclimated one hour prior to measurements.

PAM fluorometry

For the PAM measurements, a MultiColor PAM fluorometer (Walz, Germany) coupled to an Oxygraph oxygen measurement device (Hansatech, United Kingdom) was used. A volume of

2 ml of cell sample was used for every measurement. During measurements, 0.8 second long bright light pulses of 1600 μmol photons $m^{-2}s^{-1}$ of blue light (440 nm) were applied every minute. In the result part, data from every fourth measurement is shown. Our experimental setup for measuring oxygen and chlorophyll fluorescence simultaneously, allowed usage of light intensities as high as 1600 μmol photons $m^{-2}s^{-1}$. The MultiColor PAM instrument used also enabled us to choose between saturating light pulses of white and blue light. To assure that the bright light pulses used were saturating (a saturating light pulse is usually defined as a white light pulse having a light intensity above 2000 μmol photons $m^{-2}s^{-1}$), we chose to use light pulses of blue light, having a wavelength that matches the 440 nm absorption peak of chlorophyll *a*. Plants and alga absorb only about half the photons in white light, due to the absorption properties of their pigments. The effective light intensity of blue light is therefore about twice as high as white light. The intensity of blue light used in these experiments is consistent with the intensity required to achieve saturating light pulses.

Experiments investigating the effects of anaerobic conditions and high light with and without the use of a b_6f complex inhibitor were performed with the setup combining PAM measurements and oxygen measurements. Since this experiment setup restricted the intensity of the bright light pulses to 1600 μmol photons $m^{-2}s^{-1}$, an additional experiment was conducted investigating ten bright light pulse intensities ranging from 715 to 5910 μmol photons $m^{-2}s^{-1}$. This experiment was performed in aerobic conditions, allowing a different setup where the illumination source could be moved closer to the sample, yielding a higher maximum light intensity of the bright light pulses.

The inhibitor 2,5-dibromo-3-methyl-6-isopropylbenzoquinone (DBMIB) (stock solution: 20 mM) was added to a final concentration of 20 μM.

The cells were left in complete darkness for 12 minutes before DBMIB was added. After 12 more minutes, actinic white light (960 μmol photons/m^2s) was turned on for 32 minutes. The same actinic light intensity was used for illuminating untreated cells. To obtain anaerobic conditions, cells were placed into the sealed chamber of the oxygen electrode, with respiration in the dark leading to oxygen depletion.

Processing of PAM data

The raw data was extracted from the MultiColor PAM and the Oxygraph software packages, and MATLAB was utilized to normalize and plot the data. To facilitate comparison of fluorescence signals between the different experiments, the raw data was normalized (the F_0 value prior to the first bright light pulse was set to zero, while the averaged F_m values of the first group of pulses in each experiment, were set to 100).

The variable fluorescence kinetics after bright light pulses were analysed to gain insights into the reduction state of the PQ pool. For this the rate constant (λ) of the chlorophyll fluorescence signal after a bright light pulse (A(t)) was determined by fitting the data to an exponential decay function with baseline offset (y) using MATLAB.

$$A(t) = A_0 \cdot e^{-\lambda t} + y \quad (1)$$

Results and discussion

In this study, we investigated if the saturation pulse methodology can be applied to the heterokont model alga *Nannochloropsis*. In particular, we were interested if the bright pulses of light intended to induce maximum fluorescence yield (F_m) has the same effect in *Nannochloropsis* as in green algae and plants.

Saturating light pulse analysis under different conditions

To investigate the effect of bright light pulses in *Nannochloropsis* we selected parameters routinely used for saturating light pulse analysis in plants and green algae. We chose light pulses with a length of 0.8 s and an intensity of 1600 μmol of 440 nm (blue) photons $m^{-2}s^{-1}$. To assess if these pulses fully reduce the PQ pool we investigated three conditions known to completely reduce the PQ pool in plants and green algae. These conditions include (A) high light treatment (B) anaerobic conditions and (C) blocking the photosynthetic electron transport chain by utilizing the cytochrome b_6f complex inhibitor DBMIB (Fig 1).

Following the standard methodology, light pulses in dark-adapted samples were used to assess the maximum fluorescence yield in the absence of non-photochemical quenching (Fig 1A',B' and 1C'). The fluorescence yield of these saturating light pulses is marginally lower than the fluorescence yield observed in high light conditions (Fig 1A"). In anaerobic conditions (Fig 1B"), the maximum fluorescence initially increases, and then decreases again over time. The biggest increase in pulse-induced fluorescence is seen in the presence of DBMIB in high light (Fig 1C"'). Normalized fluorescence yields from the experiments summarized in Fig 1 are displayed in Fig 2.

The maximum fluorescence levels in the *Nannochloropsis* experiments displayed in Fig 1 follow a different pattern compared to well-documented observations from plants and green algae. In these organisms, bright light pulses induce the maximum fluorescence yield in dark aerobic conditions, while reduction of the PQ pool (through light or anaerobic conditions) leads to NPQ and a reduced light pulse-induced maximum fluorescence. In *Nannochloropsis*, light pulse induced fluorescence yields that are higher than the ones observed in dark-adapted, aerobic conditions can be achieved through actinic light and anaerobic conditions.

The low fluorescence yield in dark aerobic conditions may indicate the presence of a fluorescence quenching mechanism, which is diminished in high light conditions, anaerobic conditions and especially in the presence of DBMIB. This fluorescence quenching may occur within the light harvesting complexes, or may also be caused by an incomplete reduction of the primary fluorescence modulator Q_A in dark aerobic conditions, due to an incomplete reduction of the PQ pool. In order to gain further insight into the reduction state of the plastoquinone pool of *Nannochloropsis* in different experimental conditions, the kinetics of change in variable chlorophyll fluorescence after bright light pulses were investigated.

The fluorescence level after 10 ms of bright illumination (commonly referred to as the I level in the OIDP nomenclature [23]) is thought to reflect the accumulation of electrons on Q_A. This initial level is quite similar in the dark conditions of all three experiments (Fig 2A', 2B' and 2C', and also in high light, anaerobic conditions and in the presence of DBMIB in darkness. Only in DBMIB-treated cells in high light is this initial fluorescence level visibly elevated (Fig 2C"').

There are two models to explain the fast-rise (O to the I level) and the subsequent slower phases (IDP) of chlorophyll fluorescence induction. The first model assumes the existence of different populations of PSII that differ in their ability to transfer electrons from Q_A to Q_B [24]. The basis for the difference in Q_A to Q_B transfer could be an intrinsic property of PSIIs or be based on differences in accessibility to oxidized PQ. The second model used to explain the two phases of the fluorescence induction assumes that the reduction of Q_A is the cause of the initial fast fluorescence increase (O to I), whereas the reduction of the plastoquinone pool leads to the subsequent slow increase in fluorescence (I to P). The second model assumes that oxidized plastoquinones quenches fluorescence, most likely via transient electron transfer between oxidized plastoquinones and chlorophyll *a* [10]. Light-induced reduction of the plastoquinone pool requires movement of plastoquinones through the thylakoid membrane and

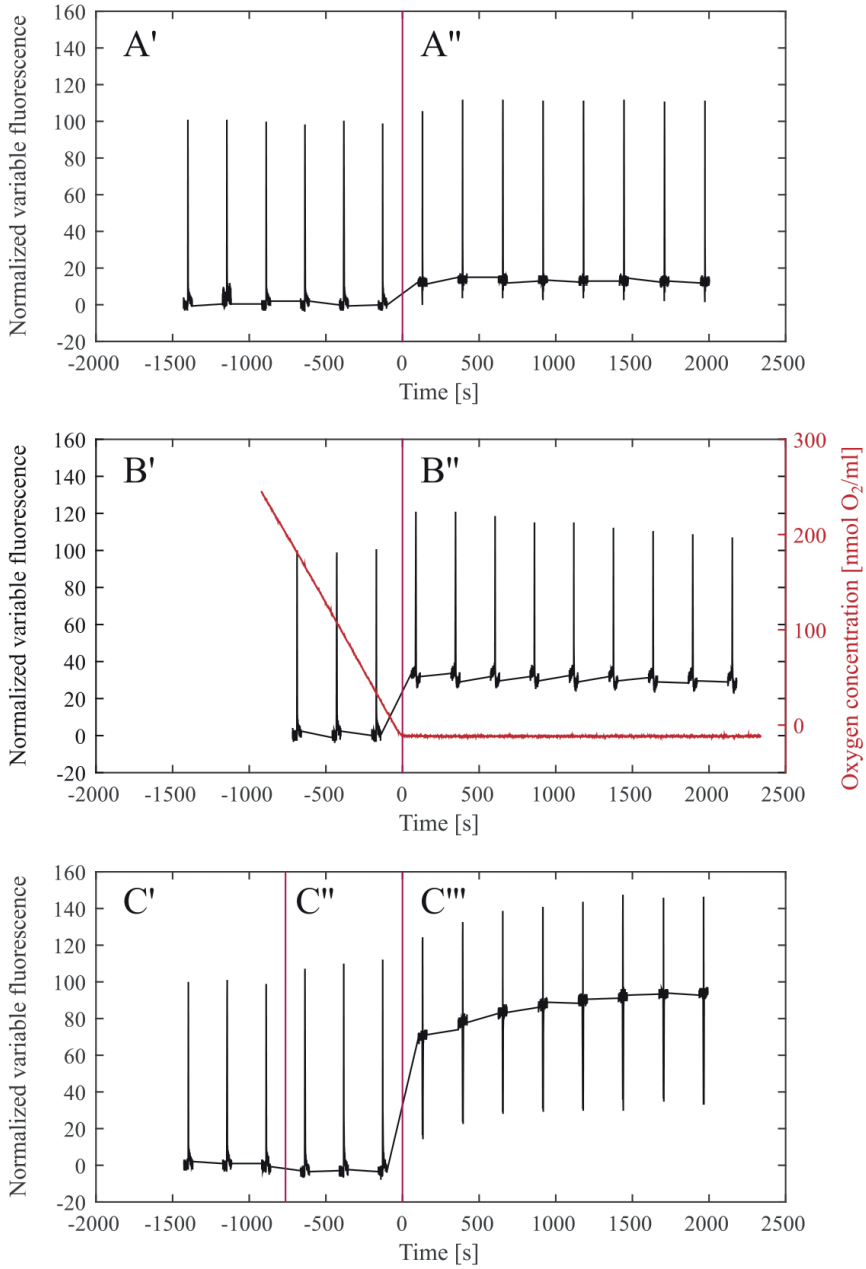

Fig 1. Variable chlorophyll fluorescence assessed by the saturation pulse method in *Nannochloropsis* cells in A) Actinic light (960 μmol photons $m^{-2}s^{-1}$), B) Anaerobic conditions, and C) Actinic light after treatment with the cytochrome b_6f complex inhibitor DBMIB. Saturating light pulses were applied every 4 minutes. Panel A, split by a

vertical line shows the data recorded in darkness (A'), and the data recorded in the presence of high actinic light (A"). The zero time point is defined as the time point when the actinic light was turned on. Panel B, also split by a vertical line, shows the data recorded when oxygen was still available to the cells (B'), and the data recorded after the cells entered anaerobiosis (B"). The red graph shows the oxygen concentration throughout the experiment, and the zero time point is defined as the moment when the oxygen was depleted. Panel C, split by two vertical lines, shows the fluorescence data recorded in darkness before the addition of DBMIB (C'), in darkness after the addition of DBMIB (C") and after the application of high actinic light (C"'). The zero time point is defined as the moment when the actinic light was turned on.

https://doi.org/10.1371/journal.pone.0175184.g001

docking of oxidized plastoquinones to PSII prior to electron transfer from Q_A [25]. The second phase being slow and showing temperature dependence is in line with the second model [26].

Common to both models is that they both predict that a fully reduced PQ pool will abolish fluorescence quenching. The saturation pulse method uses bright light pulses to reduce the PQ pool and thereby determine the maximum fluorescence yield. However, the fluorescence induction kinetics observed during bright light pulses in *Nannochloropsis* in darkness and in high light (Fig 2) do not show a typical OIDP transient. The lack of fluorescence increase beyond the first inflection point of the fluorescence induction curve (the I level in plants) can be interpreted as the PQ pool already being reduced at this inflection point, or that the PQ pool remains oxidized during the bright light pulse. Anaerobic conditions, which are known to reduce the PQ pool in a variety of organisms, reveal an OIDP transient that is similar to the one observed in plants, thus indicating that the PQ pool is oxidized in aerobic conditions, and can be reduced by bright light pulses in anaerobic conditions. Chlorophyll fluorescence kinetics in dark-adapted cells in the presence of DBMIB do not possess a typical OIDP transient. There is also no OIDP transient in DBMIB-treated and in highlight-treated cells. Surprisingly, the lack of the OIDP transient in DBMIB-treated cells could indicate that the PQ pool is not reduced by saturating light pulses, even if electron transport through the cytochrome b_6f complex is blocked.

Fluorescence decay kinetics as indicator of PQ reduction

To gain insights into the reduction state of the PQ pool after bright light pulses, the decrease in chlorophyll fluorescence immediately following the pulses was analysed. After bright light pulses, the reduced Q_A^- is re-oxidized, leading to a gradual decrease in chlorophyll fluorescence over time. In plants and green algae the oxidation of Q_A^- is due to different processes that can be kinetically grouped within three time domains.

Post-illumination oxidation of Q_A^- in the fastest time domain is dependent of the availability of oxidized Q_B that is present immediately after a bright light pulse. This Q_B-dependent Q_A^- oxidation is based on (a) the oxidation of Q_A^- by Q_B or Q_B^- (half time ~300 μs, [27, 28]), (b) the exchange of Q_B^{2-} with an oxidized PQ (half time of electron transport from Q_A to Q_B when Q_B has to bind first ~1,3–2 ms [27]), and (c) the diffusion of oxidized PQ between the cytochrome b_6f complex and PSII (half time ~15 ms [28]). Consequently, the decrease in chlorophyll fluorescence due to these fast Q_A^- oxidation events is mostly completed after 50 ms.

Post-illumination oxidation of Q_A^- in the second fastest time domain (half time 200 ms) is due to recombination of Q_A^- with the donor side of PSII. It has been demonstrated that the kinetics of Q_A^- oxidation by donor-side electron acceptors is dependent on the redox state of the PQ pool [29] and independent of oxygen concentration [30].

Post-illumination oxidation of Q_A^- the third fastest time domain (half time of several seconds) is due to the oxidation of the PQ pool by oxygen-dependent consumption of electrons [30]. The responsible oxidases may be located in the chloroplast (e.g. the plastid terminal oxidase, abbreviated PTOX), or coupled by electron shuttles to the cytoplasmic and mitochondrial electron transport chain [31].

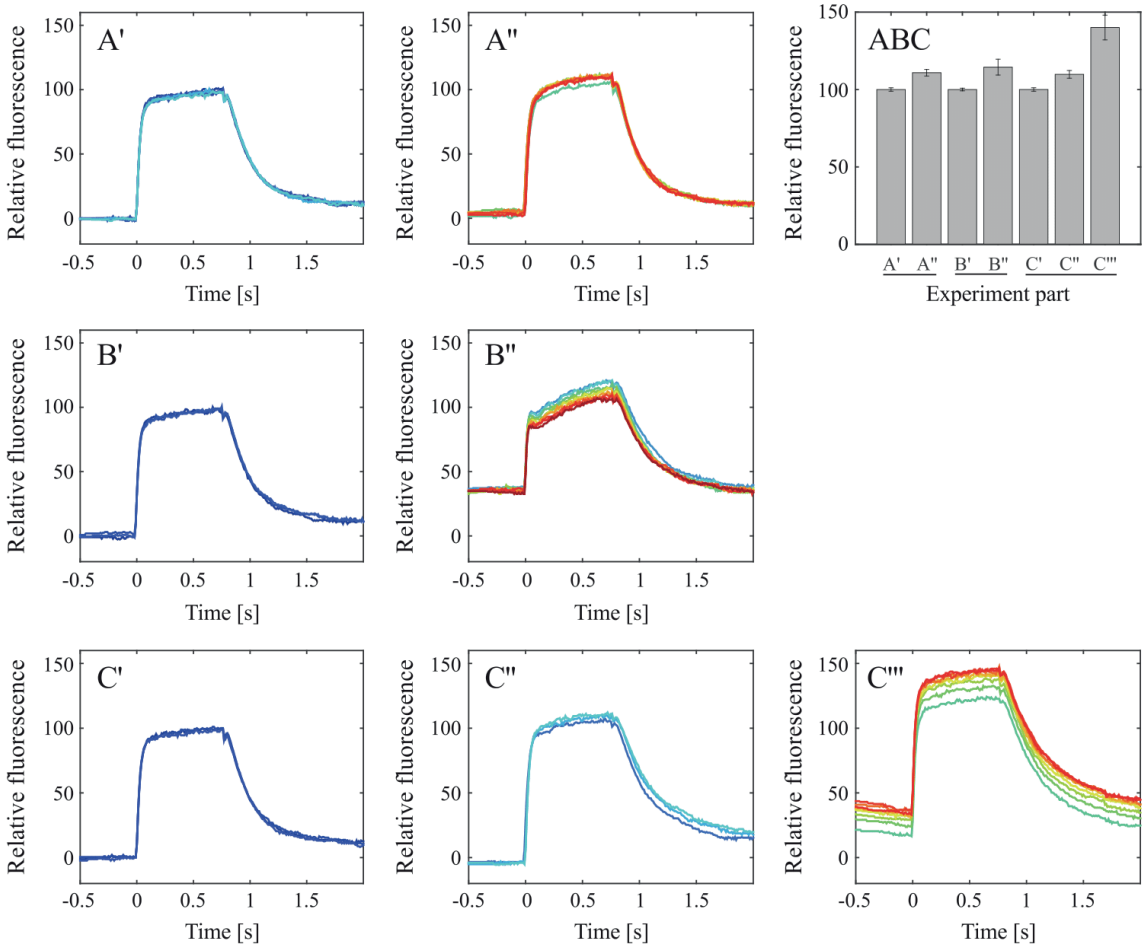

Fig 2. Variable chlorophyll fluorescence emitted by *Nannochloropsis oceanica* cells during bright light pulses. Graph series A shows the high light experiment performed without DBMIB (A'–fluorescence signal of dark adapted cells in darkness, A"–fluorescence signal in high light). Graph series B shows the anaerobic experiment (B'–fluorescence signal of aerobic cells, B"–fluorescence signal of anaerobic cells). Graph series C shows the results from the high light experiment performed in the presence of DBMIB (C'–fluorescence signal of dark-adapted cells in darkness without inhibitor, C"–fluorescence signal of cells in darkness after the addition of DBMIB, C"'–fluorescence signal of cells in high light, and in the presence of DBMIB). In both experiment A, B and C, the colour of the fluorescence curve indicates when in the experiment the particular curve was recorded. The colours of the fluorescence curves proceed from dark blue (the first recorded curves) via light blue, green, yellow and orange to red (the last recorded curves). The bar diagram (ABC) displayed in the upper right panel summarizes the F_m values in the different phases of the three experiments.

https://doi.org/10.1371/journal.pone.0175184.g002

We have analysed the chlorophyll fluorescence decrease in the second fastest phase, which–in analogy to higher plants -, we assume to rely on the recombination of Q_A^- with the donor side of PSII, to gain insights into the reduction state of the PQ pool after saturating light pulses. Fig 3A shows rate constants for the fluorescence decrease after bright light pulses in different

conditions (fluorescence curves displayed in Fig 2). The fit parameters obtained for fitting Eq 1 to fluorescence transients after a light pulse can be found in S1 and S2 Tables.

Subjecting the cells to anaerobic conditions and treatment with DBMIB (in dark-adapted conditions and high light) leads to a significant decrease in the decay constants compared to dark aerobic conditions (Fig 3A). This distribution of rate constants indicate that the PQ pool has a higher degree of reduction after saturating light pulses in anaerobic conditions and in the presence of DBMIB (dark-adapted and high light) compared to aerobic conditions (dark-adapted and high light). We therefore concluded that bright light pulses with an intensity of 1600 μmol photons $m^{-2}s^{-1}$ of blue light (440 nm) leave the PQ pool oxidized.

The apparent inability of bright light pulses to reduce the PQ pool in standard (dark aerobic) conditions was further investigated. For this we varied the light pulse intensity (from 715 to 5910 μmol photons $m^{-2}s^{-1}$) and analysed the rate constants of the fluorescence curves in aerobic dark conditions in the presence and absence of DBMIB (Fig 3B). We also determined the fluorescence kinetics subsequent to bright pulses of light in the green alga *Chlamydomonas* under the same conditions.

Increasing the light intensity does not decrease the rate constants in untreated *Nannochloropsis* cells, while a light-dependent decrease in rate constants for *Chlamydomonas* can be observed. The rate constants for untreated *Nannochloropsis* cells are higher than the rate constants for untreated *Chlamydomonas* cells. This indicates that even light pulses with very high light intensity are unable to reduce the PQ pool in *Nannochloropsis*.

Addition of DBMIB reduces the rate constants after bright light pulses in *Nannochloropsis* and *Chlamydomonas* to a similar level. This data indicate that in the presence of DBMIB, the PQ pool of both *Nannochloropsis* and *Chlamydomonas* PQ is reduced after the application of bright light pulses. This would be expected as DBMIB is thought to block electron transport at the cytochrome b_6f complex.

Conclusion and implications

Effect of bright light pulses

According to our interpretation of the fluorescence data, bright light pulses of 0.8 s are not sufficient to reduce the PQ pool in untreated *Nannochloropsis oceanica* cells.

The most likely reason for this is the unusually high PSI:PSII ratio of about 1.7 [21, S1 Fig] in *Nannochloropsis*. In plants, the PSI:PSII ratio has been found to lie between 0.53 and 0.67 [20]. The excess of PSI in *Nannochloropsis* may therefore be able to maintain a partially oxidized PQ pool, even during bright illumination.

Our finding that the PQ pool in *Nannochloropsis* is not reduced by bright light pulses has implications for interpreting results obtained by the saturating light pulse method, since a fully reduced plastoquinone pool is a prerequisite for the application of saturating light pulse analysis. Therefore, caution should be exercised when the saturating light pulse method is applied to assess photosynthetic performance in *Nannochloropsis*.

The lack of a traditional plant OIDP transient

Our experiments in anaerobic conditions show a conventional OIDP transient, while in aerobic conditions, no IDP transient can be distinguished. We can think of two likely reasons for the presence of the OIDP transient in anaerobic conditions. (1) One or more oxygen-dependent electron transport pathways may oxidize PQ, but this electron sink is lost in anaerobic conditions. The oxygen-dependent electron sink could consist of a Mehler-type reaction [32] or be mediated by a chloroplast-located oxidase. Analysis of the *Nannochloropsis gaditana* genome indicates the presence of a plastid terminal oxidase (PTOX) homologue. (2) With a

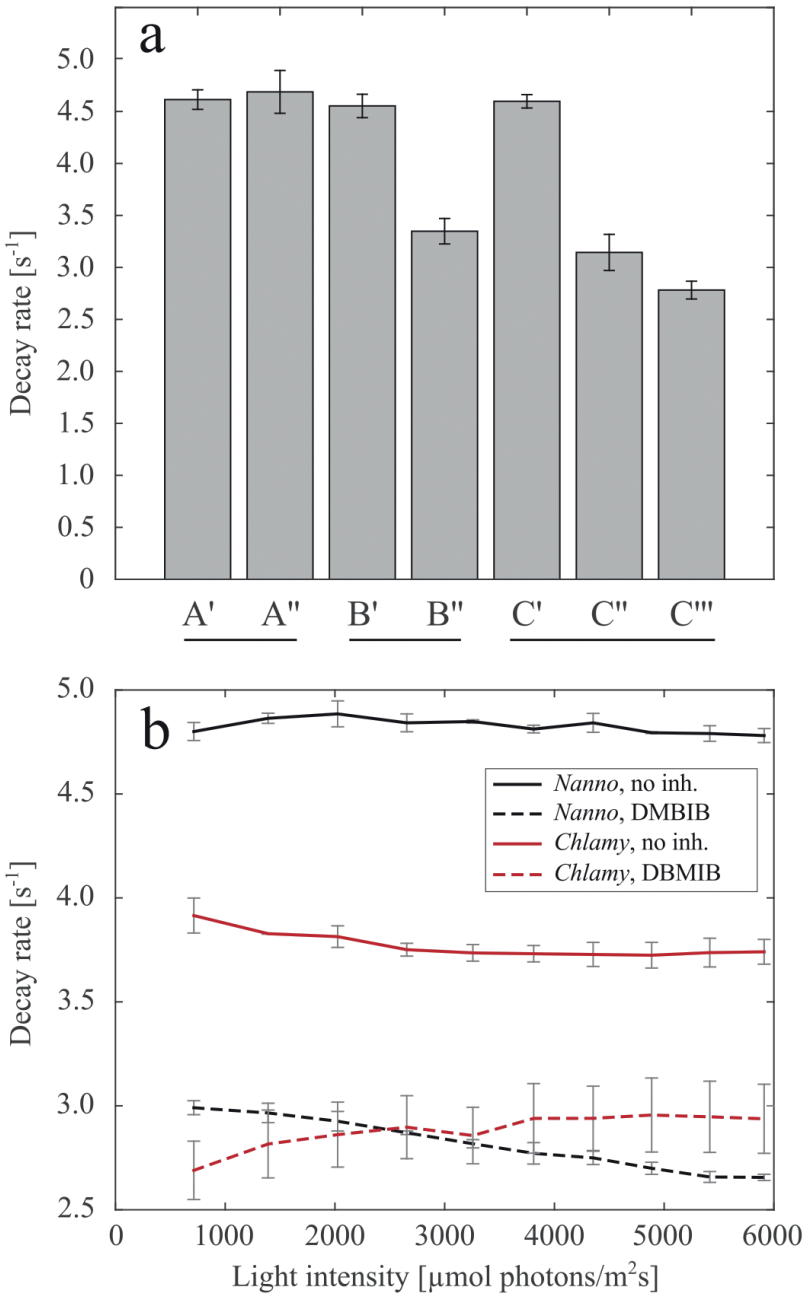

Fig 3. **(a)** Rate constants of the chlorophyll fluorescence decay after a bright light pulse for all phases of the three experiments performed. Averages of the rate constants after bright light pulses displayed in the different

groups in Fig 2 are shown. A shows the average of decay rates in the high light experiment performed without DBMIB (A'–fluorescence signal of dark adapted cells in darkness, A"–fluorescence signal in high light). B shows the anaerobic experiment (B'–fluorescence signal of aerobic cells, B"–fluorescence signal of anaerobic cells). Graph series C shows the results from the high light experiment performed in the presence of DBMIB (C'–fluorescence signal of dark-adapted cells in darkness without inhibitor, C"–fluorescence signal of cells in darkness after the addition of DBMIB, C"'–fluorescence signal of cells in high light, and in the presence of DBMIB). **(b)** Decay rates of chlorophyll fluorescence kinetics after bright light pulses in *Nannochloropsis oceanica* and *Chlamydomonas reinhardtii* without and with the addition of DBMIB under varying intensities of bright light pulses.

https://doi.org/10.1371/journal.pone.0175184.g003

limited amount of possible electron acceptors present in anaerobic conditions, *Nannochloropsis* PSI may exhibit variable fluorescence, depending on electron acceptors within PSI becoming reduced. In plants and algae it is usually assumed that PSI does not possess variable fluorescence, and only contributes to the base fluorescence level (F_0). This may be different in *Nannochloropsis*. Detailed fluorescence emission spectra may be utilized to discern a possible PSI-dependent variable fluorescence in future studies.

Effect of DBMIB

Rate constants of fluorescence kinetics after bright light pulses indicate that DBMIB blocks electron transport in *Nannochloropsis*. As in plants and algae, the cytochrome b_6f complex is the likely target for DBMIB. Interestingly, high light-induced reduction of the PQ pool in DBMIB-treated *Nannochloropsis* cells appears to abolish one or more chlorophyll fluorescence quenching mechanisms within minutes. A plant-derived interpretation of the observed increase in maximum chlorophyll fluorescence is that PSII is gaining more excitation. This interpretation is counter-intuitive for DBMIB-treated *Nannochloropsis*, as the correct physiological response would be to avoid electron generation by PSII when the PQ pool is reduced. Alternatively, the increase in fluorescence in high light and DBMIB-treated *Nannochloropsis* cells may indicate PSII damage. In any case, the high light-induced changes in DBMIB-treated cells serves as a reminder that plant-based interpretations may not be suitable for interpreting chlorophyll fluorescence in *Nannochloropsis*.

Photoprotection in *Nannochloropsis*

The inability of high light to induce a reduced PQ pool in *Nannochloropsis* is also of relevance for investigating photoprotection mechanisms in this alga. The most prominent photoprotection mechanisms observed in plants and green algae are the xanthophyll cycle and state transitions. In plants and green algae, state transitions are initiated by a reduced PQ pool [4], while the xanthophyll cycle is initiated by a low pH in the thylakoid lumen [33]. However, in *Nannochloropsis* it is unlikely that high light induces state transitions, as the PQ pool remains partially oxidized. This might be one reason why state transitions so far have not been detected in *Nannochloropsis*. Furthermore, electron transport through the PQ pool and concomitant proton translocation occurs even at high light intensities in *Nannochloropsis*. Therefore the pH-dependent xanthophyll cycle is likely more easily induced in *Nannochloropsis* than in green algae and plants, where electron transport stalls during high light illumination. When investigating mechanisms involved in photoprotection, the most common method for reducing plastoquinone is to subject the cells to high light, usually not in the presence of DBMIB [15, 34]. Thus, an oxidized PQ pool under high light intensities is in line with the observed predominance of the xanthophyll cycle as a photoprotection mechanism in *Nannochloropsis*.

Supporting information

S1 Fig. 77K spectrum of *Nannochloropsis*, indicating a high ratio of PSI:PSII. 77K spectroscopy spectrum of *Nannochloropsis* cells normalized to a chlorophyll concentration of 2.5 μmol chlorophyll ml^{-1}. The spectrum is normalized to 1.
(PNG)

S1 Table. Fluorescence decay parameters. Parameters resulting from the fitting of Eq 1 to the decay part (0.8–3 s) of the fluorescence curves shown in Fig 2. The amplitudes (A_0), decay rates (λ), constants (γ) and R^2 values are shown as averages for the parts of the different experiments. Group A' and A" correspond to the groups of fluorescence curves recorded in darkness (A') and high light (A") in the high light experiment performed without DBMIB. Group B' and B" correspond to the groups of fluorescence curves recorded in aerobic conditions (B') and anaerobic conditions (B") in the anaerobic experiment performed in darkness. Group C', C" and C"' correspond to the groups of fluorescence curves recorded in darkness without inhibitor (C'), in darkness after the addition of DBMIB (C"), and in high light (C"') in the high light experiment performed with DBMIB.
(CSV)

S2 Table. Fluorescence decay parameters. Standard deviations within the groups of variables that were averaged to obtain the parameters shown in table S1 Table.
(CSV)

Acknowledgments

The Faculty of Natural Sciences and Technology at the Norwegian University of Science and Technology (NTNU) funded the PhD position (G. R.)

Author Contributions

Conceptualization: GR MFHM.

Data curation: GR TBM.

Formal analysis: GR TBM.

Funding acquisition: MFHM.

Investigation: GR.

Methodology: GR MFHM TBM.

Project administration: MFHM GR.

Resources: MFHM.

Software: GR TBM.

Supervision: MFHM.

Validation: GR.

Visualization: GR MFHM TBM.

Writing – original draft: GR.

Writing – review & editing: MFHM TBM.

References

1. Beer S, Björk M. Measuring rates of photosynthesis of two tropical seagrasses by pulse amplitude modulated (PAM) fluorometry. Aquat Bot. 2000; 66:69–76.
2. White S, Anandraj A, Bux F. PAM fluorometry as a tool to assess microalgal nutrient stress and monitor cellular neutral lipids. Bioresource Technol. 2011; 102:1675–1682.
3. Baker NR. Chlorophyll fluorescence: A probe of photosynthesis in vivo. Annu Rev Plant Biol. 2008; 59:89–113. https://doi.org/10.1146/annurev.arplant.59.032607.092759 PMID: 18444897
4. Haldrup A, Jensen PE, Lunde C, Scheller HV. Balance of power: a view of the mechanism of photosynthetic state transitions. Trends Plant Sci. 2001; 6:301–305. PMID: 11435168
5. Finazzi G, Rappaport F, Furia A, Fleischmann M, Rochaix J-D, Zito F, et al. Involvement of state transitions in the switch between linear and cyclic electron flow in *Chlamydomonas reinhardtii.* EMBO Rep. 2002; 3:280–285. https://doi.org/10.1093/embo-reports/kvf047 PMID: 11850400
6. Kargul J, Turkina MV, Nield J, Benson S, Vener AV, Barber J. Light-harvesting complex II protein CP29 binds to photosystem I of *Chlamydomonas reinhardtii* under state 2 conditions. FEBS J. 2005; 272:4797–4806. https://doi.org/10.1111/j.1742-4658.2005.04894.x PMID: 16156798
7. Ünlü C, Drop B, Croce R, van Amerongen H. State transitions in *Chlamydomonas reinhardtii* strongly modulate the functional size of photosystem II but not of photosystem I. P Natl Acad Sci USA. 2014; 111:3460–3465.
8. Catalanotti C, Yang W, Posewitz MC, Grossman AR. Fermentation metabolism and its evolution in algae. Front Plant Sci. 2013; 4:1–17.
9. Green BR, Anderson JM, Parson WW. Photosynthetic membranes and their light-harvesting antennas. In: Green BR and Parson WW (ed) Light-harvesting antennas in photosynthesis, 1st edn. Springer Publishers, The Netherlands; 2003. pp 1–28
10. Haldimann P, Tsimilli-Michael M. Non-photochemical quenching of chlorophyll *a* fluorescence by oxidised plastoquinone: new evidences based on modulation of the redox state of the endogenous plastoquinone pool in broken spinach chloroplasts. Biochim Biophys Acta. 2005; 17:239–249.
11. Vernotte C, Etienne AL, Briantais J-M. Quenching of the System II chlorophyll fluorescence by the plastoquinone pool. Biochim Biophys Acta. 1979; 545:519–527. PMID: 427143
12. Hohmann-Marriott MF, Takizawa K, Eaton-Rye JJ, Mets L, Minagawa J. The redox state of the plastoquinone pool directly modulates minimum chlorophyll fluorescence yield in *Chlamydomonas reinhardtii.* FEBS Lett. 2010; 584:1021–1026. https://doi.org/10.1016/j.febslet.2010.01.052 PMID: 20122933
13. Ting CS, Owens TG. Photochemical and non-photochemical fluorescence quenching processes in the diatom *Phaeodactylum tricornutum.* Plant Physiol. 1993; 101:1323–1330. PMID: 12231788
14. Liu X, Duan S, Li A, Xu N, Cai Z, Hu Z. Effects of organic carbon sources on growth, photosynthesis, and respiration of *Phaeodactylum tricornutum.* J Appl Phycol. 2009; 21:239–246.
15. Cao S, Zhang X, Xu D, Fan X, Mou S, Wang Y, Ye N, Wang W. A transthylakoid proton gradient and inhibitors induce a non-photochemical fluorescence quenching in unicellular algae *Nannochloropsis* sp. FEBS Lett. 2013; 587:1310–1315. https://doi.org/10.1016/j.febslet.2012.12.031 PMID: 23474242
16. Lui B, Vieler A, Li C, Jones DA, Benning C. Triacylglycerol profiling of microalgae *Chlamydomonas reinhardtii* and *Nannochloropsis oceanica*. Bioresource Technol. 2013; 146:210–316.
17. Mitra M, Patidar SK, Mishra S. Integrated process of two stage cultivation of *Nannochloropsis* sp. for nutraceutically valuable eicosapentaenoic acid along with biodiesel. Bioresource Technol. 2015; 193:363–369.
18. Lubián LM, Montero O, Moreno-Garrido I, Huertas EI, Sobrino C, González-del Valle M, Parés G. *Nannochloropsis* (*Eustigmatophyceae*) as source of commercially valuable pigments. J Appl Phycol. 2000; 12:249–255.
19. Basso S, Simionato D, Gerotto C, Segalla A, Giacometti GM, Morosinotto T. Characterization of the photosynthetic apparatus of the Eustigmatophycean *Nannochloropsis* gaditana: Evidence of convergent evolution in the supramolecular organization of photosystem I. Biochim Biophys Acta. 2014; 1837:306–314. https://doi.org/10.1016/j.bbabio.2013.11.019 PMID: 24321505
20. Fan D-Y, Hope AB, Smith PJ, Jia H, Pace RJ, Anderson JM, Chow WS. The stoichiometry of the two photosystems in higher plants revisited. Biochim Biophys Acta. 2007; 1767:1064–1072. https://doi.org/10.1016/j.bbabio.2007.06.001 PMID: 17618597
21. Carbonera D, Agostini A, Di Valentin M, Gerotto C, Basso S, Giacometti GM, Morosinotto T. Photoprotective sites in the violaxanthin-chlorophyll *a* binding protein (VCP) from *Nannochloropsis gaditana*. Biochim Biophys Acta. 2014; 1837:1235–1246. https://doi.org/10.1016/j.bbabio.2014.03.014 PMID: 24704151

22. Guillard RRL, Ryther JH. Studies of marine planktonic diatoms. I. *Cyclotella nana* Hustedt and *Detonula confervacea* (Cleve) Gran. Can J Microbiol. 1962; 8:229–239. PMID: 13902807

23. Govindjee. Sixty-three years since Kautsky: Chlorophyll *a* fluorescence. Aust J Plant Physiol. 1995; 22:131–160

24. Cao J, Govindjee. Chlorophyll *a* fluorescence transient as an indicator of active and inactive photosystem II in thylakoid membranes. Biochim Biophys Acta. 1990; 1015:180–188. PMID: 2404518

25. Stirbet A, Govindjee. Chlorophyll *a* fluorescence induction: a personal perspective of the thermal phase, the J-I-P rise. Photosynth Res. 2012; 113:15–61. https://doi.org/10.1007/s11120-012-9754-5 PMID: 22810945

26. Neubauer C, Schreiber U. The polyphasic rise of chlorophyll fluorescence upon onset of strong continuous illumination: I. Saturation characteristics and partial control by the photosystem II acceptor side. Z Naturforsch C. 1987; 42c:1246–1254.

27. De Wijn R, Van Gorkom HJ. Kinetics of electron transfer from Q_A to Q_B in photosystem II. Biochemistry-US. 2001; 40:11912–11922.

28. Govindjee, Kern JF, Messinger J, Whitmarsh J. Photosystem II. In: Encyclopedia of Life Sciences (ELS). John Wiley & Sons, Ltd, Chichester; 2010

29. Diner BA. Dependence of the deactivation reactions of photosystem II on the redox state of plastoquinone pool A varied under anaerobic conditions; Equilibria on the acceptor side of photosystem II. Biochim Biophys Acta. 1977; 460:247–258. PMID: 870036

30. Laisk A, Eichelmann H, Oja V. Oxidation of plastohydroquinone by photosystem II and by dioxygen in leaves. Biochim Biophys Acta. 2015; 1847:565–575. https://doi.org/10.1016/j.bbabio.2015.03.003 PMID: 25800682

31. Peltier G, Cournac L. Chlororespiration. Annu Rev Plant Biol. 2002; 53:523–550. https://doi.org/10.1146/annurev.arplant.53.100301.135242 PMID: 12227339

32. Heber U. Irrungen, Wirrungen? The Mehler reaction in relation to cyclic electron transport in C3 plants. Photosynth Res. 2002; 73:223–231. https://doi.org/10.1023/A:1020459416987 PMID: 16245125

33. Jahns P, Holzwarth AR. The role of the xanthophyll cycle and of lutein in photoprotection of photosystem II. Biochim Biophys Acta. 2012; 1817:182–193. https://doi.org/10.1016/j.bbabio.2011.04.012 PMID: 21565154

34. Müller P, Li X-P, Niyogi KK. Non-photochemical quenching. A response to excess light energy. Plant Physiol. 2001; 125:1558–1566. PMID: 11299337

Paper II – Supporting information

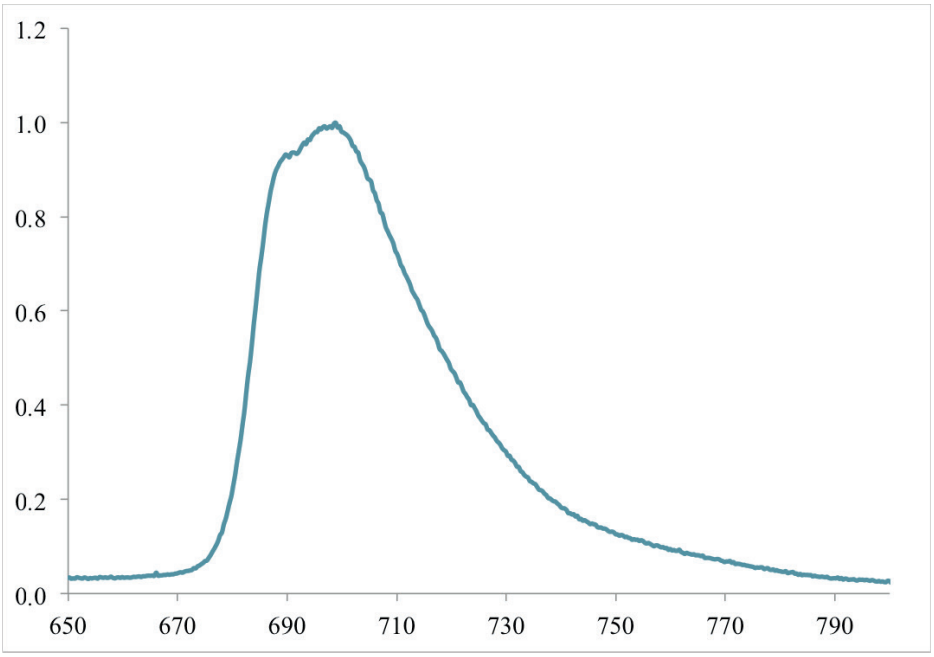

S1 Fig: 77K spectrum of *Nannochloropsis*, indicating a high ratio of PSI:PSII. 77K spectroscopy spectrum of *Nannochloropsis* cells normalized to a chlorophyll concentration of 2.5 µmol chlorophyll ml^{-1}. The spectrum is normalized to 1.

S1 Table. Fluorescence decay parameters.

Parameters resulting from the fitting of Eq 1 to the decay part (0.8–3 s) of the fluorescence curves shown in Fig 2. The amplitudes (A0), decay rates (λ), constants (y) and R2 values are shown as averages for the parts of the different experiments. Group A' and A" correspond to the groups of fluorescence curves recorded in darkness (A') and high light (A") in the high light experiment performed without DBMIB. Group B' and B" correspond to the groups of fluorescence curves recorded in aerobic conditions (B') and anaerobic conditions (B") in the anaerobic experiment performed in darkness. Group C', C" and C"' correspond to the groups of fluorescence curves recorded in darkness without inhibitor (C'), in darkness after the addition of DBMIB (C"), and in high light (C"') in the high light experiment performed with DBMIB.

	A'	A''	B'	B''	C'	C''	C'''
Amplitude	0,2172	0,2374	0,1893	0,1704	0,2034	0,2009	0,2191
Rate [s^-1]	4,6144	4,6884	4,5260	3,3483	4,5980	3,1441	2,7820
Constants	0,0218	0,0140	0,0205	-0,0019	0,0219	0,0359	-0,0018
R^2	0,0007	0,0006	0,0005	0,0005	0,0006	0,0006	0,0006

S2 Table. Fluorescence decay parameters.

Standard deviations within the groups of variables that were averaged to obtain the parameters shown in table S1 Table.

	A'	A''	B'	B''	C'	C''	C'''
StdAmp	0,0045	0,0077	0,0017	0,0105	0,0008	0,0013	0,002
StdRate	0,0939	0,2056	0,1567	0,1224	0,0644	0,1738	0,0857
StdConst	0,0009	0,0016	0,0006	0,0014	0,0009	0,0053	0,0036
StdR^2	0,0001	0,0002	0,0001	0,0001	0,0002	0,00007	0,0003

Paper III

PLOS ONE

RESEARCH ARTICLE

Unique photosynthetic electron transport tuning and excitation distribution in heterokont algae

Gunvor Bjerkelund Røkke[1], Thor Bernt Melø[2], Alice Mühlroth[3], Olav Vadstein[1], Atle M. Bones[3], Martin F. Hohmann-Marriott[1]*

1 Department of Biotechnology, Norwegian University of Science and Technology, Trondheim, Norway,
2 Department of Physics, Norwegian University of Science and Technology, Trondheim, Norway,
3 Department of Biology, Norwegian University of Science and Technology, Trondheim, Norway

* martin.hohmann-marriott@ntnu.no

Citation: Røkke GB, Melø TB, Mühlroth A, Vadstein O, Bones AM, Hohmann-Marriott MF (2019) Unique photosynthetic electron transport tuning and excitation distribution in heterokont algae. PLoS ONE 14(1): e0209920. https://doi.org/10.1371/journal.pone.0209920

Editor: Matheus C. Carvalho, Southern Cross University, AUSTRALIA

Received: June 15, 2018

Accepted: December 13, 2018

Published: January 9, 2019

Data Availability Statement: All relevant data are in the paper and its Supporting Information files.

Funding: The Faculty of Natural Sciences (https://www.ntnu.no/nv, priority programme NTNU Ocean) at the Norwegian University of Science and Technology (NTNU) founded the PhD position (G. B. R). Grant number is not available. The funder had no role in study design, data collection and analysis, decision to publish, or preparation of the manuscript.

Abstract

Heterokont algae are significant contributors to marine primary productivity. These algae have a photosynthetic machinery that shares many common features with that of Viridiplantae (green algae and land plants). Here we demonstrate, however, that the photosynthetic machinery of heterokont algae responds to light fundamentally differently than that of Viridiplantae. While exposure to high light leads to electron accumulation within the photosynthetic electron transport chain in Viridiplantae, this is not the case in heterokont algae. We use this insight to manipulate the photosynthetic electron transport chain and demonstrate that heterokont algae can dynamically distribute excitation energy between the two types of photosystems. We suggest that the reported electron transport and excitation distribution features are adaptations to the marine light environment.

Introduction

Heterokont algae have emerged as the result of a secondary endosymbiotic event [1,2] and dominate carbon fixation within the oceans [3,4]. However, the features that make heterokont algae so successful in the marine environment remain unresolved. Although separated by more than a billion years of evolution from a common ancestor, the photosynthetic machinery of Viridiplantae (green algae and land plants) and heterokont algae retains common features [2]. Both groups of organisms have two types of photosystems, which are linked by an electron transport chain that includes a pool of plastoquinone molecules. Another common feature is the presence of light-harvesting complexes, which house chlorophylls and carotenoids. There are, however, differences between Viridiplantae and heterokont algae in the type of chlorophylls and carotenoids they possess, as well as in the proteins involved in regulating light-harvesting and photoprotection [5,6]. A particularly interesting question is how these organisms utilize differences in their photosynthetic machineries to respond to the environmental conditions they encounter.

Viridiplantae dominate primary production on land, while heterokont algae dominate primary production in marine environments. Compared to *terra firma*, the light environment in

Competing interests: The authors have declared that no competing interests exist.

the oceans is more dynamic, with wave-induced lensing exposing algae to rapid variations in light intensity [7,8]. It has been established that Viridiplantae can respond to high light by redistributing light-harvesting complexes from photosystem II (PSII) to photosystem I (PSI) [9]. This "state transition", which in Viridiplantae is activated by a reduced plastoquinone pool, has not been demonstrated in heterokont algae, where a pH-dependent conversion of carotenoids [10] that is also present in Viridiplantae [11], is known to dissipate excess excitation energy [12,13]. In addition to forming a light-dependent pH-gradient, some green algae, including *C. reinhardtii* [14] and heterokont alga *P. tricornutum* [15,16] also maintain a pH-gradient during darkness, by oxygen-dependent chlororespiration.

Assessment of chlorophyll fluorescence, using a set of techniques originally developed for Viridiplantae, can provide exquisite insights into the photosynthetic electron transport chain and can be used to assess the photosynthetic performance [17]. It has been demonstrated that the maximum fluorescence yield can be obtained after applying a bright (saturating) light pulse that completely reduces the pool of electron acceptors (the plastoquinone pool), which is accepting electrons from PSII. As the plastoquinone pool is in equilibrium with the primary modulator of chlorophyll fluorescence, the PSII-bound Q_A [18], a complete reduction of the plastoquinone pool guarantees that Q_A molecules in all reaction centers are reduced, and thus that the maximum fluorescence yield is achieved [19]. Surprisingly, a detailed interpretation of chlorophyll fluorescence recently revealed that short, bright light pulses have a different effect on the electron transport chain in the heterokont alga *N. oceanica* than in Viridiplantae. While bright light pulses completely reduce the plastoquinone pool in Viridiplantae, bright light pulses applied to *Nannochloropsis* fail to do so [20]. This observation has potentially important implications for assessing photosynthetic performance that relies on achieving the maximum fluorescence yield as a reference point [21,22]. Furthermore, if the photosynthetic electron transport chain in heterokont algae also remains oxidized during longer exposures to high light, research into photoprotection mechanisms in this group of organisms has to be reinterpreted, and may uncover a novel light protection strategy. In this study, we set out to clarify the effect of high light exposure on the diatom *Phaeodactylum tricornutum* and the Eustigmatophyte *Nannochloropsis oceanica*, both marine heterokont algae.

Results

In order to determine whether bright light pulses completely reduce the plastoquinone pool, and thus induce the maximum fluorescence yield, we employed a reference condition that is known to result in a reduced photosynthetic electron transport chain. In darkness and in the absence of oxygen, metabolically generated electrons accumulate within algal cells. This leads to accumulation of electrons on electron carriers within the photosynthetic electron transport chain, including the plastoquinone pool [23,24]. If light pulse-induced fluorescence yield in the presence and absence of oxygen are identical, then the plastoquinone pool is reduced in both conditions. Using this assay, we observe that the light pulse-induced fluorescence yield in the Viridiplantae model organism *Chlamydomonas reinhardtii* is diminished in anaerobic conditions (Fig 1A) due to the state transition-associated move of light-harvesting complexes from PSII to PSI [25]. Conversely, the light pulse-induced fluorescence yield in *N. oceanica* and *P. tricornutum* increases in oxygen-free conditions (Fig 1A and 1B). We also investigated the effect of different light pulse intensities on the maximum fluorescence yield (S1 Fig) and Q_A^- oxidation after light pulses in *P. tricornutum*. In these experiments, we used the cytochrome b_6f inhibitor DBMIB as an alternative to anaerobic conditions to guarantee the reduction of the plastoquinone pool. DBMIB binds to the Q_o site of the cytochrome b_6f complex, and thereby disables the Q-cycle and electron donation to plastocyanin. Light pulses applied in

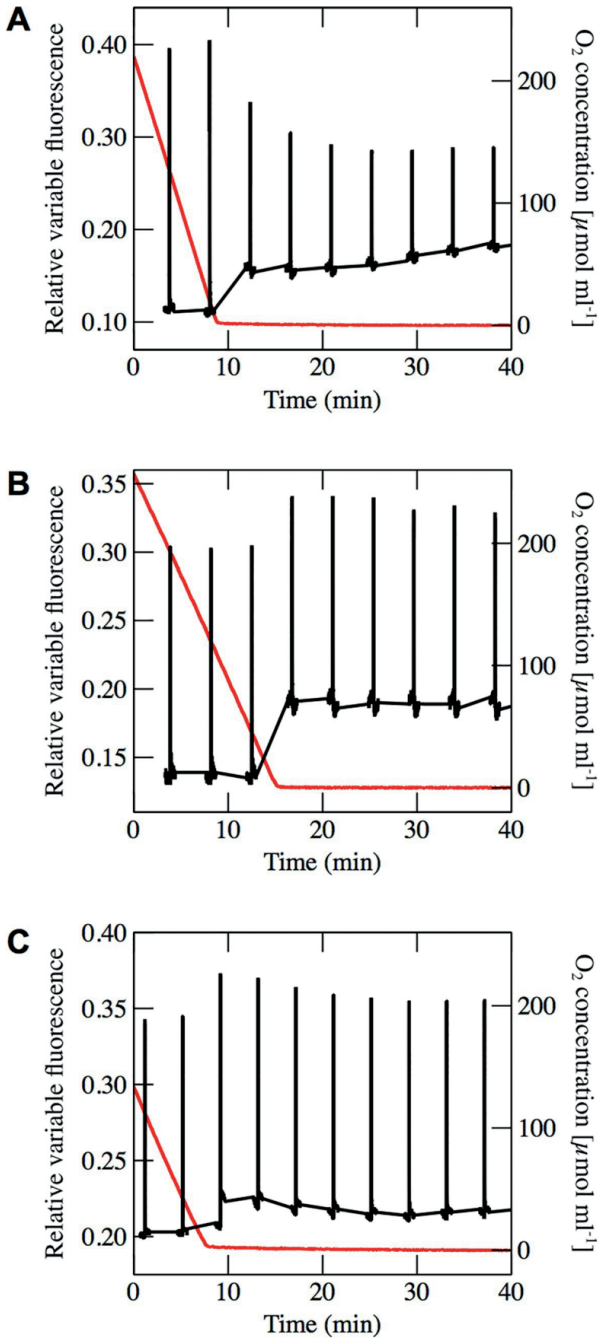
A
Relative variable fluorescence
0.40
0.30
0.20
0.10
O2 concentration [μmol ml-1]
200
100
0
0
10
20
30
40
Time (min)
B
Relative variable fluorescence
0.35
0.30
0.25
0.20
0.15
O2 concentration [μmol ml-1]
200
100
0
0
10
20
30
40
Time (min)
C
Relative variable fluorescence
0.40
0.35
0.30
0.25
0.20
O2 concentration [μmol ml-1]
200
100
0
0
10
20
30
40
Time (min)

Fig 1. Variable fluorescence recorded during the shift from aerobic to anaerobic conditions. Variable fluorescence for (**A**) *C. reinhardtii*, (**B**) *N. oceanica* and (**C**) *P. tricornutum*. Black lines show variable fluorescence, and red lines show oxygen concentration, which was recorded simultaneously.

https://doi.org/10.1371/journal.pone.0209920.g001

the presence of DBMIB therefore leads to complete reduction of the PQ pool and maximum fluorescence yield. This effect has been established for *C. reinhardtii* [26–28], *N. oceanica* [29–31] and *P. tricornutum* [32,33]. While DBMIB has been shown to have a quenching effect on chlorophyll fluorescence [34], this effect is constant, as samples were pre-incubated with DBMIB and the concentration did not change during the experiment.

Comparing untreated cells to DBMIB-treated cells indicates that in untreated cells in aerobic conditions the maximum fluorescence yield is not reached, not even at very high light intensities (S1 Fig). That the plastoquinone pool is not completely reduced can also be seen when investigating decay rates following a light pulse (S1 Fig). No matter by how much the light intensity of the light pulse is increased, the decay rates in DBMIB-treated cells was always lower, and the maximum fluorescence always higher than in untreated cells, except for in *C. reinhardtii*, where the light pulses were shown to yield a more or less reduced plastoquinone pool at higher light intensities (see S1 Discussion of S1 Fig). This conclusion is also in line with results obtained by analysing the fluorescence kinetics after light pulses. When the plastoquinone pool was reduced in the presence of DBMIB, the fluorescence decay rates were similar to the decay rates obtained in anaerobic conditions, even at low light intensities.

Similarly the decay rates of untreated cells at low chlorophyll concentration, even at very high light intensities, were similar to those obtained in aerobic conditions when a higher chlorophyll concentration was used (S1 Fig). Similar experiments to the one here presented for *P. tricornutum*, have also been published for *N. oceanica* and *C. reinhardtii* [20].

We can therefore conclude that routinely applied bright light pulses are not able to completely reduce the plastoquinone pool of the heterokont algae *N. oceanica* and *P. tricornutum* in the presence of oxygen (Fig 1B and 1C).

The obvious question arising from our initial observation of the effect of short light pulses is what effect a longer light exposure has on the reduction state of the plastoquinone pool, as it is–in analogy to Viridiplantae–generally assumed that the plastoquinone pool is reduced under high light intensities. Furthermore, we will determine whether modulating the reduction state of the photosynthetic electron transport chain induces a redistribution of excitation energy between the two photosystems in heterokont algae. This question has been previously addressed in the heterokont algae *P. tricornutum* [35], concluding that observed changes in fluorescence yield are not caused by a changing association of light-harvesting complexes between the two photosystems.

The current view in the model organisms *P. tricornutum* and other heterokont algae, is that chlorophyll fluorescence yield is modulated by pH-dependent mechanisms [12]. As chlorophyll fluorescence at room temperature cannot distinguish pH-dependent excitation quenching from other possible modes of quenching, such as a state transition, we chose to obtain spectral information of the fluorescence emission at 77 K (raw spectra shown in Fig 2, fluorescence ratios shown in Fig 3). This technique does not have as long a tradition of use in heterokont algae as it does in Viridiplantae [36], and we were initially taken aback by the dynamic behaviour we report and interpret here for the first time. These spectral dynamics allowed us to assign spectral components (Fig 4, see S2 Fig for a detailed demonstration of the procedure) that will be used to further discuss excitation distribution dynamics (Fig 3).

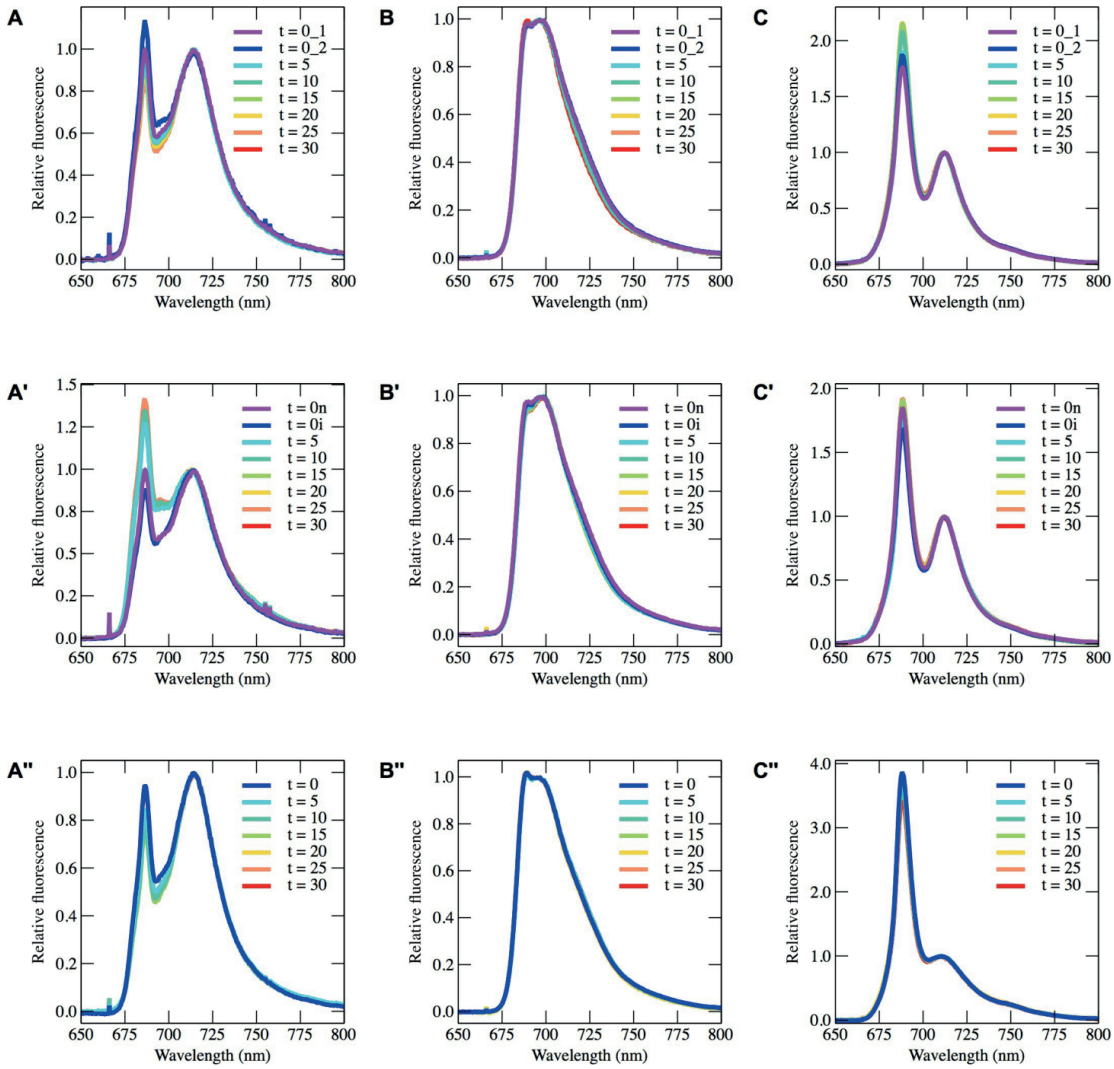

Fig 2. Raw spectra recorded by 77 K spectroscopy. 77 K fluorescence spectra from *C. reinhardtii* (**A**), *N. oceanica* (**B**) and *P. tricornutum* (**C**) recorded after exposure to high light (**A**, **B**, **C**), exposure to high light in the presence of DCMU (**A'**, **B'**, **C'**) and during oxygen-depletion in the dark (**A"**, **B"**, **C"**) using a 435 nm LED for excitation. All spectra have been baseline-corrected and normalized to the peak wavelength of PSI in each species.

https://doi.org/10.1371/journal.pone.0209920.g002

Assigning identities to fluorescent components

The wavelengths used to indicate different fluorescent components were determined by deconvoluting 77 K fluorescence spectra (an example of such a deconvolution is shown in S2 Fig).

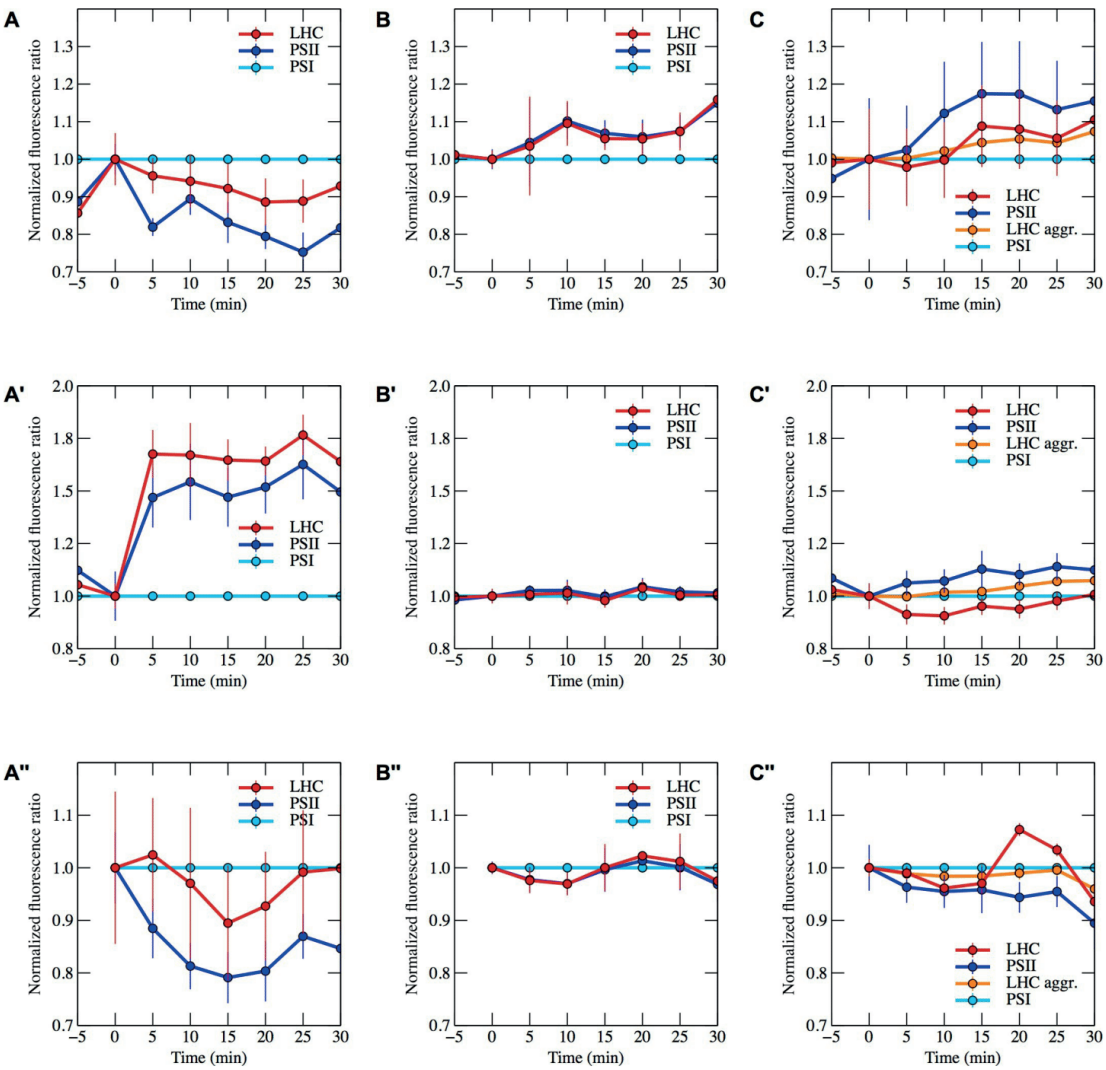

Fig 3. Fluorescence ratios for light harvesting complexes and PSII over time. Fluorescence ratios normalized to PSI over time during high light (**A**, **B**, **C**), high light in the presence of DCMU (**A'**, **B'**, **C'**) and during dark, anaerobic conditions (**A"**, **B"**, **C"**). (**A**, **A'**, **A"**) show ratios for *C. reinhardtii*, (**B**, **B'**, **B"**) show ratios for *N. oceanica* and (**C**, **C'**, **C"**) show ratios for *P. tricornutum*. Fluorescence spectra for the fluorescent components located in each organism, which led to the selection of the wavelengths representing PSII, PSI and light harvesting complexes, are shown in Fig 4.

https://doi.org/10.1371/journal.pone.0209920.g003

The fluorescence maxima of the fluorescent components found in *C. reinhardtii* were located at 680 nm, 686 nm and 716 nm (Fig 4A and 4A') and were assigned to light harvesting complexes (LHCs) [37], PSII [38] and PSI [39], respectively. For *N. oceanica*, we identified fluorescent components at 684 nm, 695 nm and at 723 nm (Fig 4B and 4B'), and assigned these components to LHCs [40], PSII [40] and PSI [40,41].

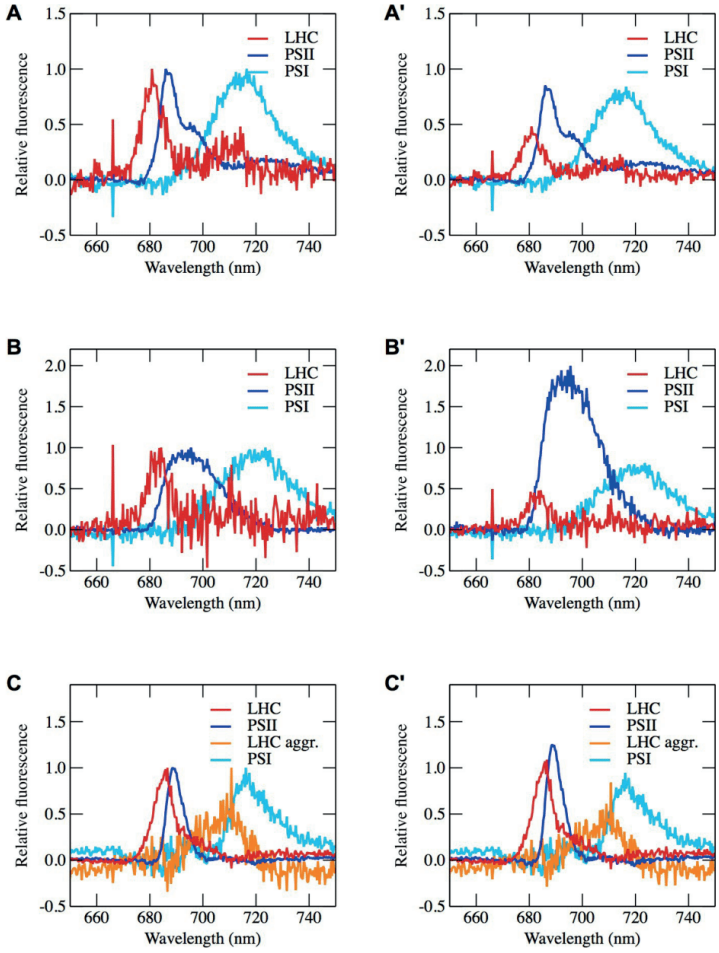

Fig 4. Fluorescent components found to be present in *Chlamydomonas*, *N. oceanica* and *P. tricornutum*. Calculated fluorescence spectra for photosynthetic components comprising fluorescence emission spectra at 77 K of (**A**) *C. reinhardtii*, (**B**) *N. oceanica*, and (**C**) *P. tricornutum*. In panels (**A**, **B**, **C**), the fluorescence spectra have been normalized to unity, while in panels (**A'**, **B'**, **C'**), the size of the respective fluorescing components correspond to their contribution to the overall fluorescence spectrum. The amplitude of the fluorescing components change throughout the experiments, but to give an example of their contribution in a spectrum, the reference sample of the high light experiments performed on *C. reinhardtii*, *N. oceanica* and *P. tricornutum* were chosen. The fluorescence components were calculated as shown in S2 Fig.

https://doi.org/10.1371/journal.pone.0209920.g004

For *P. tricornutum*, four components were identified with peak wavelengths at 686 nm, 688 nm, 710 nm and 715 nm (Fig 4C and 4C'). The component with a peak wavelength at 688 nm was assigned to PSII [42], and the 715 nm component was assigned to PSI due to spectral similarities with other diatom PSI, for example *Chaetoceros gracilis* [43] and *Cyclotella meneghiniana* [44]. The spectral component peaking at 710 nm is likely due to fluorescing light harvesting complex-aggregates, which have been demonstrated in diatoms, and particularly in

P. tricornutum [5,45–47]. Isolated fucoxanthin chlorophyll *a*/*c* binding proteins (FCPs) from *P. tricornutum* have their 77 K fluorescence maximum at 680 nm [40], while the 77K fluorescence maximum for FCPs from *Chaetoceros gracilis* has been found at 683 nm [48]. The fluorescent component having a fluorescence maximum at 686 nm does not match fluorescence components that have been previously reported for isolated diatoms. This fluorescence emission may be due to highly fluorescent red-shifted emissions by fucoxanthin-chlorophyll binding proteins (FCPs) as recently described in the diatom *Cyclotella meneghiniana* [49].

Modulation of the plastoquinone pool reduction state by high light

Exposure of *N. oceanica* and *P. tricornutum* to high light intensities results in a redistribution of excitation energy between the two types of photosystems. Upon illuminating these heterokont algae, the excitation is directed towards PSII (Fig 3B and 3C). This favouring of PSII indicates that the photosynthetic electron transport chain requires electron input, suggesting that the plastoquinone pool is largely oxidized. The response to high light is therefore opposite to what is observed in Viridiplantae, such as *C. reinhardtii*, where the plastoquinone pool is reduced during the initial exposure to bright light and excitation consequently is directed away from PSII (Fig 3A).

Oxidation of the plastoquinone pool by DCMU treatment under high light

Exposure to the herbicide DCMU blocks electron generation by PSII, and in combination with light, leads to oxidation of the plastoquinone pool. The DCMU-treated and light-exposed heterokont algae, as well as *C. reinhardtii*, show a physiological response consistent with an empty plastoquinone pool by transferring excitation to the electron-generating PSII (Fig 3A', 3B' and 3C'). The magnitude of change in the fluorescence signal in the heterokont algae is, however, small compared to in *C. reinhardtii*. This is consistent with the assumption that the plastoquinone pool in the heterokont algae is mostly oxidized in dark aerobic conditions, while being partly reduced in *C. reinhardtii*. The plastoquinone pool of *C. reinhardtii* is also more reduced if acetate is included in the growth and experimental medium, as was the case in our experiments.

Reduction of the plastoquinone pool by oxygen depletion

Exposure of algal cells to oxygen-free conditions in the dark results in an *in vivo* redox titration, as electrons accumulate within the cells, and consequently accumulate on electron carriers with increasingly negative redox midpoint potential. Oxygen depletion induces a transient increase in excitation towards PSI in the heterokont algae. A similar response to oxygen depletion is also present for the Viridiplantae model organism *C. reinhardtii*. Shifting excitation towards PSI in oxygen-free conditions is consistent with the need to oxidize a reduced photosynthetic electron transport chain. Prolonged oxygen depletion results in a clear increase in excitation directed towards PSI in *N. oceanica* (Fig 3B") and a more subtle redistribution of light energy to PSII in *P. tricornutum* and *C. reinhardtii* (Fig 3A" and 3C").

Discussion

While *C. reinhardtii* is considered a model for plants concerning excitation distribution between the two photosystems, it is noteworthy that, especially in the presence of acetate in the growth medium, chlororespiration is uniquely prominent in this alga [14], a feature shared with the diatom *P. tricornutum* [15,16].

Exposure to high light in heterokont algae induces a redistribution of excitation energy between PSI and PSII that is opposite to the distribution pattern observed in *C. reinhardtii*. This regulation of excitation distribution is consistent with a high-light induced oxidation of the electron transport chain in heterokont algae. The incomplete reduction of the plastoquinone pool upon short light-pulses in heterokont algae, as employed by the saturating pulse method [21] would lead to a systematic under-assessment of the maximum fluorescence yield, and thus influence the assessment of photosynthetic performance when this technique is utilized.

Carotenoid dependent quenching versus structural rearrangement

Are the observed changes in distribution of excitation energy between PSI and PSII in heterokont algae due to a carotenoid-specific quenching that affects light-harvesting complexes associated with PSI and PSII differently, or do light-harvesting complexes change their association between PSI and PSII? The complex dynamics of excitation distribution in high light conditions likely involve contributions by the well-characterized, pH-dependent, carotenoid-mediated excitation quenching mechanisms [10,11]. However, oxygen-depletion experiments do not change the thylakoidal pH, and application of DCMU has been shown to prevent the generation of a pH-gradient, and thus will not trigger the conversion of excitation-quenching carotenoids in *Nannochloropsis* [50] and *P. tricornutum* [51]. However, it has also been demonstrated that in dark-adapted green algae of *C. reinhardtii* [14], the prasinophycean alga *Mantoniella squamata* [52], the heterokont alga *P. tricornutum* [16] and *T. pseudonana* [53] chlororespiration can generate an oxygen-dependent pH gradient and thus potentially engage carotenoid conversion and the associated non-photochemical quenching. In addition, there is evidence that chlororespiratory activity in green algae is involved in the synthesis of carotenoids [54]. Oxygen-depletion may therefore collapse the pH-gradient, as chlororespiration is oxygen dependent, and result in the conversion to the non-quenching carotenoid and consequently cause a loss of non-photochemical quenching and an increase in chlorophyll fluorescence.

Studying the effect of high light exposure, Lepetit and co-workers [32] report the *de novo* synthesis of excitation-quenching carotenoids, which accumulate with a half time of 3–4 hours. *De novo* synthesis thus appears too slow to account for the rapid high light-induced dynamics we observe.

We observed complex spectral changes of 77 K fluorescence emission both in dark oxygen-depleted conditions and in DCMU-treated samples under high light. While abolishing chlororespiration by oxygen depletion in the dark may abolish the pH-gradient, and thus relax carotenoid-mediated non-photochemical quenching, this is not known to change energy distribution between the two photosystems. As we also observe changes in 77K fluorescence spectra in DCMU-treated cells exposed to high light, this redistribution of excitation energy appears to be independent of the thylakoidal pH and the associated carotenoid-dependent excitation quenching and may indicate a redistribution of light-harvesting systems.

Regulation of excitation energy

In *Nannochloropsis* in anaerobic conditions, an immediate response shifts excitation energy towards PSI within 10 minutes, which is followed by a shift of excitation energy back to PSII, which is completed after about 30 minutes. These two phases likely indicate a fine-tuning of excitation distribution that is mediated by a single mechanism, or the consecutive action of two independent mechanisms. Whether these mechanisms are identical to the multistep model for non-photochemical excitation quenching in *Nannochloropsis gaditana* suggested by

Chukhutsina and co-workers [55] and in *P. tricornutum* by Giovagnetti and Ruban [45] requires further study. Compared to Viridiplantae, the fluorescence signal indicative of this re-distribution is smaller in heterokont algae. It has recently been demonstrated that PSI-LHC complexes of heterokont algae possess trapping times that are three times shorter than those of plants [56]. Therefore, re-directing excitation from PSII to PSI will lower the overall PSII fluorescence emission, while only a small increase in PSI fluorescence is observed. This is unlike the situation in Viridiplantae, where redistribution results in higher PSI fluorescence emissions in addition to lower PSII emission, and these changes in emission provide a clear beacon for a changed distribution of excitation energy. The small changes in the magnitude of fluorescence emission in heterokont algae may have contributed to the original assessment by Owens [35] that excitation energy is not redistributed in the heterokont alga *P. tricornutum* in dependence of the reduction state of the plastoquinone pool. This conclusion was obtained with the assumption that the photosynthetic machinery of heterokont algae responds to light in the same manner as Viridiplantae, an assumption we can now amend.

What is the sensor that triggers the redistribution of light energy between the two photosystems? The excitation distribution induced in dark and oxygen-depleted conditions suggests that the reduction state of an electron carrier is used to modulate the distribution of excitation in heterokont algae. The plastoquinone pool is a possible candidate for this role, as it is a modulator of fluorescence, and also acts as a sensor for shifting excitation energy in cyanobacteria [57] and Viridiplantae [58].

The redox-dependent response may share components and organization with the redox-dependent pigment synthesis and synthesis of light-harvesting systems described for *P. tricornutum* [32]. A second sensing system may be responsible for the shift in excitation distribution induced by prolonged anaerobic conditions, where more electron carries with a more negative redox midpoint potential will become reduced. Here ferredoxins and thioredoxins are potential candidates, as these electron carriers are know to also have a redox-dependent regulatory function in carbon fixation in Viridiplantae and to a lesser extend in heterokont algae [59,60]. The slow change in excitation energy distribution during prolonged anaerobic condition could also indicate the conversion of carotenoids. Here the production availability of NADPH, may enable the conversion of carotenoids, as this electron carrier has been demonstrated to be required as a cofactor for the diatoxanthin epoxidase that is not available in dark aerobic condition in *P. tricornutum* [61].

Avoiding a reduced plastoquinone pool

The photosynthetic machineries of the heterokont algae *Nannochloropsis* and *P. tricornutum* are tuned to avoid reduction of the photosynthetic electron transport chain during high light illumination. As this is in contrast to Viridiplantae, it is tempting to speculate on the physiological reasons for this adaptation. We propose that differences in the characteristics of the electron transport chain are based on the different light environments that terrestrial and marine organisms experience. *C. reinhardtii* was isolated from soil, and is thus, like Viridiplantae in general, adapted to an environment that largely lacks rapid variation in light exposure. In contrast, marine heterokont algae can experience wave lensing-induced high-light [7,8], and have therefore evolved a photosynthetic electron transport chain that is tuned to avoid high light-induced over-reduction. If environmental conditions are encountered that temporarily overwhelm the photosynthetic machinery, a build up of protons is the likely consequence, which triggers the well-characterized carotenoid-dependent energy dissipation mechanism [12]. These proposed functions of electron transport poise and xanthophyll cycle in photoprotection is supported by the ability of four *P. tricornutum* species to thrive in

fluctuating light without increasing the amount of energy-quenching carotenoids [45,62]. In conclusion, our study provides key insights for re-interpreting previous studies and for directing future studies regarding the photosynthetic machinery and physiology of heterokont algae and their adaption to the marine environment.

Materials and methods

Cell cultures

Nannochloropsis oceanica CCAP 211/46 was obtained from the Culture Collection of Algae and Protozoa (Argyll, UK), *Chlamydomonas reinhardtii* CC-4532 MT- from the *Chlamydomonas* Resource Center at the University of Minnesota, and *Phaeodactylum tricornutum* CCMP 632 was obtained from the National Center for Marine Algae and Microbiota (East Boothbay, ME, USA).

N. oceanica and *P. tricornutum* were grown on f/2 medium [63] and *C. reinhardtii* was grown on TrisAcPO$_4$ (TAP) medium [64]. Pre-cultures of the algae were incubated at 18˚C and with a light intensity of 200 μmol photons $m^{-2}s^{-1}$. Before experiments, the cell cultures were harvested and either diluted with fresh medium or up-concentrated by centrifugation to a chlorophyll concentration of 1 μg Chl/mL in case of the 77 K spectroscopy experiments, and 20 μg Chl/mL (in case of *C. reinhardtii* and *N. oceanica*), and 40 μg Chl/mL (in case of *P. tricornutum*) for the PAM experiments. The chlorophyll concentration used for PAM experiments was adjusted to result in an oxygen consumption rate of approximately 15 μmol $mL^{-1}min^{-1}$ for each organism. Additional PAM experiments were performed for *Phaeodactylum* with a lower chlorophyll concentration of 0.2 μmol Chl/mL in order to be sure to avoid self-shading. In these additional experiments, DBMIB with a working concentration of 1 μM [32] was used to ensure a reduce plastoquinone pool. After being diluted or up-concentrated to the correct chlorophyll concentration, the cultures were dark-acclimated for one hour prior to experiments.

PAM experiments

The response of the photosynthetic machinery to anaerobic incubation was investigated using a PAM fluorometer (Multi-color PAM, Walz, Germany) coupled to an oxygen-measuring device (Oxygraph, Hansatech, United Kingdom). This setup allowed us to record variable chlorophyll fluorescence and oxygen concentration simultaneously. A weak measuring light of 440 nm was used to assess variable fluorescence throughout the experiment, and bright light pulses of 440 nm having a duration of 0.8 s, and a light intensity of 1600 μmol photons $m^{-2}s^{-1}$ of blue light, corresponding to an effective light intensity of 3200 μmol photons $m^{-2}s^{-1}$ of white light were applied every 4 minutes. For every measurement, 2 ml of standardized cell cultures were used. In order to analyse the fluorescence decay of the recorded induction curves, a custom written MATLAB script was used [20].

77K experiments

For the 77 K experiments, algae were exposed to three experimental conditions: (1) high light, (2) high light in the presence of the photosystem II (PSII) inhibitor 3-(3,4-dichlorophenyl)-1,1-dimethylurea (DCMU), and (3) anaerobic conditions in darkness. Samples were dark-adapted for 1 hour in aerobic conditions, before being exposed to the three experimental conditions. In the high light + DCMU experiment, DCMU dissolved in water, having a concentration of 10 mM was added 1:1000 to algae samples, to a working concentration of 10 μM. The light intensity for the high light exposure (in presence and absence of DCMU) was 1000 μmol

photons $m^{-2}s^{-1}$ of white light. In the anaerobic experiment, oxygen depletion was achieved by bubbling the algae with N_2 gas containing 0.5% CO_2. Aliquots of the algae were taken every 5 minutes in triplicate. In the high light experiments, one zero sample was taken first. Then, another zero sample was taken after the addition of DCMU. In the high light experiment performed without the addition of DCMU, two zero samples were taken at the same time points as the zero samples without and with inhibitor were taken in the DCMU experiment. This was done to standardize the sampling procedure. The experiment was continued for 30 minutes. The samples were frozen in liquid nitrogen immediately and stored in liquid-nitrogen-filled dewars before fluorescence measurements at 77K.

Fluorescence spectra at 77 K were acquired using a Jaz spectrophotometer (Ocean Optics, USA) in a custom designed setup [65]. The software used for recording spectra was the SpectraSuite software (Ocean Optics, USA). A 435 nm LED served as the excitation light source, and a long-pass filter was used to filter out the LED.

Processing of 77 K data

The fluorescence spectra recorded at 77 K were processed using custom-written MATLAB scripts. First, the 77 K fluorescence spectra, which were recorded in triplicate for each experimental condition, were base line-subtracted and normalized to the wavelength corresponding to photosystem I (PSI) for each organism (Fig 2, PSI spectra shown in Fig 4). After base line-subtraction and normalization, the triplicate spectra were combined and standard deviations were calculated.

In order to generate the plots shown in Fig 3, every wavelength in the spectrum recorded at one particular time point was divided by the same wavelength in the zero spectrum in the same experiment, which, being aerobic and dark adapted, served as the reference sample. For the high light experiment that contained DCMU, dark-adapted samples 5 minutes after exposure to the herbicide were used to obtain the reference spectra. From these ratio spectra, the wavelengths found to correspond to the fluorescing components present in the respective organisms were plotted (Fluorescence ratios over time for all fluorescent components are shown in Fig 3, while the fluorescence spectra for the individual components are shown in Fig 4).

The spectra associated with different photosynthetic components were identified by normalizing all spectra in one time series to a wavelength connected to one particular component, and subsequently subtracting one spectrum in the time series from another. Using this method repetitively allowed us to eliminate the fluorescence contribution of one fluorescing component at a time. To demonstrate the approach and its validity, a step-wise example of this process is presented in S2 Fig for the *C. reinhardtii* experiment performed with high light. The same procedure was performed on all 77 K datasets and resulted in resolving three spectral components for *C. reinhardtii* and *Nannochloropsis*, and four spectral components for *P. tricornutum* (Fig 4). The extracted spectral components were identical for all conditions for each organism, except for a slight shift in wavelengths in the case of DCMU treatment in all organisms.

Supporting information

S1 Fig. PAM fluorometry results for *P. tricornutum* cells and previously published results for *N. oceanica* and *C. reinhardtii* for comparison. (**A, B, C**) Light pulse-induced maximum fluorescence yield (normalized to F_0) for untreated and DBMIB-treated cells of *C. reinhardtii* (**A**), *N. oceanica* (**B**) and *P. tricornutum* (**C**) in dependence of light pulse intensity. The results for *C. reinhardtii* and *N. oceanica* have been published previously [20], and were included here

for comparison with the newly obtained data for *P. tricornutum* cells at low (0.2 μM chlorophyll concentration). (**A'**, **B'**, **C'**) Chlorophyll fluorescence kinetic decay rates after light pulses of untreated and DBMIB-treated cells of *C. reinhardtii* (**A'**), *N. oceanica* (**B'**) and *P. tricornutum* (**C'**) in dependence of light pulse intensity. The previously published results for *C. reinhardtii* and *N. oceanica* [20] were included for comparison with newly obtained data for *P. tricornutum* at low (0.2 μM) chlorophyll concentration. (**A"**, **B"**, **C"**) Chlorophyll fluorescence kinetic decay rates after light pulses (1600 μmol photons $m^{-2}s^{-1}$ of blue light) of *C. reinhardtii* (**A"**), *N. oceanica* (**B"**) and *P. tricornutum* (**C"**) undergoing anaerobic transition. The fluorescence data behind the decay rates shown in panels **A"**, **B"** and **C"** is shown in Fig 1.
(TIFF)

S2 Fig. Example of deduction of fluorescent components for *Chlamydomonas*. An example of the procedure used to isolate the spectra of fluorescing components. The dataset recorded for *C. reinhardtii* during high light treatment (**A**) was normalized to 675 nm (**B**). This is a wavelength that is assumed to be associated with light harvesting complexes in *C. reinhardtii*, and also a wavelength that is thought to be little impacted by changes in fluorescence from the PSII core complexes. To eliminate the fluorescence contribution of light harvesting complexes, one of the spectra in the time series was subtracted from the other. In this example, the t = 0_1 spectrum was subtracted from the other spectra, resulting in the spectra shown in (**C**). The next step was to neutralize the contribution of PSII. Therefore, all spectra in (**C**) were normalized to the local fluorescence maximum (in (**C**) seen as a minimum) around 687 nm, resulting in the spectra displayed in (**D**). The t = 0_2 spectrum was omitted in this panel because of it non-existent local peak at 687 nm. To compensate for the contribution of PSII to the spectra, one spectrum was chosen to be subtracted from the other spectra. This time, the t = 15 m spectrum was used, resulting in the spectra in (**E**), now thought to only to contain spectral information of PSI. The PSI fluorescence component can be obtained directly from (**E**), while the PSII fluorescence component can be calculated by subtracting the PSI component from a spectrum where the LHC component has already been subtracted (**C**, **D**). When both the PSI and the PSII fluorescence spectra are known, the fluorescence spectrum of LHCs can be found by subtracting a linear combination of the PSII and the PSI spectra from one of the raw spectra (**A**, **B**).
(TIFF)

S1 Discussion of S1 Fig. Discussion of the PAM fluorometry results shown in S1 Fig.
(DOCX)

S1 Dataset. Raw data from PAM fluorescence experiments and 77 K spectroscopy experiments.
(ZIP)

Acknowledgments

We want to thank Marianne Nymark at the Department of Biology, NTNU, for providing us with *P. tricornutum* cells.

Author Contributions

Conceptualization: Gunvor Bjerkelund Røkke, Martin F. Hohmann-Marriott.

Data curation: Gunvor Bjerkelund Røkke, Thor Bernt Melø.

Formal analysis: Gunvor Bjerkelund Røkke, Thor Bernt Melø.

Funding acquisition: Olav Vadstein, Atle M. Bones, Martin F. Hohmann-Marriott.

Investigation: Gunvor Bjerkelund Røkke, Alice Mühlroth.

Methodology: Gunvor Bjerkelund Røkke, Thor Bernt Melø, Martin F. Hohmann-Marriott.

Project administration: Gunvor Bjerkelund Røkke, Martin F. Hohmann-Marriott.

Resources: Thor Bernt Melø, Martin F. Hohmann-Marriott.

Software: Gunvor Bjerkelund Røkke, Thor Bernt Melø.

Supervision: Olav Vadstein, Atle M. Bones, Martin F. Hohmann-Marriott.

Validation: Gunvor Bjerkelund Røkke.

Visualization: Gunvor Bjerkelund Røkke.

Writing – original draft: Gunvor Bjerkelund Røkke, Martin F. Hohmann-Marriott.

Writing – review & editing: Gunvor Bjerkelund Røkke, Thor Bernt Melø, Alice Mühlroth, Olav Vadstein, Atle M. Bones, Martin F. Hohmann-Marriott.

References

1. Falkowski PG, Katz ME, Knoll AH, Quigg A, Raven JA, Schofield O, et al. The evolution of modern eukaryotic phytoplankton. Science. 2004; 305: 354–360. https://doi.org/10.1126/science.1095964 PMID: 15256663
2. Hohmann-Marriott MF, Blankenship RE. Evolution of photosynthesis. Annu Rev Plant Biol. 2011; 62: 515–548. https://doi.org/10.1146/annurev-arplant-042110-103811 PMID: 21438681
3. Falkowski PG, Geider R, Raven JA. The role of aquatic photosynthesis in solar energy conversion: A geoevolutionary perspective. In: Molecular to Global Photosynthesis. London: Imperial College Press; 2004. pp. 287–321.
4. Rousseaux CS, Gregg WW. Interannual variation in phytoplankton primary production at a global scale. Remote Sens. 2014; 6: 1–19.
5. Goss R, Lepetit B. Biodiversity of NPQ. J Plant Physiol. 2015; 172: 13–32. https://doi.org/10.1016/j.jplph.2014.03.004 PMID: 24854581
6. Derks A, Schaven K, Bruce D. Diverse mechanisms for photoprotection in photosynthesis. Dynamic regulation of photosystem II excitation in response to rapid environmental change. Biochim Biophys Acta. 2015; 1847: 468–485. https://doi.org/10.1016/j.bbabio.2015.02.008 PMID: 25687894
7. You Y, Stramski D, Darecki M, Kattawar GW. Modeling of wave-induced irradiance fluctuations at near-surface depths in the ocean: a comparison with measurements. Appl Opt. 2010; 49: 1041–1053. https://doi.org/10.1364/AO.49.001041 PMID: 20174174
8. Schenck H. On the focusing of sunlight by ocean waves. J Opt Soc Am. 1957; 47: 653–657.
9. Minagawa J. State transitions–The molecular remodeling of photosynthetic supercomplexes that controls energy flow in the chloroplast. Biochim Biophys Acta. 2011; 1807: 897–905. https://doi.org/10.1016/j.bbabio.2010.11.005 PMID: 21108925
10. Hager A, Stransky H. The carotenoid pattern and the occurrence of the light induced xanthophyll cycle in various classes of algae—V. A few members of cryptophyceae, euglenophyceae, bacillariophyceae, chrysophyceae and phaeophyceae. Arch Mikrobiol. 1970; 73: 77–89. PMID: 5484315
11. Demming-Adams B. Carotenoids and photoprotection in plants: A role for the xanthophyll zeaxanthin. Biochim Biophys Acta–Bioenergetics. 1990; 1020: 1–24.
12. Lavaud J, Lepetit B. An explanation for the inter-species variability of the photoprotective non-photochemical chlorophyll fluorescence quenching in diatoms. Biochim Biophys Acta. 2013; 1827: 294–302. https://doi.org/10.1016/j.bbabio.2012.11.012 PMID: 23201475
13. Niyogi KK, Truong TB. Evolution of flexible non-photochemical quenching mechanisms that regulate light harvesting in oxygenic photosynthesis. Curr Opin Plant Biol. 2013; 16: 307–314. https://doi.org/10.1016/j.pbi.2013.03.011 PMID: 23583332
14. Bennoun P. Evidence for a respiratory chain in the chloroplast. Proc Natl Acad Sci USA. 1982; 79: 4352–4356. PMID: 16593210

15. Caron L, Berkaloff C, Duval J-C, Jupin H. Chlorophyll fluorescence transients from the diatom *Phaeodactylum tricornutum*: relative rates of cyclic phosphorylation and chlororespiration. Photosynth Res. 1987; 11: 131–139. https://doi.org/10.1007/BF00018271 PMID: 24435489

16. Jakob T, Goss R, Wilhelm C. Activation of diadinoxanthin de-epoxidase due to a chlororespiratory proton gradient in the dark in the diatom *Phaeodactylum tricornutum*. Plant Biol. 1999; 1: 76–82.

17. Papageorgiou GC, Govindjee. Chlorophyll a fluorescence: A signature of photosynthesis. Dordrecht, London: Kluwer Academic; 2004.

18. Duysen LMN, Sweers HE. Mechanism of two photochemical reactions in algae as studied by means of fluorescence. In: Japanese society of plant physiologists, editor. Studies on Microalgae & Photosynthetic Bacteria. Tokyo: Univ. Tokyo Press; 1963. pp. 363–372.

19. Stirbet A, Govindjee. Chlorophyll a fluorescence induction: a personal perspective of the thermal phase, the J–I–P rise. Photosynth Res. 2012; 113: 15–61. https://doi.org/10.1007/s11120-012-9754-5 PMID: 22810945

20. Røkke G, Melø TB, Hohmann-Marriott MF. The plastoquinone pool of *Nannochloropsis oceanica* is not completely reduced during bright light pulses. PLoS One. 2017; 12(4):e0175184. 12:e0175184. https://doi.org/10.1371/journal.pone.0175184 PMID: 28403199

21. Schreiber U, Hormann H, Neubauer C, Klughammer C. Assessment of photosystem II photochemical quantum yield by chlorophyll fluorescence quenching analysis. Aust J Plant Physiol. 1995; 22: 209–220.

22. Schreiber U. Pulse-Amplitude-Modulation (PAM) fluorometry and Saturation Pulse Method: An overview. In: Chlorophyll a fluorescence: A signature of photosynthesis. Dordrecht, London: Kluwer Academic; 2004. pp. 279–319.

23. Diner B, Mauzerall D. Feedback controlling oxygen production in a cross-reaction between two photosystems in photosynthesis. Biochim Biophys Acta. 1973; 305: 329–352. PMID: 4200351

24. Schreiber U, Vidaver W. Chlorophyll fluorescence induction in anaerobic *Scenedesmus obliquus*. Biochim Biophys Acta. 1974; 368: 97–112. PMID: 4423963

25. Hohmann-Marriott MF, Takizawa K, Eaton-Rye JJ, Mets L, Minagawa J. The redox state of the plastoquinone pool directly modulates chlorophyll fluorescence in *Chlamydomonas reinhardtii*. FEBS Lett. 2010; 584: 1021–1026. https://doi.org/10.1016/j.febslet.2010.01.052 PMID: 20122933

26. Alric J, Lavergne J, Rappaport F. Redox and ATP control of photosynthetic cyclic electron flow in *Chlamydomonas reinhardtii* (I) aerobic conditions. Biochim Biophys Acta–Bioenergetics. 2010; 1797:44–51.

27. Iwai M, Takizawa K, Tokutsu R, Okamuro A, Takahashi Y, Minagawa J. Isolation of the elusive supercomplex that drives cyclic electron flow in photosynthesis. Nature. 2010; 464: 1210–1213. https://doi.org/10.1038/nature08885 PMID: 20364124

28. Frank K, Trebst A. Quinone binding sites on cytochrome *b*/*c* complexes. Photochem Photobiol. 1995; 61: 2–9. PMID: 7899491

29. De-Luca R, Bernardi A, Meneghesso A, Morosinotto T, Bezzo F. Modelling the photosynthetic electron transport chain in *Nannochloropsis gaditana* via exploitation of absorbance data. Algal Res. 2018; 33: 430–439.

30. Meneghesso A, Simionato D, Gerotto C, La Rocca N, Finazzi G, Morosinotto T. Photoacclimation of photosynthesis in the Eustigmatophycean *Nannochloropsis gaditana*. Photosynth Res. 2016; 129: 291–305. https://doi.org/10.1007/s11120-016-0297-z PMID: 27448115

31. Simionato D, Block MA, La Rocca N, Jouhet J, Maréchal E, Finazzi G, et al. Response of *Nannochloropsis gaditana* to nitrogen starvation includes a *de novo* biosynthesis of triacylglycerols, a decrease of chloroplast galactolipids and a reorganization of the photosynthetic apparatus. Eukaryot Cell. 2013; 12: 665–676. https://doi.org/10.1128/EC.00363-12 PMID: 23457191

32. Lepetit B, Sturm S, Rogato A, Gruber A, Sachse M, Falciatore A, et al. High light acclimation in the secondary plastids containing diatom *Phaeodactylum tricornutum* is triggered by the redox state of the plastoquinone pool. Plant Physiol. 2013; 161: 853–865. https://doi.org/10.1104/pp.112.207811 PMID: 23209128

33. Martinson TA, Ikeuchi M, Plumley FG. Oxygen-evolving diatom thylakoid membranes. Biochim Biophys Acta–Bioenergetics. 1998; 1409: 72–86.

34. Bukhov NG, Sridharan G, Egorova EA, Carpentier R. Interaction of exogenous quinones with membranes of higher plant chloroplasts: modulation of quinone capacities as photochemical and non-photochemical quenchers of energy in photosystem II during light-dark transitions. Biochim Biophys Acta. 2003; 1604: 115–123. PMID: 12765768

35. Owens TG. Light-harvesting function in the diatom *Phaeodactylum tricornutum*: II. Distribution of excitation energy between the photosystems. Plant Physiol. 1986; 80: 739–746. PMID: 16664695

36. Lamb JJ, Røkke GB, Hohmann-Marriott MF. Chlorophyll fluorescence emission spectroscopy of oxygenic organisms at 77 K. Photosynthetica. 2018; 56: 1–20.

37. Natali A, Croce R. Characterization of the major light-harvesting complexes (LHCBM) of the green alga *Chlamydomonas reinhardtii*. PLoS One. 2015; 10(2):e0119211. https://doi.org/10.1371/journal.pone.0119211 PMID: 25723534

38. Sugiura M, Minagawa J, Inoue Y. Properties of *Chlamydomonas* photosystem II core complex with a His-tag at the C-terminus of the D2 protein. Plant Cell Physiol. 1999; 40: 311–318.

39. Kargul J, Nield J, Barber J. Three-dimensional reconstruction of a light-harvesting complex I-photosystem I (LHCI-PSI) supercomplex from the green alga *Chlamydomonas reinhardtii*. Insights into light harvesting for PSI. J Biol Chem. 2003; 278: 16135–16141. https://doi.org/10.1074/jbc.M300262200 PMID: 12588873

40. Litvín R, Bína D, Herbstová M, Gardian Z. Architecture of the light-harvesting apparatus of the eustigmatophyte alga *Nannochloropsis oceanica*. Photosynth Res. 2016; 130: 137–150. https://doi.org/10.1007/s11120-016-0234-1 PMID: 26913864

41. Alboresi A, Le Quiniou C, Yadav SKN, Scholz M, Meneghesso A, Gerotto C, et al. Conservation of core complex subunits shaped the structure and function of photosystem I in the secondary endosymbiont alga *Nannochloropsis gaditana*. New Phytol. 2017; 213: 714–726. https://doi.org/10.1111/nph.14156 PMID: 27620972

42. Yokono M, Nagao R, Tomo T, Akimoto S. Regulation of excitation energy transfer in diatom PSII dimer: How does it change the destination of excitation energy? Biochim Biophys Acta. 2015; 1847: 1274–1282. https://doi.org/10.1016/j.bbabio.2015.07.006 PMID: 26188377

43. Ikeda Y, Komura M, Watanabe M, Minami C, Koike H, Itoh S, et al. Photosystem I complexes associated with fucoxanthin-chlorophyll-binding proteins from a marine centric diatom, *Chaetoceros gracilis*. Biochim Biophys Acta. 2008; 1777: 351–361. https://doi.org/10.1016/j.bbabio.2008.01.011 PMID: 18302929

44. Juhas M, Büchel C. Properties of photosystem I antenna protein complexes of the diatom *Cyclotella meneghiniana*. J Exp Bot. 2012; 63: 3673–3681. https://doi.org/10.1093/jxb/ers049 PMID: 22442408

45. Giovagnetti V, Ruban A. Detachment of the fucoxanthin chlorophyll a/c binding protein (FCP) antenna is not involved in the acclimative regulation of photoprotection in the pennate diatom *Phaeodactylum tricornutum*. Biochim Biophys Acta–Bioenergetics. 2017; 1858: 218–230.

46. Miloslavina Y, Grouneva I, Lambrev PH, Lepetit B, Goss R, Wilhelm C, et al. Ultrafast fluorescence study on the location and mechanism of non-photochemical quenching in diatoms. Biochim Biophys Acta. 2009; 1787: 1189–1197. https://doi.org/10.1016/j.bbabio.2009.05.012 PMID: 19486881

47. Herbstová M, Bína D, Koník P, Gardian Z, Vácha F, Litvín R. Molecular basis of chromatic adaptation in pennate diatom *Phaeodactylum tricornutum*. Biochim Biophys Acta. 2015; 1847: 534–543. https://doi.org/10.1016/j.bbabio.2015.02.016 PMID: 25748970

48. Nagao R, Yokono M, Teshigahara A, Akimoto S, Tomo T. Light-harvesting ability of the fucoxanthin chlorophyll a/c-binding protein associated with photosystem II from the diatom *Chaetoceros gracilis* as revealed by picosecond time-resolved fluorescence spectroscopy. J Phys Chem B. 2014; 118: 5093–5100. https://doi.org/10.1021/jp502035y PMID: 24773012

49. Krüger TPJ, Malý P, Alexandre MTA, Mančal T, Büchel C, Van Grondelle R. How reduced excitonic coupling enhances light harvesting in the main photosynthetic antennae of diatoms. Proc Natl Acad Sci U S A. 2017; 114: E11063–E11071. https://doi.org/10.1073/pnas.1714656115 PMID: 29229806

50. Cao S, Zhang X, Xu D, Fan X, Mou S, Wang Y, et al. A transthylakoid proton gradient and inhibitors induce a non-photochemical fluorescence quenching in unicellular algae *Nannochloropsis* sp. FEBS Lett. 2013; 587: 1310–1315. https://doi.org/10.1016/j.febslet.2012.12.031 PMID: 23474242

51. Eisenstadt D, Ohad I, Keren N, Kaplan A. Changes in the photosynthetic reaction centre II in the diatom *Phaeodactylum tricornutum* result in non-photochemical fluorescence quenching. Environ Microbiol. 2008; 10: 1997–2007. https://doi.org/10.1111/j.1462-2920.2008.01616.x PMID: 18397307

52. Wilhelm C, Duval J-C. Fluorescence induction kinetics as a tool to detect a chlororespiratory activity in the prasinophycean alga, *Mantoniella squamata*. Biochim Biophys Acta. 1990; 1016: 197–202.

53. Cruz S, Goss R, Wilhelm C, Leegood R, Horton P, Jakob T. Impact of chlororespiration on non-photochemical quenching of chlorophyll fluorescence and on the regulation of the diadinoxanthin cycle in the diatom *Thalassiosira pseudonana*. J Exp Bot. 2011; 62: 509–519. https://doi.org/10.1093/jxb/erq284 PMID: 20876335

54. Bennoun P. Chlororespiration and the process of carotenoid biosynthesis. Biochim Biophys Acta Bioenerg. 2001; 1506: 133–142.

55. Chukhutsina VU, Fristedt R, Morosinotto T, Croce R. Photoprotection strategies of the alga *Nannochloropsis gaditana*. Biochim Biophys Acta. 2017; 1858: 544–552.

56. Belgio E, Santabarbara S, Bína D, Trsková E, Herbstová M, Kaňa R, et al. High photochemical trapping efficiency in photosystem I from the red clade algae *Chromera velia* and *Phaeodactylum tricornutum*. Biochim Biophys Acta. 2017; 1858: 56–63.

57. Mullineaux CW, Allen JF. The state 2 transition in the cyanobacterium *Synechococcus* 6301 can be driven by respiratory electron flow into the plastoquinone pool. FEBS Lett. 1986; 205: 155–160.

58. Allen JF, Bennett J, Steinback KE, Arntzen CJ. Chloroplast protein phosphorylation couples plastoquinone redox state to distribution of excitation energy between photosystems. Nature. 1981; 291: 25–29.

59. Michelet L, Zaffagnini M, Morisse S, Sparla F, Pérez-Pérez ME, Francia F, et al. Redox regulation of the Calvin Benson cycle: Something old, something new. Front Plant Sci. 2013. https://doi.org/10.3389/fpls.2013.00470 PMID: 24324475

60. Buchanan BB. The path to thioredoxin and redox regulation in chloroplasts. Annu Rev Plant Biol. 2016; 67: 1–24. https://doi.org/10.1146/annurev-arplant-043015-111949 PMID: 27128465

61. Grouneva I, Jakob T, Wilhelm C, Goss R. The regulation of xanthophyll cycle activity and of non-photochemical fluorescence quenching by two alternative electron flows in the diatoms *Phaeodactylum tricornutum* and *Cyclotella meneghiniana*. Biochim Biophys Acta. 2009; 1787: 929–938. https://doi.org/10.1016/j.bbabio.2009.02.004 PMID: 19232316

62. Lepetit B, Gélin G, Lepetit M, Sturm S, Vugrinec S, Rogato A, et al. The diatom *Phaeodactylum tricornutum* adjusts nonphotochemical fluorescence quenching capacity in response to dynamic light via fine-tuned Lhcx and xanthophyll cycle pigment synthesis. New Phytol. 2017; 214: 205–218. https://doi.org/10.1111/nph.14337 PMID: 27870063

63. Guillard RRL, Ryther JH. Studies of marine planktonic diatoms. I. *Cyclotella nana* Hustedt and *Detonula confervacea* (Cleve) Gran. Can J Microbiol. 1962; 8: 229–239. PMID: 13902807

64. Gorman DS, Levine RP. Cytochrome f and plastocyanin: their sequence in the photosynthetic electron transport chain of *Chlamydomonas reinhardtii*. Proc Natl Acad Sci U S A. 1965; 54: 1665–1669. PMID: 4379719

65. Lamb JJ, Forfang K, Hohmann-Marriott MF. A practical solution for 77 K fluorescence measurements based on LED excitation and CCD array detector. PLoS One. 2015; 10(7):e0132258. https://doi.org/10.1371/journal.pone.0132258 PMID: 26177548

Paper III – Supporting information

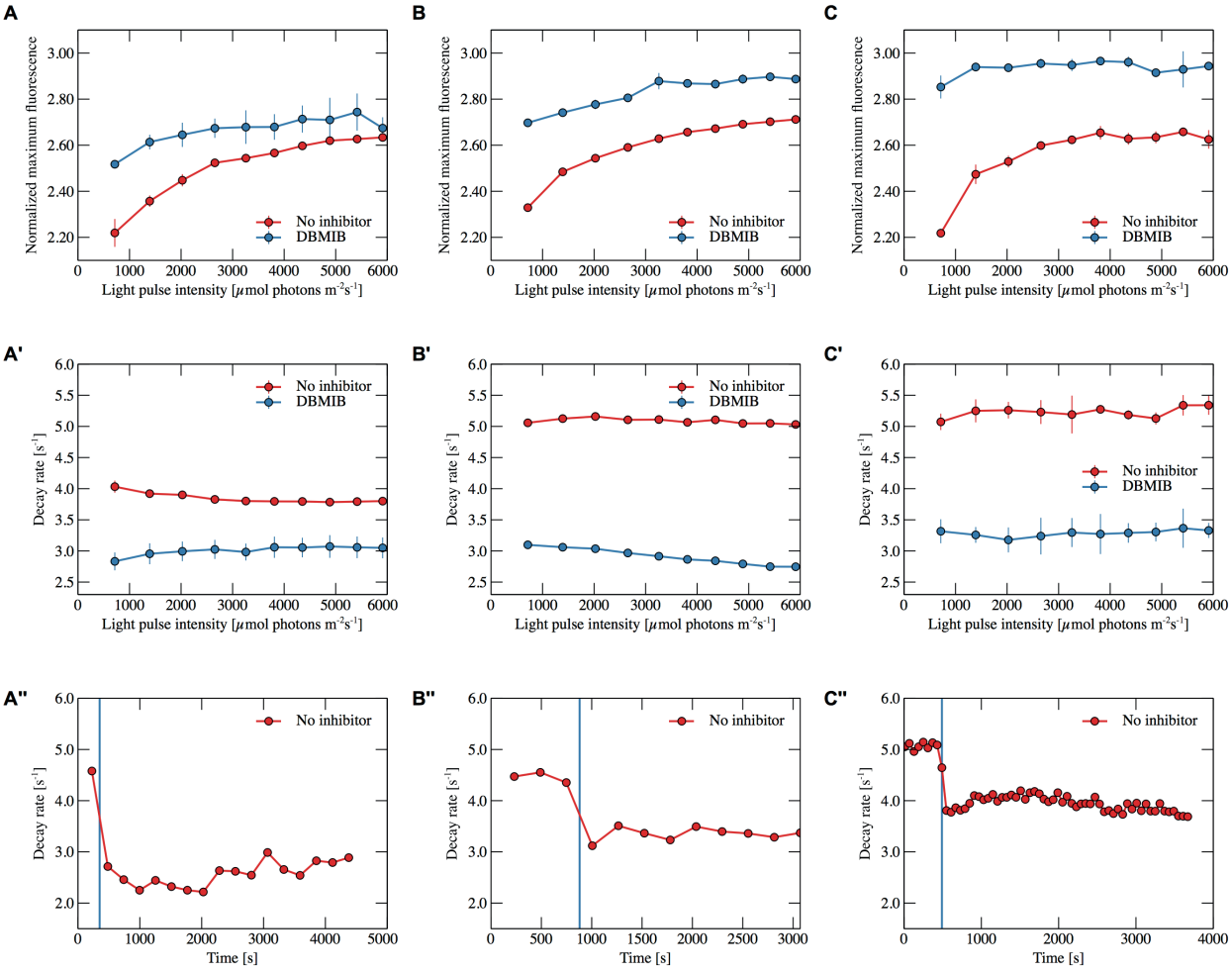

S1 Fig. PAM fluorometry results for P. tricornutum cells and previously published results for N. oceanica and C. reinhardtii for comparison.

(A, B, C) Light pulse-induced maximum fluorescence yield (normalized to F0) for untreated and DBMIB-treated cells of *C. reinhardtii* (A), *N. oceanica* (B) and *P. tricornutum* (C) in dependence of light pulse intensity. The results for *C. reinhardtii* and *N. oceanica* have been published previously [20], and were included here for comparison with the newly obtained data for *P. tricornutum* cells at low (0.2 μM chlorophyll concentration). (A', B', C') Chlorophyll fluorescence kinetic decay rates after light pulses of untreated and DBMIB-treated cells of *C. reinhardtii* (A'), *N. oceanica* (B') and *P. tricornutum* (C') in dependence of light pulse intensity. The previously published results for *C. reinhardtii* and *N. oceanica* [20] were included for comparison with newly obtained data for *P. tricornutum* at low (0.2 μM) chlorophyll concentration. (A", B", C") Chlorophyll fluorescence kinetic decay rates after light pulses (1600 μmol photons m-2s-1 of blue light) of *C. reinhardtii* (A"), *N. oceanica* (B") and *P. tricornutum* (C") undergoing anaerobic transition. The fluorescence data behind the decay rates shown in panels A", B" and C" is shown in Fig 1.

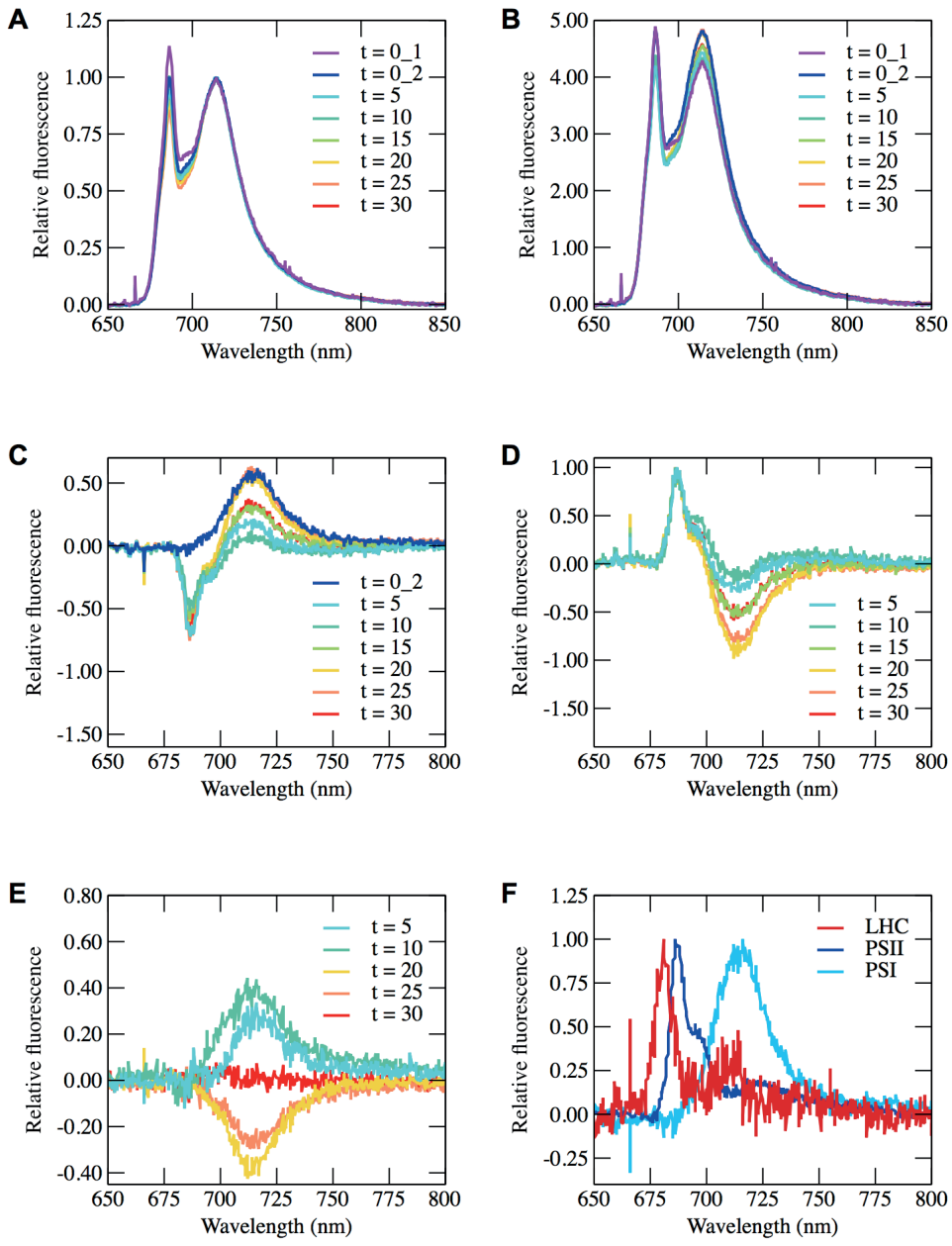
A
Relative fluorescence
Wavelength (nm)
t = 0_1
t = 0_2
t = 5
t = 10
t = 15
t = 20
t = 25
t = 30
B
Relative fluorescence
Wavelength (nm)
t = 0_1
t = 0_2
t = 5
t = 10
t = 15
t = 20
t = 25
t = 30
C
Relative fluorescence
Wavelength (nm)
t = 0_2
t = 5
t = 10
t = 15
t = 20
t = 25
t = 30
D
Relative fluorescence
Wavelength (nm)
t = 5
t = 10
t = 15
t = 20
t = 25
t = 30
E
Relative fluorescence
Wavelength (nm)
t = 5
t = 10
t = 20
t = 25
t = 30
F
Relative fluorescence
Wavelength (nm)
LHC
PSII
PSI

S2 Fig. Example of deduction of fluorescent components for *Chlamydomonas*.

An example of the procedure used to isolate the spectra of fluorescing components. The dataset recorded for *C. reinhardtii* during high light treatment (A) was normalized to 675 nm (B). This is a wavelength that is assumed to be associated with light harvesting complexes in *C. reinhardtii*, and also a wavelength that is thought to be little impacted by changes in fluorescence from the PSII core complexes. To eliminate the fluorescence contribution of light harvesting complexes, one of the spectra in the time series was subtracted from the other. In this example, the t = 0_1 spectrum was subtracted from the other spectra, resulting in the spectra shown in (C). The next step was to neutralize the contribution of PSII. Therefore, all spectra in (C) were normalized to the local fluorescence maximum (in (C) seen as a minimum) around 687 nm, resulting in the spectra displayed in (D). The t = 0_2 spectrum was omitted in this panel because of it non-existent local peak at 687 nm. To compensate for the contribution of PSII to the spectra, one spectrum was chosen to be subtracted from the other spectra. This time, the t = 15 m spectrum was used, resulting in the spectra in (E), now thought to only to contain spectral information of PSI. The PSI fluorescence component can be obtained directly from (E), while the PSII fluorescence component can be calculated by subtracting the PSI component from a spectrum where the LHC component has already been subtracted (C, D). When both the PSI and the PSII fluorescence spectra are known, the fluorescence spectrum of LHCs can be found by subtracting a linear combination of the PSII and the PSI spectra from one of the raw spectra (A, B).

S1 Discussion of S1 Fig

The decay kinetics of variable chlorophyll fluorescence after light pulses indicate recombination of an electron at Q_A with the donor side of PSII. This recombination has been shown to be dependent on the reduction state of the plastoquinone pool [66] and independent of oxygen concentration [67]. In aerobic conditions (S1 Fig 1A'', B'', and C''), the plastoquinone pool is oxidized, and a high recombination rate is observed. After transition to anaerobic conditions the plastoquinone pool becomes reduced, and the recombination rates decrease, indicating a reduced plastoquinone pool. Following this argumentation, the plastoquinone pool is reduced during bright light pulses in *C. reinhardtii* (S1 Fig 1A'), while it remains oxidized in *N. oceanica* (S1 Fig 1B') and *P. tricornutum* (S1 Fig 1C') during bright light pulses, even at higher light intensities.

The saturating behaviour of the normalized maximum fluorescence yield (F_m) under different light intensities indicates that the plastoquinone pool is reduced in *C. reinhardtii* at relatively low light intensities (convergence of the normalized maximum fluorescence yields of untreated and DBMIB-treated samples, S1 Fig 1A), while no clear saturation is achieved in *N. oceanica* (S1 Fig 1B) and *P. tricornutum* (S1 Fig 1C). The F_m for all organisms is higher in DBMIB-treated cell than in untreated cells. This is due to the differential quenching effect of DBMIB on minimum fluorescence yield (F_0) and F_m [34], where F_0 is preferentially quenched. Thus, after normalization to F_0, the maximum fluorescence yield is higher in DBMIB-treated samples. In the presented experiments, DBMIB concentrations were used that are known to inhibit electron transport through the cytochrome b_6f complex in different organisms. The DBMIB concentration for *C. reinhardtii* and *N. oceanica* was 20 μM, while the DBMIB concentration used for *P. tricornutum* was 1 μM. These differences in concentration are useful for demonstrating that the quenching behaviour of DBMIB does not influence the F_m convergence of DBMIB-treated cells and untreated cells. If this were the case, it would be expected that F_m between

DBMIB-treated and untreated samples would be most similar in *P. tricornutum*, where we see the largest difference in the data.

Together, fluorescence decay rates after light pulses, and F_m values at different light intensities indicate that the plastoquinone pool of *C. reinhardtii* is reduced at a light intensity of approximately 3000 μmol photons $m^{-2}s^{-1}$, while the plastoquinone pool remains oxidized in *N. oceanica* and *P. tricornutum* even at higher light intensities.

66. Diner BA. Dependence on the deactivation reactions of photosystem II on the redox state of the plastoquinone pool A varied under anaerobic conditions; Equilibria on the acceptor side of photosystem II. Biochim Biophys Acta. 1977;460: 247-258.

67. Laisk A, Eichelmann H, Oja V. Oxidation of plastohydroquinone by photosystem II and by dihydrogen in leaves. Biochim Biophys Acta. 2015;1847: 565-575.

Paper IV

DOI: 10.1007/s11099-018-0791-y PHOTOSYNTHETICA 56 (1): 105-124, 2018

REVIEW

Chlorophyll fluorescence emission spectroscopy of oxygenic organisms at 77 K

J.J. LAMB[*], G. RØKKE[**], and M.F. HOHMANN-MARRIOTT[**,+]

Department of Electronic Systems & ENERSENSE, NTNU, Trondheim, Norway[*]
Department of Biotechnology & CenTroN for Synthetic Biology, NTNU, Trondheim, Norway[**]

Abstract

Photosynthetic fluorescence emission spectra measurement at the temperature of 77 K (–196°C) is an often-used technique in photosynthesis research. At low temperature, biochemical and physiological processes that modulate fluorescence are mostly abolished, and the fluorescence emission of both PSI and PSII become easily distinguishable. Here we briefly review the history of low-temperature chlorophyll fluorescence methods and the characteristics of the acquired emission spectra in oxygen-producing organisms. We discuss the contribution of different photosynthetic complexes and physiological processes to fluorescence emission at 77 K in cyanobacteria, green algae, heterokont algae, and plants. Furthermore, we describe practical aspects for obtaining and presenting 77 K fluorescence spectra.

Additional key words: fluorescence; low temperature; photosynthesis.

Introduction

Historical background

"Chlorophyll fluorescence is red and beautiful" (Govindjee 1995) and has fascinated researchers for a long time (*see* reviews by Govindjee 1995, 2004). Chlorophyll (Chl) extracts prepared from leaves possess a very intense red fluorescence that caught the attention of Brewster in the 1830's (Brewster 1834). Correlations between the weaker *in vivo* Chl fluorescence emission and photosynthetic performance have been suggested (Müller 1887, as referenced by Govindjee 1995, 2004), but Kautsky and Hirsch were the first to unambiguously relate Chl fluorescence yield to the rate of photosynthesis (Kautsky and Hirsch 1931). The utility of Chl fluorescence for exploring photosynthesis was consequently demonstrated in many different photosynthetic organisms. Many breakthroughs in our understanding of photosynthesis are the result of researchers' creativity to develop techniques to resolve the spectral and temporal characteristics of Chl fluorescence in intact photosynthetic systems and by purifying individual components thereof.

One Chl fluorescence-based technique, which has been widely adopted, was developed by Seymour Steven Brody while working on his Ph. D. in the Rabinowitch laboratory at the University of Illinois at Urbana Champaign (Brody 1958, Rabinowitch and Govindjee 1969). It had been previously demonstrated that lowering the temperatures sharpens spectral characteristics, such as absorption and fluorescence, due to the loss of intramolecular vibrations. However, the improved spectral resolution was not the primary motivation for Brody to investigate fluorescence characteristics of the green algae *Chlorella* at liquid nitrogen temperatures. Brody wanted to eliminate bio-chemical and physiological processes (Hirsch and Rich

Received 27 October 2017, *accepted* 10 January 2018, *published as online-first* 8 February 2018.
[+]Corresponding author; e-mail: martin.hohmann-marriott@ntnu.no
Abbreviations: Chl – chlorophyll; LHC – light-harvesting complex; PSI – photosystem I; PSII – photosystem II.
This review is dedicated to Govindjee. In addition to Govindjee's original contributions to the field, we, the authors, are also very thankful to Govindjee for sharing historical context and personal connections, which contributed to researchers making their discoveries. In the case of 77 K fluorescence, the topic of this review, Govindjee was not only witness to its first implementation, but also went on to refine and extend the interpretation of this powerful measuring technique. The following short historical introduction into 77 K fluorescence often refers to information obtained from publications by Govindjee and coworkers.
Acknowledgements: Martin Hohmann-Marriott acknowledges support from the Research Council Norway (grant number 240741). Gunvor Røkke's research was supported by a PhD fellowship from the NT faculty of the Norwegian University of Science and Technology – NTNU. Jacob Lamb acknowledges the support from the ENERSENSE research initiative, and his research was supported by a postdoctoral fellowship from the Norwegian University of Science and Technology – NTNU.

2010), and thereby gained direct insights into excitation and electron transfer processes involved in photosynthesis using Chl fluorescence as a reporter. Around the same time during which Brody investigated fluorescence emission by the green alga *Chlorella* (Brody 1958), Litvin and Krasnovsky (1957) investigated fluorescence emission of plant material at 77 K.

One immediate finding of these measurements was that in addition to the main Chl fluorescence band at 685 nm, which is readily observed at room temperature, a second emission band with peak intensity at 720 nm becomes more prominent at lower temperatures (Fig. 1) (Brody 1958). Frederick Cho and Govindjee demonstrated that at even lower temperatures - at liquid helium temperatures (4 K) (Rabinowitch and Govindjee 1969, Cho 1970a, b, Cho and Spencer 1966) a third emission band at 695 nm can be separated (Fig. 2).

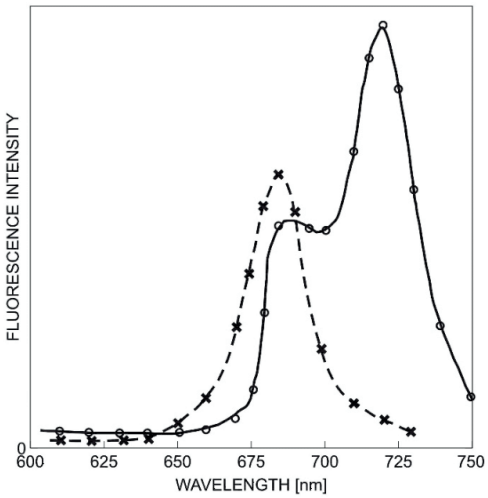

Fig. 1. Chlorophyll fluorescence emission by *Chlorella* cells at room temperature and –193°C. *The original figure legend*: „Fluorescence spectra of *Chlorella* at room temperature (*crosses*) and –193°C (*open circles*). The fluorescence intensities indicated are the same for both curves. The decrease in fluorescence yield at 690 mμ is probably due to the increased scattering of the exciting and fluorescent light".
Remarks: The fluorescence yield at 690 nm is expected to be about two times larger at –196°C compared to room temperature fluorescence yield, as suggested by Brody in the original figure legend. The term mμ is a historical notation that is equivalent with nanometer (nm).
This publication represents the first report of the increased long-wavelength chlorophyll fluorescence emission at 77 K, which has been established to be mainly associated with PSI.
Data was digitized from Brody (1958).

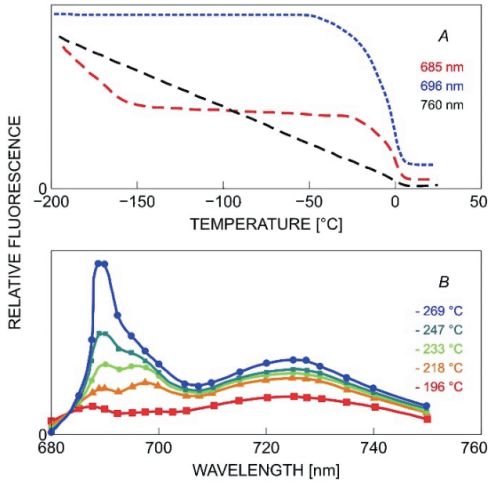

Fig. 2. Chlorophyll fluorescence emission of *Chlorella pyrenoidosa* as a function of temperature
(*A*): Chlorophyll fluorescence emission at specific wavelengths as a function of temperature in *Chlorella pyrenoidosa* as a function. The excitation light wavelength was 400 nm. *The original figure legend*: "Emission at 685 mμ (F685), at 696 mμ (F696), and at 760 mμ (F738; also referred to as F720 in the text) as a function of temperature (–196 to 20°C)." Panel *B* has been digitized from Cho *et al.* (Cho *et al.* 1966).
(*B*): Chlorophyll fluorescence emission spectra of *Chlorella pyrenoidosa* as a function of temperature (–269, –247, –233, –218, –196°C). Excitation light wavelength was 485 nm. *The original figure description*: "Fig. 1. shows the emission spectra measured in the 680–720 mμ range for several temperatures (–269, –247, –233, –218, and –196°C). Upon warming the sample, a shift from 695 mμ to 699 mμ in the location of the peak of the "F697.5" band is noticeable. As the temperature decreases from -196 to -269°C, the fluorescence increases steadily. The total intensity at –269°C is about 2 times that at –196°C. The profile of the fluorescence spectrum at –196°C shows clearly the F689, F697.5, and F725 bands; at –269°C, the F689 appears as a very sharp band and it dominates both F697.5 and 725, the F697.5 band shows only as a shoulder at –269°C" Panel *A* has been digitized from Govindjee and Yang (1966).
Remarks: The term mμ is a historical notation that is equivalent with nanometer (nm). This figure was used to demonstrate that the 738 nm (PSI) emission band is not a reabsorption artifact.

Associating these fluorescence emission bands with the concept of two types of photosystems (PSI and PSII) (Emerson 1957, Govindjee *et al*. 1960, Govindjee 1963) as part of the Z-scheme of photosynthesis, was achieved by the work of a community of researchers (reviewed by Govindjee and Björn 2017). So it was recognized that in red algae, which have a spectrally distinct light-harvesting system, preferentially exciting these light-harvesting systems, the phycobilisomes, increases the fluorescence emission at 685/695 nm (Krey 1966). Exciting Chl *b* in higher plants also increased the fluorescence at 685/695 nm, thus suggesting that Chl *b*-containing light-harvesting

systems are associated with PSII (Govindjee and Yang 1966, Rabinowitch and Govindjee 1969). Fractionation of spinach thylakoids into PSII-enriched and PSI-enriched fractions confirmed the assignments of Chl fluorescence emission bands at 685/695 nm to PSII and the emission band at 720 nm to PSI (Boardman *et al*. 1966).

That the number of light-absorbing pigments associated with PSI and PSII can be modulated in a physiologically relevant manner was shown by Murata (1969, 1970), in red alga using 77 K Chl fluorescence measurements. These "state transitions," are not unique to red algae, but have also been observed in other organism groups. Bonaventura and Myers (1969) showed dynamic adjustment of energy distribution between the photosystems in a green alga using room temperature fluorescence paired with oxygen measurements. However, 77 K Chl fluorescence emission measurements are by now the preferred method to establish changes in the association of light-harvesting systems between the two photosystems in green algae and plants (Goldschmidt-Clermont and Bassi 2015, Minagawa 2011).

We use the term "77 K Chl fluorescence" in this review article, as the majority of researchers currently uses this expression. It is derived from the fact that the boiling point of liquid nitrogen under standard conditions is 77.355 K (195.795°C). However, several expressions have been used more frequently in the past, including "Chl fluorescence at liquid nitrogen temperatures" and "Chl fluorescence at –196°C".

We have limited this review to steady-state fluorescence emission at 77 K and discuss the underlying physical processes, spectra, and its components. In addition to steady-state Chl fluorescence measurements at 77 K, many powerful techniques that use low-temperature Chl fluorescence emission have been developed, including time-resolved techniques (Strasser *et al*. 2004). Our focus here is on the physiological interpretation of information obtained from 77 K Chl fluorescence spectra. For this, we provide a visual overview of spectral features and physiological responses in different organism groups.

Physical background

Excitation of molecules

When molecules interact with light, the energy contained in the photons can be used to transfer an electron to an energetically higher orbital, thus generating a molecule in an excited state. Molecules with an extended conjugated system of bonds are likely to interact with photons in the visible spectrum. All Chls possess extended conjugated bond systems and interact with photons centered at two wavelengths that represent the first and second excited state of the Chl. The absorption band at higher energy is often termed "the blue absorption band", "B band" (consisting of several states) or "Soret band", whereas the lower energy absorption band can be referred to as the "red absorption band" or the "Q band" (consisting of two states, Q_x and Q_y) (Gouterman *et al*. 1963) (Fig. 3).

An excited Chl can return to the ground state through dissipating of the energy difference between excited state and ground state through different modes, which compete with one another. The second excited state of Chls is converted efficiently to the first excited state, and the energy difference is released as heat. The energy of the first excited state is either transferred to another pigment, or converted into: (*1*) heat, (*2*) chemical energy by driving charge separation, (*3*) a long-lived triplet state through a reversal of the spin of the electron, or (*4*) the emission of a photon. The energy of the emitted photon corresponds to the energy difference between the lower vibronic sublevels of the first excited state and ground state. This "Stokes-shifted" photon is the fluorescence that is the basis of many spectroscopic techniques, including 77 K fluorescence emission analysis.

The fluorescence characteristics of photosynthetic machinery is dependent on the emission characteristics of individual Chls and the cooperative excitation-coupling network these Chl form. A single Chl molecule possesses a fluorescence emission band, which reflects the transition from the first excited state to the ground state (Clayton 1980). This fluorescence band around 685 nm is broadened at room temperature as vibronic sublevels with higher energy are populated. Energy levels of excited states of individual Chls are also influenced by the protein and lipid environment that a Chl experiences. *In vivo*, the second broad fluorescence emission band around 735–740 nm is thought to be due to an increased emission wavelength through self-absorption at shorter wavelengths (Franck *et al*. 2002).

The overall emission of photosynthetic systems is a combination of main and vibronic sublevel emission, environment of individual Chls, and the energetic landscape of the Chl collective. For example, in plants, Chls associated with the PSII reaction center fluoresce at 685 and 695 nm – due to the main transition emission, and around 735–740 nm – due self-absorption enhanced fluorescence in this region. In intact PSII, Chls in the peripheral antennae, when isolated fluoresce at 680 nm, are coupled efficiently to the Chls within the PSII reaction center. Thus, only a small amount of 680 nm fluorescence emission is observed in intact systems, as the low energy Chls within the PSII reaction center (with a main emission at 685 and 695 nm) emit fluorescence. Furthermore, fluorescence emission from vibronic sublevels of Chls within the peripheral antennae and reaction center is emitted as a broad band centered at 730 nm. PSI has additional fluorescence emission that combines with that of PSII, light-harvesting complexes, and vibronic sublevel emission to generate the combined fluorescence emission pattern of an organism (Fig. 4).

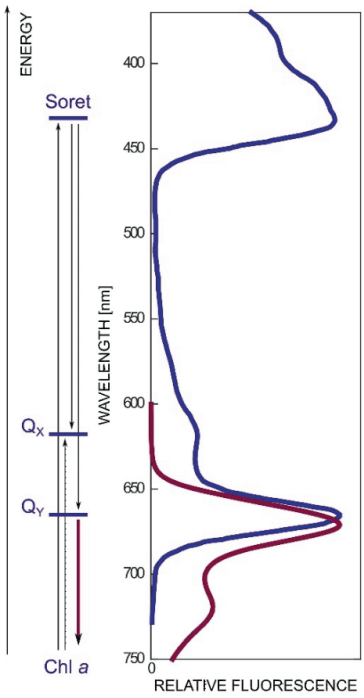

Fig. 3. Diagram relating the energy levels with the absorption spectrum and the fluorescence of chlorophyll (Chl) *a*. The data on energy levels in Chl *a* was obtained from Frank *et al.* (1994), absorption data for Chl *a* was obtained from Chen and Blankenship (2011), and the fluorescence data was retrieved from http://omlc.org/spectra/PhotochemCAD/html/122.html.

Table 1 gives an overview of major emission bands observed in various photosynthetic materials.

Excitation transfer

In whole, intact photosynthetic systems, Chl fluorescence represents a tiny fraction of all excitation energy captured by pigments in intact photosynthetic organisms, as energy is efficiently channeled into charge separation (Hillier and Babcock 2001). The bulk of the light-absorbing molecules in known photosynthetic organisms – except Heliobacteria – are not positioned within the photosynthetic reaction centers, but in separate peripheral light-harvesting systems. Light energy, absorbed by pigments in these light-harvesting systems is transferred *via* other pigments within the light-harvesting system (Förster 1965, Şener *et al.* 2011) to the reaction center antennae and finally to the reaction center core, where the excitation energy is used to accomplish a charge separation event.

Pigments

Oxygenic organisms employ three main classes of pigments for light harvesting: Chls, phycobilins, and carotenoids.

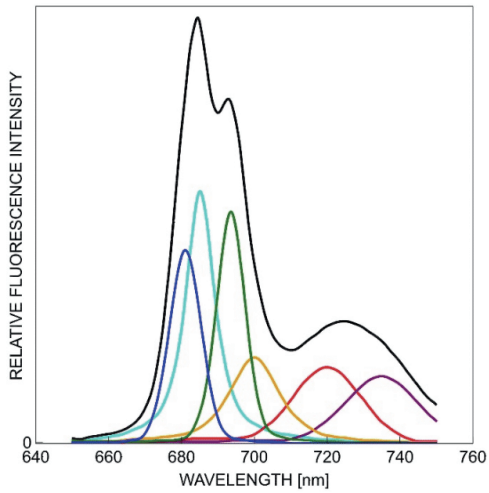

Fig. 4. Chlorophyll fluorescence emission spectra of spinach thylakoids at 77 K and decomposition in Gaussian components. A typical fluorescence emission spectrum with Gaussian decomposition representing known fluorescence emitters from spinach. The main components represent F_{680} (LHCII), F_{685} (CP47/CP43), F_{695} (CP47), F_{700} (aggregated LHCII trimer), F_{720} (PSI core complex), and F_{735} (LHCI). This figure has been digitized from Yamamoto *et al.* (2013), and a modified legend has been provided.

Chls and phycobilins possess a large absorption cross-section and are very fluorescent – features that make them well suited to participate in the Förster-type exchange of excitation. Indeed, the consortia of Chls (*i.e.*, the light-harvesting systems of plants) and phycobilins (*i.e.*, phycobilisomes, the light-harvesting system of cyanobacteria) are very efficient in channeling excitation to the Chl-containing reaction centers.

Carotenoids absorb light efficiently between 450–550 nm and display tiny fluorescence yields (Frank *et al.* 2006). Thus, the efficient excitation transfer between carotenoids and Chls cannot be understood by a Förster-type excitation transfer theory. Instead, energy transfer between carotenoids and Chls may be understood to be mediated by the singlet–singlet excitation energy transfer process (Owens 1992, Young and Frank 1996). Table 2 gives an overview of common pigments found in various organisms.

Fluorescence emission spectroscopy

A way to assess the interaction of light-harvesting systems with the reaction centers is to expose a sample to monochromatic light centered on a specific pigment absorption maximum and monitor the fluorescence emission. In cyanobacteria and red algae, phycobilins have an absorption spectrum that is distinct from the Chls of the reaction centers. For this reason, many early insights into

photosynthesis were obtained in phycobilin-containing organisms. Alga and plants expand the range of absorbed photons with Chls *b* and *c*, which are distinct from the Chl *a* of the reaction centers. The association of light-harvesting systems with the reaction centers can, therefore, be probed by exciting the light-harvesting system pigments and monitoring the fluorescence emission that is specific for PSII and PSI.

Room temperature fluorescence emission of plants

In whole, intact photosynthetic systems, only 1–2% of excitation energy captured is lost as fluorescence (Maxwell and Johnson 2000). At room temperature, PSII emits 90% of fluorescence while PSI contributes the remaining 10% (Govindjee 1995). Due to the low room temperature fluorescence emission of PSI compared to PSII, the overlapping fluorescence spectra of the main fluorescence emission band of Chls associated with PSI, and vibronic emission of Chls associated with PSII around 720–730 nm (Franck *et al*. 2002), it is difficult to assess the magnitude of PSI fluorescence emission. Another factor that makes the assignment of fluorescence to PSI and PSII difficult at room temperature is the modulation of fluorescence yield due to the reduction state of the electron acceptors within the photosystems. The prime modulator of overall Chl fluorescence at room temperature is the reduction state of the first stable electron acceptor of PSII, a quinone named Q_A (Duysens and Sweers 1963). In contrast, there is almost no modulation of PSI fluorescence yield by the reduction state of the electron acceptors of PSI at room temperature, which is due to the efficient quenching of excitation by $P700^+$ (Dau 1994a, b).

Fluorescence at low temperatures

Fluorescence emission spectra at 77 K offer a key advantage over room temperature measurements, as modulation caused by physiological acclimations and biochemical reactions are eliminated. Compared to room temperature, the 77 K fluorescence yield of the PSII core complex is about two times higher, and fluorescence yield of PSI increases by a factor of around 20 (Mukerji and Sauer 1988, Dekker *et al*. 1995), thus PSII and PSI fluorescence signatures become discernable from each other.

Electron transport reactions, apart from those involved in primary charge separation and charge stabilization within the photosystems, are inhibited at 77 K. Electrons accumulate on the acceptor side of PSII, and on the acceptor side of a fraction of PSI (Sétif *et al*. 1984, Schlodder *et al*. 1998) after brief illumination, and remain at the electron acceptors, even during low-intensity illumination, such as applied during the collection of fluorescence emission spectra. However, when samples are dark-adapted and remain unexposed to light after being frozen freezing at 77 K, fluorescence yield changes upon illumination at 77 K reflecting the electron transport within the reaction centers (Ley and Butler 1980). Lowering the temperature to 77 K also leads to a decrease in energy and thus electrons occupy lower vibrational levels, reflected by a sharpening of the fluorescence emission band compared to room temperature. Excitations are more likely trapped on the longer wavelength Chls, as the energy of the vibrational ground state is higher in the shorter-wavelength Chls. Thus, at temperatures lower than 77 K, more fluorescence within PSII is emitted at 695 nm (in addition to 685 nm), PSII and PSI fluorescence emission shifts to longer wavelengths, and emission of additional low energy pigments increase. For example, in plants fluorescence of Chls in LHCII complexes (Rabinowitch and Govindjee 1969, Cho and Spencer 1966) are thought to trap excitation below liquid nitrogen temperature increasingly, thereby contributing to fluorescence emission at 680 nm (Rijgersberg *et al*. 1979).

Having a discernible PSI-specific fluorescence signal enables the investigation of the association of light-harvesting systems with PSI or PSII, by exciting pigments (such as Chl *b*, *c*, carotenoids, and phycobilins) that are preferentially located in the peripheral light-harvesting systems. Furthermore, direct excitation of Chl *a* and the resulting fluorescence emission patterns can be used to determine the stoichiometries of the photosystems (Murakami 1997), and has provided major insights into physiological adaptations of photosynthetic organisms.

Technical and practical aspects for 77 K fluorescence measurements

Several methodologies have been developed to obtain 77 K fluorescence spectra with a variety of instruments and sample preparation procedures. The following section contains an overview of these techniques and procedures.

Fluorometer and measurements

In a fluorometer that is capable of quantifying fluorescence emission, monochromatic light is used to excite a sample at the desired wavelength. The fluorescence is detected at an angle of 90° to the incident excitation beam. The illumination and detection wavelength can be modulated by optical filters in combination with monochromators. For obtaining 77 K fluorescence emission and excitation spectra, instruments that use monochromators in combination with full spectrum excitation light sources and photomultiplier tubes have traditionally been used (Hipkins and Baker 1985). However, for obtaining fluorescence emission measurements, a less costly instrument that uses LEDs as an illumination source and a CCD-array spectrometers can also be employed (Lamb *et al*. 2015; Fig. 5).

To obtain useful spectral data that lacks artifacts, care must be taken to avoid spectral distortions by self-shading (*see* Fig. 6) (Govindjee and Yang 1966, Weis 1985). A dilution series of the sample can be used to find the concentrations where spectral distortions occur. Comparing these dilution spectra reveals that self-shading

Table 1. Assignment of fluorescence emission signals at 77 K.

Band assignment	Origin of 77 K fluorescence	Key reference
F_{640}	phycoerythrin	Sobiechowska-Sasim *et al*. 2014
F_{645}	phycocyanin	Sobiechowska-Sasim *et al*. 2014
F_{660}	allophycocyanin	Sobiechowska-Sasim *et al*. 2014
F_{680}	LCM, Lhca, Lhcb, Lhcf (Lhcv), Lhxr, RedCLH	Rijgersberg *et al*. 1979
F_{685}	PSII core: CP43, IsiA	Andrizhiyevskaya *et al*. 2005
F_{695}	PSII core: CP47	Andrizhiyevskaya *et al*. 2005
$F_{710–720}$	Lhc aggregates	Yamamoto *et al*. 2013
$F_{720–760}$	PSI reaction center antenna (cyanobaceria) PSI peripheral antenna (plants) chlorophyll vibronic sublevels	Karapetyan *et al*. 2014

Table 2. Distribution of photosynthetic pigments. [1]Many cyanobacterial species contain Chl *a* as their only chlorophyll-type pigment. [2]Heterokont algae.

	Bilins	Chl *a*	Chl *b*	Chl *c*	Chl *d*,*f*
Cyanobacteria	√	√	√[1]	√[1]	√[1]
Red algae	√	√			
Diatoms[2]		√		√	
Eustigmatophyta[2]		√			
Brown algae[2]		√		√	
Dinoflagellates[2]		√		√	
Cryptomonads	√	√		√	
Green algae		√	√		
Plants (Viridiplantae)		√	√		

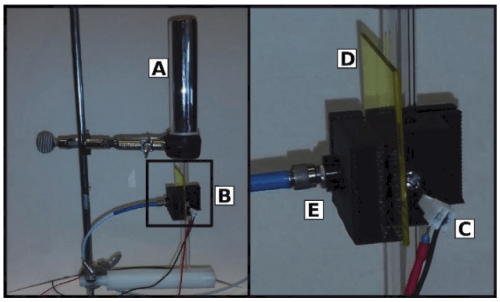

Fig. 5. Custom-built fluorometer. Images of a custom-built instrument setup published by Lamb *et al.* (2015). During data acquisition the instrument is covered by a black cloth, which has been omitted to show the setup. A: Dewar that holds the samples immersed in liquid nitrogen. The dewar part that orientates the sample in regards to the LED and detection fiber is supported by a white piece of plastic at the bottom, B: a 3D-printed housing, C: an excitation LED, D: a long-pass filter, and E: an optical fiber detector (at right angle to excitation LED). (Lamb *et al.* 2015).

leads to decrease in fluorescence yield of the bands associated with PSII (685/695 nm) compared to the PSI band, and a red shift of fluorescence emission spectra. With the sensitivity of modern instruments, compromises between spectra quality and signal-to-noise levels are unlikely to occur, but strategies and models for compensating for unavoidable self-absorption artifacts in tissues have been developed (Cordón and Lagorio 2006).

Optical filters can be employed to avoid spectral artifacts that are inherent to the optical components of the instruments and the characteristics of the sample. A (narrow) band pass filter can be used to eliminate stray light that has been transmitted by the excitation monochromator. Another artifact that can be removed by inserting a (narrow) band pass filter is the elimination of photons due to harmonic transmission by the excitation monochromators (*i.e*., photons with 1.5-times the excitation wavelength and 2-times the excitation wavelength may also pass the monochromators). This 1.5-times wavelength harmonic is of relevance when Chl is exited by 435-nm light (resulting in an artefactual peak at 652.5 nm), whereas the 2-times wavelength transmission artifact is of relevance if Chl is excited in the UV part of the spectrum.

Furthermore, a long-pass filter can be used to avoid excitation light, which is scattered by the sample, from entering the detector (Lakowicz 1983a, b).

Data processing of fluorescence spectra

Before measurements are reported, it is necessary to correct the spectra, and explicitly state the measuring configuration used. Corrections to spectra are necessary due to spectral features of the illuminating light source, as well as the spectral response of the detector used. Useful instructions and background for obtaining corrected spectra have been provided before (Lakowicz 1983a,b; Hofstraat *et al*. 1992).

A feature of most Chl fluorescence data is that they are reported in “relative fluorescence units.” The reason that most of the time non-quantified spectra, which report the fluorescence yield per absorbed photon, are reported, is the impracticality imposed by the lack of suitable equipment, as well as differences in the optical properties of samples, including scattering. Other factors that limit quantitative reporting of Chl fluorescence are changes in optical properties of the samples due to freezing, and difficulty in attaining reproducible orientation of the sample within the

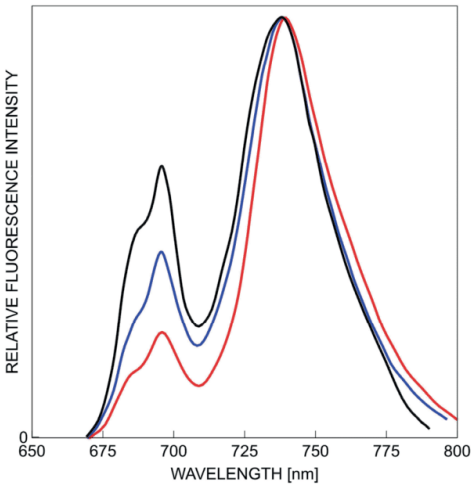

Fig. 6. Chlorophyll fluorescence emission of chloroplast fragments as a function of chlorophyll concentration. *The original figure legend*: "Emission spectra at –196°C of chloroplast fragments of spinach showing the effect of using different concentrations of chloroplasts. Exciting wavelength is 430 mμ. Further information from the text explaining the data: "The concentration is expressed on the graphs in per cent absorption at 680 mμ, ranging from about 100°-~ to 2%. These experiments show that reabsorption of the 696 mμ and 685 mμ emission bands is insignificant at less than 5%~ absorption at 680 mμ, but becomes significant at the higher concentrations. Thus, the 738 mμ band must be a "real" band (*i. e.* not due to reabsorption of the main band). (Further quantitative investigation is, however, required because our present data have not been corrected for reabsorption within a single chloroplast fragment.)"
This figure has been digitized from Govindjee and Yang (1966). *Remarks*: The term mμ is a historical notation that is equivalent with nanometer (nm). This figure was used to demonstrate that the 738 nm (PSI) emission band is not a reabsorption artifact.

used dewar. One way of standardizing the fluorescence measurements is the inclusion of a known quantity of fluorescent dye. The emission spectra of the included dye can then be used to normalize spectra against each other (*see* section on fluorescein below).

Dewars and cryostats

The dewar is at the heart of 77 K fluorescence measurements as it maintains the sample at low temperatures. Named after its inventor Sir James Dewar, a dewar is a specialized vacuum flask that houses low-temperature liquids, such as nitrogen or helium. For 77 K fluorescence measurements, the dewar takes the form of an open vessel, where a vacuum separates two glass walls. The dewar consists of a larger reservoir that houses the majority of liquid nitrogen and a thinner extension, which orientates the sample within the fluorometer. Samples that have already been frozen in liquid nitrogen are transferred to the dewar and maintained at a temperature of 77 K for the duration of the measurement. Dewars that have been designed to hold tubes for EPR experiments and other spectrophotometric measurements are commercially available. However, researchers who are lucky enough to have access to a good glassblower may find custom-designed dewars to be a cheaper alternative.

In addition to the relatively simple dewar-based setup, which can be adapted to many fluorometers, highly sophisticated instruments that interface with a defined suite of devices is also available. These instruments use cryostats, which allow precise temperature control down to liquid helium temperatures (4°C) and have optical interfaces for specific instruments or fiber optics.

Sample tubes

Unlike the situation for spectrophotometers, no standardized optical path length is used for 77 K experiments. In some laboratories, dewars made for EPR experiments are used, and thus matching EPR tubes with an inner diameter of 3–5 mm are used for measurements. An alternative to these commercial, closed-end tubes is an open-ended tube design, which provides a very cost-effective and practical alternative. The liquid samples can enter the tube by simply lowering the tube into the sample liquid. Once the tube is filled with the desired amount, the user seals the tube using their thumb and then freezes the sample in liquid nitrogen. The frozen liquid may escape from an open tube during measurements, and it is good practice to measure Chl fluorescence without a sample to assess contamination. In our experience, contamination does not occur even after measuring up to one hundred tubes. The real advantage of the open tube design is the ease of cleaning the tube so they can be reused continuously. When tubes are stored in a liquid nitrogen dewar for a long time, a film of ice can form, which should be removed with tissue paper, before inserting the sample into the dewar for measurements.

Fluorescein

An approach to compare the amplitude of fluorescence spectra is to introduce a fluorescent molecule to the sample at a known concentration. This allows the spectra from different samples to be normalized irrespective of their sample preparation properties, thus providing a quantitative insight into the changes between samples. One such molecule that can be included in the sample is fluorescein (Sjöback *et al*. 1995). When light is used to excite Chl *a*, it has an excitation maximum between 435–460 nm, and this light also excites fluorescein. The emission maximum of fluorescein is then observed at 508 nm (El Bissati *et al*. 2000), 545 nm (Walters and Horton 1991), or 535 nm (Krause *et al*. 1983, Krause and Weis 1984).

Glycerol

Glycerol has frequently been added to samples before freezing to 77 K as a cryoprotectant. This treatment reduces the formation of ice crystals during the freezing

procedure, therefore reducing damage to the sample and preventing light scattering. Unfortunately, glycerol treatment has been found to alter 77 K spectra in cyanobacteria (Mullineaux 1994) by reducing the affinity of phycobilisomes to PSII, resulting in increased fluorescence emission by the phycobilisomes (Mullineaux 1994). A detailed study on the effect of glycerol on the photosynthetic machinery of the cyanobacterium *Spirulina platensis* (Li *et al*. 2007) revealed that glycerol weakens energy transfer of the terminal phycobilisome emitter (L_{CM}) to the reaction center of PSII as well as interfering with energy transfer between phycobilins.

Sample preparation

Samples for measurement of fluorescence at 77 K can either be suspensions, such as algae, extracted thylakoids, and chloroplasts, or photosynthetic tissues, such as whole leaves. Dependent on the sample type, different sample preparation methods for measurements at 77 K have been developed. For standardization, samples are diluted or concentrated to the same Chl concentration. This concentration must be low enough to avoid self-shading of excitation and re-absorption of the emission light, yet high enough to obtain a high signal to noise ratio.

Cell suspensions and thylakoids

The fluorescence emission of many single-celled organisms can be measured in their respective growth medium. However, some cyanobacteria and alga accumulate fluorescent molecules within their growth medium, and thus washing with fresh culture medium may be required. When cells are spun down for washing with the fresh medium, it is crucial to develop a rapid procedure to do so, as prolonged exposure to new conditions, such as the absence of light within the centrifuge or changes in pH may elicit a physiological response. A physiological response that has severe consequences for Chl fluorescence within a short period is anaerobic incubation (Hohmann-Marriott *et al*. 2010) that can rapidly occur within cell pellets.

Thylakoids of cyanobacteria, algae, and plants contain the photosynthetically active protein complexes. For some experiments, it is desirable to remove the thylakoids from the organisms to control physical conditions, such as pH and the concentrations of ions, and to administer artificial electron donors and acceptors. Isolated chloroplasts and thylakoid membranes can be stored (Farkas and Malkin 1979) in the freezer. Once isolated and resuspended in their buffered media, samples can be inserted directly into sample tubes and frozen using liquid nitrogen, and are ready for 77 K fluorescence analysis. An alternative to freezing cells and thylakoids within the medium is to soak these samples up within filter paper and then rapidly freeze the sample by plunging it in liquid nitrogen. The resulting samples can then be treated like leaf tissue.

Photosynthetic tissues

For the photosynthetic tissue of multicellular organisms, such as plants and macroalgae, sample preparation differs from that of unicellular organisms. Leaf disks can be prepared readily and inserted into a dewar. However, the orientation of the tissue is a crucial parameter, as is the case for plant leaves, where the upper and lower side of the leaves have different spectroscopic properties (Björkman and Demmig 1987). Therefore, a tissue sample must have a known orientation that is stable during measurements. Due to the high Chl concentration, there is substantial self-shading in most intact photosynthetic tissues. To overcome self-shading, Egelbert Weis developed a method that dilutes the Chl concentration within tissues to a lower concentration (Weis 1985). For this, the tissue sample is ground up in a liquid nitrogen-cooled mortar, and water (Pfundel and Pfeffer 1997) or quartz (Weis 1985) is added to dilute the sample. The ground sample is then inserted into a closed, cooled glass tube with a small diameter. The original description of the method for “diluted leaf powder” (Weis 1985) also demonstrates the spectral shifts of fluorescence emission spectra that occur due to self-shading.

Processing of 77 K fluorescence emission data

Recorded raw 77 K fluorescence spectra are usually processed, before presenting them in publications, in order to remove artifacts. After compensating spectra for light source and instrument response curves (*see* “Data processing section”), remaining artifacts arise from the fluorescence of the medium the samples are suspended in, and scattering. Recording of media fluorescence emission spectra can be used to compensate for these artifacts. Spectral features of the medium that fall outside the fluorescence spectra of the sample can be used to scale the medium fluorescence and subtract it from the sample spectrum. Some bacteria and algae produce fluorescent molecules that accumulate in the medium. The fluorescence of these molecules together with scattering artifacts can form a broad spectral band that extends into the Chl fluorescence spectra. This spectral band can often be effectively subtracted from the Chl fluorescence spectrum by an exponential or Gaussian function. These functions can be anchored at a wavelength were no, or very little Chl fluorescence is expected, which is usually at 800 nm or 850 nm in oxygenic organisms. Adjusting the fluorescence level at 850 nm to zero, even without the subtraction of a logarithmic function for artifact removal, is often performed to display data in figures.

77 K fluorescence emission of isolated complexes and organisms

Photosystems

The dominant room temperature fluorescence emitted by PSII, together with its variability, has been an early focus of spectral analysis in photosynthesis research. The insight that two photosystems are working in concert in oxygenic photosynthesis (Rabinowitch and Govindjee 1969) lead to a hunt for the fluorescence signal that is emitted by the second type of reaction center. Fluorescence measurement at 77 K played a crucial part in establishing the identity of the second type of photosystem we now know as PSI. The discovery and miss-assignments of Chl fluorescence signals have been reviewed by Govindjee (2004) and Strasser *et al*. (2004).

Photosystem II

In this section, we focus on the fluorescence emitted by PSII. As PSII is associated with different light-harvesting systems in different organisms, we only discuss the fluorescence characteristics of the PSII reaction center antennae that contain Chl *a,* which are well established. There remains uncertainty about a functional assignment within PSII in Chl *d*-containing *Acaryochloris* species, as well as Chl *d*- and *f*- containing cyanobacteria capable of red light photoacclimation (FaRLiP) (Gan *et al*. 2015). The 77 K spectra of Chl *d*- (Miyashita *et al*. 1996) and Chl *f*- (Chen *et al*. 2012) containing PSII are discussed in details in the original literature.

PSII is composed of the reaction center core and the reaction center antenna. The PSII reaction center core houses 6 molecules of Chl *a*, and 2 *β*-carotenes, 2 phaeophytins, and 2 quinones are associated with D1 (PsbA) and D2 (PsbD). Four of these Chls are part of the special set of Chls that mediates charge separation, while the remaining 2 Chls energetically couple the special set of Chls to the reaction center core antenna. The 32 Chl *a* molecules, and 6 *β*-carotenes, which make up the core antennae pigments, are housed in the proteins CP43 (PsbC) and CP47 (PsbD). The absorption and fluorescence spectra of isolated CP43 and CP47 (Fig. 7*A*,*B*) and isolated PSII (Fig 7*C*,*B*) reaction centers of plants and cyanobacteria are very similar indicating a very stringent conservation through evolution.

At room temperature, PSII emission originates predominantly from Chls fluorescing at 695 nm. Upon further cooling to 77 K, a distinct fluorescence at 685 nm also gains prominence. The emission at 695 nm was early on correctly assigned to be emitted by Chls within PSII (reviewed by Govindjee 2004). The fluorescence emission at 685 nm, however, was first thought to emanate from the antenna complexes of plants (reviewed by Strasser *et al*. 2004). This fluorescence emission was later also assigned to the PSII reaction center antenna proteins CP43 (Rijgersberg *et al*. 1979) and CP47 (Nakatani *et al*. 1984). More recent studies on isolated plant PSII particles (Andrizhiyevskaya *et al*. 2005) confirm the association of

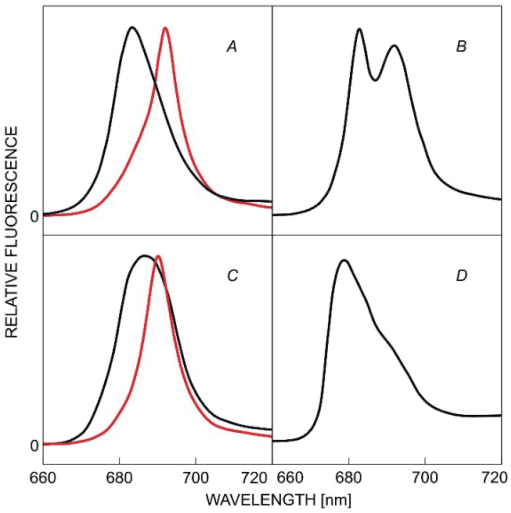

Fig. 7. Fluorescence emission from PSII, isolated PSII and CP43 and CP47 from cyanobacteria and plants. Fluorescence emission spectra of CP43 (*black*) and CP47 (*red*) (*A*) excited at 488 nm, isolated PSII that contains a histidine-tag, (*B*) excited at 435 nm from the cyanobacterium *Synechocystis* sp. PCC 6803. Fluorescence emission spectra CP43 (*black*) and CP47 (*red*) (*B*) excited at 488 nm, and isolated PSII (*D*) excited at 435 nm from plant *Arabidopsis thaliana*. The fluorescence spectra have been digitized from Boehm *et al*. (2011) (*A*, *C*), Liu *et al*. (2011), and Irrgang *et al*. (1988) (*D*).

695 nm emission with CP47, but indicate that the 685 nm emission arises from fluorescence emitted by both CP47 and CP43 at 77 K. Compared to room temperature, the fluorescence emission by PSII increases by a factor of about two when cooled to temperature of 77 K. At this temperature, PSII still contributes to long wavelength fluorescence, which overlaps with PSI fluorescence emission at 720/740 nm (Butler 1977).

PSII assembly and repair

The *de novo* assembly of PSII subunits is a fascinating topic (Eaton-Rye and Sobotka 2017) that also informs our understanding of the evolution of photosynthesis (Cardona 2016). In both cyanobacteria and plants, the assembly of PSII begins with binding of cytochrome b_{559} to the D2 subunit in the thylakoid membrane, forming the D2 pre-complex (Komenda *et al*. 2012, Nickelsen and Rengstl 2013). The D1 pre-complex is then bound, resulting in the heterodimeric reaction center pre-complex. Addition of the CP47 pre-complex to the heterodimeric reaction center pre-complex forms the RC47 complex (Boehm *et al*. 2012). The CP43 core antenna also forms a pre-complex with other subunits that bind to the RC47 complex.

Repair of damaged PSII shares common features with the assembly of PSII (Järvi *et al*. 2015). Damage to PSII reaction centers by light often affects D1 and results in the removal and consequent degradation of the damaged D1 protein (Komenda *et al*. 2012, Mulo *et al*. 2012). The repair of the damaged PSII involves the synthesis and insertion of a new D1 polypeptide into the PSII complex (Kyle *et al*. 1984, Järvi *et al*. 2015). This repair mechanism allows minimal energy expenditure during this process (Nixon *et al*. 2005, Takahashi and Badger 2011). Subcomplexes can be characterized by the presence or absence of fluorescence signal specific for the CP43 and CP47. In addition, increased fluorescence yield of peripheral light-harvesting complexes indicates that the assembly is not well coordinated or that PSII is damaged. Fluorescence spectroscopy at 77 K has provided valuable insights into the assembly and repair of the photosynthetic machinery (McCormac *et al*. 1996, Mysliwa-Kurdziel *et al*. 1997, Komenda *et al*. 2012, van Wijk *et al*. 1995).

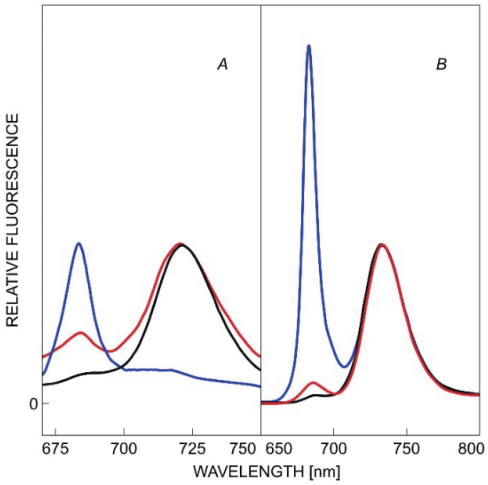

Fig. 8. Fluorescence emission from isolated PSI and PSI super complexes from cyanobacteria and plants. The fluorescence emission spectra (excited at 440 nm) of isolated PSI (*black*), isolated CP43' and (*blue*) isolated CP43'-PSI supercomplex (*red*) of the cyanobacterium *Synechocystis* PCC 6803 are shown in panel *A*. The fluorescence emission spectra (excited at 440 nm) of isolated PSI-Lhca-super complex (*black*), Lhcb-trimers (*blue*) PSI-Lhca-(Lhcb-trimer) super complex (*green*) of the plant *Arabidopsis thaliana* is shown in panel *B*. The emissions in both panels are normalized to the maximum of the Soret band.
The fluorescence spectra in panel *A* have been digitized from Bibby *et al*. (2001a).
The fluorescence spectra in panel *B* have been digitized from Galka *et al*. (2012).

Photosystem I

The discovery and assignment of the fluorescence emission at 720/730 nm to PSI is closely linked to the establishment of the two photosystem model for oxygenic photosynthesis (reviewed by Govindjee 2004). PSI complexes show a wide variety of emission spectra depending on the species and physiological conditions, but are located between 720–730 nm in oxygenic phototrophs, with some cyanobacteria having emission bands centered at wavelengths as long as 760 nm (Karapetyan *et al*. 2014).

The PSI reaction center of cyanobacteria (Fig. 8*A*), green algae, and plants (Fig. 8*B*) consists of two proteins (PsaA and PsaB) which together house around 85 Chls (Jordan *et al*. 2001). In addition, several smaller protein complexes contain about 10 Chl *a* molecules in cyanobacteria and plants. Cyanobacteria – which can form PSI trimers – are known to expand the trimeric PSI in stress conditions by circular antenna system that contributes an additional 180 (Boekema *et al*. 2001) to 218 (Bibby *et al*. 2001a) Chl *a* molecules.

The absorption cross-sections of PSI of green algae, red algae, heterokont algae, and plants are further expanded by light-harvesting systems that belong to the three trans-membrane helix family of light-harvesting complexes (Busch *et al*. 2010). In plants, four of these light-harvesting complexes (Lhca) are associated with PSI, adding 52 Chl *a* and 9 Chl *b* molecules. An additional 20 Chl *a* molecules interface the Lhca with the reaction center (Mazor *et al*. 2015). An unknown number of light-harvesting systems are associated with the PSI of red algae and heterokont algae.

In cyanobacteria and plants, fluorescence around 720 nm is emitted by Chls within the reaction center antennae (Karapetyan *et al*. 2014). Plants also possess an additional pool of long wavelength emitters located in the Lhca antenna (Morosinotto *et al*. 2003), specifically within Lhca3 and Lhca4 (Wientjes *et al*. 2011). This assignment is in agreement with previous greening studies, which indicated that the fluorescence emission at 736 nm is emitted by peripheral antennae complexes (containing Chl *b*), while the emission around 724 nm is emitted by the PSI reaction center antennae (Mullet *et al*. 1980a,b).

In plants, the fluorescence emission of PSI at 77 K is not modulated by the reduction state of P700. However, in red alga (Ley and Butler 1977) and cyanobacteria, (Karapeyan *et al*. 2014), modulation of the fluorescence yield dependent on the reduction state of P700 have been reported, but during steady-state fluorescence emission measurements, this modulation can be neglected.

Interpretation of 77 K fluorescence in different organism groups

Cyanobacteria and red algae

Cyanobacteria are a diverse group of oxygen-producing organisms, which share many features of their photosynthetic machinery with their ancestors, which gave rise to the chloroplasts of photosynthetic eukaryotes (Hohmann-Marriott and Blankenship 2011). This evolutionary relationship is reflected in the photosynthetic machinery of red algae, which uses similar pigments and protein structures as cyanobacteria. Several cyanobacteria have achieved model status, including unicellular *Synechocystis* and *Synechococcus* species, as well as multicellular, nitrogen-fixing *Anabaena* and *Nostoc* species, while the unicellular *Cyanidioschyzon* and multicellular *Porphyridium* species are red algal model systems. In the following section, we mainly discuss the well-characterized photosynthetic machinery of cyanobacteria with the inference that the photosynthetic machinery of red algae is similar.

Peripheral light-harvesting systems and supercomplexes

What makes cyanobacteria a rewarding species for spectroscopic studies are their light-harvesting pigments, the phycobilins, which are covalently linked within phycobiliproteins. The phycobiliproteins can be assembled into large structures, the phycobilisomes (de Marsac 2003, Marx *et al*. 2014). Phycobilins absorb light within the "green gap" between the two main absorption bands of Chl *a*. Phycobilisomes are in many conditions primarily associated with PSII, but as discussed in detail later, can dynamically (Mullineaux 2014) adjust this association and can form supercomplexes with both photosystems (Liu *et al*. 2013). There are several types of phycobilins; including phycoerythrobilin, phycocyanobilin, and allophycocyanobilin, but not all species of cyanobacteria contain all of these phycobilins. For example, *Synechocystis* sp. PCC 6803 contains phycocyanin, allophycocyanin, and phycoerythrin, while the latter is absent in *Synechococcus* sp. PCC 7002. Phycoerythrin absorbs excitation between 475–575 nm (maximum 565 nm), and fluoresces maximally at 640 nm; phycocyanin absorbs excitation between 525–635 nm (maximum 620 nm), and fluoresces at maximally at 644 nm; allocyanophycin absorbs between 550–665 nm (maximum 650 nm), and fluoresces maximally around 660 nm (Sobiechowska-Sasim *et al*. 2014). Excitation of phycobilins in cyanobacteria and red algae at 77 K induces fluorescence emission by phycobilins, which are pronounced when the interactions of phycobilisomes with the reaction centers are disturbed (Kaňa *et al*. 2014). The terminal phycobilisome emitter, *i.e*., the protein containing the pigments that energetically couple the phycobilisomes to the core reaction center antenna, is different for PSI and PSII. An allophycocyanin (ApcD) interfaces with PSI (Dong *et al*. 2009), while PSII interfaces with a multidomain protein named L_{CM} (encoded by *apcE*) (Tang *et al*. 2015), which contains a phycocyanobilin with a geometry usually found in phytochromes. This pigment within L_{CM} absorbs maximally around 655 nm and fluoresces maximally around 670 nm. As the number of Chl per reaction center is higher in PSI (96 Chl *a* molecules) (Jordan *et al*. 2001) than that in PSII (35 Chl *a* molecules) (Umena *et al*. 2011), exciting Chls at 435 nm preferentially excites PSI, while photons with a wavelength of 590/635 nm preferably excite PSII in cyanobacteria. The PSI/PSII ratio in cyanobacteria is much higher than 1, and consequently more than 90% of Chls can be associated with PSI.

Some cyanobacteria can utilize other Chls, in addition to Chl *a,* to perform oxygenic photosynthesis. A polyphyletic group of organisms, the prochlorophytes, possess a membrane-embedded antenna system that houses Chl *b* along with Chl *a,* which is related to the stress-induced antenna protein isiA and the PSII-subunit CP43 (La Roche *et al*. 1996), with similar fluorescence emission spectra. Chl *d* is used by the *Acaryochloris marinus*, and Chl *d* and Chl *f* (Li and Chen 2015) are used by a diverse group of cyanobacteria that take advantage of environments rich in far-red photons.

Photosystem I

Cyanobacterial PSI has species-specific long wavelength-emitting Chls ranging from 727–760 nm with 2-7 Chls estimated to contribute to the emission (Karapetyan *et al*. 2014). There is also a spectral range of emission in red algal PSI, ranging from 708 nm for *P. cruentum* to 728 nm for *C. caldarum*. Trimeric PSI complexes are commonly found in cyanobacteria under a variety of conditions (Fig. 8*A*) (Boekema *et al*. 1987, 2001; Garczarek *et al*. 1998) and *Synechocystis* sp. PCC 6803 (Bibby *et al*. 2001a,b). Some cyanobacteria can form monomeric, trimeric, and tetrameric PSI, with each possessing different optical characteristics including Chl fluorescence emission bands at 77 K (monomer at 725 nm, trimer at 730 nm, and tetramer at 715 nm) (Li *et al*. 2014). In red algae, however, PSI appears to be monomeric (Gardian *et al*. 2007).

Red algae have light-harvesting complexes related to the Lhca and Lhcb of alga and plants, which are absent in cyanobacteria (Busch *et al*. 2010). These three-transmembrane helix proteins, named Lhcr, are exclusively associated with the PSI of red algae. As in cyanobacteria (Kondo *et al*. 2007, Watanabe *et al*. 2014), there is good evidence that a specific pool of phycobilisome proteins is associated with PSI in red algae also (Busch *et al*. 2010).

State transition

State transitions are dynamic adjustments of the

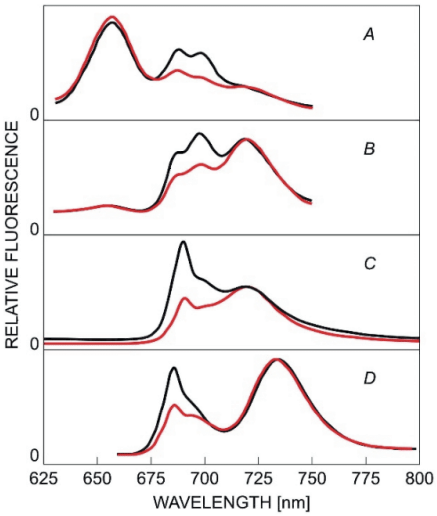

Fig. 9. Fluorescence emission characteristics of state transition in cyanobacteria, green algae, and plant during state transition. State 1 is indicated by the black trace while state 2 is indicated by the red trace. The cyanobacterium *Synechococcus* 6301 was excited at 600 nm (*A*) and 430 nm (*B*). S*ynechococcus* cells were locked in the state 1 by treating the cells with far-red light, which preferentially excites PSI, while the cells investigated in the state 2 were dark-acclimated. The green algae *Chlamydomonas reinhardtii* was excited at 455 nm (*C*). *Chlamydomonas* cells were locked in the state 1 by application of the PSII inhibitor DCMU under the light, and in the state 2 by treatment with the uncoupler FCCP. The plant *Arabidopsis thaliana was* excited at 435 nm (*D*). To lock the *Arabidopsis* cells in different states, excitation light favoring PSII and PSI, respectively, was utilized. Spectra were and normalized to the Soret emission band for all figures.
Data has been digitized from Mullineaux and Allen (1990) for *Synechococcus* 6301, Iwai *et al*. (2008) for *Chlamydomonas reinhardtii*, and Dietzel *et al*. (2011) for *Arabidopsis thaliana*. State 1 is shown in black and state 2 is shown in red.
Remarks: Excitation light at 600 nm preferentially excites phycobilins over chlorophyll *a*, thus panel *A* indicates that phycobilisomes donate more energy to PSII in state 1. *Synechococcus* 6301 can synthesize phycocyanin and allophycocyanin, while genes for phycoerythrin synthesis are missing, and therefore no fluorescence emission characteristic of phycoerythrin is observed.

photosynthetic machinery that modulate the distribution of absorbed light energy between PSI and PSII (Fig. 9*A*) (Mullineaux 2014). 77 K fluorescence studies in cyanobacteria and red algae (Murata *et al*. 1966), played a crucial role in establishing the concept of state transition, as changes in energy distribution could be easily investigated by preferentially illuminating the phycobilins while monitoring the fluorescence emission bands specific for PSI and PSII (Murata 1969). These studies indicate that both PSI and PSII receive excitation that was absorbed by phycobilins (Mullineaux 1992). Whether state transitions are based on a physical movement of phycobilisomes between PSI and PSII, or energy transfer occurs between Chl *a* in PSII and PSI, in a process called "spillover" (Biggins and Bruce 1989), was debated for a long time (McConnell *et al*. 2002, Li *et al*. 2004). However, there is now good evidence that the movement of phycobilisomes is a critical part of state transitions (Joshua and Mullineaux 2004), while spill-over appears not to be the major route for transferring energy from the phycobilisomes to PSI (Mullineaux 2008). A recent detailed study on the movement of phycobilisomes in different red algae (Kaňa *et al*. 2014) found that phycobilisomes have very limited mobility in the thermophilic red algae *C. caldarium*, while the mesophilic red algae *P. cruentum* exhibited phycobilisome movement in analogy to state transitions observed in cyanobacteria.

Stress-induced adaptations

Iron limitation induces changes in the composition of the photosynthetic machinery in cyanobacteria. Under iron limitation, proteins encoded by the *isiAB* operon are expressed (Pakrasi *et al*. 1985a,b, Laudenbach *et al*. 1988, Riethman and Sherman 1988, Burnap *et al*. 1993). While *isiB* codes for a thioredoxin that can functionally replace ferredoxin, IsiA possesses homology to the Chl *a*-binding PSII protein CP43 (Burnap *et al*. 1993, Falk *et al*. 1995), and can function as a PSI antenna system under stress conditions. During iron limitation, 18 IsiA from an antenna ring around trimeric PSI in *Synechococcus* sp. PCC 7942 (Boekema *et al*. 2001) and *Synechocystis* sp. PCC 6803 (Fig. 8*A*) (Bibby *et al*. 2001a,b). It was also suggested that IsiA could replace CP43, thus acting as an alternative antenna complex for PSII (Pakrasi *et al*. 1985b), or as an excitation energy dissipater, with the ability to protect PSII from photoinhibitory damage during iron starvation (Park *et al*. 1999). The induction of the IsiA protein under strong light, even in the presence of iron, confirmed its photoprotective role (Havaux *et al*. 2005). The presence of IsiA can be discerned by an increase in 685 nm emission (Burnap *et al*. 1993, Falk *et al*. 1995, Park *et al*. 1999), and an increase in energy partitioning to PSI. The latter is reflected by a more prominent fluorescence emission by the red Chls of the PSI reaction center antenna Chls around at 720 nm.

Green algae and plants

Green alga and plants share a common ancestor and consequently share features of their photosynthetic machinery (Keeling 2013). The green algae *Chlamydomonas reinhradtii* has many features that make it a valuable

organism for photosynthesis research, such as toolboxes for genetic manipulation, and the ability to grow non-photosynthetically. However, *Chlamydomonas* possesses many features that are altered or unique compared to plants (Erickson *et al*. 2015).

Peripheral light-harvesting systems and super-complexes

In plants and green algae, the absorption cross-section of the reaction center is extended by membrane-embedded light-harvesting systems. In addition to Chl *a* that is also found in the reaction center core and reaction center antennae, plants and green algae also synthesize Chl *b* that is associated with peripheral membrane-bound antenna complexes (LHCs). These antenna complexes and non-pigment-containing linker complexes form different supercomplexes with PSI and PSII, some of which can be isolated and structurally and spectroscopically characterized (Fig. 10) (Tokutsu and Minagawa 2013, Wei *et al*. 2016).

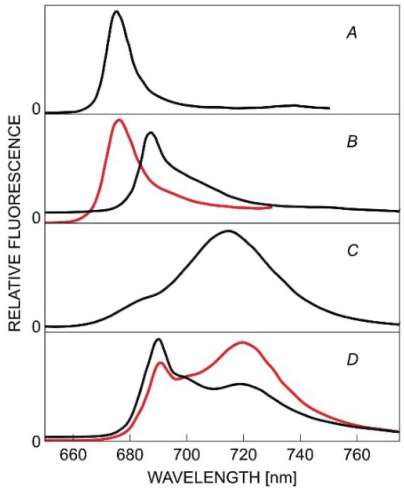

Fig. 10. Fluorescence emission spectra of photosynthetic components of the green algae *Chlamydomonas reinhardtii*. (*A*) The 77 K fluorescence emission spectrum (excitation wavelength 440 nm) of trimeric LHCII complexes isolated from *C. reinhardtii* (Natali and Croce 2015). (*B*) The 77 K fluorescence emission spectra of an isolated His-tagged PSII core complex (*black*) (excitation wavelength 435 nm) (Sugiura and Inoue 1999), and the 77 K fluorescence emission (excitation wavelength 440 nm) of PSII-LHCII super complex (*red*) (Drop *et al*. 2014). (*C*) The 77 K fluorescence emission spectra of LHCI-PSI super complex (excitation wavelength is 435 nm) (Kargul *et al*. 2003). (*D*) The 77 K fluorescence emission spectrum of a whole cell in state 1 (*black*) and state 2 (*red*) (excitation wavelength 440nm) (Iwai *et al*. 2008).
Panel *A* was digitized form Natali and Croce (2015). Panel *B* was digitized from Sugiura and Inoue (1999) and Drop *et al*. (2014). Panel *C* was digitized from Kargul *et al*. 2003 (2003). Panel *D* was digitized from Iwai *et al*. 2008 (2008).

Major and minor light-harvesting complexes

The protein complexes that house the pigments of the peripheral antennae can be grouped into monomeric Chl-binding complexes often called minor antennae complexes and trimer-forming LHCs (Busch *et al*. 2010) that are predominantly associated with PSII (Lhcb) or PSI (Lhca). Some Lhcb proteins in plants and algae can change the association between PSII and PSI during state transitions. Lhcb can form homo- and hetero-trimers that house 24 Chl *a* molecules, 18 Chl *b* molecules, and 12 carotenoids, with isolated trimers emitting fluorescence maximally between 678–680 nm at 77 K (Standfuss and Kühlbrandt 2004). Modeling in combination with mutational deletion of Chl ligands (Novoderezhkin *et al*. 2005) identified a spatially clustered group of three Chls as the final emitters, *i.e*., these Chls are likely to donate excitation to the PSII reaction center. These Chls are likely responsible for fluorescence emission at 680 nm (F_{680}). Lhcb can also form aggregated states that may be involved in photoprotection through excitation quenching, and exhibit a red-shifted fluorescence emission at 77 K (700–715 nm) (Ruban *et al*. 1997, 2012).

Photosystem II

The PSII of green alga and plants is organized in a dimer and Lhcb trimers can interface with both reaction centers of this dimer. Excitation transfer from the trimer to the reaction center is accomplished *via* three pigment-containing protein subunits (CP29, CP26, and CP24) associated with each reaction center monomer. Structural studies show that the subunit CP29 contains 10 Chl *a* molecules, 3 Chl *b* molecules, 3 carotenoids, and CP26 contains 9 Chl *a* molecules, 3 Chl *b* molecules, 3 carotenoids (Wei *et al*. 2016). Mutational analysis and modeling suggest that CP24 contains 5 Chl *a* molecules, 5 Chl *b* molecules, and two carotenoids (Passarini *et al*. 2009). These minor Chl-containing complexes are not known to contribute to 77 K fluorescence in intact systems largely.

Photosystem I

In contrast to PSI of cyanobacteria, the green algal and plant PSI possess tightly associated Lhca (Ben-Shem *et al*. 2003). The PSI supercomplex of *Pisum sativum* contains the reaction center proteins (PsaA and PsaB) as well as four Lhca (Lhca1–4) that form the peripheral antennae as a “dimer of dimers” (Mazor *et al*. 2015). Around 20 additional Chls energetically link the PSI reaction center with the peripheral antennae (Ben-Shem *et al*. 2003). The fluorescence emission of plant PSI is mainly due to Chl *a* in the Lhca antenna (Croce *et al*. 1998). Specifically, it is thought that one Chl *a* dimer within each Lhca (Qin *et al*. 2015) is the emitter of long wavelength fluorescence, whereas the reaction center core is only a minor contributor to this emission. Interestingly, no long wavelength emission was observed in PSI isolated from a prasinophyte green algae (Swingley *et al*. 2010).

State transition

The term "state transition" and its historical development has been introduced in the section on cyanobacteria. It became apparent that algae and plants also perform state transitions (Bonaventura and Myers 1969). As in cyanobacteria, the physiological basis for state transitions in green algae and plants appears to be the imbalance of electrons produced by PSII and utilized by carbon fixation (Minagawa 2011). However, in green algae and plants, the excitation coupling of Lhcb, not the excitation coupling of phycobilisomes to the two photosystems, is modulated. In the presence of a (partly) oxidized PQ pool, Lhcb are tightly excitationally coupled to PSII. Upon reduction of the PQ pool, some Lhcb are phosphorylated (Allen 1992) and consequently more Lhcb donate excitation to PSI. Whether much physical movement of the Lhcb is required for state transition is still unclear. It seems unlikely that a substantial mass migration of Lhcb between PSII-rich grana and PSI-rich stroma occurs, but instead, Lhcb may make additional contact with PSI. State transitions can be readily observed (Fig. 9*B*) by exiting samples at either the Chl *a* (430/440 nm) or Chl *b* (450/455 nm) Soret absorption band, while observing the emission bands of PSII (685/695 nm) and PSI (720/740 nm), with Chl *b* excitation providing a more specific signal for changes in excitation distribution.

Heterokont algae

Heterokonts comprise many photosynthetic algae including diatoms (*Bacillariophyceae*), brown algae (*Phaeophyceae*), and *Eustigmatophyceae*. Four membranes surround the chloroplast of these algae, indicating a secondary (Cavalier-Smith 1999) or even more complex endosymbiotic history (Keeling 2013).

Phaeodactylum

Major and minor light-harvesting complexes

Phaedactylum tricornutum is a pennate diatom that, despite several clade-unspecific features regarding its live cycle and morphology, has achieved model status. The photosynthetic machinery of *Phaeodactylum,* however, shows features that are consistent and typical for most diatoms. In addition to light absorbed by Chl *a,* diatoms use alternative pigments, in particular, *c*-type Chls (c_{1-3}) and carotenoids, with fucoxanthin being the most common. This composition of pigments was used to name the light-harvesting systems that are typical of many heterokont algae, the fucoxanthin-Chl-binding proteins (FCP) (Gundermann and Büchel 2014). The peripheral light-harvesting systems of most heterokont algae can be preferentially excited using the Soret band of Chl *c* (465 nm) and fucoxanthin (530 nm), while Chl *a*-specific photons can be used to excite the reaction center antenna preferentially.

FCP is related to the three transmembrane-helix LHCs of plants and algae. The FCP can be grouped into three fractions: (1) FCPs, which are unique to heterokont algae (Lhcf), (2) FCPs, which are related to red algal Lhca (Lhcr), and (3) FCPs, which related to LhcSR, a protein complex characterized in the green algae *Chlamydomonas* and the moss *Physcomitrella* (Lhcx) (Gundermann and Büchel 2014). Homology modeling in combination with spectroscopic and biochemical characterization suggest that each Lhcf can bind 6 Chl *a* molecules, 4 Chl *c* molecules, and 5–6 carotenoids, which in addition to fucoxanthin may also include lutein, diadinoxanthin, and diatoxanthin (Gundermann and Büchel 2014). In addition to Lhcf, another distantly related three-transmembrane helix protein belonging to the "red lineage Chl *a*/-binding-like proteins" (RedCAP) is also present in heterokont algae.

Lhcf can form trimers (Lepetit *et al*. 2007, Nagao *et al*. 2013) analogous to the Lhcb trimers in plants and algae. While some uncertainty about the association of Lhcf to PSII to heterokont algae remains, there is good evidence that Lhcf associates predominantly with PSI (Juhas and Büchel 2012).

The fluorescence emitted by PSI-associated FCP has two prominent bands at 685 nm and 697 nm (Fig. 11*A*). These fluorescence bands, however, are emitted by a group of Chl *a*, which are unlikely to be at homologous locations to the terminal emitter in the Lhca and Lhcb of plants (Gundermann and Büchel 2014). The absence of emission bands associated with Chl *c* species indicates that all Chl *c* is efficiently coupled to Chl *a* within the FCPs.

Photosystem II

PSII core complexes form dimers in diatoms, such as *Phaeodactylum*, and exhibit a fluorescence emission band with a maximum at 692 nm (Fig 10*B*) (Yokono *et al*. 2015). This emission band appears to be a combination of a 692 nm and a 684 nm emitter located in CP47 (Yokono *et al*. 2015), while CP43 fluorescence emission is absent at 77 K. A different 77 K fluorescence emission pattern is observed in monomeric PSII, where the maximum fluorescence is emitted around 687 nm (Yokono *et al*. 2015). There is little biochemical evidence that any FCPs are associated with PSII to form stable super complexes in heterokont algae (Grouneva *et al*. 2011) or at least not into very stable super complexes (Nagao *et al*. 2010). However, spectroscopy-based studies reveal that the functional antenna size of PSII can be dynamically adjusted, thus suggesting a functional association between PSII and some FCPs (Miloslavina *et al*. 2009).

Photosystem I

Isolated PSI of diatoms has a long wavelength emission at

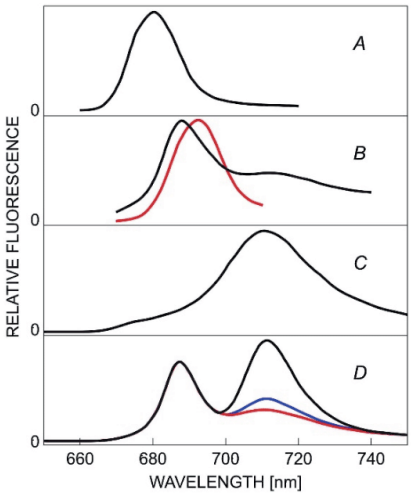

Fig. 11. Fluorescence emission spectra of photosynthetic components of heterokont diatom algae (*Phaeodactylum and Chaetoceros gracilis*). (*A*) The 77 K fluorescence emission spectrum (excitation wavelength 435 nm) of FCP from *Phaeodactylum tricornutum* (Litvín *et al*. 2016). (*B*) The 77 K fluorescence emission spectrum (excitation wavelength 425 nm) of PSII monomer (*red*) and dimer (*black*) from *Phaeodactylum tricornutum*, excited at 425 nm (Yokono *et al*. 2015). (*C*) The 77 K fluorescence emission spectrum (excitation wavelength 425 nm) of FCP-PSI super complexes from *Chaetoceros gracili*s, excited at 450 nm (Ikeda *et al*. 2008). (*D*) The 77 K fluorescence emission spectra (excitation wavelength 425 nm) of whole cells of *Phaedactylum tricornutum* with different levels of non-photochemical quenching (Lavaud and Lepetit 2013).
Panel *A* was digitized form Litvín *et al*. (2016).
Panel *B* was digitized from Yokono *et al*. (2015)
Panel *C* was digitized from Ikeda *et al*. (2008)
Panel *D* was digitized from Lavaud and Lepetit (2013).

715–720 nm (Fig. 11*C*) (Berkaloff *et al*. 1990, Veith and Büchel 2007, Ikeda *et al*. 2008). In addition, there is also a broad emission centered at 740–750 nm, which is a combination of vibronic sub-bands of all Chls within the sample.

Nannochloropsis

Nannochloropsisis species are heterokont algae belonging to the Eustigmatophyceae family. *Nannochloropsis oceanica* and *gaditana* have received increased attention as they can accumulate high amounts of lipids. The architecture of the photosynthetic machinery of *Nannochloropsis* species has recently been investigated in detail (Herbstová *et al*. 2015, Litvín *et al*. 2016).

Eustigmatophyceae are unique among the heterokont algae in lacking Chl *c* and fucoxanthin in their LHCs. Thus, Chl *a* serves as the only Chl of both PSI and PSII, as well as in the peripheral LHCs. *Nannochloropsis* species

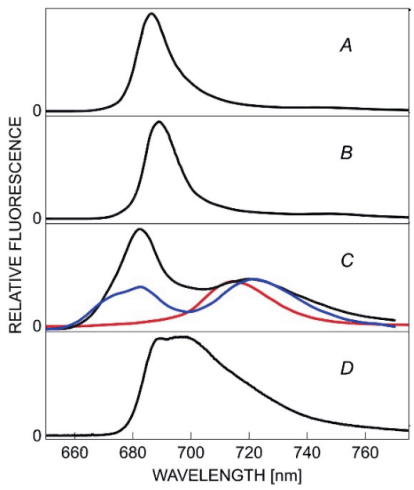

Fig. 12. Fluorescence emission spectra of photosynthetic components of heterokont algae *Eustigmataphyceaen* alga *Nannochloropsis.* (*A*) The 77 K fluorescence emission spectrum (excitation wavelength 440 nm) of isolated VCP from *Nannochloropsis oceanica* (excited at 435 nm) (Litvín *et al*. 2016). (*B*) The 77 K fluorescence emission spectrum of isolated PSII from *Nannochloropsis oceanica* (excitation wavelength 435 nm) (Litvín *et al*. 2016). (*C*) The 77 K fluorescence emission spectrum of isolated PSI-LHC complexes isolated from *Nannochloropsis gaditana* (mainly dimeric: *black*, mainly monomeric: *blue*) (Alboresi *et al*. 2017) and PSI-supercomplex (*red*) (Litvín *et al*. 2016) (excitation wavelength 440 nm). (*D*) The fluorescence emission spectrum of whole cell *Nannochloropsis oceanica* (excitation wavelength 435 nm). Panels *A* and *B* were digitized from Litvín *et al.* (2016). (*C*) was digitized from Alboresi *et al*. (2017).

use predominantly the carotenoids violaxanthin and vaucheroaxanthin as light-harvesting pigments and for photoprotection. Chl *a* and the carotenoids are housed in LHCs, called VCP for viola-/vaucheriaxanthin Chl protein (Fig. 12*A*) (Litvín *et al*. 2016).

Light-harvesting complexes

Nannochloropsis species possess LHCs that can be clustered according to their evolutionary origin as diatoms including Lhcx and Lhcv – the *Eustigmatophycean* version of the diatom Lhcf, and Lhcr. Furthermore, RedCLH, a light-harvesting protein first identified in *Chromera velia,* is also present (Litvín *et al*. 2016). Biochemical isolation suggests that VCP can form trimers (Litvín *et al*. 2016). VCP seems to be very rich in carotenoids, with about one carotenoid per two Chls, with violaxanthin and vaucheria-xanthin being the dominant carotenoids (Litvín *et al*. 2016). Until high-resolution structural data of Lchv is available, it may be assumed that VCPs bind pigments analogous to Lhca, Lhcb (in green algae and plants), and Lhcf (in diatoms).

Photosystem II

Biochemical separation procedures suggest that the PSII complexes can contain about 4–5 VCPs per PSII core (Litvín *et al*. 2016) that belong to the Lhcr family. Interestingly, 77 K fluorescence spectra of isolated PSII particles show no fluorescence emission band at 685 nm and PSII that lack CP43 are present when PSII is isolated (Fig 11*B*) (Litvín *et al*. 2016). Whether this 77 K fluorescence emission pattern in combination with the CP43-lacking PSII complexes indicate that PSII has structural features, which are different from green algae and plants, needs to be resolved in the future.

Photosystem I

The PSI reaction center core complex of *Nannochloropsis* has very similar fluorescence emission characteristics (Fig. 11*C*) to those observed in diatoms (Herbstová *et al*. 2015)**,** with a single emission band around 715 nm. However, *Nanochloropsis* PSI supercomplexes with associated complexes can be isolated, which contain Lhcr, Lhcx, and RedCAP (Bína *et al*. 2017, Litvín *et al*. 2016), the latter being a Chl-binding protein also present in other heterokont algae.

References

Alboresi A., Le Quiniou C., Yadav S.K.N. *et al*.: Conservation of core complex subunits shaped the structure and function of photosystem I in the secondary endosymbiont alga *Nannochloropsis gaditana*. – New Phytol. **213**: 714-726, 2017.

Allen J.F.: Protein phosphorylation in regulation of photosynthesis. – BBA-Bioenergetics **1098**: 275-335, 1992.

Andrizhiyevskaya E.G., Chojnicka A., Bautista J.A. *et al*.: Origin of the F685 and F695 fluorescence in photosystem II. – Photosynth. Res. **84**: 173-180, 2005.

Ben-Shem A., Frolow F., Nelson N.: Crystal structure of plant photosystem I. – Nature **426**: 630-635, 2003.

Berkaloff C., Caron L., Rousseau B.: Subunit organization of PSI particles from brown algae and diatoms: polypeptide and pigment analysis. – Photosynth. Res. **23**: 181-193, 1990.

Bibby T.S., Nield J., Barber J.: Iron deficiency induces the formation of an antenna ring around trimeric photosystem I in cyanobacteria. – Nature **412**: 743-745, 2001a.

Bibby T.S., Nield J., Barber J.: Three-dimensional model and characterization of the iron stress-induced CP43′-photosystem I supercomplex isolated from the cyanobacterium *Synechocystis* PCC 6803. – J. Biol. Chem. **276**: 43246-43252, 2001b.

Biggins J., Bruce D.: Regulation of excitation energy transfer in organisms containing phycobilins. – Photosynth. Res. **20**: 1-34, 1989.

Bína D., Gardian Z., Herbstová M., Litvín R.: Modular antenna of photosystem I in secondary plastids of red algal origin: a *Nannochloropsis oceanica* case study. – Photosynth. Res. **131**: 255-266, 2017.

Björkman O., Demmig B.: Photon yield of O_2 evolution and chlorophyll fluorescence characteristics at 77 K among vascular plants of diverse origins. – Planta **170**: 489-504, 1987.

Boardman N., Thorne S., Anderson J.: Fluorescence properties of particles obtained by digitonin fragmentation of spinach chloroplasts. – P. Natl. Acad. Sci. USA **56**: 586-593, 1966.

Boehm M., Romero E., Reisinger V. *et al*.: Investigating the early stages of Photosystem II assembly in Synechocystis sp. PCC 6803 isolation of CP47 and CP43 complexes. – J. Biol. Chem. **286**: 14812-14819, 2011.

Boehm M., Yu J., Reisinger V. *et al*.: Subunit composition of CP43-less photosystem II complexes of Synechocystis sp. PCC 6803: implications for the assembly and repair of photosystem II. – Philos. T. R. Soc. B **367**: 3444-3454, 2012.

Boekema E.J., Dekker J.P., van Heel M.G. *et al*.: Evidence for a trimeric organization of the photosystem I complex from the thermophilic cyanobacterium *Synechococcus* sp. – FEBS Lett. **217**: 283-286, 1987.

Boekema E.J., Hifney A., Yakushevska A.E., Piotrowski M.: A giant chlorophyll-protein complex induced by iron deficiency in cyanobacteria. – Nature **412**: 745-758, 2001.

Bonaventura C., Myers J.: Fluorescence and oxygen evolution from *Chlorella pyrenoidosa*. – BBA-Bioenergetics **189**: 366-383, 1969.

Brewster D.: On the colours of natural bodies. – Earth Env. Sci. T. R. So. **12**: 538-545, 1834.

Brody S.: New excited state of chlorophyll. – Science **128**: 838-839, 1958.

Burnap R.L., Troyan T., Sherman L.A.: The highly abundant chlorophyll-protein complex of iron-deficient *Synechococcus* sp. PCC7942 (CP43 [prime]) is encoded by the *isiA* gene. – Plant Physiol. **103**: 893-902, 1993.

Busch A., Nield J., Hippler M.: The composition and structure of photosystem I□associated antenna from *Cyanidioschyzon merolae*. – Plant J. **62**: 886-897, 2010.

Butler W.L.: Chlorophyll fluorescence: a probe for electron transfer and energy transfer. – In: Trebst A., Avron M. (ed.): Photosynthesis I. Pp. 149-167. Springer, Berlin – Heidelberg 1977.

Cardona T.: Reconstructing the origin of oxygenic photosynthesis: Do assembly and photoactivation recapitulate evolution? – Front. Plant Sci. **7**: 257, 2016.

Cavalier□Smith T.O.M.: Principles of protein and lipid targeting in secondary symbiogenesis: euglenoid, dinoflagellate, and sporozoan plastid origins and the eukaryote family tree. – J. Eukaryot. Microbiol. **46**: 347-366, 1999.

Chen M., Blankenship R.E.: Expanding the solar spectrum used by photosynthesis. – Trends Plant Sci. **16**: 427-431, 2011.

Chen M., Li Y., Birch D., Willows R.D.: A cyanobacterium that contains chlorophyll *f* – a red□absorbing photopigment. – FEBS Lett. **586**: 3249-3254, 2012.

Cho F., Spencer J.: Emission spectra of *Chlorella* at very low temperatures (−269° to −196°). – Biochim. Biophys. Acta **126**: 174-176, 1966.

Cho F.: Low-temperature (4–77° K) spectroscopy of *Anacystis*; temperature dependence of energy transfer efficiency. – BBA-Bioenergetics **216**: 151-161, 1970a.

Cho F.: Low-temperature (4–77° K) spectroscopy of *Chlorella*;

temperature dependence of energy transfer efficiency. – BBA-Bioenergetics **216**: 139-150, 1970b.

Clayton R.K.: Photosynthesis: Physical Mechanisms and Chemical Patterns. Vol. 4. Pp. 19-35. Cambridge University Press, Cambridge 1980.

Cordón G.B., Lagorio M.G.: Re-absorption of chlorophyll fluorescence in leaves revisited. A comparison of correction models. – Photochem. Photobio. S. **5**: 735-740, 2006.

Croce R., Zucchelli G., Garlaschi F.M., Jennings R.C.: A thermal broadening study of the antenna chlorophylls in PSI-200, LHCI, and PSI core. – Biochemistry **37**: 17355-17360, 1998.

Dau H.: Molecular mechanisms and quantitative models of variable photosystem II fluorescence. – Photochem Photobiol **60**: 1-23, 1994a.

Dau H.: New trends in photobiology: Short-term adaptation of plants to changing light intensities and its relation to Photosystem II photochemistry and fluorescence emission. – J. Photoch. Photobio. B **26**: 3-27, 1994b.

de Marsac N.T.: Phycobiliproteins and phycobilisomes: the early observations. – Photosynth. Res. **76**: 193-205, 2003.

Dekker J., Hassoldt A., Petterson A. *et al*.: On the nature of the F695 and F685 emission of photosystem II. – In: Mathis P. (ed.): Photosynthesis: From Light to Biosphere, Vol III. Pp. 53-56. Kluwer, Dordrecht 1995.

Dietzel L., Bräutigam K., Steiner S. *et al*.: Photosystem II supercomplex remodeling serves as an entry mechanism for state transitions in *Arabidopsis*. – Plant Cell **23**: 2964-2977, 2011.

Dong C., Tang A., Zhao J. *et al*.: ApcD is necessary for efficient energy transfer from phycobilisomes to photosystem I and helps to prevent photoinhibition in the cyanobacterium *Synechococcus* sp. PCC 7002. – BBA-Bioenergetics **1787**: 1122-1128, 2009.

Drop B., Webber-Birungi M., Yadav S.K.N. *et al*.: Light-harvesting complex II (LHCII) and its supramolecular organization in *Chlamydomonas reinhardtii*. – BBA-Bioenergetics **1837**: 63-72, 2014.

Duysens L., Sweers H.: Mechanism of two photochemical reactions in algae as studied by means of fluorescence. – In: Tamiya H. (ed.): Studies on Microalgae and Photosynthetic Bacteria. Pp. 353-372. University of Tokyo Press, Tokyo 1963.

Eaton-Rye J.J., Sobotka R.: Assembly of the photosystem II membrane-protein complex of oxygenic photosynthesis. – Front. Plant Sci. **8**: 884, 2017.

El Bissati K., Delphin E., Murata N. *et al*.: Photosystem II fluorescence quenching in the cyanobacterium *Synechocystis* PCC 6803: involvement of two different mechanisms. – BBA-Bioenergetics **1457**: 229-242, 2000.

Emerson R.: Dependence of yield of photosynthesis in long-wave red on wavelength and intensity of supplementary light. – Science **125**: 746, 1957.

Erickson E., Wakao S., Niyogi K.K.: Light stress and photoprotection in *Chlamydomonas reinhardtii*. – Plant J. **82**: 449-465, 2015.

Falk S., Samson G., Bruce D. *et al*.: Functional analysis of the iron-stress induced CP 43′ polypeptide of PS II in the cyanobacterium *Synechococcus* sp. PCC 7942. – Photosynth. Res. **45**: 51-60, 1995.

Farkas D.L., Malkin S.: Cold storage of isolated class C chloroplasts optimal conditions for stabilization of photosynthetic activities. – Plant Physiol. **64**: 942-947, 1979.

Förster T.: Delocalizing Excitation and Excitation Transfer. Modern Quantum Chemistry Istanbul Lectures. Pp. 93-137. Academic Press, New York 1965.

Franck F., Juneau P., Popovic R.: Resolution of the photosystem I and photosystem II contributions to chlorophyll fluorescence of intact leaves at room temperature. – BBA-Bioenergetics **1556**: 239-246, 2002.

Frank H.A., Cua A., Chynwat V. *et al*.: Photophysics of the carotenoids associated with the xanthophyll cycle in photosynthesis. – Photosynth. Res. **41**: 389-395, 1994.

Galka P., Santabarbara S., Khuong T.T.H. *et al*.: Functional analyses of the plant photosystem I–light-harvesting complex II supercomplex reveal that light-harvesting complex ii loosely bound to photosystem ii is a very efficient antenna for photosystem I in state II. – Plant Cell **24**: 2963-2978, 2012.

Gan F., Shen G., Bryant D.A.: Occurrence of far-red light photoacclimation (FaRLiP) in diverse cyanobacteria. – Life **5**: 4-24, 2015.

Garczarek L., van der Staay G.W.M., Thomas J.C., Partensky F.: Isolation and characterization of Photosystem I from two strains of the marine oxychlorobacterium *Prochlorococcus*. – Photosynth. Res. **56**: 131-141, 1998.

Gardian Z., Bumba L., Schrofel A. *et al*.: Organisation of photosystem I and photosystem II in red alga *Cyanidium caldarium*: encounter of cyanobacterial and higher plant concepts. – BBA-Bioenergetics **1767**: 725-731, 2007.

Goldschmidt-Clermont M., Bassi R.: Sharing light between two photosystems: mechanism of state transitions. – Curr. Opin. Plant. Biol. **25**: 71-78, 2015.

Gouterman M., Wagnière G.H., Snyder L.C.: Spectra of porphyrins: Part II. Four orbital model. – J. Mol. Spectrosc. **11**: 108-127, 1963.

Govindjee, Björn L.O.: Evolution of the Z-scheme of photosynthesis: a perspective. – Photosynth. Res. **133**: 5-15, 2017.

Govindjee, Ichimura S., Cederstrand C., Rabinowitch E.: Effect of combining far-red light with shorter wave light in the excitation of fluorescence in *Chlorella*. – Arch. Biochem. Biophys. **89**: 322-323, 1960.

Govindjee, Yang L.: Structure of the red fluorescence band in chloroplasts. – J. Gen. Physiol. **49**: 763-780, 1966.

Govindjee: Emerson enhancement effect and two light reactions in photosynthesis. – In: Kok B., Jagendorf A.T. (ed.): Photosynthetic Mechanisms of Green Plants. Pp 318. National Academy of Science – National Research Council Publication, Washington DC 1963.

Govindjee: Chlorophyll *a* fluorescence: a bit of basics and history. – In: Papageorgiou G.C., Govindjee: Chlorophyll *a* Fluorescence: A Signature of Photosynthesis. Pp. 1-41. Springer, Dordrecht 2004.

Govindjee: Sixty-three years since kautsky: chlorophyll *a* fluorescence. – Aust. J. Plant Physiol. **22**: 131-160, 1995.

Grouneva I., Rokka A., Aro E.-M.: The thylakoid membrane proteome of two marine diatoms outlines both diatom-specific and species-specific features of the photosynthetic machinery. – J. Proteome Res. **10**: 5338-5353, 2011.

Gundermann K., Büchel C.: Structure and functional heterogeneity of fucoxanthin-chlorophyll proteins in diatoms. – In: Hohmann-Marriott M.F. (ed.): The Structural Basis of Biological Energy Generation. Pp. 31-27. Springer, Dordrecht 2014.

Havaux M., Guedeney G., Hagemann M. *et al*.: The chlorophyll□binding protein IsiA is inducible by high light and protects the cyanobacterium *Synechocystis* PCC6803 from photooxidative stress. – FEBS Lett. **579**: 2289-2293, 2005.

Herbstová M., Bína D., Koník P. *et al*.: Molecular basis of chromatic adaptation in pennate diatom *Phaeodactylum tricornutum*. – BBA-Bioenergetics **1847**: 534-543, 2015.

Hillier W., Babcock G.T.: Photosynthetic reaction centers. – Plant Physiol. **125**: 33-37, 2001.

Hipkins M.F., Baker N.R.: Photosynthetic energy transduction: A practical approach. – In: Hipkins M.F., Baker N.R.: Photosynthesis: Energy Transduction, A Practical Approach. Pp 1. IRL Press, Arlington 1986.

Hirsch R.E., Rich M., Govindjee: A tribute to Seymour Steven Brody: in memoriam (November 29, 1927 to May 25, 2010). – Photosynth. Res. **106**: 191-199, 2010.

Hofstraat J.W., Rubelowsky K., Slutter S.: Corrected fluorescence excitation and emission spectra of phytoplankton: toward a more uniform approach to fluorescence measurements. – J. Plankton. Res. **14**: 625-636, 1992.

Hohmann-Marriott M.F., Blankenship R.E.: Evolution of photosynthesis. – Plant. Physiol. **154**: 434-438, 2011.

Hohmann-Marriott M.F., Takizawa K., Eaton-Rye J.J. *et al.*: The redox state of the plastoquinone pool directly modulates minimum chlorophyll fluorescence yield in *Chlamydomonas reinhardtii*. – FEBS Lett. **584**: 1021-1026, 2010.

Ikeda Y., Komura M., Watanabe M. *et al.*: Photosystem I complexes associated with fucoxanthin-chlorophyll-binding proteins from a marine centric diatom, *Chaetoceros gracilis*. – BBA-Bioenergetics **1777**: 351-361, 2008.

Irrgang K.D., Boekema E.J., Vater J., Renger G.: Structural determination of the photosystem II core complex from spinach. – FEBS J. **178**: 209-217, 1988.

Iwai M., Takahashi Y., Minagawa J.: Molecular remodeling of photosystem II during state transitions in *Chlamydomonas reinhardtii*. – Plant Cell **20**: 2177-2189, 2008.

Järvi S., Suorsa M., Aro E.-M.: Photosystem II repair in plant chloroplasts – regulation, assisting proteins and shared components with photosystem II biogenesis. – BBA-Bioenergetics **1847**: 900-909, 2015.

Jordan P., Fromme P., Witt H.T., Klukas O.: Three-dimensional structure of cyanobacterial photosystem I at 2.5 angstrom resolution. – Nature **411**: 909-917, 2001.

Joshua S., Mullineaux C.W.: Phycobilisome diffusion is required for light-state transitions in cyanobacteria. – Plant Physiol. **135**: 2112-2119, 2004.

Juhas M., Büchel C.: Properties of photosystem I antenna protein complexes of the diatom *Cyclotella meneghiniana*. – J. Exp. Bot. **63**: 3673-3681, 2012.

Kaňa R., Kotabová E., Lukeš M. *et al.*: Phycobilisome mobility and its role in the regulation of light harvesting in red algae. – Plant Physiol. **165**: 1618-1631, 2014.

Karapetyan N.V., Bolychevtseva Y.V., Yurina N.P. *et al.*: Long-wavelength chlorophylls in photosystem I of cyanobacteria: origin, localization, and functions. – Biochemistry **79**: 213, 2014.

Kargul J., Nield J., Barber J.: Three-dimensional reconstruction of a light-harvesting complex I-photosystem I (LHCI-PSI) supercomplex from the green alga *Chlamydomonas reinhardtii.* Insights into light harvesting for PSI. – J. Biol. Chem. **278**: 16135-16141, 2003.

Kautsky H., Hirsch A.: [New attempts for carbon dioxide assimilation.] – Naturwissenschaft **19**: 964-964, 1931. [In German]

Keeling P.J.: The number, speed, and impact of plastid endosymbioses in eukaryotic evolution. – Annu. Rev. Plant Biol. **64**: 583-607, 2013.

Komenda J., Sobotka R., Nixon P.J.: Assembling and maintaining the photosystem II complex in chloroplasts and cyanobacteria. – Curr. Opin. Plant Biol. **15**: 245-251, 2012.

Kondo K., Ochiai Y., Katayama M., Ikeuchi M.: The membrane-associated CpcG2-phycobilisome in *Synechocystis*: a new photosystem I antenna. – Plant Physiol. **144**: 1200-1210, 2007.

Krause G.H., Briantais J.M., Vernotte C.: Characterization of chlorophyll fluorescence quenching in chloroplasts by fluorescence spectroscopy at 77 K I. ΔpH-dependent quenching. – BBA-Bioenergetics **723**: 169-175, 1983.

Krause G.H., Weis E.: Chlorophyll fluorescence as a tool in plant physiology. – Photosynth. Res. **5**: 139-157, 1984.

Krey A., Govindjee: Fluorescence studies on a red alga, *Porphyridium cruentum*. – Biochim. Biophys. Acta. **120**: 1-18, 1966.

Kyle D.J., Ohad I., Arntzen C.J.: Membrane protein damage and repair: Selective loss of a quinone-protein function in chloroplast membranes. – P. Natl. Acad. Sci. USA **81**: 4070-4074, 1984.

La Roche J., van der Staay G.W.M., Partensky F. *et al.*: Independent evolution of the prochlorophyte and green plant chlorophyll *a/b* light-harvesting proteins. – P. Natl. Acad. Sci. USA **93**: 15244-15248, 1996.

Lakowicz J.R.: Fluorescence polarization. – In: Lakowicz J.R. (ed): Principles of Fluorescence Spectroscopy Pp. 111-153. Springer, Boston 1983a.

Lakowicz J.R.: Quenching of fluorescence. – In: Lakowicz J.R. (ed): Principles of Fluorescence Spectroscopy. Pp. 257-301. Springer, Boston 1983b.

Lamb J., Forfang K., Hohmann-Marriott M.: A practical solution for 77 K fluorescence measurements based on LED excitation and CCD array detector. – PLoS ONE **10**: e0132258, 2015.

Laudenbach D.E., Reith M.E., Straus N.A.: Isolation, sequence analysis, and transcriptional studies of the flavodoxin gene from *Anacystis nidulans* R2. – J. Bacteriol. **170**: 258-265, 1988.

Lavaud J., Lepetit B.: An explanation for the inter-species variability of the photoprotective non-photochemical chlorophyll fluorescence quenching in diatoms. – BBA-Bioenergetics **1827**: 294-302, 2013.

Lepetit B., Volke D., Szabó M. *et al.*: Spectroscopic and molecular characterization of the oligomeric antenna of the diatom *Phaeodactylum tricornutum*. – Biochemistry **46**: 9813-9822, 2007.

Ley A.C., Butler W.L.: Energy distribution in the photochemical apparatus of *Porphyridium cruentum* in state I and state II. – BBA-Bioenergetics **592**: 349-363, 1980.

Li D., Xie J., Zhao J. *et al.*: Light-induced excitation energy redistribution in *Spirulina platensis* cells: "spillover" or "mobile PBSs"? – BBA-Bioenergetics **1608**: 114-121, 2004.

Li H., Yang S., Xie J., Zhao J.: Probing the connection of PBSs to the photosystems in *Spirulina platensis* by artificially induced fluorescence fluctuations. – J. Lumin. **122-123**: 294-296, 2007.

Li M., Semchonok D.A., Boekema E.J., Bruce B.D.: Characterization and evolution of tetrameric photosystem I from the thermophilic cyanobacterium *Chroococcidiopsis* sp TS-821. – Plant Cell **26**: 1230-1245, 2014.

Li Y., Chen M.: Novel chlorophylls and new directions in photosynthesis research. – Funct. Plant Biol. **42**: 493-501, 2015.

Litvin F.F., Krasnovsky A.A.: Investigation by fluorescence spectra of intermediate stages of chlorophyll biosynthesis in etiolated leaves. – Dokl. Acad. Nauk+ **117**: 106-109, 1957.

Litvín R., Bína D., Herbstová M., Gardian Z.: Architecture of the light-harvesting apparatus of the eustigmatophyte alga *Nannochloropsis oceanica*. – Photosynth. Res. **130**: 137-150, 2016.

Liu H., Roose J.L., Cameron J.C., Pakrasi H.B.: A genetically tagged Psb27 protein allows purification of two consecutive

photosystem II (PSII) assembly intermediates in *Synechocystis* 6803, a cyanobacterium. – J. Biol. Chem. **286**: 24865-24871, 2011.

Liu H., Zhang H., Niedzwiedzki D.M. *et al.*: Phycobilisomes supply excitations to both photosystems in a megacomplex in cyanobacteria. – Science **342**: 1104-1107, 2013.

Marx A., David L., Adir N.: Piecing together the phycobilisome. – In: Hohmann-Marriott M.F. (ed): The Structural Basis of Biological Energy Generation. Pp. 59-76. Springer, Dordrecht 2014.

Maxwell K., Johnson G.N.: Chlorophyll fluorescence – a practical guide. – J. Exp. Bot. **51**: 659-668, 2000.

Mazor Y., Borovikova A., Nelson N.: The structure of plant photosystem I super-complex at 2.8 Å resolution. – Elife **4**: e07433, 2015.

McConnell M.D., Koop R., Vasil'ev, S., Bruce D.: Regulation of the distribution of chlorophyll and phycobilin-absorbed excitation energy in cyanobacteria. A structure-based model for the light state transition. – Plant Physiol. **130**: 1201-1212, 2002.

McCormac D.J., Marwood C.A., Bruce D., Greenberg B.M.: Assembly of Photosystem I and II during the early phases of light□induced development of chloroplasts from proplastids in *Spirodela oligorrhiza*. – Photochem. Photobiol. **63**: 837-845, 1996.

Miloslavina Y., Grouneva I., Lambrev P.H. *et al.*: Ultrafast fluorescence study on the location and mechanism of non-photochemical quenching in diatoms. – BBA-Bioenergetics **1787**: 1189-1197, 2009.

Minagawa J.: State transitions – the molecular remodeling of photosynthetic supercomplexes that controls energy flow in the chloroplast. – BBA-Bioenergetics **1807**: 897-905, 2011.

Miyashita H., Ikemoto H., Kurano N. *et al.*: Chlorophyll *d* as a major pigment. – Nature **383**: 402, 1996.

Morosinotto T., Breton J., Bassi R., Croce R.: The nature of a chlorophyll ligand in Lhca proteins determines the far red fluorescence emission typical of photosystem I. – J. Biol. Chem. **278**: 49223-49229, 2003.

Mukerji I., Sauer K.: Temperature Dependent Steady State and Picosecond Kinetic Fluorescence Measurements of a Photosystem I Preparation from Spinach. Pp. 30. Lawrence Berkeley Laboratory, Berkeley, 1988.

Müller N.: [Relationships between assimilation, absorption and fluorescence in the chlorophyll of the living leaf.] – Jahrb. Wiss. Bot. **9**: 42-49, 1887. [In German]

Mullet J., Burke J., Arntzen C.: A developmental study of photosystem I peripheral chlorophyll proteins. – Plant Physiol. **65**: 823-827 1980a.

Mullet J., Burke J., Arntzen C.: Chlorophyll proteins of photosystem I. – Plant Physiol. **65**: 814-822, 1980b.

Mullineaux C.W., Allen J.F.: State 1-State 2 transitions in the cyanobacterium *Synechococcus* 6301 are controlled by the redox state of electron carriers between Photosystems I and II. – Photosynth. Res. **23**: 297-311, 1990.

Mullineaux C.W.: Electron transport and light-harvesting switches in cyanobacteria. – Front. Plant Sci. **5**: 7, 2014.

Mullineaux C.W.: Excitation energy transfer from phycobilisomes to photosystem I in a cyanobacterial mutant lacking photosystem II. – BBA-Bioenergetics **1184**: 71-77, 1994.

Mullineaux C.W.: Excitation energy transfer from phycobilisomes to photosystem I in a cyanobacterium. – BBA-Bioenergetics **1100**: 285-292, 1992.

Mullineaux C.W.: Phycobilisome-reaction centre interaction in cyanobacteria. – Photosynth. Res. **95**: 175-182, 2008.

Mulo P., Sakurai I., Aro E.-M.: Strategies for *psbA* gene expression in cyanobacteria, green algae and higher plants: from transcription to PSII repair. – BBA-Bioenergetics **1817**: 247-257, 2012.

Murakami A.: Quantitative analysis of 77K fluorescence emission spectra in *Synechocystis* sp. PCC 6714 and *Chlamydomonas reinhardtii* with variable PS I/PS II stoichiometries. – Photosynth. Res. **53**: 141-148, 1997.

Murata N., Nishimura M., Takamiya A.: Fluorescence of chlorophyll in photosynthetic systems. III. Emission and action spectra of fluorescence – three emission bands of chlorophyll *a* and the energy transfer between two pigment systems. – Biochim. Biophys. Acta **126**: 234-243, 1966.

Murata N.: Control of excitation transfer in photosynthesis I. Light-induced change of chlorophyll *a* fluoresence in *Porphyridium cruentum*. – BBA-Bioenergetics **172**: 242-251, 1969.

Murata N.: Control of excitation transfer in photosynthesis. IV. Kinetics of chlorophyll a fluorescence in *Porphyra yezoensis*. – BBA-Bioenergetics **205**: 379-389, 1970.

Mysliwa-Kurdziel B., Barthélemy X., Strzalka K., Franck F.: The early stages of photosystem II assembly monitored by measurements of fluorescence lifetime, fluorescence induction and isoelectric focusing of chlorophyll-proteins in barley etiochloroplasts. – Plant Cell Physiol. **38**: 1187-1196, 1997.

Nagao R., Takahashi S., Suzuki T. *et al.*: Comparison of oligomeric states and polypeptide compositions of fucoxanthin chlorophyll *a/c*-binding protein complexes among various diatom species. – Photosynth. Res. **117**: 281-288, 2013.

Nagao R., Tomo T., Noguchi E. *et al.*: Purification and characterization of a stable oxygen-evolving Photosystem II complex from a marine centric diatom, *Chaetoceros gracilis*. – BBA-Bioenergetics **1797**: 160-166, 2010.

Nakatani H., Ke B., Dolan E., Arntzen C.: Identity of the photosystem II reaction center polypeptide. – BBA-Bioenergetics **765**: 347-352, 1984.

Natali A., Croce R.: Characterization of the major light-harvesting complexes (LHCBM) of the green alga *Chlamydomonas reinhardtii*. – PLoS ONE **10**: e0119211, 2015.

Nickelsen J., Rengstl B.: Photosystem II assembly: from cyanobacteria to plants. – Annu. Rev. Plant Biol. **64**: 609-635, 2013.

Nixon P.J., Barker M., Boehm M. *et al.*: FtsH-mediated repair of the photosystem II complex in response to light stress. – J. Exp. Bot. **56**: 357-363, 2005.

Novoderezhkin V.I., Palacios M.A., van Amerongen H., van Grondelle R.: Excitation dynamics in the LHCII complex of higher plants: modeling based on the 2.72 Å crystal structure. – J. Phys. Chem. B **109**: 10493-10504, 2005.

Owens T.G.: Dynamics and mechanism of singlet energy-transfer between carotenoids and chlorophylls-light harvesting and nonphotochemical fluorescence quenching. – In: Murata N. (ed.): Research in Photosynthesis. Pp. 179-186. Kluwer Acad. Publ., Dordrecht 1992.

Pakrasi H.B., Goldenberg A., Sherman L.A.: Membrane development in the cyanobacterium, *Anacystis nidulans*, during recovery from iron starvation. – Plant Physiol. **79**: 290-295, 1985a.

Pakrasi H.B., Riethman H.C., Sherman L.A.: Organization of pigment proteins in the photosystem II complex of the cyanobacterium *Anacystis nidulans* R2. – P. Natl. Acad. Sci. USA **82**: 6903-6907, 1985b.

Park Y.I., Sandström S., Gustafsson P., Öquist G.: Expression of the *isiA* gene is essential for the survival of the cyanobacterium *Synechococcus* sp. PCC 7942 by protecting photosystem II

from excess light under iron limitation. – Mol. Microbiol. **32**: 123-129, 1999.

Passarini F., Wientjes E., Hienerwadel R., Croce R.: Molecular basis of light harvesting and photoprotection in CP24 unique features of the most recent antenna complex. – J. Biol. Chem. **284**: 29536-29546, 2009.

Pfundel E., Pfeffer M.: Modification of photosystem I light harvesting of bundle-sheath chloroplasts occurred during the evolution of NADP-malic enzyme C4 photosynthesis. – Plant Physiol. **114**: 145-152, 1997.

Qin X., Suga M., Kuang T., Shen J.-R.: Structural basis for energy transfer pathways in the plant PSI-LHCI supercomplex. – Science **348**: 989-995, 2015.

Rabinowitch E., Govindjee: Photosynthesis. Pp. 273. John Wiley & Sons, Inc, New York 1969.

Riethman H.C., Sherman L.A.: Purification and characterization of an iron stress-induced chlorophyll-protein from the cyanobacterium *Anacystis nidulans* R2. – BBA-Bioenergetics **935**: 141-151, 1988.

Rijgersberg C.P., Amesz J., Thielen A., Swager J.A.: Fluorescence emission spectra of chloroplasts and subchloroplast preparations at low temperature. – BBA-Bioenergetics **545**: 473-482, 1979.

Ruban A.V., Calkoen F., Kwa S.L.S. *et al.*: Characterisation of LHC II in the aggregated state by linear and circular dichroism spectroscopy. – BBA-Bioenergetics **1321**: 61-70, 1997.

Ruban A.V., Johnson M.P., Duffy C.D.P.: The photoprotective molecular switch in the photosystem II antenna. – BBA-Bioenergetics **1817**: 167-181, 2012.

Şener M., Strümpfer J., Hsin J. *et al.*: Förster energy transfer theory as reflected in the structures of photosynthetic light-harvesting systems. – ChemPhysChem. **12**: 518-531, 2011.

Sétif P., Mathis P., Vänngård T.: Photosystem I photochemistry at low temperature. Heterogeneity in pathways for electron transfer to the secondary acceptors and for recombination processes. – BBA-Bioenergetics **767**: 404-414, 1984.

Schlodder E., Falkenberg K., Gergeleit M., Brettel K.: Temperature dependence of forward and reverse electron transfer from A1-, the reduced secondary electron acceptor in photosystem I. – Biochemistry **37**: 9466-9476, 1998.

Sjöback R., Nygren J., Kubista M.: Absorption and fluorescence properties of fluorescein. – Spectrochim. Acta A **51**: 7-21, 1995.

Sobiechowska-Sasim M., Stoń-Egiert J., Kosakowska A.: Quantitative analysis of extracted phycobilin pigments in cyanobacteria – an assessment of spectrophotometric and spectrofluorometric methods. – J. Appl. Phycol. **26**: 2065-2074, 2014.

Standfuss J., Kühlbrandt W.: The three isoforms of the light-harvesting complex II spectroscopic features, trimer formation, and functional roles. – J. Biol. Chem. **279**: 36884-36891, 2004.

Strasser R.J., Tsimilli-Michael M., Srivastava A.: Analysis of the Chlorophyll *a* Fluorescence Transient. – In: Papageorgiou G.C., Govindjee (ed.): Chlorophyll *a* Fluorescence: A Signature of Photosynthesis. Pp. 321-362. Springer, Dordrecht 2004.

Sugiura M., Inoue Y.: Highly purified thermo-stable oxygen-evolving photosystem II core complex from the thermophilic cyanobacterium *Synechococcus elongatus* having His-tagged CP43. – Plant Cell Physiol. **40**: 1219-1231, 1999.

Swingley W.D., Iwai M., Chen Y. *et al.*: Characterization of photosystem I antenna proteins in the prasinophyte *Ostreococcus tauri*. – BBA-Bioenergetics **1797**: 1458-1464, 2010.

Takahashi S., Badger M.R.: Photoprotection in plants: a new light on photosystem II damage. – Trends Plant Sci. **16**: 53-60, 2011.

Tang K., Ding W.-L., Höppner A. *et al.*: The terminal phycobilisome emitter, LCM: A light-harvesting pigment with a phytochrome chromophore. – P. Natl. Acad. Sci. USA **112**: 15880-15885, 2015.

Tokutsu R., Minagawa J.: Energy-dissipative supercomplex of photosystem II associated with LHCSR3 in *Chlamydomonas reinhardtii*. – P. Natl. Acad. Sci. USA **110**: 10016-10021, 2013.

Umena Y., Kawakami K., Shen J.-R., Kamiya N.: Crystal structure of oxygen-evolving photosystem II at a resolution of 1.9 Å. – Nature **473**: 55-60, 2011.

van Wijk K.J., Bingsmark S., Aro E.-M., Andersson B.: *In vitro* synthesis and assembly of photosystem II core proteins. the D1 protein can be incorporated into photosystem II in isolated chloroplasts and thylakoids. – J. Biol. Chem. **270**: 25685-25695, 1995.

Veith T., Büchel C.: The monomeric photosystem I-complex of the diatom *Phaeodactylum tricornutum* binds specific fucoxanthin chlorophyll proteins (FCPs) as light-harvesting complexes. – BBA-Bioenergetics **1767**: 1428-1435, 2007.

Walters R.G., Horton P.: Resolution of components of non-photochemical chlorophyll fluorescence quenching in barley leaves. – Photosynth. Res. **27**: 121-133, 1991.

Watanabe M., Semchonok D.A., Webber-Birungi M.T. *et al.*: Attachment of phycobilisomes in an antenna – photosystem I supercomplex of cyanobacteria. – P. Natl. Acad. Sci. USA **111**: 2512-2517, 2014.

Wei X., Su X., Cao P. *et al.*: Structure of spinach photosystem II-LHCII supercomplex at 3.2 Å resolution. – Nature **534**: 69-87, 2016.

Weis E.: Chlorophyll fluorescence at 77 K in intact leaves: characterization of a technique to eliminate artifacts related to self-absorption. – Photosynth. Res. **6**: 73-86, 1985.

Wientjes E., van Stokkum I.H.M., van Amerongen H., Croce R.: The role of the individual Lhcas in photosystem I excitation energy trapping. – Biophys. J. **101**: 745-754, 2011.

Yamamoto Y., Hori H., Kai S. *et al.*: Quality control of Photosystem II: reversible and irreversible protein aggregation decides the fate of Photosystem II under excessive illumination. – Front. Plant Sci. **4**: 433, 2013.

Yokono M., Nagao R., Tomo T., Akimoto S.: Regulation of excitation energy transfer in diatom PSII dimer: How does it change the destination of excitation energy? – BBA-Bioenergetics **1847**: 1274-1282, 2015.

Young A.J., Frank H.A.: Energy transfer reactions involving carotenoids: quenching of chlorophyll fluorescence. – J. Photoch. Photobio. B **36**: 3-15, 1996.

Paper V